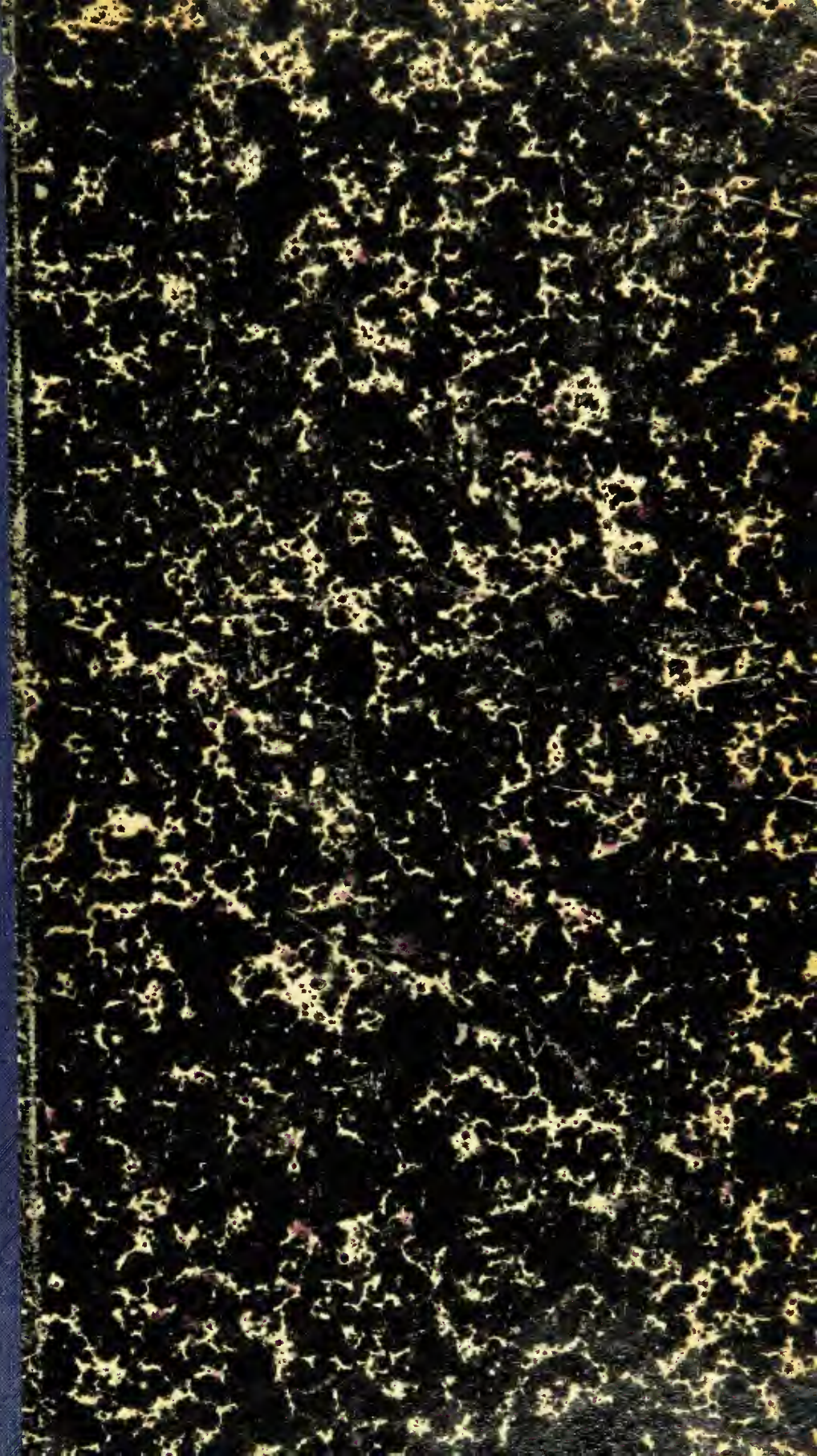
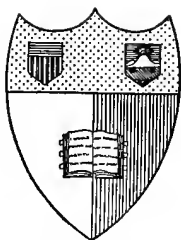


QC  
411  
B29  
I58+  
v.3



411  
B29 I58+  
V.3



**Cornell University Library**  
**Ithaca, New York**

---

FROM

Carnegie Institution

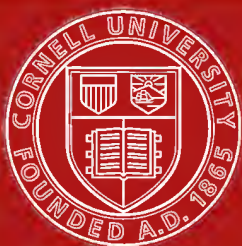
---

---

To renew this book copy the call No. and give to the librarian.

Readers are asked to report all cases of books marked or mutilated.

olin, ove1



Cornell University  
Library

The original of this book is in  
the Cornell University Library.

There are no known copyright restrictions in  
the United States on the use of the text.

<http://www.archive.org/details/cu31924012330100>

# INTERFEROMETER EXPERIMENTS IN ACOUSTICS AND GRAVITATION *ack*

## PART III

By CARL BARUS, Ph. D., LL. D.

*Hazard Professor of Physics and Dean of the Graduate Department  
in Brown University*



PUBLISHED BY THE CARNEGIE INSTITUTION OF WASHINGTON  
WASHINGTON, JUNE, 1925



# INTERFEROMETER EXPERIMENTS IN ACOUSTICS AND GRAVITATION

## PART III

By CARL BARUS, Ph. D., LL.D.

*Hazard Professor of Physics and Dean of the Graduate Department  
in Brown University*



PUBLISHED BY THE CARNEGIE INSTITUTION OF WASHINGTON  
WASHINGTON, JUNE, 1925

A547122

CARNEGIE INSTITUTION OF WASHINGTON

PUBLICATION No. 310, PART III

*The Lord Baltimore Press*  
BALTIMORE, MD., U. S. A.



## PREFACE.

The following papers contain the experiments made in this laboratory during the last two years, chiefly with the aid of the mercury U-gage, the rise and fall of the free surfaces of which are read off with the interferometer. In most cases relative values of the small pressures in question are alone of interest, and as these are proportional to the corresponding fringe displacements with white light, it suffices to report the latter graphically. Unfortunately, the range of the gage is restricted by the tendency of the surfaces of mercury gradually to lose parallelism in their reciprocal motion. This has been partially counteracted by making the free mercury surfaces of large (10 cm.) diameter, by filling the gage in vacuo, etc. The success of these devices is but partial. Moreover, pressures within  $5 \times 10^{-4}$  cm. of mercury are liable to be more or less distorted by capillary forces and thus not registered in the surface depressions of the gage. Finally in a closed region with rigid walls, small pressure increments, if accruing in the lapse of time, are not determinable, owing to coincident relatively enormous temperature discrepancies which may supervene. The hope of measuring slowly accumulating pressure increments easily and directly, a frequent desideratum in physical chemistry and biology, has not borne fruit, as shown by a number of typical examples in Chapter I.

If, however, the walls of a region are elastic in such a way as to determine a definite small-pressure increment within, the temperature difficulties vanish. Thus the measurement of variations of surface tension by the pressures observed within a bubble works out nicely, though it must be acknowledged that the work requires both patience and expedition. It is possible to trace the increase of surface tension in this way almost as far as the solid state. The experiments succeed not with soap-bubbles only, for colloidal solutions are very generally available. An interesting result, moreover, is the possibility of thinning out of a soap solution to a degree approaching pure water with continually increasing surface tensions.

In the case of gases, there are many measurements to which the U-tube interferometer lends itself. Thus it is easy to find the viscosity of a gas from very small pressure increments, though here the temperature discrepancy referred to above is already menacing, in spite of the small times of transpiration. In the case of efflux, I have not been able to produce a hole small enough to admit of trustworthy results. The large increase of gas viscosity, produced by the heat of a flame carried at the end of a fine jet, is strikingly noticeable. The flame thus virtually plugs the gas-jet; and since the plug is removed with the flame, there is here a mechanism favorable to turbulency in flames.

A most promising application of the U-gage was found in the endeavor to measure the density and diffusion of gases. For here it is merely necessary to determine the pressures at the end of a long tube in the lapse of time. I have, therefore, investigated this subject at some length, using a variety of gases and with special reference to the gage discrepancy already stated. The densities found may be shown to conform satisfactorily with known data. The diffusion coefficients come out consistently for all lengths and widths of tubes; but for some reason which I have not ascertained, the coefficients found are larger than the standard data. From measurements of the pressure at the top of hot gas columns, the coefficient of expansion may be derived approximately, and more precisely as the pipe is longer. The attempt to find the hygrometric state of the air, however, failed, probably from the difficulty of actually drying the tube and appurtenances adequately.

In Chapter IV, I have returned to the pressures generated acoustically when pin-hole probes are placed at the nodes of vibrating systems. These pin-holes, which are ideally salient and reëntrant cones, respectively, with a prescribed size of hole, are always used in pairs; for in such a case the fringe displacement of the tube interferometer is nearly doubled. If a region of pulsating air has access to still air through a pin-hole probe only, the pin-hole being placed at the boundary, the resulting stream-lines point from the apex to the base of the pin-hole cone. Their strength varies with the diameter of the pin-hole (critical maximum of efficiency), the obliquity of the walls, and the intensity of the pulsation (node). The result is a pressure increment or decrement, respectively, in the pulsating region. The first part of the paper describes the vibration in branched pipes excited by a telephonic siren, as it were, or by paired sirens in unison. The pipes are of different diameters, but the branched region is closed and preference is given to quill tubes. The character of the motion within is mapped out both with the telephones in sequence (plate displacement respectively in and out) and in phase (plate displacement in and out together) for a great variety of tube-lengths. If the survey is made in pitch, the maxima of fringe displacement (crests) show the pipe-notes in any given case. The endeavor is then made to distribute the observed pipe-lengths determined by the crests in relation to the free wave-length of the pipe-note. A curious feature in all this work is the appearance of strong low-frequency crests (2 and 4 foot octave) in connection with pipes less than 10 cm. long, and the repeated occurrence of multiple resonance.

Among the allied results, the use of currents arising in the electromagnetic mechanism of a loud-speaker horn, receiving diapason pipe-notes from different distances, may be mentioned. The most interesting method of exciting vibration, however, is the small spark-gap placed at one end of a doubly capped tube. For in such a case, in addition to the acoustic resonance (frequencies of the tube) the electromagnetic frequency of the coil, if low enough, may also be recognized by an anomalous crest, the pitch of which is controlled by the capacity and inductance of the coil.

In Chapter V, I have collected such experiments as grew out of the work incidentally and seemed to require further investigation. Thus, when Mayer's phenomenon of acoustic pressure is evoked by telephones, it shows a systematic distribution of both attractions and repulsions along the pipe axis, and these are best exhibited when the resonators or disks are swung from a bifilar mechanism or a torsion balance. In the work done with interferometers, the peculiar asymmetrical sequence of fringes produced by the aid of the extraordinary ray of a calcite rhomb used as a compensator is noteworthy. A suggestion for the use of long-distance interferometry in connection with earthquake phenomena to detect slight changes of shear is given a preliminary trial, etc.

In the last chapter I have put together the work done on the constant of gravitation. The chief purpose of this chapter is to compare the night observation for the Newtonian constant made under reasonable laboratory surroundings, in 1922, throughout a number of months in the summer, with corresponding data obtained in 1921. The result is disappointing; for the mean data of the two series differ in spite of all precautions by nearly 2 per cent. Incidentally, it is shown that the static displacement of the needle, its period, and logarithmic decrement are interdependent, all being similarly influenced by the presence of dominating radiant forces, which it was found impossible to bring under adequate control. They are considerably reduced by the partial exhaustion of the needle-case and all observations were made in rarefied air; but they are increased again by high exhaustions, and the anomalous results obtained under these circumstances, where attractions are frequently inverted and repulsive forces appear, are a curious incident in the work. For this reason, the endeavors to interpret the motion of the needle in terms of the viscosity of the gas, etc., are illusory, since the chief resistances are radiant forces. In fact, the blight which seems to descend upon the apparatus after high exhaustion, reversing all normal behavior for days, is an astonishing phenomenon. I have been tempted at times to find more in it than a mere consequence of the law of cooling to ultimate equilibrium.

My thanks are due to Miss Mildred E. Carlen for her efficient assistance in preparing this volume for the press.

CARL BARUS.

BROWN UNIVERSITY,  
*Providence, Rhode Island.*



# CONTENTS.

## CHAPTER I.—*Modified Interferometer U-tube with Applications.*

	U-TUBE.	PAGE
1. Apparatus. (Fig. 1.)	.....	I
2. Mercury charged in vacuo.	.....	2

### APPLICATION.

3. Gas evolution and absorption. Figs. 2 to 5.	.....	3
4. Water absorption. Fig. 6.	.....	5
5. Water evaporation. Figs. 7 to 10.	.....	5
6. Differential experiments. Fig. 11.	.....	9
7. Summer experiments. Figs. 12 to 14.	.....	10

## CHAPTER II.—*Pressures in Connection with Surface Tension.*

### SOAP, GLUE, AND SUGAR BUBBLES.

8. Pressure within a soap-bubble. Fig. 15.	.....	12
9. Observations. Fig. 16	.....	13
10. Glue-bubbles. Figs. 17, 18. Table 1.	.....	15
11. Molasses. Fig. 19	.....	18
12. Sugar. Figs. 20, 21.	.....	18
13. Charged bubbles. Sparkless sparks. Fig. 22.	.....	22

### OIL BUBBLES.

14. Oil and rubber surface tensions.	.....	25
15. Canada balsam. Figs. 23, 24.	.....	26
16. Pitch. Fig. 25	.....	29
17. Nitrocelluloid	.....	30

## CHAPTER III.—*Viscosity, Density, and Diffusion of Gases.*

### VISCOSITY AND EFFLUX.

18. Viscosity of air. Fig. 26.	.....	31
19. Observations. Fig. 27	.....	32
20. Efflux through pin-holes. Fig. 28.	.....	34
21. Sensitive flames. Adjustment. Fig. 29.	.....	35
22. Same. Telephonic excitation	.....	35
23. Apparent flame pressure and viscosity. Fig. 30.	.....	35
24. Inferences	.....	36

### DENSITY AND DIFFUSION OF GASES.

25. Apparatus. Fig. 31	.....	37
26. Equations and data (coal gas) for density. Figs. 32, 34.	.....	37
27. Equations for diffusion	.....	40
28. Data for diffusion (coal gas). Fig. 33.	.....	41
29. Hydrogen. Density	.....	41
30. Diffusion of hydrogen. Fig. 35.	.....	42
31. Air. Coefficient of expansion. Fig. 36.	.....	43
32. Vapor pressure. Hygrometry	.....	45
33. Gage tests by direct compression. Figs. 37, 38.	.....	45
34. U-gage with fresh mercury. Figs. 39 to 41.	.....	47
35. New quill-tube experiments with hydrogen. Fig. 42.	.....	48
36. Experiments in wider and longer tubes.	.....	49
37. Capillary gage correction, $\delta x$ , in case of hot air.	.....	50
38. Diffusion in one direction only. Fig. 43.	.....	51
39. Incidental results. Density. Table 6.	.....	52

	PAGE
40. Data for diffusion. Figs. 44 to 50. Table 7.....	54
41. Inferences relative to equations.....	56
42. Diffusion in case of a longer tube. Fig. 51. Tables 8, 9.....	58
43. Diffusion. Very long tube. Table 10.....	60
44. Diffusion. Short tube. Figs. 52, 53.....	61
45. Diffusion. Quill tube again. Fig. 54.....	63
46. Conclusion .....	63

#### CHAPTER IV.—*Pin-hole Probe Experiments, Chiefly with Branched Tubes.*

##### BRANCH PIPES.

47. Branch adjustments. Figs. 55 to 58.....	64
48. Experiments. Figs. 59 to 62.....	65
49. Multiple resonance; narrow tubes. Location of pin-holes. Figs. 63 to 67.....	66
50. The same. Wide tubes. Figs. 68 to 70. Tables 11, 12, 13.....	68
51. Modes of vibration within the H-tube. Figs. 71, 72. Tables 14, 15.....	71
52. Continued. Deep resonances. Figs. 73 to 75.....	74

##### STRAIGHT AND TRANSVERSE PIPES.

53. Straight tubes 2 cm. diameter. Figs. 76, 77.....	76
54. Transverse tubes, 2 cm. diameter. Figs. 78 to 84.....	76
55. Comparison of constants for wide tubes. Figs. 85 to 88.....	78
56. Telephones in parallel.....	80

##### QUILL PIPES CAPPED AT BOTH ENDS.

57. Vibration in closed straight quill tubes. Figs. 89 to 94.....	80
58. Vibration in transverse quill tubes. Figs. 95 to 98.....	82
59. The same. Overtones, viscosity effect. Figs. 99 to 102. Tables 16, 17.....	83
60. The same. Single telephonic exciter. Figs. 103 to 107. Table 18.....	86
61. The same. Single telephone and single tube. Figs. 108 to 114.....	89
62. Reversal of pin-holes, etc. Figs. 115 to 118.....	91
63. Successive telephones in cascade. Figs. 119, 120.....	93
64. Experiments with high resistance (binaural) telephones. Apparent hysteresis. Figs. 121, 122.....	93
65. Telephonic effect at different air pressures.....	94
66. Telephonic response to varying current. Figs. 123 to 125.....	95

##### MISCELLANEOUS PIPES AND EXCITATION.

67. Experiments with pin-hole resonators.....	97
68. Interference of resonators. Fig. 126.....	98
69. Immediate junction of U-gage and telephone. Fig. 127.....	98
70. The same. Different telephones. Figs. 128 to 134.....	99
71. Specially tuned H-pipes. Figs. 135, 136.....	100
72. Experiments with horns. Figs. 137, 138.....	101

##### ELECTRIC EXCITATION OF CAPPED PIPES.

73. Electric-spark excitation of quill tubes. Figs. 139 to 143.....	104
74. Effect of spark-length, etc. Figs. 144 to 146.....	106
75. Electric oscillation recognized. Inductance. Figs. 147 to 150.....	108
76. The same. Further experiments. Figs. 151 to 153.....	110
77. Computation .....	111

#### CHAPTER V.—*Miscellaneous Experiments.*

##### EXHIBIT OF TELEPHONIC EXCITATION OF ACOUSTIC PRESSURE.

78. Apparatus. Fig. 154 .....	113
79. Observations. Figs. 155 to 158.....	113
80. Estimates .....	114
81. Equation .....	114
82. Further experiments. Figs. 159 to 166.....	115
83. Disk explorer. Figs. 167 to 170.....	117

##### PNEUMATIC GAGE FOR THE PIN-HOLE RESONATOR.

84. Apparatus. Observations. Fig. 171 .....	118
---	-----

## EXPERIMENTS WITH INTERFEROMETERS.

PAGE

85. Modification of the Michelson interferometer. Fig. 172.....	119
86. Achromatic fringes. Figs. 173 to 175, 177, 178, 187.....	120
87. Iceland-spar compensator. Extraordinary ray. Figs. 179 to 181.....	122
88. Theoretical remarks .....	124

## INTERFEROMETER AT LONG DISTANCES.

89. Purpose. Figs. 182, 183.....	125
90. Interferences resembling Michelson's diffractions for small angles. Fig. 184..	126
91. Same. Outer plate for angular measurement.....	127
92. Same. Data .....	127
93. Same. Diffraction substituted for interferences.....	127

## THE CAPILLARY ELECTROMETER.

94. Electrolysis. Figs. 185 to 187.....	128
95. Capillary electrometer .....	130
96. Dilution of electrolyte. Figs. 188, 189.....	131

CHAPTER VI.—*Gravitational Experiments.*

## THE CONSTANT OF GRAVITATION IN TERMS OF THE VISCOSITY OF AIR.

97. Introductory .....	134
98. Apparatus and method. Fig. 190. Table 19.....	135
99. Excessive arcs .....	137
100. Recent summer tests.....	137

## PERIODS, LOGARITHMIC DECREMENT, AND STATIC DISPLACEMENT.

101. Apparatus newly installed. Fig. 191.....	138
102. Data. Logarithmic decrement. Figs. 192, 193.....	138
103. Periods. Fig. 193 .....	140
104. Static displacements. Table 20.....	141
105. Comparison of $\lambda$ , $T$ , $\Delta y$ . Fig. 194.....	142
106. Observations in plenum. Table 21.....	142
107. Comparison with computed values of frictional resistance.....	143

## FURTHER INVESTIGATIONS.

108. Change of apparatus. Figs. 195, 196 (197 below).....	144
109. Remarks on the graphs. Figs. 198, 199.....	146
110. New observations. Figs. 197, 200, 201.....	148
111. Values of $\lambda$ , $T$ , $\Delta y$ . Figs. 202 to 210. Table 22.....	149

## INFERENCES.

112. Summary. Figs. 211, 212.....	153
113. Comparison of the equilibrium curves $F$ , $R$ , of 1921, 1922. Figs. 213 to 216....	154
114. Static deflections ( $\Delta y$ ) a year apart. Fig. 217. Table 23.....	157

## CONCLUDING OBSERVATIONS AND COMPARISONS.

115. Further observations. Figs. 218 to 220.....	159
116. Same. Higher exhaustions repeated. Fig. 221.....	161
117. Conclusion. Observations of 1921.....	163
118. Same. Observations of 1921.....	165





## CHAPTER I.

### MODIFIED INTERFEROMETER U-TUBE WITH APPLICATIONS.

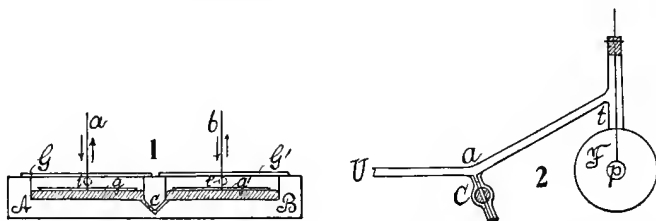
1. **Apparatus.**—The mercury U-tube heretofore used, at the end of a long interval of time, developed increasingly annoying viscous discrepancies, probably due to the aging of the mercury; at least, on cleaning and refilling the apparatus with fresh mercury they vanished. The other difficulty, however, was not so overcome; *i. e.*, the two free surfaces of mercury do not rise and fall rigorously in parallel. They remain practically so only within a small displacement ( $dh$ ), usually not exceeding 50 fringes. This not only reduces the limits within which the gage may be used, but introduces an error of obliquity. All methods used hitherto to overcome this failed, and even the practically unavailable naked mercury surface is not free from the discrepancy.

A method of at least improving the gage by enlarging the area of the free surfaces suggests itself as promising. This is done in the apparatus shown in figure 1, where  $AB$  is an iron block containing two shallow cisterns about 9.5 cm. in diameter and 2 cm. deep. They are joined by the canal  $C$  made by the junction of two oblique  $\frac{1}{8}$ -inch drill-holes. This is narrow enough to guarantee nearly aperiodic and sufficiently rapid deflections at the interferometer, so that a vertical screw to choke off  $C$ , partially, is needless. Mercury is poured into the cistern to a depth of less than a centimeter and covered by the two equally thin glass plates,  $g, g'$ , beveled at the edges. These not only make admirable mirrors, but they almost completely dampen the natural quiver of the mercury surface in an agitated environment. The cisterns are closed by the equally thick glass plates ( $G, G'$ ), laid upon the flat surface of iron and sealed with molten soft sealing-wax at their edges when the block is warm. A linear gas-flame from a pin-hole is very serviceable for the purpose. This simple method of closing the shanks of the U-tube is preferable to the use of reëntrant receptacles in the iron, because the plates  $GG'$  may be so easily removed and very low pressures or partial vacua alone come in question. Access for pressure measurements to either cistern is obtained through the two tubulures ( $t, t'$ ) in front. The two beams of the quadratic interferometer  $a, b$ , about 10 cm. apart, are reflected from the mercury mirror, so that glass thicknesses must be nearly equal.

The gage constructed in this way, and used in connection with the fringes of white light, behaved admirably within the field of the ocular micrometer, *i. e.*, within about 200 or 300 fringes. Beyond this, however, the growing obliquity of surfaces gradually puts a stop to further measurement. Possibly anchoring small plates ( $g, g'$ ) with fibers of silk in the middle of the pools of mercury would be a further remedy; but the exposed surfaces of mercury

would then be free to quiver annoyingly. With the further aid of the slide micrometer on the interferometer, supplementing the ocular plate micrometer, I was able to carry the pressure measurements as far as 0.2 mm. of mercury before the fringes became too vague to be easily recognized. The useful interval lies between  $10^{-4}$  mm. and 0.1 mm., the size of fringes (usually within 0.1 mm. in the ocular) being modified to suit the experiment. The ocular micrometer should be placed in the wide slit-image of the *collimator*, in which case the telescope is free to move to and fro. If one of the shanks of the U-tube is closed or communicates with a closed region, the U-gage becomes a very sensitive air thermometer. Hence, if pressure measurements are in question, it is necessary to work in an environment of practically constant temperature; for spurious pressure increments in millimeters would be interpreted numerically over twice the actual temperature increments.

2. **Mercury charged in vacuo.**—Some time after this, in endeavoring to use the U-tube as a vacuum gage, I noticed that the tendency of the plates



to lose accurate parallelism on measuring relatively high pressure differences (0.02 mm. to 0.1 mm.) had disappeared. The inference is that in order to give the gage the largest possible range, the mercury charge must be added in vacuo. When the gage which has been filled in a plenum is exhausted, air-bubbles are apt to rise and cling to the lower face of the glass plate, from which they are difficult to remove, particularly if the mercury is no longer quite clean. This succeeds, however, with a trigger arrangement by which the plates may be tilted and manipulated, through the rubber-tube connections, in vacuo. It is not uncommon to find the cast-iron cistern (*AB*, fig. 1), though perfect as a mercury container, apparently leaky under exhaustion, so that large bubbles appear under the glass plate when the internal pressure falls to a few millimeters. It is even probable that films of air between glass or iron and the mercury may on exhaustion be thrown into a bubble-shape and become appreciable. The experiments which show this are convincing. Thus, if the gage is kept exhausted for 1 or 2 hours, no bubbles appear under the plate *g*, the mirror remaining smooth. If, now, air is allowed to enter and plenum is retained for a few hours, large bubbles half an inch in diameter will separate out as soon as the gage is again exhausted. After the lapse of a day (the gage being open to the air), the air-bubbles formed on exhaustion will cover the lower face of the plate. Thus, the bubbles date back to the plenum, and they arise from the infiltration of air between mercury and the

glass or iron surfaces, previously exhausted. The next exhaustion merely exhibits the result by expanding the air.

The largest crop of such bubbles was obtained on exhausting the gage in the presence of saturated water-vapor within. Removing the water-tube and exhausting again, the plate was fairly deluged with bubbles, and the effect only ceased after the complete removal of water-vapor by successive exhaustion.

The vacuum-filled gage will be used for a variety of experiments below, where relatively long-range pressure increments are demanded. With very pure mercury charged in the way stated, the annoyances of separating slit-images were found to be absent. Nevertheless, in the lapse of time they reappeared and the range was correspondingly shortened. This aging seems to introduce a peculiar error to be discussed in §§ 37, *et seq.*, below, under the name of capillary error; for it appears that the whole pressure is not expressed in the displacement of the mercury surfaces  $g, g'$ , but that a correction term, nearly constant in a given series of measurements, must be added, even when the zero of the gage (*i. e.*, the fringe position for no pressure) is quite fixed.

#### APPLICATION.

**3. Gas evolution and absorption.**—It was hoped that the interferometer U-gage might here be of some interest, particularly in chemical and bacteriological researches; but the work is delicate, inasmuch as it calls for rigorous constancy of temperature. Specific pressure production within rigid walls is probably not measurable. For not only is the closed U-region with appurtenances an air thermometer, but the vapor-pressure of a solution, if present, also changes. If we write  $dp/p = d\tau/\tau$ , the spurious pressure increment is more than double the discrepant temperature increment. Moreover, for an aqueous solution at  $25^\circ \text{C.}$ ,  $dp = 1.5d\tau$  millimeters of mercury. Thus together,  $dp = \left(\frac{760}{300} + 1.5\right) d\tau = 4d\tau$ , nearly. Hence  $d\tau = \frac{\lambda/2}{4} < 10^{-4}^\circ \text{C.}$  is a sufficient temperature discrepancy to produce a spurious pressure discrepancy (0.0003 mm. of mercury) equivalent to one fringe. Such experiments are, therefore, essentially summer basement work. Nevertheless, it seemed to me desirable to give the apparatus a preliminary trial under winter conditions.

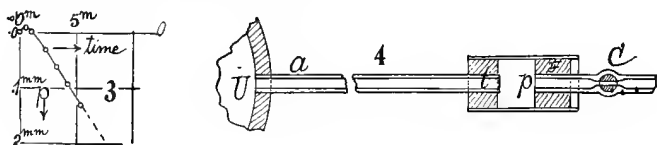
The experiment first performed was very simple and consisted in mounting a small boiling-flask 3 cm. diameter ( $F$ , fig. 2) connected with the U-gage at  $U$ , and the stopcock  $C$  by a branch tube. The absorption agency  $p$  was placed in the tube with  $C$  open and the fringes at zero, by aid of a rubber stopper. Thereafter  $C$  was quickly closed and the march of fringes observed with a stop-watch.

The test was made with phosphorus, pressed between bits of wire gauze about 1 cm. square. A variety of these experiments was tried, the typical example given in figure 3 corresponding to the following results:

Time = 0	.5	1	2.25	3.25	4.25	5.42	minutes.
Deflection = 0	.11	0	—50	—100	—150	—210	Scale parts, s.
$\Delta p \times 10^2 = 0$	+7	$\pm 0$	—3.1	—6.3	—9.4	—13.2	mm. Hg.

Within the first minute pressure rises to a maximum (sometimes  $2 \times 10^{-2}$  mm.) after which it falls regularly at a rate of about 0.03 mm./minute, within the available interval of observation almost linearly. The rise is the excess of the air-thermometer action of the flask  $F$ , registering the heat of the phosphorus oxidation or the desiccating effect of the  $P_2O_5$  produced, over the cotemporaneous absorption. Since the air is initially moist, the latter may be the greater heat contribution. After 1 minute the pressure reduction resulting from oxygen absorption supervenes.

As the reduction in pressure after 5 minutes is but 0.13 mm., out of the many centimeters of mercury available, it might seem as if the motion of oxygen through the quill tube  $Uat$ , figure 2, had hardly begun, the oxygen in  $F$  sufficing. For this quill tube was only about 0.3 cm. in diameter and 10 cm. long, apart from the elbow and rubber joints, which contributed an additional 5 cm. of length and 0.5 cm. in diameter. To obtain results more definitely bearing on such a diffusion-like contribution, the volume of  $F$  should be as nearly as possible deleted. This device is shown in figure 4, where the stopper  $F$  has a phosphorus grid or the like on its front face and



may be moved quite up to the quill tube  $Uat$ . The air within the  $U$ -gage at the other end thus becomes practically the sole oxygen reservoir. The cock  $C$  is open on adjusting the tube in place (to avoid turbulence on compression) and closed immediately thereafter.

In the following examples a rough disk of phosphorus had previously been placed between  $t$  and  $p$  of figure 4 and the grid dispensed with. The oxygen consumption was now apparently slower than before, the diffusion-tube being 17 cm. long and 0.5 cm. in diameter. Nevertheless, because of the limits of the  $U$ -gage, the experiment had to be made in successive sections and the slide micrometer ( $\Delta x \cos i = \Delta h$ ) used. The range of the ocular micrometer was too small, and its middle 50 merely served as a fiducial point to bring the fringes back to their starting-point. The cock  $C$  was opened after about 10 or 12 minutes for about 6 or 7 minutes and the new stage of the experiment begun afresh. This is of course an interruption of the experiment, as fresh air enters at  $C$ . As it does not penetrate beyond the large charge of phosphorus, its effect on the oxygen contribution from  $U$  should be secondary, but for the fact that it seems to wear out the efficiency of the phosphorus surface. At all events the graphs given in figure 5 are distinctly curved from the beginning and the rates of diffusion persistently diminish, viz :

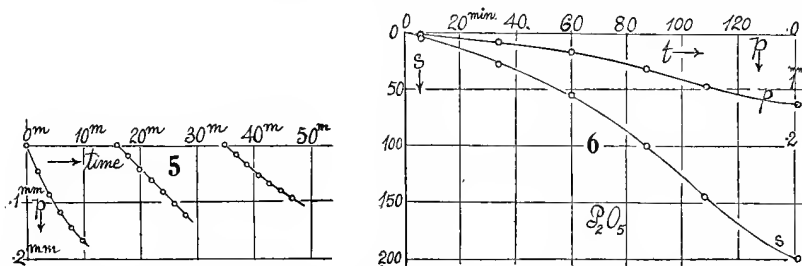
First stage, 0-10<sup>m</sup>  
Initial  $dp/dt = -0.023$   
Final  $dp/dt = -0.012$

Second stage, 16-28<sup>m</sup>  
—0.011  
—0.010

Third stage, 35-47<sup>m</sup>  
—0.009 mm./min.  
—0.006 mm./min.

Much of this distortion, since thermal and absorption effects act differentially, is no doubt due to temperature irregularities. The total pressure reduction may be estimated as not much above 0.5 mm. of mercury, so that the oxygen exhaustion in  $U$  is insignificant. The retardation in rates is thus to be ascribed to the diminished effectiveness of the phosphorus surface just referred to, which was no doubt already too much tarnished in the beginning.

**4. Water absorption.**—In this case a tube similar to figure 4 was used, without phosphorus, the cork  $F$  being withdrawn towards the rear and the space filled with dry  $P_2O_5$  behind a loose cotton plug as a partition. After  $at$  was attached to  $U$ , the cock  $C$  was closed again. The diffusion of the residual water-vapor in  $U$  through the quill tube  $at$  (15 cm. long, 0.5 cm. in diam.), into the desiccator  $F$ , is here an apparently very slow process, as shown in figure 6. The absorption proceeds at a gradually accelerated rate within the first 100 minutes; but thereafter it is again retarded. The latter must occur



eventually from deficiency of moisture in  $U$ ; yet it is rather difficult to account for earlier acceleration. The mean results are:

Time = 0	6	34	60	87	109	141	minutes.
$\Delta s = 0$	6	26	52	100	148	200	s. p.
$\Delta p \times 10^{12} = 0$	.4	1.6	3.3	6.3	9.3	12.6	mm. Hg.

Though there was not much moisture in  $U$ , the slow drain is rather unexpected, the rates during successive half-hour sections being about

$$10^5 \times dp/dt = 47 \quad 65 \quad 115 \quad 136 \quad 103 \quad \text{mm./min.}$$

The complications here are much like those discussed in the case of phosphorus, with the addition of the variable humidity of  $U$ . There must also be a large counteracting thermal effect.

**5. Water evaporation.**—On replacing the phosphorus in  $F$ , figure 2, by a wad of wet filter-paper at  $p$  and then closing  $C$ , data were obtained in which the first trial showed larger evaporation pressures than the second, taken an hour or more later. It was thought that the flask, after the phosphorus experiment, was initially drier. The maximum pressures appeared about 5 minutes after closing  $C$ , and they were but 0.044 and 0.026 mm. of mercury respectively. Thus it seemed as if the increase of pressure were confined to the inside of the flask  $F$ , the diffusion of water-vapor through  $Uat$  having

scarcely begun. After the occurrence of the maxima, the pressures in both cases dropped off.

Using an apparatus of the form of figure 4, in which the stopper  $F$  (phosphorus removed) was pushed toward the rear and a wad of wet filter-paper placed between  $F$  and the end of the tube  $at$ , much more definite results were obtained, as shown in figure 7, curve  $a$ . The tube was here 16 cm. long and 0.5 cm. in diameter and the cock  $C$  closed immediately after the adjustment had been made; nevertheless there are complications in the pressure increments ( $h$  mm. of Hg) within the first 10 minutes. Recovering thereafter, they show an almost linear progress at the rate of 0.0016 mm. per minute within the ensuing 90 minutes, as follows:

Time = 0	15	39	63	87	minutes.
$\Delta p \times 10^2 = 0$	2.1	6.7	10.4	14.4	mm. Hg.

Unlike the complicated case of phosphorus, the present experiment may possibly be modified into a real exhibit of diffusion, and therefore seemed deserving of further trial. Nevertheless, it is essential to bear in mind that slow, uncontrollable elevation of room temperature, increasing both the air-pressure and vapor-pressure in the closed region, would give rise to a march of pressure indistinguishable from those obtained. Furthermore, since the saturated vapor-pressure is independent of volume, it is a question whether the occurrence of diffusion would leave any pressure record in  $U$ , at all; for the whole region  $Uatp$ , figure 4, is from the outset under pressure  $p_{air} + p_{vapor}$ , the latter certainly being saturated at  $tp$ . If the vapor advances at all it can do so only by depressing the mercury in  $U$ , which would thus become interpretable evidence for diffusion, provided discrepancies of the kind enumerated above can be eliminated.

The repetition of the experiment with a shorter diffusion-tube of the same diameter ( $l=7$  cm.,  $a=0.2$  cm.<sup>2</sup>) gave the results (fig. 7, curve  $b$ ):

Time = 0	23	26	56	minutes.
$\Delta p \times 10^2 = 0$	2.6	3.1	7.2	mm. Hg.

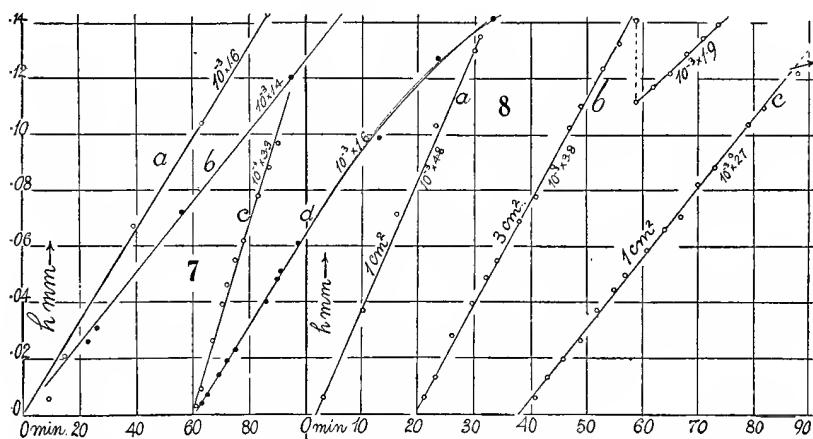
and a rate of but 0.0014 \* mm. per minute. In other words, for a tube less than half as large as the preceding, the coefficient  $dp/dt$  is smaller. Thus, unless the air in  $U$  was less dry in the present case as compared with the preceding, for which there was no evidence, the experiments being made some time apart, the interpretation of these experiments in terms of diffusion only is out of the question. Moreover, the extreme smallness of the coefficients  $dp/dt$  falling within 0.08 mm. per hour, when the saturated pressure is over 15 mm., points in the same direction. What was observed could at best be a residual diffusion, after the pressure gradient had all but vanished. Similarly, adverse results are given in figure 7, curves  $c$  and  $d$ , obtained from tubes 9 cm. long and respectively 0.5 cm. and 0.17 cm. in diameter. The former shows a high coefficient  $10^{-3} \times 3.3$  mm. per minute, while the latter, in spite of its small bore and length, is not inferior in its coefficient ( $10^{-3} \times 1.6$ ) to the case  $a$ .

---

\* Corrected for change of size of fringes.

There is a further consideration: Like the case of phosphorus above, it is possible that what is at present being measured is the rate of evaporation from a surface. Pieces of thick, wet blotting-paper,  $1 \text{ cm.}^2$  and  $3 \text{ cm.}^2$  in area, were therefore selected as sources of moisture and inclosed between the end of the tube  $t$  and the stopper  $F$  of figure 4.

The results of figure 8 were obtained in this way, at intervals of about 1 hour apart in a warm, dry room. The attempt to desiccate the volume  $v$  of  $U$  showed no advantages. As to the observations (both fringe displacement  $\Delta s$  and the slide micrometer  $\Delta x$  being employed), they are remarkably good, with only an occasional lag in the U-tube, which later soon recovers itself. The zero-point was always nicely regained at the end of each experiment, and accidental changes of fringe-breadth were allowed for. The same tube,



8 cm. long and about 0.4 cm. in diameter ( $a=0.13 \text{ cm.}^2$ ), was used in all cases. The successive rates obtained are thus

Experiment .....	(a)	(b)	(c)
Area evaporating .....	2	6	2
$10^3 \times dp/dt$ .....	4.8	3.8	2.7
			mm. Hg/min.

From the first and second experiments, it is seen that the area evaporating is of no consequence, for the area 3 times the larger has the smaller coefficient.

In the second and third curves of figure 8, a peculiar feature presents itself. In the former, after 40 minutes, the rate suddenly breaks down to  $19 \times 10^{-4}$ ; in the latter after 50 minutes the break is even more pronounced, falling to  $6 \times 10^{-4}$  (data not given). This looks as if the pieces of blotting-paper had become dry; but from the small amount of water evaporated such a result is impossible. Again, if it were a question of vanishing gradient, the evanescence would not occur abruptly, as the observations imply.

One is thus eventually driven to the conclusion that what is being observed is in large measure the result of thermal expansion, inasmuch as the closed region is necessarily an air thermometer, exposed in a room of not rigorously

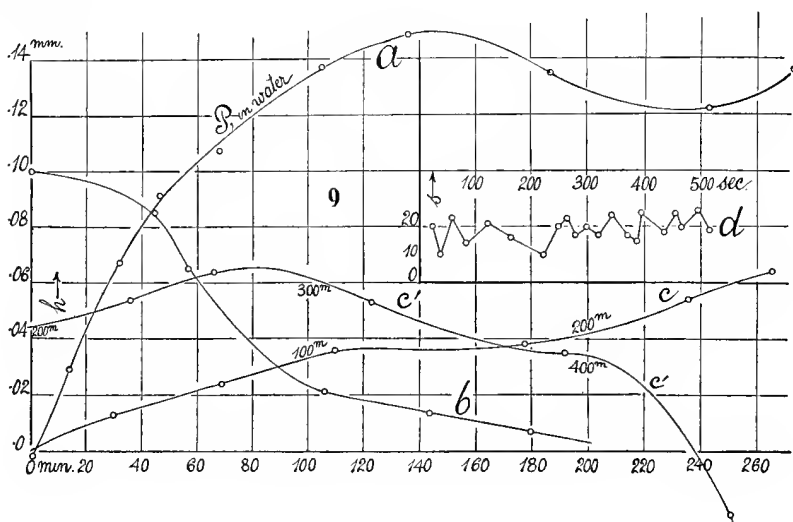
constant temperature. For if we take the largest of the coefficients just obtained,  $dp/dt = 5 \times 10^{-8}$  mm./min., and if the **U**-region is the bulb of an air thermometer of constant volume at about  $27^\circ \text{C}$ .,

$$(dp/dt)/p = (d\tau/dt)/\tau$$

or,

$$d\tau/dt = \frac{5 \times 10^{-8}}{760} 300 = 2 \times 10^{-8} \text{ C./min.}$$

Thus an increase of the mean temperature of the massive apparatus of only about  $0.1^\circ \text{C}$ . per hour would suffice to account for the higher results obtained. To this the vapor-pressure increment of the evaporating water further contributes.



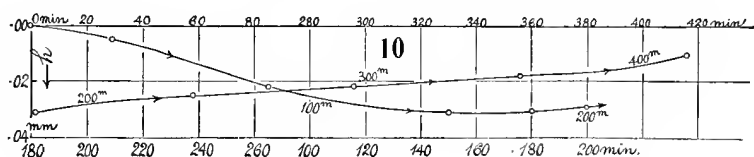
In spite of these discouragements, I made a number of further experiments with the object of capturing a coefficient, actually negative. Small coefficients were rather frequent; but the only negative value obtained is given in figure 9, curve *b*, for the case of a tube 9 cm. long and 0.17 cm. in diameter. The curve is not straight (the usual result), but is such as would be expected in a room slowly cooling, eventually at a decreasing rate. Again, figure 10, the two shanks of the **U**-tube were joined by a short piece of rubber hose which was then closed in the middle with a pinch-cock. But for the almost complete recovery after 420 minutes, the results (fig. 10) would suggest a slight leak in one shank, which was thus not present. On opening the pinch-cock, the zero at once reappeared. Thus the **U**-tube alone makes some contribution to the pressure variations for reasons rather difficult to understand, seeing that the mercury wells are close together in a block of iron.

The pressure decrement in figure 10, where both shanks of the **U**-tube are closed, scarcely exceeds 0.03 mm. The test will be much severer if but



one shank of the tube is closed, the other freely communicating with the atmosphere. Results of this kind, recorded through 450 minutes, are given in figure 9, curves  $c$  and  $c'$ . These would be in conformity with slowly increasing room temperatures to a maximum at about 300 minutes and a fall thereafter, eventually relatively rapid. In the main, pressure increments exceeding a total of 0.06 mm. of Hg are present. In the same figure (curve  $a$ ), I have given (by way of contrast) the results observed on joining the same shank to a tube containing phosphorus *submerged* in water. The phosphorus tube must be kept in a water-bath. From this arrangement I anticipated pressure decrements resulting from slow phosphorus oxidation under water. The results (maximum, 0.15 mm. of Hg) reproduced in curve  $a$ , however, compare with the largest pressure increments recorded, and the high values, though fluctuating, are sustained for over 270 minutes. The rise is less abrupt than in figures 7 and 8.

When one shank of the U-tube is closed, the other being open, atmospheric-pressure variations on a micrometric scale are very well indicated. I have



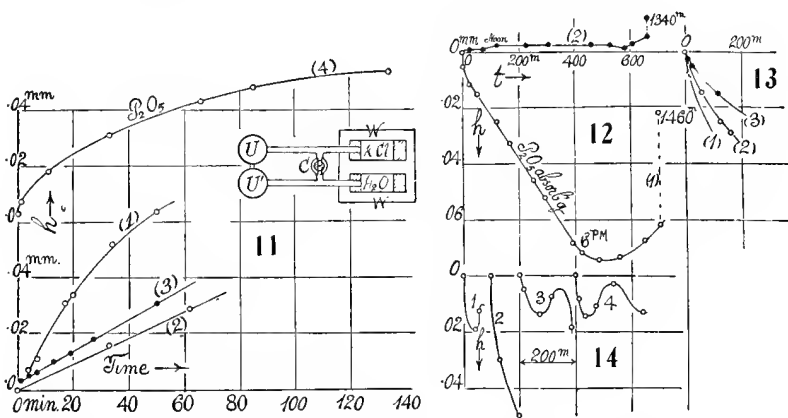
given an example of such cases in the jagged curve  $d$  of figure 9, the behavior being followed within 500 seconds. On a windy day these rapid fluctuations of the mercury surface are very marked. In the figure the mean displacement may be taken as within  $\Delta s = 10$  scale-parts, or  $\Delta p = 0.006$  mm. of mercury. It is not impossible that a micrometric registry of this kind may be of meteorological value.

**6. Differential experiments.**—In addition to the above work, a number of experiments were made by using the U-tube differentially. Thus, figure 11 (inset), a dilute solution of KCl ( $\rho = 1.1184$  at  $20^\circ$ ) and pure water, were joined respectively to the two shanks of the U-tube, the liquids being kept in a water-bath,  $W$ . A glass three-way cock, to shut off atmospheric connection, and to separate the KCl chamber from the water chamber, is necessary. I shall give but one example, figure 11, summarizing four successive experiments. It is seen (1) that pressures in the right shank, which happens to be the KCl solution, increase faster; but the rate soon falls off. On exchanging the liquids, (2) pressure still increases faster in the right shank, about at the final rate of the case (1). On again exchanging the tubes (curve 3), the final increase on the right is maintained. The left side was now placed in contact (4) with a small closed  $P_2O_5$  drying-tube in the place of the water (removed). The curve, however, except at the beginning, shows no striking rates, which are throughout inferior to curve (1).

Thus it seems that secondary occurrences, to be associated with temperatures, completely obscure the results looked for, whether of diffusion or vapor-pressure, and that it is only in the summer time, in a non-heated room, that interpretable data can be expected. Meanwhile, the graphs show the extent of annoyances to be guarded against.

**7. Summer experiments.**—During an interval of steady summer temperature I gave these experiments with pressure increments another trial, using the method indicated in the inset of figure 11. The first test was made with a solution of KCl ( $\rho = 1.1184$  at  $20^\circ$ ) compared with water. The results (time  $t$ , pressure increment  $h$  mm. of mercury),

$t = 0$	17	37	82	117	400 minutes.
$10^4 h = 0$	15	20	15	15	—25 mm.



are merely incidental errors. Similarly with a solution of  $\text{CaCl}_2$  ( $\rho = 1.19650$  at  $20^\circ$ ),

$t = 0$	30	63	228 minutes.
$10^4 h = 0$	10	0	—220 mm.

actually show an apparent excess of pressure over the solution. This can only indicate a temperature difference at the two shanks of the U-gage. It seems to me probable that the walls of the gage in such experiments are soon covered with a film of distilled water and that this contributes the effective equality of vapor-pressure, the surface of solution in the tube being relatively inactive.

These experiments are thus inconclusive. I therefore made a further trial of the water-vapor absorption of  $\text{P}_2\text{O}_5$ , the two tubes containing water and  $\text{P}_2\text{O}_5$ , respectively, being placed as in figure 11. The initial test (graph 1, fig. 12) at first proceeded with vigor; but after 400 minutes' absorption ceased and the reaction is apparently reversed. The tubes were then exchanged. The resulting graph 2 merely shows that water absorption is practically absent. The same was true when the tubes were again exchanged.

The  $P_2O_5$  was therefore replaced by a fresh sample. The graphs 1, 2, 3, figure 13, were now obtained on successive exchanges of the water and  $P_2O_5$  tubes. These graphs are consistent as to absorption, but the reactions are nevertheless so slow and the general run of the curves so complicated with secondary issues and so difficult to interpret, that I abandoned the work as unpromising. In figure 14 a few supplementary results are given with the tubes separated, the water tube being open to the atmosphere. The sinuous curves obtained in the successive changes of tubes show that the temperature discrepancy is prohibitive, even in summer.

Finally I tested the same method (inset, fig. 11) with the U-gage exhausted, comparing  $H_2O$  and the  $CaCl_2$  solution specified in a vacuum of the vapor-pressure of water. With the cock between the  $H_2O$  and  $CaCl_2$  tubes open, the fringes were easily found and steady. With influx of air they remained nearly fixed and could be recognized, even through a fog which often formed. On closing the cock between the tubes, however, so that each liquid operated alone, the fringes speedily vanished, too rapidly for control. The method is further objectionable, inasmuch as any slight leak through the glass exhaustion-cocks, etc., would have the same effect. It was therefore not pursued further because of its difficulty. It required four successive exhaustions subsequently to free the gage of the water-vapor which had filtered in between the mercury and the solid parts of the gage, large bubbles forming under the glass plate.

## CHAPTER II.

### PRESSURES IN CONNECTION WITH SURFACE TENSION.

#### SOAP, GLUE, AND SUGAR BUBBLES.

8. The pressure within a soap-bubble.—If both surfaces of the bubble cooperate, this pressure ( $p$ ) is written  $p=4T/r$ , where  $T$  is the surface tension and  $r$  the radius of the bubble. The ease with which  $p$  may now be measured by the interferometer **U**-gauge suggests a number of observations. One may ask, for instance, whether both surfaces cooperate with unimpaired strength until the bubble bursts from excessive thinness; whether  $T$  increases or decreases as the result of concentration of the film during evaporation; or the value of  $T$  in modified soap solutions may be read off, etc. If the quadratic interferometer is used with plates at an angle  $i=45^\circ$ , for reading the displacement  $\Delta h$  of the free surface of the mercury in the **U**-gauge, we may write as above

$$T = (\rho g r \cos i/4) c \Delta s$$

where  $\Delta n$  is the number of fringes of wave-length  $\lambda$  passing, and  $\Delta x$  the displacement of the slide micrometer, at an angle equivalent to  $i$ , the screw being normal to the displaced mirror. Hence

$$4T/r = \rho g \cos i \cdot \Delta x = (\rho g \lambda / 2) \Delta n$$

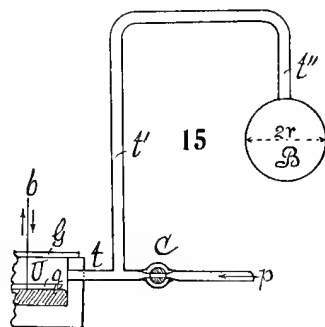
or

$$T = (\rho g r \cos i/4) \Delta x = (\rho g \lambda / 8) \Delta n$$

If the ocular micrometer is used, a trial measurement would give  $\Delta x = c \Delta s$  cm., where  $c$  is the value of  $\Delta x$  corresponding to one ocular scale-part (0.01 cm.), so that finally

$$T = (\rho g r \cos i/4) c \Delta s$$

The apparatus used is simple, consisting of a bent glass tube  $tt''$ , figure 15, about 5 or 7 mm. in diameter, from one end  $t''$  of which, the soap-bubble  $B$  is blown. The other end  $t$  communicates with one shank of the **U**-gauge  $U$ , closed by glass plates  $G, g$  being the floating plate. The other shank of the gage is in free communication with the air. One of the interferometer beams is shown at  $b$ . Pressure is applied at  $p$ , the air being blown in through a cotton wad or a capillary tube to avoid excessive vibration (relatively speaking) of the mercury. When



the requisite size of bubble is obtained, the cock  $C$  is closed and the displacement of fringes read off. The difficult measurement in relation to the equation

is the diameter ( $2r$ ) of the bubble. In the present experiments I contented myself with a projection against a white centimeter scale closely behind the bubble. This is a rough method, but it suffices for the present tentative purposes.

9. **Observations.**—The micrometer test showed  $\Delta x = 1.07 \times 10^{-4} \Delta s$  cm. (in later work  $1.03 \times 10^{-4}$ , or  $\Delta h = 7.3 \times 10^{-5} \Delta s$  cm.), so that  $\Delta h = 7.6 \times 10^{-5} \Delta s$  cm.,  $\theta$  being  $45^\circ$ . The results taken in succession were ( $T = 0.24r\Delta s$ , etc.)

$2r = 9$	7	9	6.5	4.5	3.0	4.2	2.5	3.0	6.0	cm.
$\Delta s = 25$	30	25	33	50	70	50	85	74	37	s. p.
$10^3 \Delta p = 19$	23	19	25	36	51	36	62	54	27	mm. Hg.
$T = 28$	27	28	27	27	25	26	26	27	27	dyne/cm.

The irregularity here may be due to the  $r$  measurement, which is necessarily inadequate and too large; but the different samples need not be identical. The soap mixture was a commercial solution adapted for blowing persistent bubbles; nevertheless the order of value found for  $T$  is surprisingly small. Data of the same value were also obtained from fringes only. The pressure seemed to be sustained until the bubble burst, when the fringes fell back to zero. Changes of pressure resulting from deformations of the bubble were easily shown.

In later experiments better results for  $r$  were obtained by the shadow of the soap-bubble as cast by a distant electric lamp, on a white centimeter scale. The fringes were somewhat large,  $\Delta h = 8.9 \times 10^{-5} \Delta s$  mm.,  $T = 0.21r\Delta s$ . I found—

$2r = 3.0$	3.0	5.0	5.0	cm.
$\Delta s = 80$	80	50	50	s. p.
$10^3 \Delta p = 71$	71	44	44	mm. Hg.
$T = 25$	25	26	26	dynes/cm.

Here a definite increase of  $\Delta x$  was registered while the bubble slowly dried out to the bursting-point, the increase of  $T$  being 6 to 10 per cent. Though the soap-bubble is the bulb of an air thermometer, and slight changes of temperature produce passing fluctuations of fringe positions, on the whole the registry is good, as  $r$  accommodates itself to the pressures.

Common commercial soap solution, not intended for soap-bubble experiments, was also tried. The bubbles here burst much more rapidly and bubbles larger than about 4 cm. could not be obtained comfortably with quiet fringes. The results were (the preceding fringes being used,  $T = 0.210r\Delta s$ ):

$2r = 4.5$	3.0	4.0	4.0	3.0	cm.
$\Delta s = 67$	100	75	73	100	s. p.
$10^3 \Delta p = 60$	89	67	65	89	mm. Hg.
$T = 31.7$	31.5	31.5	30.7	31.5	dynes/cm.

Thus the tension is definitely larger here, there being no extra ingredients.

A small quantity of liquid glue was added to this soap solution, the mixture thoroughly shaken up, and tested the next day. Bubbles were now much more persistent, and they shrank to an iridescent viscid soap-glue film (with evaporation of water), which gradually crumpled up. The mean surface tension

found was  $T=25$  dynes/cm., so that the  $T$  had decreased by the admixture of the glue. It also slightly increased at first on evaporation to about 6 per cent, after which, with the crumpling of the film,  $T$  decreased relatively fast but regularly (while the bubble shrank) to about one-third of its original value (not allowing for the  $r$ ). Here the viscid bubble usually broke and the fringes fell back to zero. The occurrence of a much reduced size of viscid bubble with temporarily stationary but relatively small surface tension may be regarded as evidence in favor of Kelvin's suggestion, viz, that the film puckers to accommodate the energy-content in view of diminished surface tension. Probably in shrinking with deformation, the bubble becomes fissured and springs little leaks, but in such a way that pressure diminishes gradually and regularly. Diffusion would be a slower occurrence. With a broken bubble the fringes instantly fall to zero.

Diluting the glue-soap solution to one-half, the bubbles usually burst; but occasionally one would be captured which shrank, being pervious, in the manner just described.

A variety of further experiments were made with the glycerine-soap solution, using greater care in the measurement of  $2r$  (shadow); but not much improvement was observed in the data, probably, I think, because the colloidal structure or phase mixture of successive bubbles is not exactly the same. Taking the means of about 5 observations for each diameter  $2r$ , the results were (internal pressures decreasing from about 0.015 to 0.0016 mm. of Hg):

$2r =$	1.16	2.0	4.9	7.0	8.8	10.4	cm.
$10^3 \Delta h =$	15	...	...	...	...	1.6	mm. Hg.
$T =$	28.7	29.6	29.3	29.8	32.7	31.8	dynes/cm.

so that  $T$  (fig. 16) seems to increase about  $\Delta T=0.4$  per centimeter of increase of the diameter of the bubble. In the same way,  $T$  here increased slightly at all diameters, just before the bubbles burst. This would be in keeping with the enormously greater effect observed with glue-bubbles in the next paragraph.

Some time after, the contrasting behavior of common liquid soap and the soap mixture prepared for bubbles was taken up again. The common soap in its  $T$  values, for example,

$$T = 32.7 \quad 31.7 \quad 32.7 \quad 32.7 \quad 32.4 \quad \text{mean } 32.4,$$

was usually very constant; but the bubbles lasted only 10 or 20 seconds, not long enough to detect variations. With the prepared mixture, however, the life of 2-cm. bubbles was at times nearly 10 minutes. During this time the drop at the bottom was gradually absorbed, the film showing continual agitation in these parts, while  $T$  regularly increased. The following is a good example observed up to the bursting-point.

$$\begin{array}{ll} \text{Time} = & 0^m \\ & T = 27.7 \end{array} \quad \begin{array}{l} 8^m \\ 31.7 \end{array}$$

When the bubble burst, therefore, its  $T$  was nearly that of the common soap solution. The lowest value obtained in a number of experiments was 27, the rate of increase  $dT/dt$  being 0.5 per minute. Thus, the effect of concen-

tration during evaporation, though not nearly so marked, resembles the behavior of the glue-bubbles below. Other persistent soap mixtures were tried and give about the same rate. For instance, after adding glycerine to the liquid soap above,  $T$  changed from 28.4 to 30.8 in 5 minutes; in another case from 30.3 to 32.4 in 3 minutes, the rates  $dT/dt$  being thus 0.5 to 0.7 per minute. Similarly in a glue soap,  $T$  increased from 27 to 28.4 in 4 minutes; again from 27 to 28.9 in 3 minutes. The rates  $dT/dt$  are thus 0.4 to 0.6 per minute.

The rate is slower if a drop is at the bottom of the bubble, and faster as the drop vanishes. After this the bubble bursts. Thus

0 <sup>m</sup> 29	0 <sup>m</sup> 28	0 <sup>m</sup> 28
3 32	9 31	1.5 29
	12 33	2 30

the second sample holding a large drop, the colors throughout being in agitated motion. With increasing  $T$  operating on a film gradually growing thinner, conditions favorable to bursting increase (*cf.* celluloid bubbles, below).

**10. Glue-bubbles.**—Common liquid glue was dissolved in 5 to 10 parts of distilled water, thoroughly warmed, shaken, and allowed to stand for a day or more. The bubbles obtainable in this way rarely exceed 2 cm. in diameter and most of them break before the measurements of  $2r$  and  $\Delta h$  can be completed. The work, therefore, is an exercise of patience, for only occasionally a result is obtained. Still more rarely (I succeeded only twice in many hundred trials), a bubble is obtained which actually solidifies to a film of gelatine, highly iridescent and lasting indefinitely.

Samples of dilute glue are apt to vary widely in  $T$ . Thus, for instance,  $2r=2$  cm.,  $T=32$ ;  $2r=1.5$  cm.,  $T=43$  were obtained from short-lived bubbles of the same solution. Longer-lived bubbles suggest the reason for this variability. In the case of bubbles bursting after 2 minutes, the data were:

Persistence:	0	1	2 min.	
$T$	28.3	39.7	34.1	First case.
$T$	30.4	36.9	49.9	Second case.

In the first example  $T$  passes through a maximum before the bubble bursts; in the second,  $T$  has enormously increased and is apparently still growing.

But the full exhibition of these phenomena was not reached until one of the bubbles,  $2r=1.7$  cm., actually dried to a solid iridescent spherical film of glue. The drop at the bottom of the bubble, in this case, evaporated very slowly, but without marked distortion of the shape of the bubble. When dry and detached it was quite flexible and robust but sticky, the folds easily cohering.

Table 1 and figure 17 (1), give a full account of the observations made in the lapse of about 4.5 hours, after which the internal pressure excess had nearly vanished. It will be seen that there were successive stages marked  $a$ ,  $b$ ,  $c$ ,  $d$ ,  $e$  in the graph at which the pressure was temporarily stationary. The successive intervals of stability decreased, and the one at  $d$  was very short, prior to the persistent stage  $e$ . One would be inclined to infer that these

stages represent successive phases or types of colloid, each with its appropriate  $T$ . But it is obvious from the mottled color-fields on the bubbles that at each stage a large number of phases must contribute to the temporary equilibrium. At  $f$ , at the limit, the colloid is probably solid. Thereafter the nearly regular decrease of  $T$  between 20 and 265 minutes is merely apparent, and to be ascribed to the continued diffusion of air outward, from within the thin solid sphere at a pressure excess, into the atmosphere. The water has first largely evaporated and the air follows after, probably along the same channels between the colloidal molecules.

In the preceding case the surface tension of the phase conglomerate  $a$  ( $T=30$ ) has nearly doubled ( $T=57$ ) in the phase  $e$ . In the present experiment, figure 17(2), the initial surface tension ( $T=35$ ) is more than doubled

TABLE 1.—*Dilute glue-bubbles evaporating to the solid state.*

Bubble.	Time.	$10^3\Delta h$	$T$	Bubble.	Time.	$10^3\Delta h$	$T$
	<i>min.</i>	<i>cm. Hg</i>			<i>min.</i>	<i>cm. Hg</i>	
Sphere $2r = 1.7$ cm.	0	12.7	29.8	Sphere	0	10.6	35.2
	2	11.2	31.5	$2r = 2.0$ cm	1	11.3	37.4
	4	11.9	33.4	becoming	2	13.3	44.2
	6	12.5	35.3	pear-shaped	5	25.2	83.4
	8	20.4	57.3	$1.7 \times 2.0$ cm.	10	25.2	83.4
	20	20.4	57.3		12	24.5	81.1
	35	17.3	48.7		15	24.1	79.9
	40	16.7	47.0		21	22.6	74.7
	45	16.1	45.4		95	11.7	38.8
	65	13.3	37.4		150	.5	1.7
	75	12.3	34.5				
	80	10.6	29.8				
	110	7.9	22.3				
	140	5.0	14.3				
	165	1.3	3.5				

( $T=83$ ) in the persistent phase. Here, however, the drop at the bottom of the bubble later expanded on its own account, so that the solid bubble was symmetrically pear-shaped, while the top diameter in the final distortion shrank from about  $2r=2$  to  $2r=1.7$ . The data are thus complicated by change of form. Moreover, the phenomenon ran through its cycle from the minimum at  $a'$  to the maximum at  $b'$ , much more rapidly, so that only these two temporary stages could be recognized. Here and in the preceding experiment, however, there may be phase equilibria antedating the first observation; for it takes some time to set the fringes with the slide micrometer and to measure the diameter  $2r$ . Beyond  $c'$  the phenomenon is the same as before, indicating diffusion of air outward through the solidifying film. In the present case the diffusion after everything is dry is apparently accelerated; but this is probably thermal discrepancy.

Between  $e$  and  $f$  or  $b'$  and  $c'$ , the film is still liquid and contractile and the values of  $T$  obtained are probably true surface tensions. Beyond  $f$  or  $c'$  the film is less and less contractile and the values of  $T$  cease to have a meaning.



One can not argue, therefore, that  $T$  has been measured quite into the solid state; but it has been measured as far as a highly viscous, but still liquid, film of glue.\*

Promiscuous work with the glue-bubbles led to no further striking results. I shall therefore give mean values. Four experiments with the original solution, after long standing, showed ( $2r=2.1$  cm.)  $T=25$ ; warming and shaking the solution,  $T=26.8$ . Two drops of soap solution were now added to 10 c. c. of the glue. The mean results with small bubbles ( $2r=2.2$ ) were  $T=27$ ; with four large bubbles ( $2r=4.4$  cm.),  $T=28.7$ . These differences are merely incidental, the glue-soap mixture being perhaps more expansible.

Again, a drop of caustic soda in solution was added to the original gelatine. Three tests gave ( $2r=2.3$  cm.)  $T=26.8$ . The alkaline glue solution was then diluted over one-half, an advantageous procedure, for large persistent bubbles were now very easily obtained. The mean result of six tests ( $2r=4.7$  cm.) was  $T=28.2$ . The latter solution, further diluted to more than one-half, was

TABLE 2.

Successive dilution.	$2r$	$T$	Remarks.
1/8	4.2	29	Colors not striking, just before breaking. Colors absent, nearly.
1/16	4.8	28	
1/32	4.3	30	
1/64	4.1	41	No color.
1/128	4.2	53	Do.
1/256	2.7	55-62	Very variable in $T$ .

found to be equally available, 3 large bubbles ( $2r=4.7$ ) giving  $T=29.1$ . At this stage the usually promiscuous grouping of drifting interference colors began to conform to well-developed broad, horizontal color-bands, still in motion, however. In fact, surging, broad color-patches, which keep moving till the bubble bursts, are the noteworthy feature of these glue-bubbles. It is indicative, of course, of the high degree of heterogeneity, which has not been eliminated even in these excessively thin films. In a further dilution to over one-half, the bubble became more fragile. Incidentally  $T$  had decreased, the mean of four cases being ( $2r=4.6$  cm.)  $T=26.8$ . All this is still far remote from the  $T$  of pure water. After allowing the last solution to stand for some time, the following mean results (4 to 5 tests each) were obtained for successive further dilutions (table 2).

Thus (fig. 18)  $T$  shows no tendency to increase, except in the last three cases. Nevertheless, the bubbles had been continually growing more fragile. Interference colors are quite absent when the marked increase of  $T$  begins, as the relatively thick bubbles only can withstand the rapidly increasing capillary stress. In the last solution, the original liquid glue was diluted nearly

---

\* From another point of view, the arrest at  $e$  and  $b'$ , respectively, may be regarded as evidences of incipient solidification, so that the growth of  $T$  ceases.



however, 1 or 2 drops of common soap solution are added to 10 c. c. of the 10 per cent sugar solution and the mixture thoroughly stirred, bubbles at least as large as 2 cm. are easily obtained. Many of them survive through a number of observations and some actually pass into the solid state. Smooth, iridescent bubbles of solid sugar were in fact detachable, having lasted under pressure one or more hours. Success is usually assured when the solutions are freshly put together. After standing a day they are liable to become turbid and the bubbles burst. Additions of 1 or 2 drops of fresh soap solution, however, is apt to clarify the mixture and restore its usefulness. A drop of dilute caustic alkali (NaOH) has the same effect. Curiously enough, neither from the soap solution nor from the sugar solution can adequately persistent bubbles be obtained. The advantages of adding sugar to soap solutions is of course well known; but what I here wish to accentuate is the profound effect on  $T$  of a mere trace of soap. But this, too, is not out of keeping with the nature of  $T$ .

In the first experiment, figure 20(1), the zero of fringes was accidentally shifted and the absolute data may be slightly displaced. The relations, however, are trustworthy, and they indicate a marked increase of  $T$  during the first half hour. After about 40 minutes the pressure was removed, whereupon the bubble shrank in its lower half (drop). The attempt to blow it out again broke it. This bubble, like all the rest, was vividly colored in bands parallel to the equator. The next experiment, figure 20(2), proceeded satisfactorily. There was no appreciable change of diameter  $2r=2.10$  cm. After about 2 hours the solid bubble broke off under the pressure. The film, smooth (without puckering) and iridescent, remained so indefinitely (days) thereafter. As the curve shows,  $T$  rose regularly from 28.7 to 33.6, after which the leakage from diffusion of air outward supervenes. Next day the solution had become turbid and persistent bubbles were not obtainable. The addition of 2 drops of soap solution restored it and the data, figure 20(3), were thus obtained. The maximum,  $T=33.6$ , happens to be the same as before; but the final apparent decrease of  $T$  does not occur (temperature discrepancies). After the observations of figure 20(3), the following were successively taken:

Time .....	85	112	153	minutes.
$T$ .....	28.9	31.2	31.5	

which probably indicate thermal fluctuations. This bubble shrank somewhat in drying to the solid state. With another fresh solution the results

Time .....	0	3	6	minutes.
$T$ .....	29.6	31.5	31.5	

are of the same nature. In a great variety of individual experiments (10 cases), with similar solutions, initial values of  $T$  from 26 to 29 were obtained, the mean value being  $T=27.9$ .

The endeavor was now made to obtain bubbles of sugar solution by adding 2 drops of caustic-soda solution, but none persisted. On supplying 2 drops of soap solution, however, bubbles were again obtained, but in this case they

remained colorless and lasted only a few minutes. The following examples may be given:

$2r = 2.10$	2.05	2.20	2.10	2.05 cm.
$T = 36.2$	37.1	37.1	38.8	36.7

Thus the surface tension in these thick bubbles has been increased in marked degree. It was, moreover, found to decrease in the same bubble ( $\Delta T = -0.0012$  per minute being observed) in the lapse of time; but the bubble did not last long enough for adequate tests.

Tried again next day (means of three observations each), the data were  $T = 35.6$ ; with 2 more drops of soap solution,  $T = 34.1$ ; with further 2 drops of soap solution,  $T = 34.1$ ; with 2 more drops of NaOH solution,  $T = 34.2$ . The bubbles remained relatively brittle and colorless. Finally, diluting the solution one-half, the mean results were  $T = 35.8$ ; with 2 drops of soap,  $T = 35.4$ . Thus throughout all these modifications, the solution retained about the same high  $T$ , with bubbles that throughout were clear, thick, and of slight persistence, as compared with the same solutions (approximately) above.

To meet this dilemma fresh sugar solutions were taken and tested with 2 drops of soap solution. It was astonishing to find that  $T$  had increased further in all of the 7 tests made, to over  $T = 40$ . Moreover,  $T$  fell at first and later usually rose again. Thus, for example:

Time .....	0	2	4 minutes.
$T$ .....	43.5	38.8	41.4

The bubbles ( $2r = 2.1$ ) were uniformly thick, colorless, short-lived, and  $T$  a continually variable quantity.

This experiment suggested that probably the soap solution, kept in a covered glass and remaining perfectly clear, was nevertheless continually undergoing change owing to exposure to the air. Fresh soap solution from a supply in a stoppered bottle was therefore taken and two drops of it added to fresh 10 c. c. of the sugar solution. The result was immediately decisive and the highly colored bubbles with low  $T$  were again obtained. For example:

TABLE 3.

$2r$	Time	$T$
cm.	min.	
2.21	.....	28.7
1.95	3	23.3
	6	25.6
2.30	1	30.1
	2	27.5
	3	24.9
	4	26.3
etc.		

Notwithstanding the occasional occurrence of solid-sugar bubbles, it thus seems as if the sugar had very little to do with the  $T$  values, these being determined in the above tests by the 2 or 3 drops of progressively changing

soap solution. To test this, 2 drops of soap solution were added to 10 c. c. of distilled water, care having been taken to clean all apparatus until distilled water itself produced no results. The bubbles obtained with these dilute mixtures were naturally short-lived, bursting within a minute or two. The surface tensions in 10 successive tests, though consistent in a single test, were very variable, ranging from  $T=35$  to  $T=50$ . The feature throughout was the marked and rapid decrease of  $T$ , for the same bubble, within a minute of its life. For example, with bubbles each  $2r=1.1$  cm., the  $T$  values successively obtained were

42.1	42.1	49.8	36.9	43.9	46.5
39.2	29.5	44.6	31.7	41.4	42.5
36.9	34.8	...	29.1	...	...

The bubbles were all thick and colorless. Some of them could be blown to a diameter of even 4 cm., but they burst before any color appeared.

The interesting question paralleling the above experience with glue solutions may now be asked, as to the degree of approach to the surface tension of pure water which may be reached by successively diluting soap solutions. Mixtures were therefore prepared of 10 c. c. distilled water with 1 drop of soap solution. Estimating the drop as less than 0.01 c. c., the dilution of the solution is greater than 0.001. The first of these gave the values

10 c. c. $H_2O + 1$ drop:	$2r = \frac{2.2}{36}$	$\frac{2.1}{36}$	$\frac{2.2}{31}$	$\frac{1.9}{31}$ cm.
---------------------------	-----------------------	------------------	------------------	----------------------

which are unexpectedly low. The tube and other parts were therefore further cleansed and a fresh solution prepared showing (successive values of  $T$ )

10 c. c. $H_2O + 1$ drop:	$2r = \frac{2.0}{41}$	$\frac{1.90}{39}$	$\frac{2.00}{48}$	$\frac{2.10}{48}$ cm.
	$T = \frac{36}{36}$	$\frac{37}{37}$	$\frac{45}{45}$	$\frac{43}{43}$

which is an improvement. The bubbles last less than a minute, and during this time  $T$  regularly falls. The solution was now diluted one-half, giving

10 c. c. $H_2O + 0.5$ drop:	$2r = \frac{1.90}{52}$	$\frac{1.90}{59}$	$\frac{2.20}{60}$	$\frac{1.90}{54}$	$\frac{1.80}{58}$ cm.
	$T = \frac{50}{50}$	$\frac{54}{54}$	$\frac{58}{58}$	$\frac{50}{50}$	$\frac{56}{56}$

$T$  decreasing as usual. The preceding solution on further dilution to one-half gave

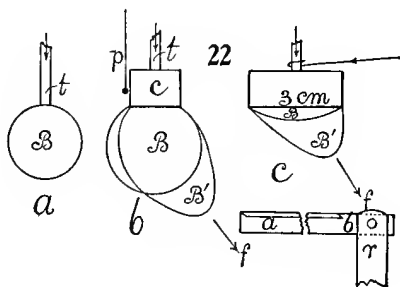
10 c. c. $H_2O + 0.25$ drop:	$2r = \frac{1.90}{63}$	$\frac{1.80}{64}$	$\frac{1.80}{66}$
	$T = \frac{61}{61}$	...	$\frac{63}{63}$

A final dilution to one-half was also tried, but the bubbles were now too short-lived for one observer to manipulate. One bubble was caught showing about  $T=62$ . This was a late and low value. With two observers there would have been no difficulty, but the experiment similarly made in §10 with glue is much less trying.

The mean data, viz, 1 drop,  $T=44$ ; 0.5 drop,  $T=55$ ; 0.25 drop,  $T=64$ , have been constructed in figure 21. A linear extrapolation for pure water would make  $T$  somewhere near 70; a quadratic extrapolation nearer 80. Since

$T$  decreases rapidly, since it takes time to blow the bubble and set the fringes with the slide micrometer, even the first  $T$  observed is itself probably low. At all events, the data are in good accord with the surface tension of a clean surface of water.

As to the cause of the rapid decline of  $T$  after the bubble is blown, two reasons may be adduced. In the first place, the outer surface, at least in contact with air, becomes contaminated, or again, colloidal matter within the bubble may accumulate at the surface. In the second place, we may suppose the forces embodied in  $T$  act not merely at the surface of the film, but throughout its cross-section. Hence if this cross-section decreases in thickness from evaporation, the thinning of the walls is expressed in a continued reduction of  $T$ . The water-bubbles are throughout colorless; but if with continued addition of soap solution one eventually reaches the iridescent stage of film, one should expect the least values of  $T$  (such as found) to accompany the thinnest bubbles.



**13. Charged bubbles. Sparkless sparks.**—The initial experiments, in which the bubble was charged by a micrometer screw electrophorus, showed no appreciable fringe displacement for the available potentials. It was necessary to use a small Wimshurst machine to electrify the bubbles. The first of these were blown from a 0.25-inch tube  $t$ , figure 22a; but on charging they were too easily pulled off the tube along the lines of force. A similarly charged plate below and a drop at the bottom of the bubble to weight it down, however, were the means of obtaining a few preliminary results. The internal pressure of the uncharged bubble,  $10^{-3}$  6.4 cm. Hg, fell to  $10^{-3}$  5.5 cm., developing a difference of  $p = 9 \times 10^{-4}$  cm. Hg before the bubble was torn off. Since for the potential  $V$  the charge is  $Q = rV$ , where  $r = 2$  cm. is the radius of the bubble,

$$p = 2\pi(Q/4\pi r^2)^2 = V^2/8\pi r^2 \quad \text{or} \quad V = r\sqrt{8\pi p}$$

Thus

$$V = 2\sqrt{25.1 \times 9 \times 10^{-4} \times 13.6 \times 981} = 35 \text{ electrost. units or } 10,500 \text{ volts}$$

nearly. Very high potentials are therefore needed even in these simple performances.

The purpose of the experiments, however, is the nearly complete removal of internal pressure and with this in view the device, figure 22b, with a cylin-

drical funnel  $tc$  and therefore a larger base of attachment, was adopted. The bubbles are now no longer spherical, at least when charged. A pith ball  $p$  may be added to indicate the rise or drop of potential. The cylinder  $c$  was about 3 cm. in diameter and 1.5 cm. deep. Larger sizes up to 6 cm. were also tried, and abandoned, as it would have been much less easy to produce the large number of films needed. The effect of gradually charging the exposed bubble  $B$  is to draw it out into a blunt spindle  $B'$  along the incidental lines of force  $f$ , to a maximum of distortion; at a definite potential, however, the stretched bubble suddenly, almost spasmodically, returns to the form  $B$ , usually with vigorous quivering, right and left.  $B'$  may even touch objects and be discharged; but frequently the bubble parts at an unstable constriction and the end flies off. The aerial discharges take place in free air and at each such discharge the repelled pith ball falls back slightly toward the vertical. The discharges from the bubble, in spite of the violent jerking, are thus only partial, just noticeable with the pith ball and probably within 10 per cent. At the same time the reduced pressure rises. Potential must be increased very gradually coincidently with the slow expansion. This means, therefore, that at each jerk some of the lines of force  $f$  break loose with an outrush of ions from the film. The phenomenon is very interesting, as it takes place without any light effect even in the dark, so far as I could observe, and without noise. Such a result, when occurring with metal electrodes, is usually estimated as equivalent to an electrical pressure of  $p = 2\pi\sigma^2 = 68$  dynes/cm.<sup>2</sup> The forces are thus of the same order as those depending on the surface tensions  $T = 30$  dynes/cm. It may, therefore, be anticipated that they will be observable together.

With the larger part of the bubble  $B$  outside, as in figure 22*b*, the experiment is short-lived, as the bubble soon parts and the pressure within can not be wholly removed. To accomplish this, only a small segment of the bubble must protrude, as in figure 22*c*. The radius of such bubbles may be estimated as 4 to 3 cm., for a depth of the protruding part of 0.6 to 1 cm. These bubbles are also drawn out along the lines  $f$ , to return with a jerk, and the experiment may now be repeated 10 to 50 times before the bubble breaks. During the earlier spasms all superfluous water is thrown off, so that at the end the film is very even throughout, more actively stimulated, and requiring higher potentials to contend with the effective surface tensions. At first there is perhaps little more than a flutter.

Using the small Wimshurst machine, giving a spark within 1 cm., the run of pressure in a large number of experiments was typically as follows:

Discharged	..... $10^3 p = 4.9$	4.9	4.9 cm. Hg.
Charged	..... $10^3 p = 1.4$	1.4	1.0
Kept charged	..... $10^3 p = 3.5$	3.5	3.5 etc.

the same bubble being successively discharged at the poles of the machine and then gradually charged again. Pressure here falls off to a minimum; but on further continued play of the machine this rises as if the potential were being dropped by brush discharge or other increasing leakage of ions. The potential

was scarcely sufficient to remove all pressure, nor to reach the jerking stage. Frequently the  $T$  of the uncharged bubble regularly increased by this successive charging and discharging, as, for instance,

Discharged . . . . .	$10^3 p = 4.9$	5.2	5.4	5.5	5.5	5.6 cm. Hg.
Charged . . . . .	$10^3 p = 1.7$	1.7	1.7	1.7	1.7	1.4
Kept charged . . . . .	$10^3 p = 2.8$	2.8	2.1	2.8	2.8	2.8

Common soap solution behaved similarly, except that but 1 or 2 discharges were possible before the bubble burst, and the pressure could not be so fully reduced; thus, uncharged  $p \times 10^3 = 5.6$ ; charged  $10^3 p = 2.1$ ; later  $10^3 p = 3.5$ .

The charge here was negative, the positive pole being put to earth. The latter pole was less efficient as a charger and there was no rise in pressure in time; thus, uncharged  $p \times 10^3 = 4.9$ ; charged,  $p \times 10^3 = 3.5$  (minimum permanent).

The above peculiar minima may of course be attributed to the bubble, its  $T$  changing under electrification; but they are more probably to be ascribed to the machine. So also the inferior efficiency of positive charge is more liable to be a defect of the machine. To elucidate this point, a large Holtz machine was installed, operating on a holder of the form figure 22c. With common soap solution pressures were brought down from  $4.9 \times 10^{-3}$  to  $0.7 \times 10^{-3}$  cm. Hg. Drops being shed in the earlier flutters, the bubble after the final violent oscillation soon broke, however carefully and slowly the potential was increased.

With the prepared soap solution, the whole of the internal pressure of the uncharged bubble, if low enough, was easily removed, on very slow rotation of the machine, and the resultant pressure even became negative; as for example, uncharged  $p \times 10^3 = \text{below } 4$ ; charged  $p \times 10^3 = 0$ ; later  $p \times 10^3 = -0.7$  cm. Hg. There was now no minimum  $p$  with subsequent recovery. The pressure, even below  $p = 0$ , could be maintained indefinitely by very slowly rotating the machine. It was not always possible, however, to bring the internal pressure down to zero. Selecting a few cases (fig. 22c), the run in successive shallow bubbles was

Uncharged . . . . .	$10^3 p = 5.1$	5.2	4.7	4.9	4.9 etc. cm. Hg.
Charged . . . . .	$10^3 p = 1.7-1.6$	1.4-1.0	0.7	1.0-0.7	0.7-0.5

the charged bubble jerking continually with but slight change of pressure or voltage. Large bubbles were liable to break apart prematurely with differences less striking, as for instance,

Charged . . . . .	$10^3 p = 4.1$	4.2	3.0 etc. cm. Hg.
Uncharged . . . . .	$10^3 p = 2.1-1.8$	2.1-1.8	1.4

The differences in the first instance were on the average about  $10^3 \Delta p = 4.0$  cm. of mercury. With the machine at rest,  $p$  slowly rose, owing to the leakage. Both poles behaved alike. Discharge effects in pressure and potential, produced by the jerks as above, were slight when compared with those produced at the poles of the machine.

The correctness of the theory of partial discharge may be proved by an aluminum electroscope (*abr*, fig. 22c) below the bubble. The electroscope



consists of a horizontal hacksaw blade against which a very thin (0.03 mm.) elastic strip of aluminum foil  $ab$ , 8 inches long, is appressed, both being carried by the hard-rubber stem  $r$ . To give the strip  $ab$  rigidity, it is bent at right angles throughout its length, except at the end  $b$ , where the flexure is to take place when the strip is charged and diverges from the saw-blade. This simple contrivance works admirably; the slightest spasm of the bubble  $B'$  communicates an increment of potential and increases the divergence to a final maximum. Meanwhile the pith ball  $p$  only just changes its obliquity to the vertical at the successive jerks. The amount of outrush or intermittent current thus depends on the supply of removable ions at the outer surface of the soap-bubble. Possibly a skin layer of molecules free from surface tension ( $T$  counterbalanced by  $2\pi\sigma^2$ ) strips off bodily, seeing that  $2\pi\sigma^2$  like electric charge can reside only on the surface molecules. On the same plan all drops, etc., are removed at the beginning. Successive molecular layers thus exfoliate till the bubble breaks.\*

Owing to the distortion of the bubble, computations are not easily possible. As the form  $B'$  (fig. 22c) becomes more spindle-shaped, the surface density at the blunt point rapidly increases. It is here, therefore, that the inward components of the surface tensions are first balanced by the rigorously superficial outward electric pressures. At the beginning, when there is a drop, etc., at the bottom of the bubble, the excess of moisture is shed at once and the pressure reductions needed are below 25 dynes per square centimeter. Later, when the bubble has become very even and thin, pressure reductions (as instanced above) of the value of 55 dynes per square centimeter are registered at each exfoliation. It is here, therefore, that the surface tensions proper compete with the electric pressures. Hence the surface molecules slide off with much greater difficulty at the end of the experiment. If the pressure needed to produce a spark be estimated at 68 dynes/cm.<sup>2</sup>, the lines of force might seem to break off to this extent with greater ease of slip from a liquid than from a solid surface; but from the variable curvature of the bubble the inference is not warranted. The difference only of internal and external pressures is constant throughout and is observed.

#### OIL BUBBLES.

**14. Oil and rubber surface tensions.**—Sweet oil was first tested; but the bubbles producible, 1 to 2 cm. in diameter, broke at once. No value of  $T$  (single observer) could be obtained after many trials. A drop of soda solution, warming, etc., rather made the behavior worse. Drops or small quantities of liquid soap were also unavailing; but on adding a larger quantity of soap solution (10 to 20 per cent) and shaking, opaque bubbles were easily obtained from the emulsion, with surface tensions  $T=25, 28, 27, 29, 26$ , etc. Another

---

\* This type of exfoliation has recently been discussed by Sir W. H. Bragg (Nature, Feb. 21, 1925) in relation to the work of Perrin and of Wells, with evidence given by X-ray investigation.

emulsion behaved similarly, showing mean  $T=26$ . The oil was not present as a merely neutral body, however, for a reduction of  $T$  from the normal value 32 is in evidence. The white bubbles, originally opaque, cleared to films decorated with white patches, during which time  $T$  decreased markedly; for instance, in a later experiment after heating, originally,  $T=29.6$ ; just before bursting,  $T=23.7$ ; another trial giving the same result.

The behavior of paraffine (vacuum) oil, both alone and with admixtures of small quantities of soap solution, was the same. With larger admixtures of liquid soap, the oil in emulsion behaved rather more like a neutral body than sweet oil. Bubbles over 5 cm. in diameter were easily produced and the surface tensions obtained from the opaque bubbles had a mean value  $T=30$ . On standing (days) the emulsion separated into clear oil below and a long column of pasty emulsion above. From this after weeks of standing a short layer of clear soap solution appeared on top.

The question now arises whether the phenomenal reduction of the  $T$  of pure water by addition of soap solution is an isolated case, or whether something similar can be done with oil on addition of another suitable colloid. Pure rubber (not vulcanized) was therefore dissolved in the paraffine (vacuum) oil by heating and digestion, the oil becoming distinctly more viscid. Bubbles were now easily produced even over 2 cm. in diameter and lasting 1 or 2 minutes. Good values of surface tension were thus obtainable, viz ( $2r=2$  cm. throughout),  $T=30.7$ ,  $31.9$ ,  $31.4$ ,  $30.7$ , etc., and these values were constant till the bubbles burst. The colloid can thus have had very little effect on  $T$  (Magie's value for sweet oil, for instance, is 32); but it does contribute in marked degree to the persistence of bubbles, as in the case of soap.

Rubber dissolved in a mixture of sweet oil and paraffine oil gave the same order of results,  $T=30$  to  $31$ .

Rubber dissolved in kerosene (illuminating oil) was much less available, the bubble bursting almost before the fringes came to rest. The value of  $T$  obtained in several experiments was of the order  $T=26$ ; but this is merely an estimate.

The partial success of these results induced me to test other oils, with a view to obtaining the surface tension of pure rubber, if possible. For this purpose a gasoline solution seemed specially adaptable, for with the speedy evaporation of gasoline a rubber film would remain. It is necessary to use a gasoline solution thick enough to only just flow. Even then the bubbles are too short lived for the successive measurements of  $2r$  and  $\Delta x$ . After many trials, three cases occurred in which the fringes were glimpsed in position. The estimate so obtained ( $2r=1.5$  cm.,  $\Delta x=0.0170$  cm.) was  $T=30$ , which is the usual order of values for the preceding colloid solutions.

**15. Canada balsam.**—This substance seemed particularly favorable for  $T$  measurements, as the bubble remains viscous for a long time. The solution in turpentine, however, failed of success, the bubbles bursting almost at once.

The viscid liquid itself was therefore tried, warmed to facilitate the blowing. The results obtained for  $T$  are shown in figure 23, in a scale of minutes. The first series is the most complete and indicates the uniform occurrence of a rise of  $T$  during the first 5 or 10 minutes, after which  $T$  regularly but slowly decreases. This is to be ascribed, as I think, to the diminished contractility or incipient solidification of the tissue with loss of the air within the bubble. At 74 minutes the original clear iridescent bubble was found to be opalescent or opaque. It had roughened and shrunk from 2.3 to less than 2.2 cm. in diameter. At 85 minutes it had shrunk further to 2.0 cm. Breaking it at 102 minutes, it was still flexible, but very tough. In series 2, the bubble became opaque after about 60 minutes and then broke of its own accord. In the series 3, the bubble sprang a leak (?) early, but seemed afterward to have resealed itself again.

As the production of persistent bubbles is thus easy with this substance, a thick solution of Canada balsam in chloroform was next tested, and the data obtained are given in figure 24. As a whole, they show a close resemblance to figure 23. The results of the first series are low; but it was found that the lower end of the tube had become choked with an excess of the solution, a danger to be guarded against in all these experiments. The diminution is thus a thermal effect and  $T$  eventually runs into negative values. The second series, however, is trustworthy, the data being

Time .....	0	3	12	26	38	53	66	170 minutes.
$10^3 \times \Delta h$ .....	17.4	13.5	11.8	9.6	7.7	5.7	4.8	4.8 cm. Hg.
$T$ .....	49.1	49.4	43.2	35.1	28.1	20.8	17.4	14.3

At 170 minutes the originally clear iridescent bubble was found to be opalescent with a satin-like luster. It had decreased in size from a diameter of 2.2 cm. to 1.8 cm., but was otherwise quite intact. Observed next day, it had shrunk further to a white dry pendant, but was still whole, giving an apparent value of  $T=3.6$ . The bubble crumbled at the touch, however, to a white, chalk-like powder. It is noteworthy that between 66 minutes and 170 minutes there was no difference of internal pressure, the reduction of apparent  $T$  being due to shrinkage. In the third series the initial  $T$  is somewhat smaller, but the general behavior is the same, remembering that the fall of  $T$  during incipient solidification can not be independent of temperature. The data were

Time .....	0	3	6	12	29	48	79	117	129	360 minutes.
$\Delta h \times 10^3$ .....	12.3	12.9	12.6	11.7	9.5	8.1	5.3	4.6	5.0	4.8 cm. Hg.
$T$ .....	43.6	45.9	44.6	41.6	33.8	28.7	18.9	16.4	17.6	16.9

After 117 minutes this bubble had also become opalescent and stringy, showing creases on the surface; though the bag was still whole, for after 360 minutes scarcely any change of internal pressure was observable. In this respect, therefore, series 2 and 3 are in accord; for long periods (hours) after incipient opalescence, the internal pressure remains nearly fixed.

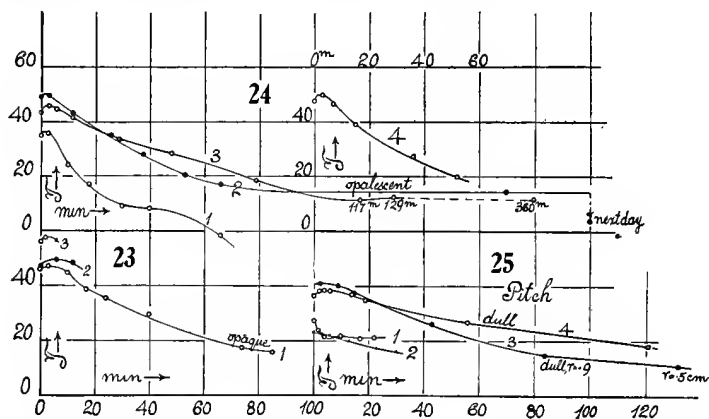
In the case of series 4, the bubble obtained was a very thin, highly iridescent sphere, and it was with regret that the observations could not be extended

beyond 50 minutes. They are separately given in figure 24, and are (bubble clear throughout) :

Time .....	0	3	7	15	36	52 minutes.
$10^3 \times \Delta h$ .....	14.4	15.1	14.0	11.9	8.3	6.0 cm. Hg.
$T$ .....	47.7	49.8	46.3	39.2	27.5	20.0

From the initial high  $T$  value, there is a rapid descent similar to the case of series 2. Next day this bubble had shrunk to a white bag about 1.3 cm. in diameter. The internal pressure was zero, suggesting a rent.

The surface tension of these thick chloroform solutions differs but little (as a whole) from the behavior of warmed Canada balsam. The difference of viscosity is thus merely incidental. Since the fall of  $T$  following the rise during the first 3 or 4 minutes occurs while the bubble is perfectly clear and therefore probably still a viscous fluid, and since the pressure within the opaque bubble remains constant for hours, I am in some doubt whether the reference



of this feature of the experiment to diminished contractility is quite warranted. The assumption of incipient solidification is thus merely a reasonable hypothesis, for the air does leak out. Under the microscope patches of the white, solid, friable chalk-like bubble residues appear minutely cellular, like transverse sections of wood, but more finely porous. A measurement of the pores (granting that they may be the illusion produced by a rough surface) showed them no longer than 0.0001 cm. in diameter and evenly distributed. If we consult again curve 1, figure 23, and particularly curves (2) and (3), figure 24, it will be seen that the fall of  $T$  (which means escape of air and a leaking bubble) occurs while the bubble is clear and iridescent, whereas the nearly constant low values of  $T$  thereafter (bubble now impervious to air) occur when the bubble has become opalescent and rough, or white, and opaque. During the clear stage the bubble does not appreciably shrink. It does so during the opaque stage, keeping the pressure nearly constant within. The decrease of  $T$  in the graphs as stated is purely due to this fact. Thus the bubble is impervious when the liquid solvents (chloroform, etc.) have prac-

tically evaporated, but not so when they are present and the bubble clear and glass-like. One may infer that the diffusion of the high-pressure air within the bubble outward is conditioned by the presence of a liquid solvent. Furthermore, that toward the end of the evaporation, at least, the resin and the solvent separate so that the latter occurs in an indefinite number of minute droplets, not exceeding 0.001 mm. in diameter, throughout the tissue of the resin. It may have been so distributed throughout, but the separated resin and solution in some measure recalls the ejection of the solute on the freezing of a salt solution. In the final bright white residue, air only is present in the pores. To resume: The clear bubble leaks, but does not appreciably shrink and pressure within diminishes; the opaque bubble often shrinks in excess of the leakage, if any, and the internal pressure may be constant or even rise.

With mastic in alcohol similar experiments were tried at length, but failed in all cases. Bubbles were producible, but they did not last.

**16 Pitch.**—The sample used was rather old and stiff and it was necessary to blow the bubbles warm, after the fusion of the pitch. The results for  $T$  in the lapse of minutes are summarized in figure 25, graphs 1 and 2. In both cases the surface tensions are low values, even at the beginning, and they apparently decrease as usual in the lapse of time. The bubble of No. 2 was elliptical and the absolute results of the graph are therefore too low. It was curious to note that the bubbles remained black throughout, but were initially glossy.

This sample of pitch was therefore diluted with a small addition of turpentine, fused, and stirred. With the nearly cold mixture a bubble was blown and examined for over two hours. The graph, figure 25, No. 3, summarizes the data. It will be seen that they show a very close resemblance to the behavior of Canada balsam throughout, even as to the absolute values, which were

Time .....	2	9	15	43	83	132 minutes.
$\Delta h \times 10^3$ .....	13.1	12.8	12.0	8.4	5.1	5.5 cm. Hg.
$T$ .....	41.1	40.2	37.8	26.3	15.0	12.4

At 83 minutes the bubbles had assumed a dull surface, with shrinkage from diameter 1.9 to 1.8 cm., and at 132 minutes it had shrunk further to a black paper bag, as it were, about one-half its original diameter. The pressure within had actually increased. We have here the same tendency to maintain constant pressure inside the bubble that characterized the opaque stage of Canada balsam, and the same inferences might be drawn.

Further turpentine was now added; but it was not possible to obtain bubbles from the solution until the greater part of the turpentine had been boiled away. The bubble finally obtained was small,  $2r=1.7$  cm. After about 120 minutes it had shrunk to 1.6 cm., with a dulled surface; after 180 minutes to 1.4 cm. with distortion, the dull bubble being more or less cushion-shape, embraced by a bright ring around the edge. The data were (curve 4)

Time .....	0	2	4	6	14	19	56	121	180	212 minutes.
$\Delta h \times 10^3$ .....	13.1	13.7	13.8	13.7	13.2	12.4	9.6	6.8	6.2	5.5 cm. Hg.
$T$ .....	36.7	38.5	38.8	38.5	37.1	35.0	27.0	18.1	14.6	12.7

The relative constancy of pressure during the long period of shrinkage (121 to 212 minutes, dull surface) is again noteworthy, so that while the glossy bubble does not shrink appreciably, the dull bubble sometimes shrinks in excess of leakage, if any. Pitch of course remains viscous, never becoming solid.

**17. Nitrocelluloid.**—With thick collodion, bubbles are easily producible, but they last but 1 or 2 seconds. Occasionally one is caught which solidifies; but on so doing it shrinks to a puckered cylindrical tube, by shrinking equatorially and additionally blowing out liquid adhesions like the drop at the bottom. All is complete in a few seconds. Under these circumstances the pressure goes up many fold and is beyond the range of the U-gage interferometer. I caught but one measurable bubble,  $2r=1.5$  cm., iridescent and spherical. The internal pressure was  $\Delta h \times 10^8 = 11.4$  cm. Hg and  $T=30$ . Thus the colloidal solution presents no abnormal values, however the tough solid resulting may behave. With celluloid varnish (thick), bubbles are also producible, but none of them persist.

Celluloid thus differs from the preceding colloids in speed and intensity of reaction. Speed is referable to the volatile solvents, and a determination of the air leakage of the clear bubble is thus out of the question. In the second stage, with evaporated solvent, the period of shrinkage is similarly rapid. Pressures, instead of remaining constant as heretofore, actually increase impulsively many times and they furnish only a lower limit of value for the cohesional forces in action. In other words, while the solid residues of Canada balsam are brittle and friable, those of nitrocelluloid are flexible and tenacious, and we have thus an interesting transition from the surface tension of the liquid bubble to the elastic forces (probably) of the solid film.

In a corroborative experiment some time later, a bubble  $2r=1.4$  cm. in diameter showed an initial  $T=29$ . It shrank in a few seconds to an elliptical puckered solid bubble, which later became rounded to a crumpled sphere, about  $2r=0.7$  cm. in diameter. Pressures were increased about 5 times after shrinking, which after 7 minutes (leakage) became 3 times, after 22 minutes 2 times, after 39 minutes and long thereafter once the pressure in the liquid bubble. If we compute the solid data as surface tension,  $T=74$ , necessarily a lower limit. The size and form changed no further. Under the microscope no structure was detected in the crumpled bubble. Certain parts of it were iridescent, but as a whole it was free from the colors seen on the liquid film.

## CHAPTER III.

### VISCOSITY, DENSITY, AND DIFFUSION OF GASES.

#### VISCOSITY AND EFFLUX.

**18. Viscosity of air.**—The observation made above, of a more rapid transpiration of air through one pin-hole as compared with the other, in case of a common pressure difference, suggested an actual measurement of the viscosity  $\eta$  of air, by capillary-tube method. For this purpose (inset, fig. 26), it is merely necessary to attach such a tube, by a piece of pure rubber tubing, to one shank of the U-gage, the other remaining open to the atmosphere. On pushing the tube in question inward slightly, the pressure will rise from  $p$  (atmosphere) to  $P$  a little above (excess of the order of 0.05 mm. of mercury), and this is indicated by the displacement,  $s$ , of fringes. The change of  $s$  in the lapse of time is, then, to be measured with a stop-watch. Thus the method is extremely simple and capable of indefinite repetition, either for  $P > p$  or  $P < p$ . Any other gas may replace air on the side of the U-tube in question. The serviceable equation for this purpose was deduced long ago by O. E. Meyer,\* in the form

$$(1) \quad \eta = \frac{\pi}{16} \frac{P^2 p^2}{p_1 V_1/t} \frac{R^4}{L} \left(1 + 4 \frac{\xi}{R}\right)$$

where  $P$  and  $p$  are the pressures at the two ends of the capillary tube of length  $L$  and radius  $R$ , and  $V_1/t$  is the volume of air transpiring per second at the mean pressure  $p_1$ . The coefficient of slip,  $\xi = \eta/\epsilon$ , (the ratio of internal and external friction) will have to be neglected. In this equation  $P + p$  may be written  $2P$ , since  $P - p$  is very small compared with  $P + p$ . But  $p_1 V_1/t = R(m_1/t)\tau$ , if  $m_1/t$  is the mass of air transpiring per second; and since this comes out of the closed volume  $V$  of air, of mass  $m$ , of the shank of the U-gage,

$$(2) \quad m_1/t = -dm/dt$$

Hence if the volume  $V$  is preliminarily taken as constant, while the pressure  $P$  decreases,

$$(3) \quad p_1 V_1/t = R(m_1/t)\tau = -R(dm/dt)\tau = -VdP/dt$$

so that the equation (2) now becomes

$$(4) \quad \eta' = -\frac{\pi}{16} \frac{R^4}{LV} \frac{2P(P-p)}{dP/dt} = -\frac{\pi}{8} \frac{R^4}{LV} \frac{P(P-p)}{d(P-p)/dt}$$

as  $p$  is the constant atmospheric pressure without. Therefore,

$$(5) \quad \eta' = -\frac{\pi}{8} \frac{R^4}{LV} \frac{P}{d(\log(P-p))/dt}$$

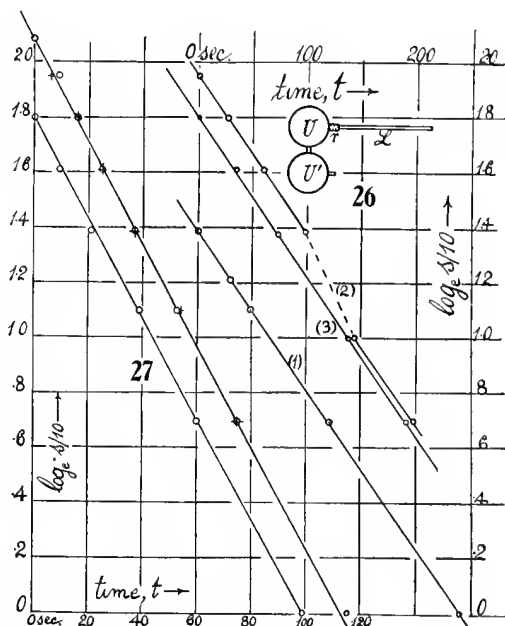
---

\* O. E. Meyer: Pogg. Ann. cxxvii, p. 269, 1866.

But since  $P-p$  is proportional to the fringe displacement  $s$ , the logarithmic time differential is simply  $d(\log s)/dt$ . Hence finally,

$$(6) \quad \eta' = -\frac{\pi}{8} \frac{R^*}{LV} \frac{P}{d(\log s)/dt}$$

$V$  being supposed not appreciably variable. Thus  $d(\log s)/dt$  is constant, and it is merely necessary to record the decrease of the fringe displacement  $s$  in the lapse of time, after the capillary tube is affixed under slight pressure,  $P-p$  to the U-gage on one side.



Equation (6) is incomplete, inasmuch as  $V$ , though very nearly constant, nevertheless varies in the same order as  $P$ , so that  $p_1 V_1/t = V dP/dt + P dV/dt$ . It is desirable, however, to test (6) preliminarily, in order to ascertain to what degree the method is feasible.

**19. Observations.**—The first tube selected had a length of 15.1 cm. and an internal diameter (as found by the microscope) of 0.0354 cm. Attached by an inch of pure rubber tube to one shank of the U-tube with a slight pressure excess, the relations of  $\log_e s$  (or for convenience  $\log_e s/10$ ) in the lapse of time were such as shown in the three graphs of figure 26. Of these, No. 1 is as nearly linear as may be expected, seeing that no attempt was made at precision, the time  $t$  being taken when the fringes passed successive equidistant scale divisions of the ocular micrometer. The same is true for the third graph. The second is for some reason irregular, owing possibly to an accidental



small displacement of the zero at 100 seconds (about). The mean rates in the three cases are respectively

$$10^3 d(\log s)/dt = 5.74, 5.84, 5.79$$

giving a mean value of 0.00579, as a whole.

The volume  $V$  of the closed shank of the U-gage was about 70 cm.<sup>3</sup>, the reduced barometric height  $B = 75.4$  cm. Hence the equation

$$\eta' = -\frac{\pi}{8} \frac{R^4}{LV} \frac{B\rho g}{d(\log s)/dt}$$

or

$$\eta' = \frac{\pi}{8} \frac{10^{-8} \times 9.81}{15.1 \times 70} \frac{75.4 \times 13.6 \times 981}{.00579} = 0.00633$$

Thus, while the logarithmic variation is sustained, the incomplete  $\eta'$  is enormously too large. This implies that most of the air is pushed bodily through the capillary tube by the advancing piston  $U$ , at nearly constant pressure.

The second tube was of larger bore, the diameter being 0.0454 cm. and the length 11.7 cm. The three graphs of  $\log s/10$  and  $t$  obtained for this tube are much steeper and shown in figure 27 in a different scale. Here all three graphs are as nearly linear as may be expected from the straightforward method of record. The individual mean rates are respectively

$$10^3 d(\log s)/dt = -18.8, -17.9, -18.5$$

with a mean rate therefore of 0.0184. Applying the preceding equation to this case

$$\eta' = \frac{\pi}{8} \frac{10^{-7} \times 2.65}{11.7 \times 70} \frac{75.4 \times 13.6 \times 981}{0.0184} = 0.00696$$

an order of value about the same as the preceding case, while the logarithmic variation is again substantiated.

It is therefore necessary to complete the equation for  $\eta$ , which is easily done by replacing  $VdP/dt$  by the full coefficient. If  $a$  is the area,  $H$  the normal depth of the cylindrical volume  $V$ , at  $U$ , and if the mercury head is  $h$ ,

$$V = a(H + h/2) \quad \text{or} \quad dV = adh/2$$

and

$$p_1 V_1/t = R(dm/dt) \tau = VdP/dt + PdV/dt = (V\rho g + aP/2)dh/dt$$

If  $B$  is the barometer height, since  $P - p = h\rho g$  and  $V = aH$  (nearly),

$$\eta = \frac{\pi}{8} \frac{R^4}{LV} \frac{B\rho g}{(B/2H + 1)d(\log s)/dt}$$

since  $d(\log h)/dt = d(\log s)/dt$ ,  $s$  being the fringe displacement from zero. Thus

$$\eta = \eta'/(1 + B/2H) = \eta'/(1 + 75.4/2) = \eta'/38.7$$

as  $H = 1$  cm. in the apparatus. Hence in the two cases,

$$\begin{aligned} L &= 15.1 \text{ cm.}; \quad 2R = 0.0350 \text{ cm.}; \quad \eta = 0.00633/38.7 = 0.0000164 \\ L &= 11.7 \text{ cm.}; \quad 2R = 0.0454 \text{ cm.}; \quad \eta = 0.00696/38.7 = 0.0000180 \end{aligned}$$

Both values are now correct in order; but the first, in which the transpiration is much slower, has been more influenced by the concomitant and inevitable changes of temperature in the U-gage reservoir  $V$ . It is obvious that the difficulties of Chapter I enter. For this reason, a more accurate determination of  $R$ , etc., and a consideration of the initially adiabatic temperature increment in  $V$  after compression, is of no interest, except in connection with observations made under very constant temperature conditions in summer.

**20. Efflux through pin-holes.**—This apparently simpler experiment does not succeed by the present method. In the first place, the hole must be considerably finer than 0.1 mm. or finer than can be punctured by the most delicate cambric needle. It will not, therefore, be round, and its area  $a'$  would have to be estimated. In the second place, the equation for this case ( $v = \sqrt{2(P-p)/\rho}$ ), reduces in the same notation to

$$\frac{dh}{dt} \frac{d \log h}{dt} = \left(\frac{a'}{a}\right)^2 \frac{2R^2 \tau^2 \rho_a}{H^2 \rho_m g (1 + B/2H)^2}$$

where  $R$  is the gas constant,  $\tau$  the absolute temperature,  $\rho_a$ ,  $\rho_m$  the densities of the gas and of mercury, and  $a$  the area of the U-gage. Thus neither of the rates are linear, and the head  $h$  must be known throughout, since  $(dh/dt)^2/h$  is constant. Using the equations, the rates would be (hole  $2r=0.027$  cm.,  $h=10^{-5} \times 6.3s$ )

50 s. p.	$dh/dt = 0.00439$	$ds/dt = 69$ s. p./sec.
25	310	49
12.5	219	35
6.2	155	25
3.1	110	17

which is too rapid for observation, as I found.

The equation if written in the form

$$(dh/dt)^2 = Ah$$

is integrable and becomes

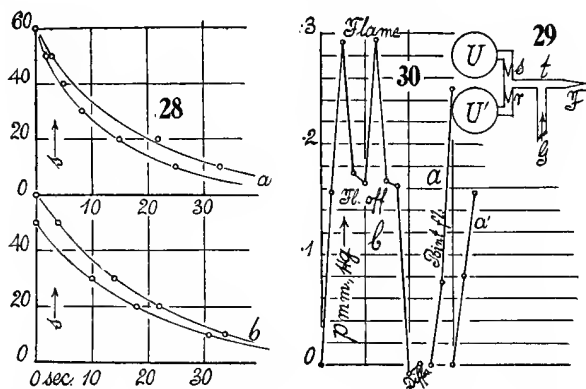
$$\sqrt{H} - \sqrt{h} = \sqrt{A/2t}$$

and thus, curiously enough, terminates in  $h=0$ , thereafter to increase again in the lapse of time, indefinitely.

I endeavored to get further light on the subject by inserting a fine wire ( $2r=0.02$  cm.) into the above pin-hole ( $2r=0.0272$  cm.), whereby the flow became sufficiently slow to be observable; but the efflux conditions of the experiments are thereby spoiled by the friction along the wire. Examples of the curves obtained are given in figure 28,  $a$ ,  $b$ , still difficult to observe, and which differ materially from each other, depending on the initial rapid fall before observation is possible. They are not in numerical conformity with the equation or otherwise, as may be seen by using the constants  $10^6 a = 267$ ;  $a\tau = 70$ ;  $(1 + B/2H) = 39$ ;  $\tau = 300^\circ$ ; etc., which makes  $\sqrt{A}/2 = 0.0179$  quite out of proportion. The actual efflux is much too slow as compared with the

equation, so that Torricelli's law in case of efflux into air, instead of vacuum, and a very small pressure difference, is here not warranted.

**21. Sensitive flames. Adjustment.**—The disposition of apparatus is shown in figure 29, where  $UU'$  is the interferometer  $U$ -gage,  $r$  and  $s$  the reëntrant and salient pin-holes,  $t$  the quill tube, and  $F$  the fine conical gas-jet about 1 mm. in diameter (salient outward) for the sensitive flame.  $F$  is preferably placed vertically. The gas inlet  $G$  is at the middle of  $t$ , so that  $r$ ,  $s$ , and  $F$  may function as nodes.  $G$  is provided with a stopcock to vary the gas-pressure. Since this pressure acts at both  $U$  and  $U'$ , it is only the acoustic pressure due to vibration within the quill tube which will influence the gage  $U$ .



The pin-holes  $rs$  are rarely quite of the same diameter. Hence the fringes will move for any sudden change of pressure at  $G$ , temporarily, but they soon return to zero. The flame  $F$  was very sensitive, but no acoustic pressure under any conditions could be observed. There was no effect even when the flame was purposely made turbulent by high gas-pressure. Thus the sensitive-flame phenomenon must be considered to exist outside of the quill tube  $tF$  and there is no corresponding vibration apparent within.

**22. Same. Telephonic excitation.**—On removing  $t$  from  $rs$  and the gage and joining the open end of  $t$  to a telephone mouthpiece, excited by a little induction coil with a break of variable pitch, one gets a beautiful exhibition of König's flames at  $F$ . In this case a small, sharp flame, 2 or 3 cm. or less, is of course desirable. However, the attempt to detect the resonances in the quill tube in this way failed. The method may, however, be useful in detecting the harmonies of the telephone plate and appurtenances.

**23. Apparent flame pressure\* and viscosity.**—Joining the quill tube  $t$  with the shank  $U$  only ( $s$ , fig. 1, may be left in place, as it does not function,  $r$ , also

\* Prof. A. T. Jones (Thesis, Clark Univ., 1913) seems to have first come across these phenomena and is inclined to accentuate the flame-pressure aspect (Science, LX, 1924, p. 315).

inactive, must be open to the atmosphere), one observes an increased pressure within  $t$  (cæ. par.), whenever the flame  $F$  is ignited. These pressures are in excess of the normal registry of the gage, so that small flames, from a point like a split pea to 2 or 3 cm., are to be used. Figure 30 gives examples of the results. The curve  $a$  (points spaced horizontally to show different conditions) beginning with no pressure (millimeters of mercury), when the cock is closed, registers about 0.075 mm. with the cock just open, owing to the resistance at the jet, and 0.25 mm. after the flame is lighted. At  $a'$ , the lower graph, is a less well chosen adjustment. The point flame, therefore, acts like a stopper, virtually narrowing the jet. Figure 30*b* gives a more extended series, with a flame 2 to 3 cm. long. Hence the gas-pressure at  $t$  in the absence of flame is larger, about 0.16 mm. With the flame lighted, the pressure reaches nearly 0.3 mm. It is not, however, relatively as much larger as in the case of the point flame. When the flame is blown out, the intermediate gas-pressure is restored, first at a rapid rate, finally very gradually, the progress obviously corresponding to a case of cooling of the mouth of the jet. The phenomenon is remarkably steady, and the experiment may be repeated indefinitely, two cases being given in figure 30. When the gas is finally shut off, the fringes dip below zero, which, however, is regained in the lapse of time. This is optic (refraction) evidence of the diffusion of hydrocarbon gas into the  $U$ -gage and of the subsequent diffusion outward; or in accord with the next sections, it may be due to the density difference at  $U$  and  $U'$ .

24. Inferences.—I was at first inclined to believe that an actual pressure increment within the flame locus had been observed. What happens, however, is probably no more than a large increase of the viscosity of the gas at the jet. Because of the high temperature there, the jet with the flame lighted temporarily conveys a much more viscous gas-current. Thus the asymptotic cooling effects in figure 30 are accounted for (hot-jet tube), as well as the striking steadiness of the phenomenon when the flame is on, and the disproportionately great effect of point flames. For in the latter, the colder blue base is lacking.

It follows from the above that if for any reason the flame is removed, there is an instantaneous excessive *outrush* of gas from the jet. When the flame is restored this excess is at once cut off. Here, then, is a mechanism that contributes to periodic motion of flame and must be effective in turbulent flames. Since pin-holes are sensitive at nodes, I have supposed that temperature occurrences might here be effective also; but this can not be the case in a phenomenon which is symmetrically either positive or negative, depending on the slope of the pin-hole.

With regard to the pin-hole probe itself, however, which is virtually a hollow cone, it would seem that on compression towards the point the adiabatic increase of temperature is accompanied by diminished flow outward, whereas

on dilatation from the point, there is a corresponding rapid flow of air inward. The result must be an excess of flow inward until the increased air-pressure within the closed region compensates for the viscosity differences at the point. Reversing the pin-hole, therefore, reverses the sign of the pressure, just as observed. Relaying is a failure, because adequate motion after the first pin-hole is quenched.

#### DENSITY AND DIFFUSION OF GASES.

**25. Apparatus.**—The present method, which in practice is singularly expeditious and simple, should nevertheless, it was hoped, eventually be capable of giving results well within 1 per cent. I have carried it through preliminarily to exhibit its entire feasibility, the plan being to compare the pressure of a column of gas with that of the surrounding air. A diagram of the apparatus is given in figure 31, where  $tt$  is a quill tube 68 cm. long, in which the gas (here supposed lighter than air) is to be stored. This communicates by the three-way stopcock  $C$  with one shank (10 cm. diameter, 1 cm. deep)  $G$  of the interferometer  $U$ -gauge.  $M$  shows the flat charge of mercury,  $p$  the sealed cover-glass, and  $L$  one component beam of the interferometer. The other shank of the  $U$ -tube (not shown) is open to the atmosphere.

With  $C$  set as in the figure, the gas arriving at  $g$  is passed in excess through  $tt$ . After a few minutes the plug in  $C$  is suddenly rotated  $90^\circ$  and the pressures produced at  $M$  read off by the fringe displacement in the telescope of the interferometer. The zero of the scale may be set by the slide micrometer. It is desirable to repeat this operation many times, as in the first instance there is a large throw of fringes. After this, with the tube filled with gas, the fringes are more steady and may be read off within 5 seconds or less. Diffusion, though relatively slow, nevertheless sets in from the beginning, the gas escaping both at the bottom and the top of  $tt$ , to be regularly replaced by air. If a stop-watch is started when the gas is definitely turned off, the progress of the diffusion phenomenon is registered by the displacement of fringes from minute to minute. To keep the gas within  $tt$ , the channel in  $C$  must be slightly above the tubulure in  $G$ , so that the connector  $s$  rises toward the left. This adjustment of diffusion from top and bottom is advantageous in requiring but very little gas; but for precision it is far preferable to so design the apparatus that the gage  $G$  and tubes  $sCt$  are filled with gas, and diffusion can take place out of the bottom of  $tt$  only.

**26. Equation and data for density.**—If  $\Delta p$  denotes the pressure difference on the two sides (gas and air),  $\Delta h$  the difference of heads of mercury of density  $\rho_m$  and  $\Delta x$  the corresponding displacement of the mirror on the screw slide-micrometer, for an angle of reflection  $\theta$  of the rays of the quadratic interferometer

$$(1) \quad 2\Delta h = 2\Delta x \cos \theta$$

$$(2) \quad \Delta p = \Delta x \cos \theta \rho_m g$$

Similarly, if  $\Delta\rho$  is the difference in density of the gas examined and the known density of the surrounding air,

$$(3) \quad \Delta p = H \Delta \rho g$$

$H$  being the length of the quill tube  $tt$  used. Thus

$$(4) \quad \Delta \rho = \rho_m \cos \theta \Delta x / H$$

The tube was 68.4 cm. long and  $\theta$  (which is difficult to measure) was taken as  $45^\circ$ . It was, however, frequently convenient to read the fringe displacement  $\Delta s$  off on the ocular micrometer, where by preliminary comparison

$$(5) \quad \Delta x = 10^{-5} 2.25 \Delta s \text{ cm.}$$

Accepting this provisionally

$$(6) \quad \Delta p = 9440 \Delta x = 0.212 \Delta s$$

and

$$(7) \quad \Delta \rho = 0.1415 \Delta x = 10^{-8} 3.184 \Delta s$$

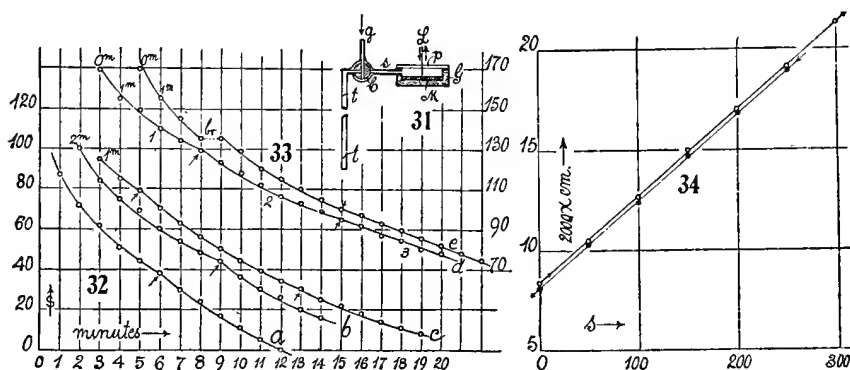
The linear relation of  $\Delta x$  and  $\Delta s$  must also be tested.

For convenience, ordinary coal-gas was first taken. The results are adequately given in the graphs figure 32,  $a$ ,  $b$ ,  $c$ , and figure 33  $d$ ,  $e$ , where the abscissas denote the time of observation in steps of 1 minute each. The initial time (0 minute) is frequently indicated. In curves  $a$  and  $b$ , 2 and 1 minutes, respectively, passed before the fringe reading could be taken. In curves  $d$  and  $e$ , however, with the advantage of the method of repeated filling, the reading could be made within 5 seconds, to this extent eliminating the initial diffusion. One may note that the curves are as a rule regular; but that certain discontinuities occur in the places marked by the arrow. They may be due to release from the surface viscosity of the mercury, as the gage was not tapped; or they may result from different components of the coal-gas diffusing out at different rates. Thus, in the curve  $d$  there are three branches, the last being nearly straight. In curve  $e$ , however, there is an actual break at  $br$  and some adhesion and slip in the gage under so gradual a release is more probable. It would seem to make little difference here; for the densities are determined from the beginning and the diffusion coefficients from the ends of the curves. In case of curves  $c$ ,  $d$ ,  $e$ , rubber-pipe connectors were so far as possible avoided.

As the curves  $a$ ,  $b$ ,  $c$  (fig. 32) begin with initial diffusion (1 to 2 minutes), they are less available than figure 33,  $d$  and  $e$ , for these (multiple filling) begin with the same pressure (equivalent to  $s=168$  scale-parts of displacement) and after 15 minutes show respectively  $s=83$  and 81 scale-parts of pressure, and this in spite of the break in curve  $e$ , which must have been in the gage. From equations (5 to 7),  $\Delta x=0.00425$  cm. whence  $\Delta p=35.7$  dynes/cm.<sup>2</sup>, and  $\Delta \rho=0.000535$ . The density of air being (at  $25^\circ$  and 76.4 cm.)  $\rho'=0.001190$ , it follows that the gas density observed is  $\rho'-\Delta \rho=0.000655$ ; or under normal conditions about  $\rho=0.000712$ . This is correct in order of value, but as yet

problematical. To improve it,  $\theta$  in equation (4) must be measured and the interpolation equation (5) tested. The other curves (*b*, *c*) gave values of the same order, after the initial diffusion was estimated.

The endeavor was now made to correct both the provisional values of  $\Delta x$  and  $\cos \theta$ . In the latter case the angle between incident and emergent rays was  $3.6^\circ$  in excess of  $90^\circ$ , so that the values of  $\theta = 46.8^\circ$ . This is equivalent to a diminution of  $\rho$  by 3.2 per cent. Again a long-range comparison was made between  $\Delta x$  of the slide micrometer and the  $\Delta s$  of the ocular micrometer, by applying steps of pressure to one shank. These results are given in figure 34 for increasing and decreasing pressures. It is interesting to note that the ratio is the same, but the lines differ by a lag of two or three ocular scale-parts, or a little over a fringe. I at first inferred this to be merely a question of the time needed for the final flow to equilibrium as the pressure vanishes. To have waited for its full disappearance would have introduced temperature



disturbances into the closed region. The ratio given by the new graph is  $\Delta x = 10^{-6} 21.5 \Delta s$ , which accounts for an addition 4.4 per cent. Thus the difference becomes  $\Delta \rho = 10^{-6} 2.94 \Delta s = 0.000494$ , whence  $\rho = 10^{-6} 696$ , or, reduced to normal conditions,  $\rho = 0.000757$ .

Some error may reside in a frictional temperature effect of the gas passing *tt*, and temperature should preferably be measured in the tube; but the following paragraphs indicate pronouncedly that a static error referable to surface tension of the mercury in the gage needs attention.

A few incidental results on different days may be recorded. The first at  $23.5^\circ$  and 75.1 cm. of the barometer gave  $\Delta s = 166$ , whence the reduced  $\rho = 0.000758$ . Another at  $22.5^\circ$  and about the same barometer gave  $\rho = 0.000755$ . In all cases it is best to set the screw micrometer so that the displaced fringes may be nearly at zero. Measurement is then made directly in terms of  $\Delta x$ , while  $\Delta s$  is a small correction. This avoids the serious use of the relations  $\Delta x$  and  $\Delta s$  of the two micrometers, a quantity which varies with incidental conditions of fringe size. It is even better to take the limit of the ocular throw of fringes as the zero of the slide micrometer.

27. **Equations for diffusion.**—If  $\partial\rho/\partial t = A^2\partial^2\rho/\partial x^2$ , where  $\rho$  is the density of the gas at a time  $t$  and at a distance  $x$  from the end of the tube, the coefficient of diffusion is  $a^2$  in [cm.<sup>2</sup>/sec.]. The problem in case of the tube is practically that of diffusion in one direction in infinite space bounded on one side by a plane, at which  $\rho=0$  at all times. Initially  $\rho=\rho_0$  was constant throughout all gas-filled space. The general solution, given by Riemann (see Partielle Differentialgl., Hattendorf, 1876), for the present particular case leads to

$$(8) \rho = \frac{2\rho_0}{\sqrt{\pi}} \int_0^{x/2a\sqrt{t}} e^{-\beta^2} d\beta = \frac{2\rho_0}{\sqrt{\pi}} \left\{ \frac{x}{2a\sqrt{t}} - \frac{x^3}{3(2a\sqrt{t})^3} + \frac{x^5}{5.2(2a\sqrt{t})^5} - \dots \right\}$$

Since for the vertical tube  $d\rho = \rho g \cdot dx$ , the pressure value is found on integration for a tube-length  $x$  to be

$$p = \frac{2\rho_0 g}{\sqrt{\pi}} \left( \frac{x^2}{2(2a\sqrt{t})} - \frac{x^4}{12(2a\sqrt{t})^3} + \frac{x^6}{60(2a\sqrt{t})^5} - \dots \right)$$

or, on replacing  $\rho_0 g x$  by  $p_0$ , the initial pressure,

$$p = \frac{p_0}{\sqrt{\pi}} \frac{x}{2a\sqrt{t}} \left( 1 - \frac{x^2}{24a^2t} + \frac{x^4}{480a^4t^2} - \dots \right)$$

Thus, if  $l$  is the tube-length,

$$a = \frac{1}{\sqrt{\pi}} \frac{p_0}{p} \frac{l}{2\sqrt{t}} \left( 1 - \frac{l^2}{24a^2t} + \frac{l^4}{480a^4t^2} - \dots \right)$$

seeing that approximate values of  $a$  suffice in the correction terms.

A subsidiary explanation is needed here. If  $\rho'$  is the air density and  $\rho$  the density of mixed air and gas in the tube  $tt'$ ,  $\Delta\rho = \rho' - \rho$ , where  $p = Hg\Delta\rho$  at the U-gage. But  $\rho = \frac{B-B_h}{B} \rho' + \frac{B_h}{B} \rho_h$ , if  $\rho'$  and  $\rho_h$  are the gas densities at the barometric pressures  $B$ , whereas  $B$  has fallen for the gas to  $B_h$  by diffusion. Hence  $\Delta\rho = \frac{B_h}{B} (\rho' - \rho_h)$ , and therefore

$$p = Hg\Delta\rho = H \frac{B_h}{B} (\rho' - \rho_h)$$

$$p_0 = H \frac{B}{B} (\rho' - \rho_h)$$

whence

$$\frac{p}{p_0} = \frac{B_h}{B} = \frac{\rho_h t}{\rho_0}$$

The ratio of U-gage pressures is the same as the ratio of the barometric pressures which determine the dilution of the gas after  $t$  seconds of diffusion at constant temperature. It is here tacitly assumed that the  $a$ 's for diffusion of  $H_2$  into air and of air into  $H_2$  are the same. The subject is resumed in § 41.

But since  $p$  is nearly proportional to the fringe displacement  $s$ , the first term reduces finally to

$$a = \frac{1}{\sqrt{\pi}} \frac{s_0}{s} \frac{l}{2\sqrt{t}} (1 - \text{etc.})$$



It is thus merely necessary to observe the initial fringe displacement  $s_0$  and a final displacement  $s_2$ , after say 15 minutes, to obtain  $a^2$ , the diffusion coefficient.

In the above experiment, however, diffusion takes place at both ends of the tube, which is equivalent to using two tubes of length  $l/2$ . This reduces the main term one-half (since  $p_0$  and  $l$  are both reduced), so that

$$a = \frac{1}{\sqrt{\pi}} \frac{s_0}{s} \frac{l}{4\sqrt{t}} \left( 1 - \frac{l^2}{96a^2t} + \frac{l^4}{7680a^4t^2} - \right)$$

would be used in the experiments.

**28. Data for diffusion.**—The curves, figure 33,  $d$  or  $e$ , are available. Taking the former with  $t=15$  minutes=900 seconds,  $s_0=168$ ;  $s=83$ ;  $l=68.4$  cm., the first term is

$$a' = \frac{1}{\sqrt{\pi}} \frac{s_0}{s} \frac{l}{4\sqrt{t}} = \frac{1}{1.77} \frac{168}{83} \frac{68.4}{4 \times 30} = 0.6508$$

whence

$$a'^2 = 0.4236$$

The term

$$-l^2/96a^2t = -(68.4)^2/(96 \times 0.42 \times 900) = -0.1278$$

The term

$$l^4/7680a^4t^2 = (68.4)^4/7680 \times (0.42)^2 \times (900)^2 = 0.0196$$

And the correction therefore

$$1 - 0.1082 = 0.8918$$

so that  $a=0.580$  and  $a^2=0.337$ .

The datum is again of the right order of value, but probably in need of the same kind of corrections already instanced in the preceding paragraph. In particular, the diffusion from both ends not strictly identical is objectionable.

**29. Hydrogen. Density.**—The next test made was possibly too severe for the method, for the very rapid initial diffusion of hydrogen will facilitate an escape of gas from the quill tube before the fringes come to rest (5 seconds). Whether from this cause or whether from some other error still to be detected, the hydrogen data for  $\rho$  came out much too large. It is curious that the initial fringe displacements in any given experiment are remarkably constant (to about 1 part in 300), even when the quill tube is successively refilled 25 to 50 times.

The hydrogen was generated by sheet zinc with dilute  $H_2SO_4$  in a Kipp apparatus and passed directly through a cotton filter into the quill tube. An example of results obtained on different days follows.  $\rho'$  refers to air,  $\rho$  to hydrogen corrected for moisture,\*  $\rho_0$  refers to normal conditions. Tube-length 68.4 cm. (Table 4.)

---

\* In winter for dry air and wet  $H_2$ ,  $\rho_h (B - \pi)/B = \rho_a - \rho_w - C\Delta x$ ; in summer for wet air and  $H_2$ ,  $\rho_a - \rho_h = (BC/(B - \pi))\Delta x$ .

The values of  $\rho_0$  are thus about twice too large and vary erratically from day to day. The presence of 3 or 4 per cent of  $\text{H}_2\text{S}$  would account for the excess value, but so much is improbable. Temperature, which should be measured in the quill tube, would account for some slight variations. The optic flatness of the plates of the interferometer may not have warranted the large  $\Delta x$  displacement. A value of  $\theta = 40^\circ$  in the first three experiments in place of  $46.8^\circ$  taken would have given a correct order of value, but this is out of the question. The rapidity of initial diffusion, already referred to, may be mentioned in explanation. The compression of the volume of air in the gage is negligible. The displacement of fringes on opening and closing the cock did not exceed  $\Delta s = 10$  or  $\Delta x = 10^{-6} \times 215$  cm. Hence if the gage reservoir is 10 cm. in diameter and 1 cm. deep, while the quill tube is but 0.3

TABLE 4.

Date.	Temp.	Bar.	$\Delta x \times 10^3$	$\Delta \rho \times 10^6$	$\rho' \times 10^6$	$\rho \times 10^6$	$\rho_0 \times 10^6$	$10^3 \Delta s$ deficient.
	°	cm.	cm.					
Feb. 18	26.0	77.0	7.25	993	1196	179	193	0.87
Feb. 20	24.5	75.2	7.30	999	1174	155	170	.66
Feb. 21	23.5	75.3	7.06	966	1179	195	211	.94
Feb. 22	23.8	76.0	†7.10	1005	1189	163	178	.60

†  $\theta$  changed to  $45^\circ$ ;  $\Delta \rho = 0.1415 \Delta x$  here; in other cases  $\Delta \rho = 0.1370 \Delta x$ .

cm. in diameter, the equivalent length  $\Delta l$  of quill tube would be  $\Delta l \times 0.07 = 10^{-6} 78 \times 215$  or  $\Delta l = 0.24$  cm. when the total length is  $l = 68.4$  cm.

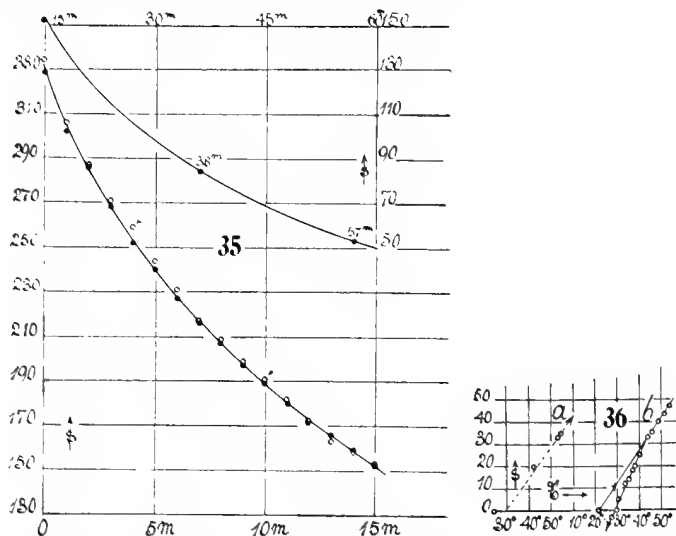
Taking the behavior as a whole, it appears, in spite of these minor misgivings, as if the initial pressures or thrusts were not fully given by the gage, but in part resisted, for instance, by capillary counterforces of the mercury surface. Moreover, the mercury was old and no longer quite bright. In fact, if we compute backward from the known density of hydrogen ( $\rho_0$ ), the values of  $\Delta x$  in the table are on the average 0.00077 cm. too small. This is the  $\Delta x$  equivalent of the capillary reaction, and since  $\Delta h = \Delta x \cos \theta$ , the corresponding pressure would be 0.00054 cm. of mercury. In § 31 below a reaction of the same order is encountered in measuring the relatively small  $\Delta x$  observed when warm air is compared with cold air, so that the reaction is actually in a measure static. It was thus necessary to recharge the U-gage with fresh pure mercury preliminarily, as the reaction would seem to be associated with the dulled surface of the metal.

**30. Diffusion of hydrogen.**—Two series of experiments made several days apart are given in figure 35, the ordinates being ocular scale-parts  $s$ , equivalent to  $21.5 \times 10^{-9}$  cm. each ( $\Delta x = 10^{-6} \times 21.5 \Delta s$ ). Considered as a whole, the agreement is quite satisfactory, although the former hold and release of the gage is again apparent. One of the series was prolonged 57 minutes, the fringe displacement being still 50 scale-parts. Even after several hours, the presence of  $\text{H}_2$  in the open tube was quite apparent. If the observable initial density

is too large and the initial pressure therefore too small, the coefficient of diffusion will also come out too small, and that is the case. We shall have in the two cases for a time interval of 15 minutes

$$t=0 \text{ sec. } s_0 = \frac{334}{328} \quad t=900 \text{ sec. } s = \frac{153}{152}$$

The  $l=68.4$  cm. is the same as above. The ratio  $s_0/s$  is thus 2.18 and 2.16 respectively, so that the mean 2.17 may be taken. This gives for the first term of the diffusion equation  $a'=0.698$ , whence  $a'^2=0.487$ . The first term in the correction is  $-0.1112$ ; the second  $+0.0148$ , whence  $a=a' \times 0.904=0.631$  and therefore  $a^2=0.398$ . This, as was anticipated, is too small, the standard value being near 0.66. The initial  $s_0$  falls short, as before, but the essential



discrepancy lies in the hypothesis, *i. e.*, the upper mouth of the quill tube is too much constricted by the stop-cock and hence the assumption of two identical half tubes is not valid. The true value of  $a$  must therefore lie somewhere between  $a=0.631$  and twice this value. It is actually 0.81, which indicates the diminished diffusion (one may estimate it as only about 17 per cent) at the top. Again, when  $a$  and  $l$  increase together, the value of the parenthesis in the equation for  $a$  remains unchanged. Computed for diffusion at the lower end only, the result after 15 minutes is  $a=1.396 \times (1-0.1112+0.0148)=1.262$ ; after 30 minutes,  $a=1.544(1-0.0454+0.0024)=1.544$ ; after 60 minutes about  $a=1.9$ . The equation, therefore, does not here respond adequately to the observed occurrences, as a whole, in the lapse of time.

**31. Coefficient of expansion of air.\***—By surrounding the tube  $tt'$ , figure 31, with a water or steam jacket, the expansion of the air within the quill

\* §§31, 32, 33, are a digression, and contain experiments made to throw light on the gage discrepancy in question. The subject is resumed in §34.

tube should be determinable. This was accordingly tried, using a heavy brass tube 2 cm. in diameter for the jacket and placing a thermometer and stirring apparatus within the brass envelope. The mixture was made more thorough by siphoning the water from lower to higher levels.

In the first experiment (fig. 36, graph *a*) the outside of the brass jacket was directly heated by a burner and readings taken in steps of temperature at the ocular micrometer. Contrary to expectations, this curve is roughly linear, but its slope is only 1.4 scale-parts per degree centigrade. In this case the fringes were larger than above, so that  $\Delta x = 10^{-6} \times 15 \Delta s$ , where ( $\alpha$  is the coefficient of expansion)

$$\alpha = \frac{\Delta \rho / \rho_0}{\Delta t} = \frac{\rho_m \cos \theta}{\rho_0 H} \frac{\Delta x}{\Delta t} = 109 \frac{\Delta x}{\Delta t} = 10^{-3} \times 1.63 \frac{\Delta s}{\Delta t}$$

Thus the coefficient found is but  $\alpha = 0.0024$ .

A number of subsequent experiments indicated that  $\alpha$  was always small if measured in a temperature-rising series, but approached a normal value if measured on cooling. Figure 36, curve *b*, shows a case of this kind. To guard against incidental temperature disturbance, the compensating cold-air tube was placed at a distance and connected with  $\frac{1}{8}$ -inch lead pipe with its shank of the U-tube. It will be seen that in the up-going branch the curve rises with almost the same slope as before, so that  $\alpha = 0.0024$  here also. The down-going slope soon becomes steeper. Hence  $\Delta s / \Delta t = 2.15$ , so that  $\alpha = 0.00163 \times 2.15 = 0.0035$ , which is a closer approach to the standard value, but still definitely short of it.

Although the curve *b* runs below  $s=0$ , on further cooling in the lapse of time, the micrometer zero was nevertheless quite regained. Thus there is something here cyclic and viscous in character. As one can hardly fancy any difficulty for the heat to get through the thin quill tube, the thrusts on the mercury surfaces in the gage are met by an apparent static resistance there. On cooling these relations are reversed. What is rather striking is the parallelism of the up-going curves *a* and *b* in spite of the deficiency, particularly as all the other experiments behaved similarly.

Taking the work as a whole, it seems as if the above capillary resistance to thrust is effective here also, so that the pressures, if increasing, are not fully registered in a depression of the surface of the U-gage. A few experiments were thereafter made with a steam jacket. In the first the heating was done too near the interferometer, so that a displacement of fringes occurred. The zero was therefore taken after the exposure to  $100^\circ$ . The results were  $\Delta x = 0.00171$  cm. for a rise of temperature from  $25^\circ$  to  $100^\circ$ , so that

$$\alpha = 109 \frac{0.00171}{75} = 0.00248$$

In the second the fringes returned to zero before and after the exposure to  $99.7^\circ$  (boiling-point); but the fringe displacement was only equivalent to  $\Delta x = 0.00145$ , so that

$$\alpha = 109 \frac{0.00145}{72.7} = 0.00218$$

Both values are as usual too small. Curiously enough, no fault could be found with the technique in the second, which is the smallest, the heating apparatus, etc., being placed at a distance. The fringe displacement should have been equivalent to 0.00247 cm. or 4.94 scale-parts in place of the 2.9 obtained. The deficiency is thus 2 scale-parts or  $\Delta x = 0.001$  cm.

This difference tends to be static. If we turn again to the case of hydrogen (§ 29, with the same constants),  $\Delta p$  is roughly  $10^{-4}$  too small, so that the observed  $\Delta x$  is  $10^{-4}/0.1415 = 0.7 \times 10^{-3}$  cm. short of its true value, which is even less than the discrepancy just considered, although the hydrogen  $\Delta x$  is 5 times larger.

**32. Vapor pressure. Hygrometry.**—A few other incidental experiments were made with the old gage, as follows: To determine the atmospheric vapor-pressure, dry air and wet air were alternately pumped through the tube  $tt'$ , figure 31. In the latter case the air was passed in a tube over wet filter-paper. As but a small fringe displacement is to be expected, the method is not good, for there is considerable commotion of fringes incidental to the pumping, so that the zero is not quite trustworthy. Many alterations of the kind specified gave a mean value of about 4 scale-parts as the excess pressure for wet air at  $23.8^\circ$  and 75.3 cm. of the barometer. Hence  $\Delta p = p' - p = p' - \left( \frac{p - \pi}{p} p' - p_w \right)$  if  $\pi$  is the vapor-pressure and  $p_w$  the saturation vapor density of water-vapor at  $23.8^\circ$ . Thus

$$\Delta p = \frac{\pi}{p} p' - p_w = \Delta x \cos \theta_{pm} / H = 0.1415 \Delta x = 10^{-6} 2.1 \Delta s$$

if  $\Delta x = 10^{-6} 15 \Delta s$ , as here found. Hence for  $\Delta s = 4.5$ ,  $\Delta p = 10^{-6} 2.1 \times 4.5 = 10^{-6} 9.4$ , and

$$p_w = \frac{2.22}{75.3} 0.00118 - 10^{-6} \times 9.4 = 10^{-6} \times 25$$

The actual saturation vapor density is  $10^{-6} \times 22$ , which is as close as one can expect to come.

Repeating these experiments at some length in the summer time, no certain fringe displacement could be detected equivalent to the alternate passage of dry air ( $\text{CaCl}_2$ ) and of wet air (bubbled through water) through the tube. The computed displacement should have been over  $\Delta s = 20$  scale-parts. I failed to detect a reason for this persistently negative result, unless it is much more difficult to dry the tube than I anticipated. Heating the tube was of course out of the question.

**33. Gage tests by direct compression.**—Measurements of this kind were made when I first used the interferometer U-gage (Carnegie Inst. Wash. Pub. 310, p. 2, 1921), but only cursorily. The method consists in closing one shank of the U-tube and compressing the air within by advancing a fine-threaded thin screw by a definite number of turns. Unfortunately, the closed region is a sensitive air thermometer and the results obtainable in a steam-

heated room will show a cyclic progress due to the slight change of temperature. Figure 37 gives data of this kind, the abscissa showing the number of turns of screw and the ordinates  $\Delta x$  the displacement of the slide micrometer to bring the fringes back to zero. Ascending and descending series are indicated by arrows. I worked as quickly as the micrometer could be set, and though the zero in  $\Delta x$  was finally nearly regained, the curves are cyclic.

Figure 38 (decreasing pressure positive) summarizes corresponding results when the room was unfavorable. In the ascending branch the rate is  $10^{-6}$  575 cm. per turn before the break at  $a$ , where the fringes were incidentally shaken. In the return branch there is initially a kind of back-lash, after which the uniform rate  $10^{-6}$  680, much higher than before, appears. Many other examples of the same kind might be given, of which figure 37 is the best available.

The screw had a pitch of  $\Delta l = 0.073$  cm. and its mean section was  $a = 0.204$  cm.<sup>2</sup> Thus for one turn the volume decrement of the region is  $dv = 0.204 \times 0.073 = 0.0149$  cm.<sup>3</sup> On the other hand, the area of the shank was (diameter 9.5 cm.)  $A = 70.9$  cm.<sup>2</sup>, and its volume excursion therefore  $dV = 70.9 \Delta x \cos \theta / 2$ , since but half the total head  $\Delta h = \Delta x \cos \theta$  is allotted to one side. At constant temperature we may write

$$-\frac{dv}{V} + \frac{dV}{V} = \frac{dp}{p} = \frac{dh}{H} = \frac{\Delta x \cos \theta}{76}$$

if  $V$  is the total volume of the closed region and  $H$  the barometric height. If now we eliminate the common area

$$-\frac{dV}{V} = \frac{dh}{2h}$$

where  $h$  is the height of the cylindrical volume of the shank. If  $h$  can be estimated

$$V = \frac{adl}{\Delta x \cos \theta} \frac{1}{1/2h + 1/76}$$

where  $dl$  is the advance of the screw of cross-section  $a$ . This gives a fairly good value of  $V$ ; but the height  $h$  is difficult to measure for the closed shank. If, on the other hand,  $h$  is not introduced, the equations lead to

$$-V = (76A/2) \left( 1 - \frac{2adl}{A\Delta x \cos \theta} \right)$$

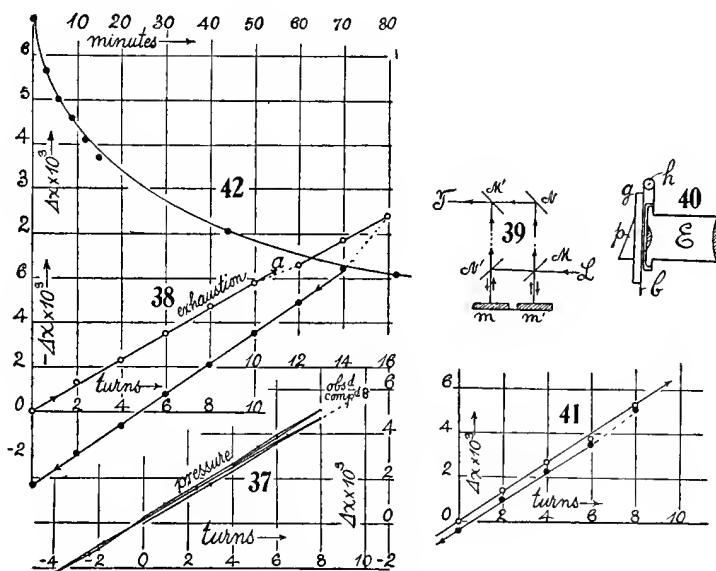
but the observations are not sharp enough to accurately evaluate the last factor, which is nearly zero. Thus, in the experiment and from figure 37, per turn of screw  $a = 0.204$  cm.<sup>2</sup>;  $dl = 0.073$  cm. (pitch);  $\theta = 45^\circ$ ;  $A = 70.9$  cm.<sup>2</sup>;  $\Delta x = 0.000595$  (cm./turn); whence

$$2adl/A\Delta x \cos \theta = 0.9986$$

and the parenthesis is thus but 0.0014 and is made up of errors of observation in the relatively large number 0.9946. In other words, the small piston  $a$  and the large piston  $A$  have moved as if the air were an incompressible fluid, if figure 37 is used for  $\Delta x$ .

In fact, if one accepts an estimate of  $V = Ah = 70.9 \times 1.5 \text{ cm.}^3$ , the corresponding value of  $\Delta x$  comes out  $10^6 \Delta x = 571 \text{ cm.}$  Figure 37 shows that this lies quite within the range of thermal variation and could easily have been taken. Hence no discrimination can be carried out in this way unless the temperature conditions are ideal. Moreover, figure 37, while containing thermal cycles, curiously enough suggests no static effect in the values of  $\Delta x$  observed. Thus this leaves the whole question at issue open, and I am at a loss how further to approach it, except possibly with the change of apparatus indicated.

**34. U-gage with fresh mercury.**—The disquieting feature of the above work with hydrogen, viz, that the deficient pressures might be referable to



viscous or capillary resistances in the old mercury of the U-gage, induced me to introduce a fresh change of distilled mercury. A larger quantity, moreover, was taken, which makes the mercury more mobile than the shallow disk-like charge. The fringes are thus harder to read, but the quivering mercury surface is more liable to conform to a true reading. The fringes were at first hard to find. In the quadratic interferometer the spectrum fringes (in view of the fact that the component rays pass through the half-silvers  $M, N', M'$ , fig. 39, twice) are too faint to be seen if very small and if a prism grating is used in front of the objective of the telescope at  $T$ . The visibility can be very greatly improved, however, by placing the grating in front of the ocular. For this purpose prism grating  $pg$ , figure 40, is attached to a brass plate hinged at  $h$  to a second plate clamped to the edge of the ocular. The plates are perforated. When not needed, the grating  $pg$  is therefore swiveled

out of range and the fringes of white light become available. When  $pg$  is used the collimator is provided with a slit parallel to the edge of the prism. In the case of white light the slit is widened at right angles to the fringes, so that they may play across the plate micrometer which now replaces the slit. An ocular plate micrometer is not desirable, as the telescope must frequently be shifted.

The advantage of the spectrum fringes, or channeled spectra, lies in their range of visibility. They are easily identified long after the white fringes have left the field. The type of spectrum fringes which usually appear in this adjustment is fan-shaped, as they open out from violet to red. Those of maximum size and coinciding with the white fringes are normal to the slit. From this they diverge on both sides symmetrically, growing continually finer, until the hair fringes are nearly parallel to the slit.

The behavior of the new gage when tested with the air-compression screw was apparently better than the old gage. One example of results is given in figure 41, in which the ascending and descending rates are  $\Delta x = 0.00067$  cm. and  $0.00066$  cm. per turn of screw. Nevertheless, between the two graphs there is something akin to the former back-lash, which amounts on the average to nearly  $\Delta x = 0.0005$  cm. Granting that by reason of the inevitable thermometer errors of a closed region these data are not very searching, the breadth of loop here obtained is nevertheless of the order of the discrepancy of the data in tables for  $H_2$  gas (§ 29), the mean deficiency in the old gage for thrusts being  $\Delta x = 0.00077$ . It thus begins to look as if an increment of the order of about  $0.0005$  cm. of mercury (say  $7$  dynes/cm.<sup>2</sup>) is not a gravitational resistance when obtained with the mercury gage, owing to the appearance of capillary and similar surface forces. This critical question will have to be left for conditions of constant temperature such as occur in the summer only.

**35. New quill-tube experiments with hydrogen. (Fresh mercury.)**—The endeavor was now made to obtain better results for hydrogen by aid of the new gage. In the first series the glass quill tube ( $l=68.4$ ,  $2r=0.3$  cm.) was again used, a number of useful improvements having been added. The essential data are given in table 5.

TABLE 5.

Bar.	$t$	$\Delta x \times 10^4$	$\Delta p \times 10^6$	$\rho_t \times 10^6$	$10^6 \rho_0$	Deficiency $\Delta x \times 10^4$
cm.	.	cm.				cm.
74.9	23.6	68.5	969	183	201	8.6
	24.0	70.5	998	151	160	5.9
	24.0	70.0	991	158	174	6.5
	24.0	70.0	991	158	174	6.5
	24.0	68.0	976	173	190	7.8

The mean of these results, taken independently at different times of the day, is  $\rho_0 = 0.000181$ , practically the same value as that obtained above (§ 29,



$\rho_0 = 0.000188$ ), the difference being referable to the  $\cos \theta$  of the interferometer, which is here newly adjusted. Hence the change of gage, the supply of fresh pure mercury, etc., has made no appreciable difference in the run of density values obtained. The mean deficiency in  $\Delta x$  is again about  $0.71 \times 10^{-3}$  cm., which compares closely with the  $0.77 \times 10^{-3}$  cm. above. This means that a pressure of about  $5 \times 10^{-4}$  cm. of mercury is borne by the capillary forces of the U-gage and does not appear in the gravitational or fringe displacement of the surfaces of the mercury.

In case of the first experiment of the table, the diffusion of the gas in the quill tube into the air was followed for over 80 minutes. The results are given in figure 42. The slide micrometer alone was used, the fringes being brought back to the fiducial mark in the ocular at the times given in the figure. It is interesting to note that after an hour and a half considerable hydrogen pressure is still evident in the charged tube. The coefficient of diffusion from both ends of the tube would naturally be low as before; but the constants of the curve (fig. 42), if taken for diffusion from the bottom of the quill tube only, were much nearer the correct datum, 0.81 (the coefficient being  $a^2$ ), than heretofore. The march of  $a$  in the lapse of time, though still apparent, is reduced. The data are

$t = 15^m$	$a = 1.160$	$(1 - 0.161 + 0.031) = 1.009$	$\Delta x_0 / \Delta x = 1.80$
$t = 30^m$	$a = 1.133$	$(1 - .084 + .008) = 1.046$	2.49
$t = 60^m$	$a = 1.434$	$(1 - .025 + .001) = 1.434$	4.56

One may note in relation to the sequel, §§ 43, 46, that  $a$  has not fallen below 1.

**36. Experiments in wider and longer tubes (gas-pipes).—**The results obtained when  $\frac{1}{8}$ -inch and  $\frac{1}{2}$ -inch iron gas-pipes held the charge of hydrogen were as follows:

Tube.	Bar.	$t$	$\Delta x \times 10^4$	$\Delta p \times 10^6$	$\rho_1 \times 10^6$	$\rho_0 \times 10^6$
$2r = 0.5$ cm. $l = 70.5$ cm.	75.1	.				
1.6 cm. 74.0 cm.	75.1	25.1 26.2	72.5 75.0	996 975	151 157	168 174

These data for about the same length of tube as before are of the same order of value. It was interesting to note that even for the wide tube (diameter 1.6 cm.), the experiments as such proceeded smoothly. The question of a more critical import, however, would be answered by longer tubes; for with these the true density should be approached more closely as the length is greater, seeing that the static character of the capillary error had been retained. This proved to be the case, as shown by the next table.

Tube.	Bar.	$t$	$\Delta x \times 10^4$	$\Delta p \times 10^6$	$\rho_1 \times 10^6$	$\rho_0 \times 10^6$	$\frac{\Delta p}{\text{cm. Hg.}}$
$2r = 0.5$ cm. $l = 158$ cm.	cm. 75.2 75.2	" 20 20	170.0 173.5	1,034 1,056	141 119	153 129	0.0120 .0122

In the first experiment the freshly made hydrogen probably still contained a little air. As stated above, the pipe was repeatedly refilled by turning the three-way cock. Fringe displacements of such readings are remarkably constant; but even if the cock is closed for but a minute, there is considerable throw of fringes on opening, showing that the initial diffusions, together with temperature accommodations, are marked.

Unfortunately, to accommodate this long tube below the interferometer, it was necessary to poke it through the floor into the basement. As a result the temperature (winter) varied from  $15^\circ$  below to  $25^\circ$  above the floor, so that a mean value was taken. The static discrepancy is of the same order as before, about 0.0005 cm. The total pressure difference is roughly  $\Delta p = 0.012$  cm. of mercury here.

Thus it seems that for pressures below  $\delta h = 0.0005$  cm. of mercury, or the corresponding  $\Delta x$  increments, little can be done but to add this discrepancy  $\delta x$  to the  $\Delta x$  obtained. This  $\delta x$  in other words is the capillary or viscous resistance which attaches itself to the gravitational resistance of the depressed mercury column of the U-gage. Hence our equations would read at the given temperature  $t$  ( $\rho_t$  to be corrected for vapor-pressure)

$$\rho_t = \rho_a - C(\Delta x + \delta x) - \rho_w$$

where  $\rho_w$  is the density of water vapor at  $t$ , if present,  $\rho_a$  the density of air, and  $C = \rho_m \cos \theta / H$  for the tube-length  $H$ . In the last series ( $\delta x = 0.0006$  accepted)

$$\begin{aligned}\rho_t &= 0.001192 - 0.0608(0.0173 + 0.0006) - 0.000017 = 0.000083 \\ \rho_0 &= 0.0000897\end{aligned}$$

which is nearer than one would expect to come, considering the variable temperature  $15^\circ$  to  $25^\circ$  of the pipe, the non-rigorous purity of the gas, and the capricious character of the correction  $\delta x$ , the latter being not smaller than 0.0005 cm. as taken, and may run to 0.0007. The correction for vapor-pressure would reduce  $\rho_0$  a few per cent. To minimize the capillary effect, the diameter of the shanks of the U-tube was made large (10 cm.). There may be a further advantage in diminishing the size of mirror (glass plate) anchored in the middle of the vat. Another feature is not to be overlooked, viz, in a gage, like the present, not filled in vacuo, the mirrors do not move rigorously in parallel. Hence a small obliquity error is introduced.

If the mirror on the slide micrometer is not quite plane parallel, but a wedge of small angle  $\phi$ , a path difference of  $(\mu - 1) \phi \tan \theta \cdot \Delta x$  would be introduced. This, however, from the smallness of both  $\phi$  and  $\Delta x$ , is negligible.

**37. Capillary gage correction,  $\delta x$ , in case of hot air.**—It has already been inferred that this correction is the same in the hydrogen and hot-air experiment, though the pressures  $\Delta x$  are widely different, relatively. The measurement of the coefficient of expansion of air is thus an extreme test; for here the  $\delta x$  is over one-third as large as  $\Delta x$ . Conformably with the data already obtained (§ 31), the coefficient must thus come out much too small. If we write

$$-(d\rho/\rho)/d\tau = 1/\tau \text{ and } 1/\tau_0 = (1/\tau)(\rho_0/\rho)$$

at constant pressure, where the subscript refers to zero centigrade, the coefficient of expansion may be computed as

$$1/\tau_0 = (\rho_0/\rho) (d\rho/d\tau)/\rho = a$$

A new apparatus was used, consisting of a vertical  $\frac{1}{8}$ -inch gas-pipe 70 cm. long, open below and communicating with the U-gage above, as in figure 31. This pipe was surrounded by a steam jacket of  $\frac{3}{4}$ -inch gas-pipe, the whole firmly screwed together, with an addition of other improvements.

In the first experiment with the room temperature at  $27^\circ$  and  $\delta x = 0.0006$  cm. accepted, the data were  $\Delta x = 0.0015$ ,  $\Delta x + \delta x = 0.0021$  cm.,  $\Delta \tau = 73^\circ$ ,  $\rho/\rho_0 = 0.90$ ,  $\rho = 0.00117$ ; whence  $\Delta \rho = 0.137(\Delta x + \delta x) = 0.000288$ ;  $(\Delta \rho/\Delta \tau)/\rho = 0.0034$ ,  $(\Delta \rho/\Delta \tau)/\rho_0 = 0.0037 = 1/\tau_0 = a$ , which is as near the coefficient of expansion as one may hope to approach conformably with the micrometer reading to  $\Delta x = 10^{-4}$  cm. An error of 3 or 4 per cent in the coefficient of expansion is to be expected from this source alone.

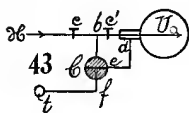
In a variety of subsequent experiments, values of  $a$  rather higher than the one given were found, so that capillary discrepancies as low as  $\delta x = 0.0004$  cm. may have been operative. But as the whole the presence of this quantity, of the order of values given, may in this particular work be regarded as substantiated, even for such small total density increments as are here in question ( $\Delta \rho = 3 \times 10^{-4}$ ;  $\Delta \rho = 2 \times 10^{-3}$  cm. of mercury).

**38. Diffusion in one direction only.**—In the above work, two discrepancies were left outstanding. One related to the diffusion from the top and bottom of the vertical quill tube under conditions not identical. Here, moreover, the possibility of practically exhausting the tube of its charge of hydrogen at its middle point is not to be overlooked. The other is the error of  $\Delta x$ , resulting from quasi-capillary phenomena at the mercury surface of the U-gage. These were counteracted by adding a correction  $\delta x$  to the  $\Delta x$  observed, and the group of experiments made seemed to conform to a nearly constant positive value of  $\delta x$ .

Two methods were now employed in the endeavor to remove these disturbances. These consisted in filling the whole system  $tCG$ , figure 31, of diffusion tube and shank of U-gage with the gas (hydrogen) to be tested; or if this should be inadvisable, to diminish the bore of the cock  $C$  to a mere crevice, while increasing the bore of the diffusion tube  $t$ . In such a case loss by diffusion at the top could be considered negligible.

The modification of the apparatus (fig. 31) is shown in figure 43, in plan, where  $H$  is the source of hydrogen,  $U$  one shank of the U-gage (closed),

$C$  the three-way cock,  $t$  the vertical diffusion tube. The influx pipe is branched at  $b$  and provided with two glass stop-cocks  $c$  and  $c'$ . If  $C$  is adjusted as in the figure,  $c$  and  $c'$  open, the gas fills the gage  $U$  first and then by the branch  $de$  and  $C$ , enters the diffusion pipe  $t$  and leaves at its open lower end. On completed filling,  $c'$  is permanently closed, after which  $t$  may receive  $H_2$  via  $bf$  by properly turning the cock  $C$ , and may be alternately



placed in connection with  $U$  only, as in figure 43 ( $c'$  being closed). The cock  $c'$  is as fine in bore as possible, as is also the cross-branch in  $C$ , thus preventing the rapid influx of gas into  $U$ , which might dislocate the fringes. Other devices were tried, but figure 43 sufficiently indicates the general method.

The attempt to flood the  $U$ -gage with hydrogen, no matter how carefully done, always resulted in a large displacement of the zero-point of the gage; and to my astonishment this displacement was now in the *opposite* direction to that obtained in the preceding (§ 37, etc.) paragraphs; *i. e.*,  $\delta x$  had changed from positive to negative values. In other words,  $\Delta x$  was now too large. This occurred so consistently that I was inclined to refer the effect observed to changed capillary properties of a mercury surface in an atmosphere of  $H_2$  as compared with the same surface in an atmosphere of air. But as these effects are always accompanied by a marked distortion of fringes, meaning that the mean inclination of the surface has changed, it is difficult to reach a trustworthy conclusion.

**39. Incidental results. Density.**—As all the diffusion experiments were preceded by density measurements, it is of interest to give these results separately, at the outset. In place of the density  $\rho_h$ , however, it will here be preferable to compute the micrometer displacement ( $\Delta x$ ), which should have been obtained for the hydrogen density  $89.6 \times 10^{-6}$  under normal conditions of temperature and pressure. The equation reads, at  $t$  degree,

$$\rho_h \frac{B - \pi}{B} = \rho_a - \Delta \rho - \rho_w = \rho_a - C \Delta x - \rho_w$$

whence

$$C \Delta x = \rho_a - \rho_h (B - \pi) / B - \rho_w$$

where  $B$  is the barometric pressure and  $\pi$  the vapor-pressure of saturated water-vapor,  $\rho_a$ ,  $\rho_h$ ,  $\rho_w$  the densities of air, hydrogen, and vapor all at the same temperature  $t$ . If  $\rho_a$  as in the following experiments is also moist,  $\rho_w$  disappears and

$$\Delta x = \frac{B - \pi}{BC} (\rho_a - \rho_h)$$

Thus it appears also that the rate at which  $\rho_h$  varies with  $\Delta x$  is roughly  $-C$ . Hence if the error of  $\Delta x$  is  $10^{-4}$  cm. and  $C$  is about 0.13 in these experiments, the effect on  $\rho_h$  would be  $10^{-5} \times 13$ . Since the density of  $H_2$  is below  $10^{-6} \times 90$ , this is an error of nearly 15 per cent. It will therefore be best to report the values of  $\Delta x$  as found, together with the value computed, as has been done together with the relevant data in table 6.

Thus the effect of flooding the  $U$ -gage with hydrogen is a relatively enormous displacement of the zero of fringes before and after the operation. Whenever this occurs, moreover, the  $\Delta x$  observed for the density measurement is correspondingly changed, and in the present case (unlike that of the preceding

experiments) in the direction of an increase of  $\Delta x$ , i. e.,  $\delta x$  is negative.\* As has been stated, this effect or the reversal of sign of  $\delta x$  might seem to be attributable to the behavior of a mercury surface in an atmosphere of hydrogen; but the experiment is so complicated and the data so capricious that no confidence can be placed in such an inference. When  $\Delta x$  is found without flooding and the zero before and after the measurement is the same, the values are reasonable. In two cases, series IV, third experiment, and series VI, first experiment,  $\Delta x$  is practically correct. In one case, series II, experi-

TABLE 6.

Tube 2.	Series.	Initial zero $10^4 \Delta x$ .	Final zero $10^4 \Delta x$ .	Observed $10^4 \Delta x$ .	Computed $10^4 \Delta x$ .	$\rho_a \times 10^6$ $\rho_h \times 10^6$	$\frac{(B-\pi)}{B}$ $C$	Remarks.
$l = 71$ cm. $2r = 0.7$ cm.	I	cm. 134	cm. 101	cm. 86	cm. 79	1,177 81.5	0.972 .1354	After diffus.exp't, H at U-tube.
	II	113	113	75	80	1,191 82.6	.974 .1354	Separate exp't, air at U.
	II	113	108	82	80	1,189 82.4	.974 .1354	After diffus.exp't, H at U.
	III	77	80	82	80	1,193 82.8	.975 .1354	Separate exp't, air at U.
	IV	107	83	82	80	1,192 82.7	.971 .1354	Separate exp't, H at U.
	IV	111	111	82	80	1,192 82.7	.971 .1354	After diffus.exp't, air at U.
	IV	121	121	78	78	1,183 82.1	.964 .1354	Sep. exp't, next day, air at U.
	V	119	119	84	81	1,179 81.8	.962 .1300	Separate exp't, air at U.
	V	119	120	84	81	1,179 81.8	.962 .1300	After diffus.exp't, air at U.
	VI	123	123	83	83	1,187 82.4	.974 .1300	Separate exp't, air at U.
	VI	127	57	91	83	1,187 82.4	.974 .1300	After diffus.exp't, H at U.
	VI	87	87	88	84	1,198 83	.975 .1300	Sep. exp't next day, air at U.

ment 1,  $\Delta x$  is deficient as in the earlier results. Usually it is in excess by  $2 \times 10^{-4}$  or  $3 \times 10^{-4}$  cm. After vigorous flushing, with much inevitable commotion of fringes (series I, and series VI, experiment 2) the excess may reach  $8 \times 10^{-4}$  cm. In the latter case the excess had not even vanished on the ensuing day ( $\delta x = 4 \times 10^{-4}$ ), though as a rule there is an apparent recovery after the hydrogen atmosphere around the mercury has been dissipated. When the zero is much displaced, the recovery is very obvious during the march of the ensuing diffusion and the fringes show increasing distortion. The diffusion data are then erroneous, as will presently be seen.

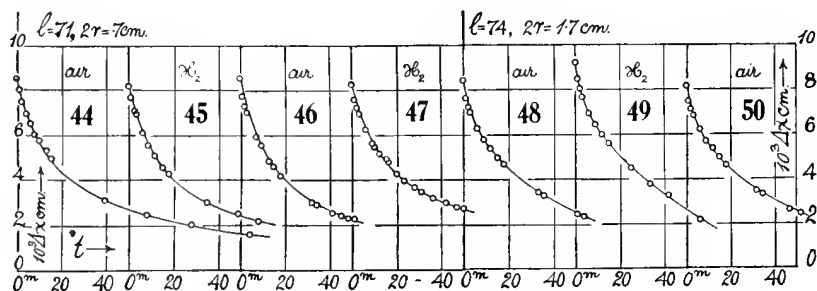
Obviously, therefore, the method of flooding the U-gage with hydrogen is not safely available. It is thus necessary to use a very fine perforation in

\* Since the U-gage has two surfaces, this merely means that  $\delta x$  is now positive on the other shank.

the cock *C* at the head of the diffusion tube and to make this as wide as practicable. In table 5 the second tube used had a diameter of 1.7 cm. and an area enormous in comparison with the crevice in the stop-cock above. A capillary-tube connection would be even preferable, if available.

**40. The same. Diffusion.**—The diffusion curves, of which seven examples are given in figures 44 to 50, require more searching examination. The curves, as a whole, when considered in relation to the behavior of an interferometer *U*-gauge, with the fringes successively placed at zero by a slide micrometer (displacement  $\Delta x$  at  $\theta=45^\circ$ ), are remarkably regular. When studied with more critical detail, however, they present many anomalies. Table 7 presents a number of these peculiarities.

In the first and second series, the cocks were of about 1 mm. bore as compared with the tube diameter of 7 mm. Curiously enough, the data here obtained are nearly as good as any of the following, in spite of later improve-



ments. The pressure ratios at the beginning and end of 50 minutes of diffusion are 3.18 and 3.30 respectively, pressures being proportional to the initial and final  $\Delta x$ .

In series III and IV the bore of the cocks was reduced to mere crevices, the same diffusion pipe being retained. In series III there must have been some incidental dislocation of fringes (marked †). The effect of this as it gradually vanishes is to increase the diffusion-rates spuriously. The same effect appears in the drop of  $\Delta x$  in 50 minutes.

In series V and VI, retaining the same fine-bore cocks, a wide diffusion tube was substituted. Series V is among the best of the lot. In series VI the commotion due to influx of  $H_2$  produces a condition similar to that in series III, but more marked. Series VII was made later. If we omit the cases marked (†), the ratio of  $H_2$ -pressure at the beginning and end of 50 minutes of diffusion has the mean value 3.19 for the thin pipe. It is rather disappointing that the laborious work of flooding the *U*-gauge and using fine-bore cocks has evidenced so little improvement on the results.

Inasmuch as the series VI is not trustworthy, a special series (VII) was investigated, using the original method of figure 31, but with a fine-bore

cock *C*. The attempt was made to connect *C* and *U* by metallic and by glass capillary tubes. It was found that diameters up to 0.5 mm. could not be used because of the viscosity of the gas. In fact, the *U*-tube behaved like a closed region with a wandering zero (Chap. I), and the results were worthless. A connecting-tube with a diameter exceeding 1 mm. was found essential. To guard against transpiration leakage, all rubber-tube connections, though used sparingly throughout the experiments, were painted over with soft sealing-

TABLE 7.—Data of diffusion measurements.

	Series.						
	I	II	III	IV	V	VI	VII
Initial zero, $x \times 10^4$ cm. ....	135	113	77	108	119	127	85
Final zero,* $x \times 10^4$ cm. ....	101	108	80	83	120	52	86
Temperature, ° C....	23.2	22.9	22.0	22.3	22.9	23.1	21.2
Initial reading, $\Delta x \times 10^4$ cm. obs. ....	86.0	82.0	†85.5	82.5	84.0	†91.5	81.0
Initial reading, computed .....	79.2	80.0	80.4	80.3	82.6	83.2	83.5
Final reading, $\Delta x \times 10^4$ cm., obs. after 50 minutes .....	27.0	24.8	22.5	26.7	25.0	26	25.0
$10^4 \times \Delta x$ drop in 50 minutes .....	59.0	57.2	63.0	55.8	59.0	65.5	56.0
Pressure ratio in 50 minutes .....	3.18	3.30	†3.80	3.10	3.36	†3.52	3.24
Mean $a$ (50 minutes). Air .....	1.111	.....	.....	.....	1.201	.....	.....
Atmosphere at U-gage	Air	H <sub>2</sub>	Air	H <sub>2</sub>	Air	H <sub>2</sub>	Air
Pipe-length, $l$ cm....	71	71	71	71	74	74	74
Pipe-diameter, $2r$ cm.	.7	.7	.7	.7	1.7	1.7	1.7
Glass-cock bore, cm.	.15	.15	crevice	crevice	crevice	crevice	crevice
Reading ( $\Delta x \times 10^4$ cm.) after 15 minutes .....	50.0	46.0	45.5	47.5	49.5	55.5	49.5
$\Delta x \times 10^4$ drop in 15 minutes .....	36.0	36.0	†40.0	35.0	34.5	†36.0	31.5
Pressure ratio (15 minutes) .....	1.72	1.78	†1.88	1.74	1.70	†1.65	1.64
Mean $a$ (15 minutes)	1.039	.....	.....	.....	1.037	.....	.....

\* The final zero, of course, was taken for the  $\Delta x$  data. † Referred to in text.

wax. Under these circumstances the observations of series VII (fig. 50) proceeded faultlessly, as appears in the zeros, which before and after the diffusion are practically the same. The displacement or pressure ratio 3.24 at the beginning and end of 50 minutes is nevertheless the same as the mean of series I and II. Hence the additional care taken seems to have been superfluous. Series V has an equally fixed zero; hence the pressure ratio 3.30, the mean of series V and VII, may be taken as holding for the wide diffusion tube (bore 1.7 cm.).

To compute the coefficient of diffusion,  $a^2$ , when the escape of hydrogen takes place at the lower mouth only, the equation

$$a = \frac{\Delta x_0}{\Delta x} \frac{l}{2\sqrt{\pi t}} (1 - l^2/24a^2t + l^4/480a^4t^2 - )$$

is available. The series converges slowly, unless  $t$  is large, and for this reason the time interval  $t=50$  minutes was taken throughout. The pressure ratio  $p_0/p = \Delta x_0/\Delta x$ , where  $\Delta x_0$  and  $\Delta x$  are the slide-micrometer displacements at the beginning and end of  $t=3,000$  seconds. For the case of series I, II, IV we therefore have  $l=71$  cm.,  $t=3,000$  seconds,  $\Delta x_0/\Delta x=3.19$ , whence uncorrected  $a'=1.167$ . The term  $-l^2/24a^2t=0.0515$  and  $l^4/480a^4t^2=0.0032$ , which makes the full correction  $1-0.0483$ ; whence  $a=1.167 \times 0.9516=1.111$  and  $a^2=1.234$ . For the case of series V and VII obtained with the wide tube,  $l=74$  cm.,  $t=3,000$  seconds,  $\Delta x_0/\Delta x=3.30$ ; whence  $a'=1.258$  and the correction terms  $-0.0481$  and  $+0.0028$ , respectively. This makes  $a=1.258 \times 0.955=1.201$  and  $a^2=1.440$ . The mean of these values,  $a^2=1.337$ , is about twice as large as the value for hydrogen (0.66) usually given. It thus becomes a question to search for the cause of this large divergence.

In view of the tendency of the values of  $a$  to rise in the lapse of time, I also made the computation for an interval of 15 minutes. The data are inserted in the bottom of table 6. It is very interesting to note that the run of the ratio of pressures,  $\Delta x_0/\Delta x$ , for narrow and wide tubes is about the same (excluding the first exceptional value marked) and that it is smaller for the wide tubes. This eliminates the appreciable occurrence of convection errors. The results came out as follows:

$$\begin{array}{l} 2r=0.7 \text{ cm., Series I, II, IV: } a=1.168 \quad (1-0.1709+0.0351)=1.009 \\ 1.7 \text{ cm., Series V, VII: } a=1.176 \quad (1-0.1832+0.0403)=1.008 \end{array}$$

Thus the values of  $a$  for the  $\frac{1}{8}$ -inch and  $\frac{1}{2}$ -inch gas-pipe happen to coincide. They are, however, smaller, as was anticipated, than the values for a lapse of 50 minutes; but they agree admirably with the values obtained with very long tubes below.

The further decrease of  $a$  does not occur; for if  $t=7.5$  minutes, the computation shows

$$\begin{array}{l} 2r=0.7 \quad a=1.342 \quad (1-0.260+0.081)=1.10 \\ 2r=1.7 \quad a=1.368 \quad (1-0.271+0.088)=1.12 \end{array}$$

Thus  $a$  has risen; but the  $t$ -interval is now too small.

**41. Inferences relative to equations.**—In spite of the minor discrepancies, the mean value of  $a$  found for long tubes of all diameters, from quill sizes to tubes over 0.5 inch in bore, for 50-minute intervals, is of the order of value  $a=1.1$  to 1.2; and this is about 50 per cent larger than the value  $a=0.8$ , estimated. So much can not be accounted for in terms of any of the capillary distortions,  $\delta x$ , discussed above. Moreover, they are not observed to vanish between the initial  $\Delta x_0$  and the final  $\Delta x$  50 minutes later. They merely account for the differences of value in  $a$  obtained in the different series. With tubes



of so many diameters, moreover, the effect of leakage or diffusion at the top must be negligible, else the thin pipes would have shown it.

The effect produced by the rise of the mercury surface in the U-tube during diffusion produces a slight current down the diffusion tube. Since  $\Delta x = 0.0057$  about, the rise of mercury surface may be put  $\Delta h = 0.004$  cm., which is equivalent to a decrement of volume of  $0.31$  cm.<sup>3</sup> This air passes through the diffusion tube of a diameter  $0.7$  cm. or greater. Hence the total displacement of the air column in the diffusion tube is about  $1$  cm. In the wide tube (diameter  $1.7$  cm.) the displacement would be  $0.14$  cm. Both may be here disregarded, as the experiments show.

Though the attempt has already been made (§ 27) to treat the concomitant effect of the influx of air at the bottom of the tube, it is necessary to examine this occurrence from the point of view of diffusion. If we denote by  $\rho_0'$  the density of air at the atmospheric temperature and pressure of the experiment and by  $a'$ , the corresponding diffusion coefficient of air into hydrogen, the problem becomes an inversion of the case for hydrogen and thus leads to

$$\rho' = \rho_0' \left( 1 - \frac{2}{\pi} \int_0^{x/2a'\sqrt{t}} e^{-\beta^2} d\beta \right)$$

where  $\rho'$  is the density of the air at  $t$  seconds at  $x$  cm. from the end of the tube. Expanding the integral as before, and integrating for the length  $l$  of tube,

$$\rho' = \rho_0' (1 - (l/2a'\sqrt{\pi t}) (1 - l^2/24a^2t + l^4/480a^4t^2 - )$$

where  $\rho'$  is the mean density at  $t$  seconds of the air left in the tube.

If we add the corresponding mean density of hydrogen at the same time, the total mean density  $\bar{\rho}$  of the mixed gas in the tube is

$$\bar{\rho} = \rho_0' - (\rho_0' l / 2a' \sqrt{\pi t}) (1 - \dots) + (\rho_0 l / 2a \sqrt{\pi t}) (1 - \dots)$$

Ignoring the correctives temporarily for brevity, this may be converted into pressures,  $p = g l \bar{\rho}$ , etc., whence

$$\bar{p} = p_0' - (l/2\sqrt{\pi t}) (p_0' (1 - \dots) / a' - p_0 (1 - \dots) / a)$$

If we solve this for  $a$ , the reduced result is

$$a = \frac{a p_0' (1 - \dots) / a' p_0 - (1 - \dots)}{p_0' / p - 1} \frac{l}{2\sqrt{\pi t}} \frac{p_0}{p}$$

apart from the correctives in both terms of the first numerator. The expression may also be written

$$a = \frac{l}{2\sqrt{\pi t}} \frac{(a/a') (p_0' - p_0) - p_0 (1 - a/a')}{p_0' - p}$$

If now,  $a = a'$  nearly,

$$a = \frac{l}{2\sqrt{\pi t}} \frac{p_0' - p_0}{p_0' - p} = \frac{l}{2\sqrt{\pi t}} \frac{\Delta x_0}{\Delta x}$$

the expression used in the above computations with the inclusion of the correctives. But if  $a$  differs from  $a'$ , the value so found is not correct. If we call the above original value  $A$ ,

$$1 = \frac{A}{a'} + \frac{p_0}{p_0' - p} \frac{l}{2\sqrt{\pi t}} \left( \frac{1}{a'} - \frac{1}{a} \right)$$

a single equation with two variables,  $1/a'$  and  $1/a$ .

Thus, if  $a^2 = 0.66$  or  $a = 0.81$ , the value of  $a'$  computed from  $A = 1.111$  from series I, II, IV above, would be  $a' = 1.126$ , somewhat lower than the  $A$  found. In this equation it is necessary to reduce  $p_0$  to its equivalent in  $(\Delta x)$  by the equation  $(\Delta x) \cos \theta \rho_m = l p_h$ , where  $p_h$  is at atmospheric temperature. This makes  $(\Delta x) = 0.000609$  cm. The  $\Delta x$  equivalent of  $p_0' - p$  is given in table 6 above, and the mean value of  $\Delta x = 0.00573$  cm.

The question is thus brought to a rather unsatisfactory conclusion; but I have not been able to find any further reason for corrections. True, there may be a release in capillary strain of the kind discussed when  $\Delta x_0$  falls to  $\Delta x$ . Since, however, the zeros are often quite the same at the beginning and end of 50 minutes of diffusion, there is little probability in this assumption. A final device, viz, to contrast a very long and a very short diffusion tube, is still worth trying.

**42. Diffusion in case of a longer tube.**—Whatever the reason for the outstanding difference may be, it will be reduced by using the longest vertical tube available in the present installment. This was of length  $l = 157$  cm. and diameter  $2r = 0.7$ , being  $\frac{1}{8}$ -inch iron gas-pipe. All rubber connections were waxed. The fringe displacement is thus about twice as large as the preceding. Unfortunately it was accompanied with considerable distortion. This distortion completely vanished in the course of the first series of data for diffusion (fig. 51), in which the observation was carried on for 3 hours. After 2 hours the diffusion curve is practically linear at a rate of  $\Delta x / \Delta t = 30 \times 10^{-6}$  cm./min. Some  $H_2$  would thus be left after 6 hours. The curve, in view of the fact that fringes were placed by the slide micrometer (displacement  $\Delta x$ ), is remarkably regular. The error of  $\Delta x$  is now again negative as originally, or the correction  $\delta x = +0.0008$  cm. (about 0.0006 cm. of mercury head) compatibly no doubt with the observed distortion. The constant  $C = \rho_m \cos \theta / l$  is here  $C = 0.0612$  and  $\Delta \rho = C \Delta x$ . This constant enters the density measurements only, the diffusion data being independent of it, and hence of  $\theta$ .

The following values (table 8) enter into the density measurement conformably with  $\Delta x = (B - \pi) (\rho_a - \rho_h) / BC$ , where  $B$  is the barometric pressure and  $\rho_a$  and  $\rho_h$  refer to it and the temperature  $\theta = 22.8^\circ$ .

TABLE 8.

Tube.	B	$\theta$	$\pi$	$\rho_a \times 10^6$	$\rho_h \times 10^6$	Com- puted $\Delta x_0 \times 10^4$ .	Ob- served $\Delta x_0 \times 10^4$ .	Diff.
	cm.	°	cm.			cm.	cm.	cm.
$l = 157$ cm., $2r = 0.7$ cm.	76.34	22.8	2.07	1,197	83.1	177	169	0.0008

With the observed  $\Delta x = 0.0169$ , the density of hydrogen under normal conditions would come out  $\rho_0 = 143 \times 10^{-6}$ , corresponding to the long-tube values discussed above (§ 36).

Since the diffusion rates are necessarily slower for long tubes, larger time intervals  $t$  will be desirable to avoid excessive correctives. The data in table 9 ( $22.8^\circ$ ) are relevant,  $a'$  being uncorrected.

TABLE 9.

$t$ sec.	$a'$	$l^2/24a^2t$	$l^4/480a^4l^2$	Factor.	$a$	$a^2$	Initial and final zero $\Delta x \times 10^4$ .	$\frac{\Delta x_0}{\Delta x}$ observed.	$\frac{\Delta x_0}{\Delta x}$ computed.
3,000	1.270	0.2123	0.0112	0.799	1.015	1.030	112	1.57	1.64
6,000	1.124	.1356	.0221	.887	.996	.992	112	1.06	2.06
9,000	1.111	.0924	.0103	.918	1.020	1.040	...	2.38	2.50

Thus the mean values  $a = 1.010$  and  $a^2 = 1.021$  have apparently been brought somewhat nearer the usual tabulated values (0.81 and 0.66), but they are still in marked degree above them. Part of this might be supposed to result from the release of capillary strain virtually complete after 100 minutes; but as the computed  $\Delta x_0 = 0.0177$  is *larger* than the observed  $\Delta x_0 = 0.0169$ , all the values of  $a$  would be 5 per cent larger, viz,

$t = 50$ minutes	$a = 1.066$	$a^2 = 1.137$
100 minutes	1.046	1.095
150 minutes	1.071	1.147

which actually brings these results nearer the short-tube values again. In the latter case one may notice that the wide-tube values, in spite of the smooth diffusion, are the largest. Hence it might seem probable that convection has something to do with the high results. Convection within the tube should accelerate diffusion or be favorable to loss at the lower end and the effect would be marked with tubes both wide and short. This inference is made untenable by the behavior of quill tubes which show the same large  $a$ , but in which convection must be negligible.

I am obliged to conclude, therefore, that values of the diffusion coefficient of hydrogen into air below  $a^2 = 1$  have not been attainable by the method pursued. In figure 51a I have drawn the curve which should be observed if  $a^2 = 0.66$ , since  $a \propto \Delta x_0 / \Delta x \propto 1 / \Delta x$ , if the correctives are small. This may be assumed to occur for values of  $t$  greater than 100 minutes. The mean difference is about 0.0020 cm. in  $\Delta x$ . The occurrence of such a discrepancy resulting from capillary forces is out of the question, as it must have been detected in the large number of density measurements made, where  $\delta x$  falls below  $\pm 0.0008$ ; one would have to assume that the mercury surface of the gage in contact with the atmosphere is always supported, or that the closed shank in contact with hydrogen is always depressed by an equivalent capillary pressure. A unilateral effect of this size has nowhere been put in evidence.

**43. Diffusion. Very long tube.**—As the mean values of the coefficient  $a$  had fallen from  $a=1.1$  or  $1.2$  to  $a=1.010$  when the tube-length was doubled, the question arises whether a real limit has been reached. Accordingly the tube-length was again increased, this time to over five times the original length. To accommodate the new tube,  $l=386$  cm. and  $2r=0.7$  cm., it had to be placed *at a slant*, the top being at the influx cock  $C$ , 94.5 cm. above the floor, while the far end rested in the distance on the floor. Hence for the density measurements,  $l=94.5$  cm., whereas for diffusion measurements  $l=386$  cm. Far from being disadvantageous, this disposition has much to recommend it. The constant  $C=\rho_m \cos \theta/l=0.1018$ , since  $l=94.5$  cm. In fact, the density measurements came out flawlessly at once, as, for instance:

Length radius.	Series.	Initial zero $x \times 10^4$ .	Final zero $x \times 10^4$ .	$\Delta x_0 \times 10^4$ observed.	$\Delta x_0 \times 10^4$ computed.	$\rho_a \times 10^6$	$\rho_h \times 10^6$	Temp. pressure.	$\pi$
$l=386$ cm. $2r=.7$ cm.	IX	cm.	cm.	cm.	cm.				cm.
		112	112	105	105	1,187	82.7	$\left. \begin{matrix} 23.5^\circ \\ 75.80 \text{ cm.} \end{matrix} \right\}$	$\left. \begin{matrix} \\ \\ \end{matrix} \right\} 2.15$

In other words, the observed and computed fringe displacement,  $\Delta x_0$ , corresponding to the hydrogen pressure, are identical, which implies the standard hydrogen density.

The diffusion measurements are given (with the *doubled* time-scale marked near the curve) in the graph *b*, figure 51, and as a whole are also remarkably smooth. At the beginning, however, there is always some irregularity which I refer to inevitable convection at the free end, just after the tube is filled. This amounts to  $3/105$  of the initial displacement  $\Delta x_0$ . One would be tempted to take the second point and a shortened tube-length, but such a selection would nevertheless be arbitrary.

Owing to the unusual length of tube, the diffusion proceeds very slowly, so that a long period of observation is necessary, if the diffusion equation is to converge rapidly. Observations were made throughout about 700 minutes on the same day and were continued the next day; but the latter were thrown out, as the zero had changed (temperature) during the night. I shall give these data as an example in full, in table 10,  $t$  being the time in minutes and  $\Delta x$  the corresponding micrometer displacement which brings the fringe back to zero. One may note that after 26 hours about 17 per cent of the original hydrogen pressure is still left in the tube.

Table 10 shows that 200 minutes is not sufficient for the practical convergence of the diffusion equation, but that after 400 minutes this may be assumed. I have, however, in the table given the mean of all results, as less arbitrary. Dropping the first  $a$ , the mean of the others is  $a=1.002$ . The mean might be diminished 3 per cent if the first observation were removed for the reasons given.

If, now, we compare the values of  $a$  obtained ( $l=35$  cm. from next section) for different tube-lengths, viz,

50-minute intervals.				10-minute interval.		10-minute interval.
$l=71$	to 74	cm.	cm.	cm.		cm.
$a=1.111$	to 1.201	157	386	71	74	35
$a^2=1.234$	to 1.440	1.010	1.043	1.009	1.008	1.045
$2r=0.7$	to 1.7	1.021	1.092	1.018	1.016	1.092
		0.7	0.7	.7	.7	1.7

remembering that the last could be reduced about 3 per cent, it is obvious that a limit has been reached within the errors of method and measurement. So far as I see, therefore, it does not seem possible to reach the relatively low values ( $a=0.81$ ) usually quoted for the diffusion of hydrogen into air by the present apparently straightforward procedure. The results for wide tubes ( $2r=1.7$  cm.), in which convection is most easily possible, are highest; but if the data for 15-minute intervals be taken, the first set ( $l=71$ ,  $2r=0.07$  and  $l=74$ ,  $2r=1.7$  cm.) leads to identical  $a$  values, 1.009 and 1.008, which fit the above data very closely.

TABLE 10.—Diffusion of  $H_2$  into air. Zero at  $x=0.0112$  cm.

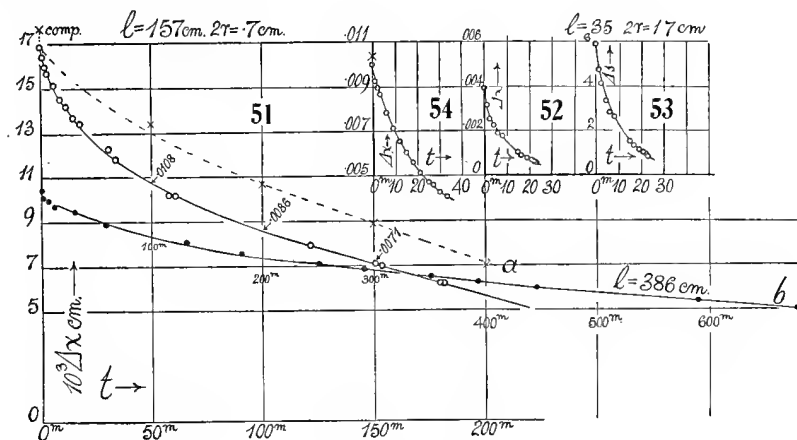
[Long tube:  $l=386$  cm.,  $2r=0.7$  cm., barometer 75.80 cm., temperature  $23.5^\circ$ .]

$t$	$\Delta x \times 10^4$	$\Delta t$	$a'$	$P/24a^2t$	$l^4/480a^4t^2$	$a$	$a^2$
<i>min.</i>	<i>cm.</i>	<i>min.</i>					
0	105	200	1.413	0.2600	0.0811	1.160	1.346
1	102						
2	101.5	400	1.192	.1824	.0400	1.018	1.036
3	101						
6	100	600	1.118	.1385	.0230	.989	.979
11	97.5						
30	95	700	1.118	.1188	.0169	1.004	1.008
58	89						
60	89				Mean	1.043	1.092
131	81						
181	76.5						
251	71						
291	68.5						
351	65						
393	62.5						
447	60						
591	54						
702	50						
(next day *) 1,485	19.5						
1,564	18						

\* Zero at  $x=0.0098$  cm.

44. Diffusion. Short tube.—By way of contrast, diffusion experiments with a short tube were finally made. They, moreover, serve as an introduction to the promiscuous experiments with gas-pressures made elsewhere. The tube

in question had the dimensions  $l=35$  cm. and  $2r=1.7$  cm., being half-inch iron gas-pipe. As the fringe displacements are small, they were read off directly ( $s$ ) and then reduced if necessary to slide-micrometer values ( $x$ ) by the equation  $\Delta x = 10^{-6} \times 668 \Delta s$ . The observed data are reproduced in figures 52 and 53, respectively, in  $\Delta x$  cm. and also in  $\Delta s$ , which are arbitrary



ocular scale-parts. In view of the shortness of the tube, the diffusion is rapid and relatively small time-intervals suffice to converge the equation, 10 to 20 minutes being deemed sufficient. As a further advantage of the small displacements, the zero remained quite the same before and after the diffusion experiment. The results of the measurement for density were ( $C = \rho_m \cos \theta / l = 0.2747$ )  $l=35$  cm.,  $\Delta s_0=5.8$ ,  $\Delta x_0=0.00389$  cm. (observed),  $B=75.41$  cm.,  $2r=1.7$  cm.,  $\Delta x_0=0.00388$  cm. (computed),  $\theta=23.5^\circ$ . Thus the normal density of hydrogen appears here at once and there happens to be no appreciable capillary correction.

For the diffusion coefficient it is convenient to take the  $s$  values directly, since

$$a = \frac{l}{2\sqrt{\pi t}} \frac{\Delta s_0}{\Delta s} (1 - l^2/24a^2t + l^4/480a^4t^2 -)$$

At  $t=0$  second,  $\Delta s_0=5.8$ , and the curve gives further (temp.  $23.5^\circ$ ),

$l$	$t$	$\Delta s$	$\Delta s_0/\Delta s$	$a'$	$l^2/24a^2t$	$l^4/480a^4t^2$	$a$
cm.	min.						
35	10	2.10	2.76	1.120	0.0678	0.0006	1.045
35	20	1.05	5.50	1.568	.0346	.0014	1.516

The diffusion thus increases for some reason, probably thermal convection, in the lapse of time. The mean value  $a=1.28$  is too large, as was anticipated. It would probably have been better to use a narrow tube, seeing that at

10 minutes the corrections are small and the  $a$  value obtained closely in accord with the preceding long-tube values.

**45. Quill tube.**—Contrawise, the concluding experiment (fig. 54) with a long vertical glass tube ( $l=94$  cm.) and a relatively fine bore ( $2r=0.15$  cm.) accentuated the leak at the top, in spite of the crevice-apertured stop-cock employed. The density results came out fairly well, viz, bar., 75.34 cm.; temp.,  $25.0^\circ$ ;  $\rho_a \times 10^6$ , 1.174;  $\rho_h \times 10^6$ , 81.5; computed  $\Delta x_0$ , 0.01035 cm.; observed  $\Delta x_0$ , 0.01005 cm., the placement of the slide micrometer being too small by  $3 \times 10^{-4}$  cm., a return to the original sign of  $\delta x$ .

The diffusion data are also smooth, but rapid. The constants were

$$\begin{aligned} 15 \text{ minutes} \dots a &= 1.480 (1 - 0.1867 + 0.0428) = 1.269. \\ 30 \text{ minutes} \dots a &= 1.478 (1 - 0.0936 + 0.0421) = 1.401. \end{aligned}$$

Again  $a$  increases in the lapse of time, which can not now be referred to convection, seeing that the bore of tube is only 1.5 mm. There seems no way of accounting for this, except in terms of the crevice-leak, on top, in relation to the small volume of gas in the vertical tube and of the gas expulsion from the tube below, where the mercury surface of the U-gage rises. The latter, since  $\Delta x_0=0.01$ , may be estimated at  $\Delta h=0.004$  cm., equivalent to a volume of 0.31 cm.<sup>3</sup> Since the area of tube is 0.018 cm.<sup>2</sup>, the displacement would be 17 cm. for the 94 cm. of tube. This is no longer negligible.

**46. Conclusion.**—Thus, finally, if we include the values for  $a$  found above for quill tubes, and use the smallest  $t$  compatible with a reasonably convergent equation, the results at about  $22^\circ$  to  $23^\circ$  are

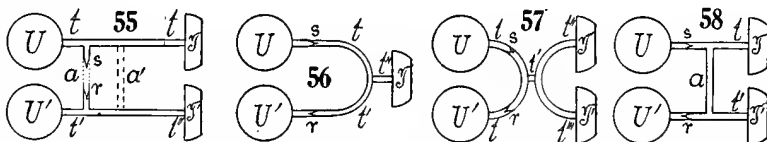
$l \dots 35$	68.4	71	74	157	386	cm.
$2r \dots 1.7$	.3	.7	1.7	7	.7	cm.
$t \dots 10$	15	15	15	50	400	minutes.
$a \dots 1.045$	1.009	1.009	1.008	1.010	1.002	cm./ $\sqrt{\text{sec.}}$

## CHAPTER IV.

### PIN-HOLE PROBE EXPERIMENTS, CHIEFLY WITH BRANCHED TUBES.

#### BRANCH PIPES.

47. **Branch adjustments.**—The simplest of these tube combinations is shown in figure 55, where  $U$ ,  $U'$  are the two shanks of the mercury U-tube, the displacements of the heads of which are read off by a vertical interferometer. The cylindrical spaces above  $U$ ,  $U'$  are closed by glass plates and these spaces are coupled with telephones  $T$ ,  $T'$  by quill tubes  $tt$  and  $t't''$ , the whole forming a closed region. The tube  $tt$  carries a  $T$  branch, into the free end of which the salient pin-hole  $s$  is inserted, short ends of pure-rubber tubing being available for junctions. Similarly, the tube  $t't''$  is provided with the reëtrant pin-hole  $r$ . Thus  $U$  responds to  $T$ ,  $U'$  to  $T'$ , and the effect of either telephone may be quite removed by withdrawing the corresponding pin-hole adjutage. The telephones may also be examined together by coupling  $s$  and  $r$  with a short length of rubber tubing at  $a$ . In such a case either may be examined separately ( $T$  for instance) by closing the quill tube (here to be short)  $t''$ . If  $s$  and  $r$  are not coupled, but open to the air, a branch  $a'$  from  $t$  to  $t''$  makes the registry impossible, the fringes remaining stationary at all frequencies.

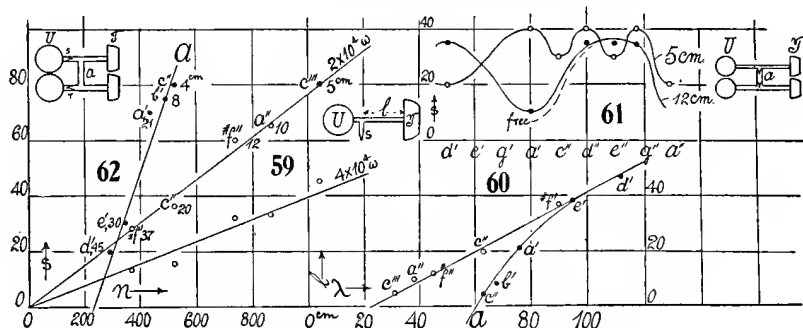


High-resistance radio telephones are preferable. A small inductor, with 20,000 to 40,000 non-inductive resistance in the secondary and one or two storage cells in the primary, is convenient for actuating the telephones. A break of variable frequency (usually  $c$  to  $c''$ ) places the note. Small interference fringes, measuring 0.01 cm. in the ocular, are usually sufficient in sensitiveness.

Figure 56 is an arrangement for a single telephone  $T$ . The quill tubes  $t$  and  $t'$ , carrying the salient and reëtrant pin-holes  $s$  and  $r$ , are joined by a T-branch at  $t''$ , with the telephone  $T$ . In figure 57 the same arrangement is duplicated at  $t''t'''$ , so as to receive the sound-waves from both telephones  $T$ ,  $T'$ . The curious feature about this arrangement is the low pitch ( $c'$ ,  $d'$ ) which it harbors at the maximum, even when the unbroken tubes used are short (10 cm.). Finally, figure 58 shows the H-branch already tested in the preceding report, with a cross-tube  $a$ . By stopping off the quill tube  $t'$ ,  $T$  alone is tested, as in the case of figure 55.



**48. Experiments.\***—It will not be possible to give more here than a few examples, as the results are often involved and too complicated for reproduction. Among these the case of a single telephone and connection,  $TtU$ , figure 55, with  $T't''U'$  removed, deserves mention. The length of rubber tubing between  $s$  and  $T$  to be called  $l$  (right insert, fig. 59) was successively increased and the intensity  $s$  and pitch of the maximum found for each value of length  $l$ . Figure 59 is a summary of the results, with  $4 \times 10^4$  and  $2 \times 10^4$  ohms in the telephone circuit, and the intensities  $s$  are exhibited in relation to  $n$ , the frequency of the maximum. The length  $l$  is also inserted at each point. Halving the resistance does not quite double the fringe displacement  $s$ . Within the limits of error  $s$  is proportional to  $n$  directly. One would be inclined to attribute this to an induced electromotive force  $e$ , varying with  $n$ ; but as the mean value of  $e$  depends on the speed of breaking the circuit and not on the number of breaks per second, this explanation is not tenable. Since  $e$



must be regarded as constant, therefore, the cause is to be sought in an acoustic pressure favored by frequency.

Another aspect of these results is reproduced in figure 60 (upper curve) in which the inserted length  $l$  and the wave-length  $\lambda$ , corresponding to  $n$ , are compared. Here also there is proportionality; but it is no longer direct, since the nearest equation would read

$$2(l + 12) = \lambda$$

In other words, the length  $l$  acts as if it were 12 cm. longer, or 12 cm. are supplied by the short but irregular length  $sU$  of the pipe  $UT$ . Since at the maximum the pin-hole is located at a node, it is difficult to understand this result.

If the combination of figure 55 be taken with a junction-pipe  $a$ , of small length, 5 cm., maxima are redundant and closely crowded, as in figure 61. The pipes have no sharp tune. If the length of the cross-piece  $a$  is increased to 12 cm., the high maxima become more definite. Finally, if the pin-holes are free ( $a$  removed) the same conditions are enhanced. Thus a junction,  $a$ ,

\* As relative intensity of sound is alone of interest, the fringe displacement,  $s$ , as directly observed, is used as the ordinate of most of the graphs.

longer than 12 cm., is ineffective. The best conditions are naturally reached if  $UT$  and  $U'T'$  have the same harmonics.

In this respect the combination (fig. 56) with but a single telephone has advantages and shows high sensitiveness. The pitch, however, is liable to be different with different telephones of the same kind. Thus, at 40,000 ohms,  $s''=50$  with a  $c''$  crest, and  $s=43$  with a  $b'b'$  crest, appeared. The design (fig. 57) is quite sensitive, in spite of low frequency. Thus with  $t=15$  cm.,  $t'=8$  cm.,  $t''$ ,  $t'''$  each 16 cm.,  $s=70$  was obtained at the low-pitched crest  $e'$ . In all cases there must be provision for flux of air. If in figure 57,  $Tt''t'sU$  and  $T't'''t'sU$  make a closed region,  $U'$  being left open and the  $r$  pipe closed, there is scarcely any response; but if  $s$  on a T-branch juts into the atmosphere, the system is very sensitive.

The importance of the cross-piece  $a$  of length  $l$  in figure 58 has already been indicated. Relevant data are also given in figures 61 and 62, graph  $a$ . Naturally there is no direct proportionality of  $s$  and  $n$ ; and the relation of  $l$  and  $\lambda$  (black dots in fig. 60) is a curved line, which seems to merge into the simpler relations (open dots) of the design (fig. 55), when  $l$  is large.

**49. Multiple resonance; narrow tubes. Location of pin-holes.**—Some time after, the H-branch-tube was taken up again (see inset 62 or fig. 58), largely in relation to multiple resonance \* which has recently gained increasing attention. A variety of examples have been given in my earlier reports; but in the present case other matters not then treated are to be considered. These are the strong resonances of very low pitch obtainable in very short tubes; the effect produced by reversing the action of one of the two telephones on the same circuit; the adjustment of salient and reëtrant pin-holes in relation to each other and to the U-gage; and finally the behavior of H-tubes of large diameter (2 cm.) and of doubly capped straight tubes.

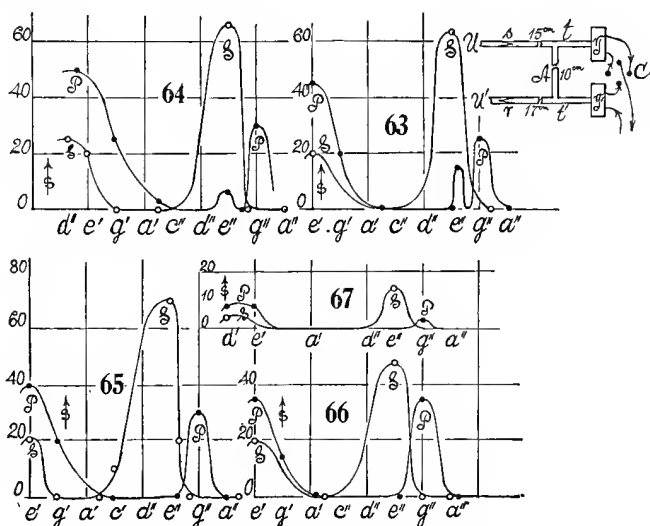
I began the work with thin tubes (fig. 63, inset,  $t$ ,  $t'$ ) about 6 mm. in diameter joined by the cross-piece  $A$  of the same diameter. The telephones  $T$ ,  $T'$  at the ends of  $t$ ,  $t'$  were of the common pattern, and supplied with the same current in series, but one of them ( $T$ ) was provided with a switch  $C$  by which its current could be reversed with reference to  $T'$ . At the other ends of  $t$ ,  $t'$  the salient ( $s$ ) and reëtrant ( $r$ ) pin-holes were inserted and joined to the shanks  $U$ ,  $U'$  of the U-gage by the shortest tubing admissible. The results obtained are summarized in figures 64 to 66. For the curves marked  $S$ , the telephones cooperated, the plates presumably advancing and retreating in amplitude, respectively; *i. e.*, telephone plates vibrating in opposed phases, being concave and convex, respectively, at the same time. For the case  $P$  the current of one was reversed, so that both plates advanced or retreated together (vibration in the same phase, both convex or both concave). The telephones were actuated by a small induction coil with over 2,000 ohms in the

---

\* An interesting digest of the subject in reference to the work of Paget, Boys, Paris, is given in *Nature*, 1923, Feb. 24, p. 254, by Mr. P. Rothwell.

telephone circuit and an appropriate break-circuit device (electric siren), as heretofore explained (*cf.* § 75).

The difference of behavior for the two adjustments are given in figure 64, the ordinates showing the fringe displacements,  $s$ , proportional to the acoustic pressures at the different stages of pitch indicated by the abscissas. One observes the very striking presence of notes of the 2-foot octave in case of quill tubes but 16 cm. long. When the telephones are in sequence  $S$ , the high notes ( $e''$ ) of the 1-foot octave resonate far more intensely than the low notes  $d' \dots e'$ . These being here at the limits of performance of the siren were difficult to locate, but the resonance interval is a little over the octave  $e'$  to  $e''$ , with the  $e''$  very abrupt.



For the case  $P$  with the telephone plates in phase, the low pitches ( $d'$  to  $e'$ ) are far more intense than the high pitches ( $g''$  with an uncertain  $e''$ ). This specific difference in the two telephone adjustments makes it quite improbable that the high pitches are in all cases called out by the upper harmonics of the telephone note, *i. e.*, that the fringe deflection, etc., is merely apparent and called out by the harmonic  $e''$  in  $e'$ . It is more reasonable to assume that both  $e'$  and  $e''$  correspond to distinct modes of vibration of the **H**-pipe.

The endeavor was now made to test each pipe  $t$  and  $t'$  separately. Accordingly,  $t'$  was detached from the **U**-gage and closed with a plug, so that  $tAt'$  now became a closed region communicating with  $U$  by the salient pin-hole  $s$ . No fringe deflection whatever was obtainable in this way, a result corroborating my earlier experiments of an analogous kind. Similarly, when  $s$  was detached from the **U**-gage and closed,  $r$  communicating with  $U'$ , no deflection was obtained at any pitch. Thus the slender closed region needs an additional vent to generate acoustic pressure. This was secured by leaving  $s$  attached to  $U$ ,

while  $r$  was detached but not closed, so that  $r$  freely communicated with the atmosphere. The results are summarized in the graphs (fig. 63) for the  $S$  and  $P$  switching of the telephones. These curves are almost identical with the corresponding cases of figure 64, not merely in pitch, but even as to intensity; and fluctuating  $e''$  in the  $P$  graph is now very definite. Since the plates here vibrate in phase, it is probably the residue of the overtone of the strong  $e'$ . The alternative case of the reëntrant pin-hole  $r$  joined to  $U'$  and  $s$  communicating with the atmosphere is given in the graph (fig. 65). The curves again are a close reproduction of figures 63 and 64; the  $e''$  in the  $R$  curves does not appear, but the  $e''$  intensity in the  $S$  curve is the highest obtained. These results (fig. 63, 65) contrasted with the first (fig. 64) are illuminating; if  $s$  communicates with  $U$ , there is no advantage in having  $r$  communicate with  $U'$ , contrary to what would naturally be supposed. The air-space above the shank  $U'$  acts merely like any other atmosphere, the acoustic-pressure difference  $s$ ,  $r$  being constant, like an electromotive force on open circuit. This recalls the impossibility of relaying a series of pin-holes discussed in a preceding report (Carnegie Inst., Washington, Pub. 310, 5, 1923).

To further elucidate this question, I closed  $t'$  at  $r$  with a plug and put the reëntrant pin-hole  $r$  in the cross-branch at  $A$ , salient outward. The results obtained in this case are given in figure 66, and they differ from the preceding graphs in intensity only, but all the relations are preserved. A still more striking result was obtained by detaching  $s$  from  $U$  and  $r$  from  $U'$  and joining the cross-piece at  $A$  with  $U$  by a short tube. The results are given in figure 67, in which the intensities are naturally low, but all features reappear identically. Thus excess pressure exists throughout the pipe. Had both pin-holes been placed at  $A$ , the  $P$  graph would have evidenced a strong overtone here, and it is suggested that paired pin-holes at a prospective node will secure the largest values.

**50. The same. Wide tubes.**—The above arrangement did not admit of the examination of the tubes  $t$  and  $t'$  individually and the closed region gave no response. It seemed probable that this difficulty could be overcome by widening the tubes as in figure 68 (inset), where the pipes  $t$ ,  $t'$  are 2 cm. in diameter and all 15 cm. long. They were also placed farther apart to accommodate the individual telephones  $T$ ,  $T'$ . The latter were first put in communication with  $t$  and  $t'$  by short rubber tubes and the high-resistance radio-telephones used; but no fringe displacement was thus obtainable. The pipes  $t$ ,  $t'$  were therefore directly mounted with cement on the mouthpieces of common telephones, as shown, and  $T'$  provided with a switch  $C$ . The far ends of  $t$  and  $t'$  were closed with well fitting perforated corks and connected with the pin-holes  $s$  and  $r$  and the shanks of the U-gage with rubber tubing. Reducing the resistance to 1,000 ohms, fringe displacements were obtained, which were enhanced by placing  $s$  and  $r$  as near  $U$  and  $U'$  as possible (short connectors). Thus I obtained for telephones in sequence,  $S$ , pitch  $e''$ ,  $s=40$  scale-parts; telephones

in phase,  $P$ , pitch  $f''$ ,  $s=53$  scale-parts; and it made little difference whether the vent at  $A$  (1 cm. nearly) was open or closed.

The reëtrant pin-hole was now detached and closed, the salient pin-hole being the sole communicator with the U-gage. This is the case of a closed region. The  $s$  pin-hole was similarly treated, in succession, and the results were: Salient pin-hole only: telephones in sequence,  $s=70$ ,  $be''$ ; telephones in phase,  $s=45$ ,  $be''$ . Reëtrant pin-hole only: telephones in sequence,  $s=38$ ,  $e''$ ; telephones in phase,  $s=60$ ,  $f''$ . Thus it appears that the closed region of sufficient volume responds, and this even more actively than when both pin-holes are used conjointly as originally. This seems to be due to the curious result that for the salient pin-hole alone, the telephones in sequence ( $S$ ) are more active, whereas for the reëtrant pin-hole the telephones in phase ( $P$ ) are the more so.

With the adjustment shown in figure 68 (inset), the occurrence of multiple resonance is very neatly shown, both for the case where the telephones are in sequence ( $S$ ), figure 69, and for the case  $P$ , figure 68. The two pin-holes were first used together as in the figure. The full curves marked  $r+s$  were

TABLE II.

Pipes and telephones.	Pin-hole.	Switch.	Pitch.	$s$	Tele-phone.	Pin-hole.	Switch.	Pitch.	$s$
$t, T$	$s$	$S$	$bd''$	85	$T'$	$s$	$S$	$bd''$	80
$t, T$	$s$	$P$	$..$	5	$T'$	$s$	$P$	$..$	0
$t', T'$	$r$	$S$	$d''$	80	$T$	$r$	$S$	$d''$	80
$t', T'$	$r$	$P$	$g'$	5	$T$	$r$	$P$	$..$	0

thus obtained with 1,000 ohms in the telephone circuit. The two tubes responding with the salient and the reëtrant pin-holes were then successively detached and plugged, so that the fringe displacement of one tube only was recorded. The curves marked  $s$  (salient pin-hole) and  $r$  were so obtained, for each switching ( $S$ ,  $P$ ) of the telephones. In the low-pitch values (fig. 69) the component resonances are nearly the same in frequency, and the compound curve is of the same type. The high-pitch components, however, are some distance apart ( $f''$  and  $a''$ ), but their compound curve is an active coalescence throughout the whole of this interval. In figure 68 for telephones in phase ( $P$ ) the low-pitch resonances are obscure. The high-pitch resonances ( $e''$  and  $a''$ ) for  $r$  and  $s$  are also less intense than in the preceding figure, but they merge in a plateau-like curve which shows sustained intensity between  $e''$  and  $a''$ .

When the pipes  $t$  and  $t'$  were opened (corks withdrawn) and the pin-holes at the end of 6-inch quill tubes used as probes and inserted close to  $T$  and  $T'$ , the behavior of each pipe was about the same as presented in table II (resistance in circuit, 1,000 ohms).

When the pin-holes were used conjointly ( $s+r$ ), the result was here summational, so that a double resistance (2,000 ohms) had to be inserted into

the telephone circuit, giving  $S$ ,  $d''$ , 80 scale-parts,  $P$ ,  $g'$ , 20 scale-parts. This experiment was now repeated with the tubes  $t$  and  $t'$  closed (as in fig. 68) with a perforated tube, through which the pin-hole probes were thrust loosely to within a centimeter of the plate of the telephone. The results are given in table 12.

The telephones switched into phase ( $P$ ) gave no result at any pitch. As the fit at the perforation was not snug, it was next waxed, giving data shown

TABLE 12.

Telephone.	Pin-hole.	Switch.	Pitch.	$s$
$T$ and $T'$	$s$ and $r$	$S$	$a'$	60 scale-parts.
$T$	$s$	$S$	..	35
$T'$	$r$	$S$	..	33

in table 13, which is practically the same result. In these cases it made little difference in pitch or intensity whether the vent in the cross-piece  $A$  was open or closed. The low-resonance pitch  $a'$  in the tube closed at both ends contrasts very strikingly with the high pitch  $d''$  for the same tube closed at one end only. In the former  $a''$  is inactive, no fringe displacement resulting.

Thus it appears that a salient and reëtrant pin-hole probe on separate tubes communicating with the shanks  $U$  and  $U'$  of the **U**-gage may probably be used together in the same pipe; and this proved to be the case. For instance: Tubes  $t$ ,  $t'$  closed at both ends,  $r+s$  in  $t$ , pitch  $b'b'$ , switch  $S$ ,  $s=50$  scale-parts;

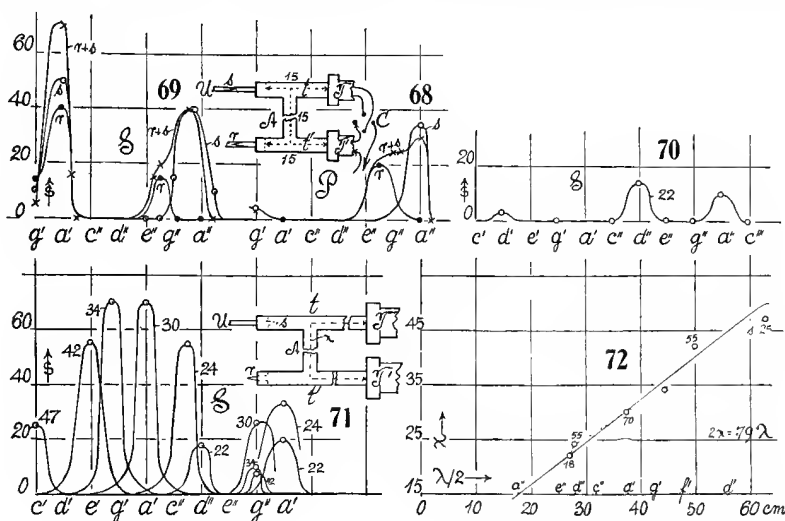
TABLE 13.

Telephone.	Pin-hole.	Switch.	Pitch.	$s$
$T$ and $T'$	$s$ and $r$	$S$	$a'$	55 scale-parts.
$T$	$s$	$S$	..	26
$T'$	$r$	$S$	..	30

tube  $t$  closed,  $t'$  open,  $r+s$  in  $t$ , pitch  $c''$ , switch  $S$ ,  $s=50$  scale-parts. In all these cases when the telephones were switched in phase no appreciable fringe displacement was obtained.

The exploration of the closed tubes  $t$ ,  $t'$  (fig. 68, inset) in depth, by passing the respective pin-holes through the perforated corks to different distances from the telephone plates, proved to be a difficult experiment both for a single pin-hole in each tube or a double pin-hole in a single tube. Pressures seemed to fall off from the plate or the cork at the end of the tubes toward the middle, but there were frequent discrepancies traced to the adjustment of the pin-hole. The telephones in adjustment  $P$  were quite ineffective; when in sequence ( $S$ ) the resonant pitch was sharply  $a'$ . The following data finally obtained are trustworthy for the pipe  $t$  and the salient pin-hole at 1 cm. from

plate,  $s=65$ ; middle of  $t$  pipe,  $s=40$ ; 1 cm. from corked end,  $s=68$ . The  $t'$  tube showed no certain difference of deflection for any position of the reëntrant pin-hole from the plate to the corked end of the pipe  $t'$ . Thus it made no difference whether both pin-holes were attached to their respective shanks of the U-tube, or whether one was free. Both could be detached, moreover (fig. 70), and the middle of the cross-tube  $A$ , figure 68, joined to the U-gage as in the preceding experiment (fig. 67), showing a small residual fringe displacement of  $s=15$ . Curiously enough, with both pin-holes saliently inward at the corks, the deflections for the usual attachment were liable to be negative ( $s=33$ ). With one tube ( $t'$ ) quite closed and the other joined



to the U-gage, there was no displacement at any pitch, the fringes merely wandering in response to temperature.

**51. Modes of vibration within the H-tube.**—From what has preceded, the character of the possible vibrations in the H-tube (fig. 68, inset) is now clear. At low pitch the ends of the  $t$  and  $t'$  tubes are nodes, from which the acoustic pressure diminishes upward 40 per cent toward the middle of each and thence to the middle of the cross-pipe  $A$ , where it nearly but not quite vanishes (reduced 80 per cent). Hence the middle of the branch  $A$  (fig. 68) is an antinode and the motion in  $t$  and  $t'$  is bifurcated towards the two ends of each, as shown in the diagram. The high pitch, however, is an individual vibration, probably arising in each doubly closed tube  $t$  and  $t'$ . The pitch here will usually differ but slightly, and hence if sounding together the graphs coalesce.

To test this matter further and deduce an equation, the pipe (fig. 71) was prepared, in which an expansible branch  $A$  could be increased in length at pleasure. The fringe deflections for the upper and lower pitch are given in

table 14 and constructed for the case of telephones in sequence (*S*) in figure 71. For the telephones in phase (*P*), the upper resonances are practically the same as when the telephones are in sequence, but the lower resonances only appear in the latter case (sequence, *S*). Moreover, while the upper pitch remains nearly the same for all values of length *A* (marked in centimeters on the graphs), the lower resonances are very sharp and move rapidly into lower pitch (*d''* to *c'*) with increase of the *A* length. Moreover, the upper resonances are usually strong when the lower are less intense. Both pass through a maximum, particularly the lower resonances, which rise from about *s*=20 at *d''* to 70 at *g'* to *a'* and then fall to 25 at *c'*.

TABLE 14.—Resonances of the H-tube.

[*x*=axial distance from plate to plate of telephones. Distance in tubes *t* and *t'*, 15 cm. Fringe displacements, *s*.]

<i>x</i>	Telephones in sequence ( <i>S</i> ).				Telephones in phase ( <i>P</i> ).			
	Pitch.	<i>s</i>	Pitch.	<i>s</i>	Pitch.	<i>s</i>	Pitch.	<i>s</i>
		<i>scale-</i> <i>parts.</i>		<i>scale-</i> <i>parts.</i>		<i>scale-</i> <i>parts.</i>		<i>scale-</i> <i>parts.</i>
47	<i>c'</i>	25	..	..	..	..	..	..
42	<i>e'</i>	55	<i>g''</i>	8	<i>e'</i>	2	<i>g''</i>	10
34	<i>bg'</i>	70	<i>g''</i>	10	<i>bg'</i>	4	<i>g''</i>	10
30	<i>a'</i>	70	<i>g''</i>	25	<i>g'</i>	4	<i>g''</i>	20
24	<i>bd''</i>	55	<i>a''</i>	33	<i>g'</i>	4	<i>g''</i>	25
22	<i>d''</i>	18	<i>a''</i>	18	<i>g'</i>	3	<i>a''</i>	20
Single tube	..	..	<i>a''</i>	30	..	..	..	..

In figure 72 I have given the length *x* from plate to plate of the telephones, along the axes of the tubes *tAt'*, in terms of the semiwave-length  $l=\lambda/2$  of the given pitch in free air. These points make a coherent grouping quite as close as the ear can well estimate pitch. It is therefore probable that a linear equation

$$(1) \quad x = (x_0/\lambda_0)\lambda = (x_0/l_0)l$$

is applicable and the the graph (fig. 72) shows  $x_0/l_0=0.79$ . Hence

$$(2) \quad x = 0.79l = 0.40\lambda$$

instead of  $\lambda/2$ , which would hold in the absence of viscosity. The independent data of figure 69 would give  $2x=0.81\lambda$ , and the other incidental values on the average also  $2x=0.79\lambda$ .

With this it is now very interesting to compare the data of figures 64 to 67 for a pipe about but 0.6 cm. in diameter (apart from the expansion at the telephones), and a prevailing lower harmonic *e'*. Here

$$x_0/l_0 = 25/50 = 0.5 \text{ or } x = 0.5l = 0.25\lambda$$

In other words, the internal friction for these narrow tubes is enormously larger, so that for a given pitch but half the normal length suffices. This accounts for the striking occurrence of very low frequencies in connection with these short pipes.



The equation given by Helmholtz for the open organ-pipe and discussed by Rayleigh (Sound, Chapter IX) is

$$u = v(1 - \sqrt{\eta/2n\rho}/R$$

where  $u$  is the velocity of sound within the pipe of radius  $R$  under conditions of viscosity  $\eta$ ,  $v$  the free velocity in air of density,  $\rho$ , and  $n$  the frequency. If we convert this into wave-lengths  $\lambda'$  corresponding to  $u$  and  $\lambda$  to  $v$  at the same  $n$ ,

$$(3) \quad (\lambda - \lambda')/\lambda = \sqrt{\eta/2n\rho}/R$$

In equation (4) if  $2x = \lambda' = 0.79\lambda$ , the corresponding value comes out experimentally

$$(4) \quad \frac{\lambda - \lambda'}{\lambda} = 0.2$$

and is, so far as figures 71 and 72 show, not appreciably dependent on frequency  $n$  within the interval  $c'$  to  $c''$  under observation. Since the diameter of pipes is  $2R = 2$  cm., the quantity  $R(\lambda - \lambda')/\lambda = 0.2$  (here experimentally constant) has the same value.

To compare this with the narrow tube of figures 65 to 67, which has unfortunately the telephone mouthpieces as terminals and possibly a tube not adequately smooth (because of the rubber-tube junctions), we may regard  $2R > 0.6$  cm., the diameter of brass pipe. The pitch at  $e'$  descended to  $b d'$ . Thus  $\lambda' = 0.5\lambda$  or  $(\lambda - \lambda')/\lambda = 0.5$  and  $\lambda' = 0.47\lambda$  or  $(\lambda - \lambda')/\lambda = 0.53$  occur. Hence  $R(\lambda - \lambda')/\lambda = 0.15$  to  $0.19$  are reasonable estimates, the latter showing a tendency to conform with this part of equation (3).

Returning to the wider tube  $R = 1$  cm. and figure 71, one may inquire whether a reasonable value of  $\eta$  is approached at any of the pitches  $d''$  to  $c'$  tested, since

$$[R(\lambda - \lambda')/\lambda]^2 = 0.04 = \eta/2n\rho$$

The values so obtained range from  $\eta = 0.06$  at pitch  $d''$  to  $\eta = 0.027$  at  $c'$ , and are thus quite out of keeping with the viscosity of a gas. The individual values computed from equation (3) directly are ( $R = 1$  cm.) (table 15).

TABLE 15.

Pitch.	$d''$	$b d''$	$a'$	$b g'$	$e'$	$c'$
$R\Delta\lambda/\lambda$	0.21	0.20	0.19	0.24	0.16	0.25
$n$	590	550	440	370	330	260
$\eta$	.070	.057	.042	.055	.022	.044

Thus the mean friction here in evidence (0.049) would be about 270 larger than the viscosity of the gas.

It has been assumed that the lower maxima in figures 69, 68, and 71 occur when the telephones are used in sequence, *i. e.*, when the plates are

respectively convex and concave at the same time, for the alternating vibration should be stimulated by an advance of one plate, coinciding with a retreat of the other. Not wishing to injure the telephones, this interpretation of  $S$  and  $P$  has not been directly investigated. Moreover, in figures 64 to 67 both commutations of the telephones are definitely active at the lower resonance, though one is about twice as much so as the other. However, it will be shown below that the  $P$  position evokes overtones, and this may be taken as adequate evidence.

At the high pitch there should be no difference, since in the case of the wide tubes each vibrates separately. For the quill tubes (fig. 64 to 67), where the best adjustment for the lower pitch is the worst for the higher, throughout, the relations are again less clear.

52. Continued. Deep resonances.—To refer the high-pitch data at  $g''$  and  $a''$  to the individual tubes  $t$  and  $t'$  (fig. 71, inset), experiments were made at some length by elongating one or the other of these tubes. The results were unsatisfactory, and no multiple resonances or coalescences of graphs were obtained. In fact, a third tube closed at both ends was inserted between  $t$  and  $t'$  and parallel to them on the cross-piece  $A$ , without any effect worth recording. The third tube merely lowered the lower resonances and modified amplitudes. Its own vibrations, if occurring, were not appreciable at the U-gage.

A more promising method of procedure, keeping the telephones always in sequence, seemed to be that of cutting down the outer lengths of the tubes  $t$  and  $t'$  as shown in the inset, figure 73, until the pin-hole lay very close (1 to 2 cm.) to the cross-tube  $A$ . The reduced effective length of each tube was now but 9 cm. A very extended survey from  $c$  to  $c'''$  was carried out, but at first no marked resonances at all were detected. With greater care in tightening all joints and reducing the effective telephonic resistance to one-third, the graphs of figure 73 were traced, and they refer to a total axial length  $x$  of 24 cm. and 29 cm.

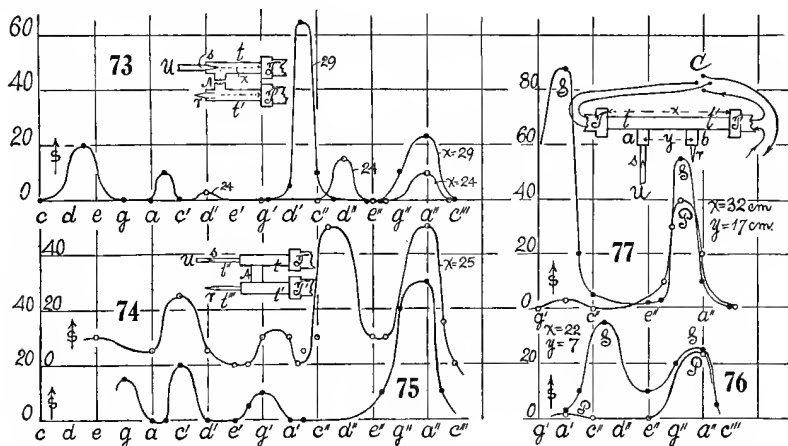
At  $x=24$  cm. (cross-piece  $A$ , 9 cm.) the resonances are very weak in spite of the low resistances, both at  $d''$  and at  $a''$ . The  $d''$  has the proper frequency in relation to  $x$ , but the  $a''$  appears here as in figure 71, and it even occurred ( $g''$  to  $a''$ ) when the tubes  $t$ ,  $t'$  of that figure were elongated 3 cm. Thus the  $a''$  frequencies can hardly be associated with the tubes  $tt'$ , but are referable to the telephones, which have remained the same throughout.

At  $x=29$  cm., *i. e.*, for an increase of length of the cross-piece  $A$  from 9 to 14 cm., the graphs show highly increased sensitiveness with the  $b'$  pitch properly salient and the  $a''$  located as before. This increase of sensitiveness, through a maximum as  $A$  increases, has already been shown in figure 71 and thus corroborates an interesting result.

The new resonance  $d'$  for  $x=24$  is probably evoked by exciting the overtone  $d''$ . Similarly,  $b$  for  $x=29$  excites the overtone  $b'$ , as the telephone note is not a simple harmonic.

The novelty in the graphs for  $x=29$  is the low  $\#d$  (frequency about 150), for which the free semi-wave-length would be over a meter. This is very salient and distinct, though the exact location of pitch between  $d$  and  $e$  is a little difficult to ascertain. With pipes but 9 cm. long and a maximum axial distance not exceeding 29 cm., the origin of this note is an interesting problem. To suppose that it awakens  $a''$  as its second overtone is not in keeping with the fixity of  $a''$  above stated.

The subtlety of the relations involved is well shown by the graphs (figs. 74 and 75), in which the pipes  $t$  and  $t'$  as above are prolonged by quill tubes  $t''$  and  $t'''$ , with the pin-holes (as before) near the U-tube. The cross-pipe  $A$  was short ( $x=25$ ). The  $a''$  maximum has its usual fixed position and the  $\#c''$  maximum, figure 74, corresponds to  $x$ ; but these two maxima now show a strong tendency to coalesce. The  $\#c'$  maximum might be associated with  $\#c''$ . One observes the multiple resonance below  $\#c'$ . The  $\#g'$  maximum here, as compared with figure 73, is new.



In case of figure 75, the quill tube  $t'''$  was removed and the pin-hole attached directly to  $t'$  as before. The resonances near  $a''$ ,  $g'$ ,  $c'$ , and even below, remain nearly intact, but the strong  $\#c''$  resonance has been quite obliterated. Hence this maximum would seem to be referable to the quill tube  $t'''$  acting independently. Similarly, the new maximum near  $g'$ , as compared with figure 73, should be associated with the quill tube  $t''$ . The maximum near  $c'$ , though more pointed in figure 75, is present in both figures and might therefore originate with the tube-length  $t'At'$ . Granting the uncertainty of these conjectures, there is nevertheless a suggestion that by connecting quill tubes with the nodal ends of the pipes  $t$ ,  $t'$ , a variety of multiple resonances might be obtained. Experiments made at some length along these lines, however, gave me nothing more than highly ornamented graphs, containing secondary maxima. I obtained no contrasts quite so clear as those of figures 74 and 75, though on lowering the resistance in the telephone a number of subsidiary maxima varying with  $t''$  and  $t'''$  were readily picked out.

## STRAIGHT AND TRANSVERSE PIPES.

**53. Straight tubes 2 cm. diameter.**—The inset, figure 77, shows the new adjustment with the telephones  $TT'$  at the ends of the pipe  $tt'$ . The latter is provided with adjutages  $a$  and  $b$ ,  $y$  cm. apart, when the total length of  $tt'$  is  $x$ . The salient ( $s$ ) and reëntrant ( $r$ ) pin-holes are here attached. The telephone current in  $T$  may be reversed at  $c$ .

The graphs, figures 76 and 77, are the results of two surveys in pitch, for  $x=22$  cm.,  $y=7$  cm., and  $x=32$  cm.,  $y=17$  cm., respectively, the adjutages being about 7 cm. from the telephone plates. The results conform closely with figure 71 for bent tubes, as would be anticipated. The chief maximum near  $c''$  in figure 76 and near  $a'$  in figure 77 being strong in the  $S$  position, but practically absent in the  $P$  position of the switch. Moreover, the intensity of this maximum increases in marked degree with  $x$ , being over twice as high for  $x=32$  as for  $x=22$ .

If the adjutages  $ab$  are placed nearer the telephone plate, the fringe displacements  $s$  may be enormously increased. Thus in figure 82 (below),  $x=32$ ,  $y=25$ , so that the plane of the pin-holes is about 3 cm. from the respective telephone plates. It was necessary to put 1,000 ohms in the telephone circuit, so that the  $a'$  maxima are here over 3 times as high as before. The pin-holes may be inserted at  $a$  and  $b$  (fig. 77), or side by side in  $a$ ,  $b$  being closed. If the reëntrant pin-hole is at the middle of  $tt'$ , a smaller displacement  $s$  is obtained, as indicated (fig. 82).

The fixed maxima near  $g''$  are as usual present in all cases, and here they also increase in intensity with  $x$ . In figure 82, however, they have not been raised in the same ratio as the  $a'$  maxima.

**54. Transverse tubes, 2 cm. diameter.**—The tube  $tt'$  was now provided with a cross-branch in the middle, shown at  $mn$  in the inset, figure 79. This not only makes it convenient to search for the occurrence of nodes midway between the telephone plates, but (as will presently appear) with the telephones in phase ( $P$ ), a complete succession of nodes may be invoked in these transverse pipes without changing the position of pin-holes. The length  $z$  of the cross-branch in relation to the length  $x$  of pipes  $tt'$  modifies the intensity of vibration obtained, though it seems to change the pitch very slowly at first.

The graphs traced in the frequency surveys are given in figures 78 and 79, for  $z=4$  and 13, respectively. In both a new maximum at  $e''$  is strikingly developed. This maximum is very high in figure 79, conformably with the large  $z=13$  cm. It occurs, moreover, for the  $P$  position of the switch and not at all for the  $S$  position, as do the maxima belonging to the ends of  $tt'$  hitherto studied. There is thus an opposition in the phase of the telephone plates in the two cases of experiment.

While the strong  $a'$  maximum has vanished, the  $g''$  maxima are still remarkably strong at the middle of  $tt'$ . In figure 78 the salient pin-hole was at the  $m$  end, but near the U-gage, while the reëntrant pin-hole was put in the cork at  $n$ . Adding a quill-tube adjutage here in the interest of greater

symmetry, the  $e''$  maximum was but slightly enhanced, but the  $g''$  maximum considerably, as the figure indicates. In figure 79 the pin-holes were tentatively placed side by side in a doubly perforated cork. In this case the  $g''$  was not marked and had coalesced with the excessive  $e''$  maximum. Placing the reëntrant pin-hole at  $n$  decreased the  $e''$  somewhat, but brought out the  $g''$  maximum more sharply, as indicated more fully in figure 80.

To produce a node in the middle of the pipe  $tt'$ , the telephone plates must be in the same phase, whereas for a neutral segment here they should be in opposite phases. It is thus curious to note the pitch  $a'$  in the latter case, as compared with the pitch  $e''$  of the former middle node, a difference interval of but a fifth. This, however, is conformable with the expansion of tube at  $mn$ , figure 79.

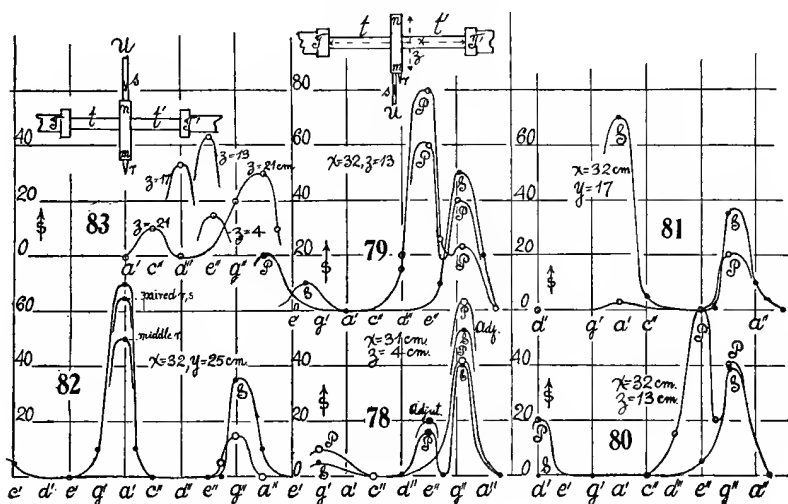


Figure 81, finally, is a repetition of the case of figure 77 ( $x=32$  cm.,  $y=17$ ), but in the presence of the cross-branch ( $z=13$  cm.). The character of the graph is unchanged, though with reduced intensity. It thus contrasts sharply with figure 79, except at the common fixed maximum at  $g''$ .

The effect of the expansion in  $z$  in intensity and pitch was next investigated, as shown in figure 83 (inset). The pin-holes were here placed at the opposite ends,  $m$  and  $n$ ,  $m$  being elongated. The graphs obtained for the different adjustments ( $z=4, 13, 17, 21$  cm.) are indicated, showing that here there is also an optimum in length at  $z=13$  cm., about, while the pitch changes from  $\sharp e''$  to  $c''$ .

The arrangement, however, is far more sensitive if the adjutage  $m$  is closed and the two pin-holes  $r$  and  $s$  are placed side by side in  $n$ ,  $s$  communicating with the U-gage. The pitch and intensity of the maxima found in the different adjustments is given in figure 84, the  $z$  lengths (4, 9, 14, 16, 21, 22 cm.) in round numbers being attached. The locus rises rapidly to the optimum and then decreases, fast at first but eventually less so, the distribution being much

as in figure 71. In the adjustment of figure 84, the pin-holes necessarily lie at the node.

The full resonance curve for the length  $z=9$  cm., given in figure 84, is interesting, 1,000 ohms being in circuit, telephones in phase ( $P$ ). All the  $e$ 's ( $e, e', e''$ ) are active. Probably the  $e$  and  $e'$  as given by the telephone plate contain the dominant  $e''$  as an overtone. Similarly,  $g, g', g''$  coalesce with  $e, e', e''$ , more or less, so that except at  $a', c'', c'''$  there is response throughout. In the case  $S$ , with the telephone plates not vibrating in phase, there is moderate response at  $g''$  only.

**55. Comparison of constants for wide tubes.**—If we collect the data of figure 71 for the tube-length  $x$  and corresponding intensity of note or fringe displacement  $s$ , and compare them with figure 84 for the transverse tube-length  $z$  and its fringe displacement  $s$ , the following correspondence appears:

Longitudinal tube	$\left\{ \begin{array}{l} x = 22 \\ s = 18 \\ d'' \end{array} \right.$	$\left\{ \begin{array}{l} 24 \\ 55 \\ b d'' \end{array} \right.$	$\left\{ \begin{array}{l} 30 \\ 70 \\ a' \end{array} \right.$	$\left\{ \begin{array}{l} 34 \\ 70 \\ b g' \end{array} \right.$	$\left\{ \begin{array}{l} 42 \\ 55 \\ e' \end{array} \right.$	$\left\{ \begin{array}{l} 47 \\ 25 \\ c' \end{array} \right.$	cm. scale-parts.
Transverse tube	$\left\{ \begin{array}{l} z = 4 \\ 25, 32 \\ b f'' \end{array} \right.$	$\left\{ \begin{array}{l} 9 \\ 75, 100, 120 \\ e'' \end{array} \right.$	$\left\{ \begin{array}{l} 14 \\ 95, 100 \\ \# c'' \end{array} \right.$	$\left\{ \begin{array}{l} 16 \\ 60 \\ b' \end{array} \right.$	$\left\{ \begin{array}{l} 21 \\ 40 \\ a' \end{array} \right.$	$\left\{ \begin{array}{l} 22 \\ 35 \\ g' \end{array} \right.$	cm. scale-parts.

These curves are given in figures 85 and 86. The  $x$  values of  $s$  could have been increased several times by placing the pin-holes nearer the telephone plates (as was done in the work of figure 82) under high resistance; but it is merely the relative values or configuration curves which are here in question. The cusplike rapidity with which the optimum is reached and lost in the case of transverse pipes (pin-holes in the middle between plates) is in contrast with the more leisurely progress in the case of longitudinal pipes; but a preferable length in  $z$  or in  $x$  is none the less clearly present in both cases. Thus a length most favorable to response exists, and for this it is not easy to account. True, the transverse tube is associated with the longitudinal tube (inset, fig. 86), so that the vibration is from  $T$  to  $m$  and  $T'$  to  $m$  simultaneously, making  $m$  a node; but the longitudinal tube is alone, the transverse section being removed.

If we use the above equation (2) in  $x$  and  $\lambda$  obtained with bent pipes

$$x = 0.4\lambda$$

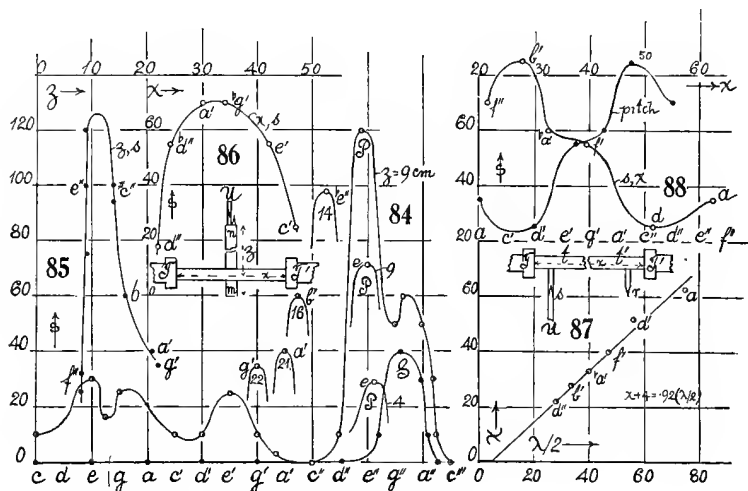
and apply it to the axial length of the semi-wave-lengths  $T$  to  $m$  and  $T'$  to  $m$  (deducting the  $n$  protuberance  $z'=2$  cm. from  $z$  so that  $z'+z''=z$ ), the following data appear:

Observed $z' + x/2 \dots\dots$	18	22	27	29	34	35
Pitch $\dots\dots f''$		$e''$	$\#C'$	$b'$	$a'$	$g'$
Computed $z' + x/2 = 0.4\lambda \dots\dots$	19	20	24	27	30	34

These values, though too small in the computed data, nevertheless show that the vibration form is correctly assumed, the node of both  $T$  and  $T'$  being at  $m$  and receding with  $m$ . The true coefficients here would be 0.44, 0.45, 0.43, 0.45, between  $e''$  and  $a'$ , or  $x=0.44\lambda$  on the average.

Thus it seems probable that additional resistance was introduced in the above experiments ( $x=0.4\lambda$ ) by the two right-angled bends in the tubes. The experiment was therefore repeated with straight tubes 2 cm. in diameter (inset, fig. 87), with the results given in the graph of that figure, 1,200 ohms in the telephone circuit. If  $x$  is the length from plate to plate of the telephones, the data range as follows (fig. 87) :

Observed $x$ .....	21	27	32	39	51	62 cm.
Observed pitch .....	$d''$	$b'$	$ba'$	$f'$	$d'$	$a$
Observed $\lambda/2$ .....	28	33	40	47	56	75 cm.
Observed $s$ .....	70	83	60	53	25	35 scale-parts.
Computed $\lambda/2$ .....	24	31	37	45	59	71 cm.
Computed pitch .....	$f''$	$c''$	$a'$	$f'$	$bd'$	$a$



The mean coefficient obtained from these results,  $x=0.43\lambda$ , agrees very very nearly with the data for transverse tubes. Though this graph is the best obtained, the equation is inadequate, as may be seen by computing the  $\lambda$  from the observed  $x$ , in which case the higher notes  $d''b'ba'$  would be too far off to have deceived the ear of the observer. In fact, an equation of the form  $x = -a + b\lambda$  must at the outset be much more satisfactory; for the  $a$  is referable to the space in the telephone mouthpiece. Thus, for instance,  $x + 4 = 0.92(\lambda/2)$  would give the data:

$x =$	21	27	32	39	51	62 cm.
$\lambda/2 =$	27	34	39	47	60	72 cm.
Observed pitch $=$	$d''$	$b'$	$ba'$	$f'$	$d'$	$a$
Computed pitch $=$	$d''$	$b'$	$ba'$	$f'$	$\sharp c'$	$a$

which is perhaps as near as the pitch obtained under chromatic conditions can be recognized. Thus there is no experimental evidence here of an effect of pitch in relation to viscosity within the octave and a half surveyed.

Figure 88 shows the fringe displacement  $s$  for the different pipe-lengths  $x$ , as well as pitch. There is also an optimum length here at  $x=30$  approximately, though the curve later (at  $a, x=80$ ) shows signs of recovery. Much depends

in such cases on the steady efficiency of the contact-breaker; so that inferences here must be made with caution. The possibility of a harmonic distribution of points is not, however, improbable.

**56. Telephones in parallel.**—A number of experiments (tubes straight, 2 cm. in diameter, as in fig. 77) were made with the telephone circuit in parallel, so adjusted that one of the currents could be reversed. The distribution of  $s$  in pitch was naturally not modified, but the sensitivity was usually much smaller. A single telephone sufficed to bring out the resonant note almost in full strength, which was quite audible,  $s=0$ , with the telephones in opposition. Thus at pitch  $c''$ ,  $s=40$  scale-parts, appeared with one telephone or both telephones cooperating  $s=0$  when they counteracted each other. In the alternative case,  $s=30$  for one and  $s=40$  for two telephones was obtained, while  $s=0$  appeared with the telephones antagonistic.

The experiments were made with the object of gradually modifying the phase of one telephone plate with reference to the other, and from this viewpoint the design is of great interest; but nothing worth recording was obtained.\*

#### QUILL PIPES, CAPPED AT BOTH ENDS.

**57. Vibration in closed straight quill tubes. Straight tubes.** Though some work of this kind was done above, it was thought well to carry it through more systematically and with thinner tubes. The plan of the apparatus is shown in the inset, figure 89, with the pin-holes  $s, r$  close to the telephones  $T, T'$  and the ends of the  $t, t'$  tubes extending very nearly to the telephone plates. A full survey from  $c$  to  $d'''$  was made both for the shortest available length,  $x=9$  cm., and for the longest,  $x=29$  cm. The results are summarized in the graphs, figures 89 and 90, both for the  $S$  and  $P$  telephone relations.

With the telephone plates vibrating in the same phase ( $P$ , currents in sequence), the two curves are practically identical, except in intensity distributions. Thus the maxima near  $a''-b''$ ,  $d''-\#d''$ ,  $a'-b'$ ,  $d'-\#d'$ , below  $a$  are present in both. Below  $a$  in the 4-foot octave, the graph is still of high intensity,  $s$ , and practically horizontal, almost to  $c$ . The pipe is in resonance with any pitch of the 4-foot octave. The intensities of the  $a''$ ,  $a'$ ,  $a$  of the pipe are in excess when  $x=9$  cm., the intensity of  $d''$ ,  $d$  slightly in excess when  $x=29$  cm.

When the telephone plates vibrate in opposite phases ( $S$ , current in contrary), the single strong movable note corresponding to the length  $x$  of the  $tt'$  pipe appears. This is at  $a'$  in figure 90,  $x=9$  cm., at  $g-a$  in figure 89,  $x=29$  cm. and in both cases very outspoken. The steady maximum near  $b''$  is now stronger for  $x=29$  cm.; that near  $c''$  coalesces below ( $x=9$  cm.) with the large  $a'$  maximum; that near  $a$  below ( $x=9$  cm.), with the large  $a$  maximum above ( $x=29$ ).

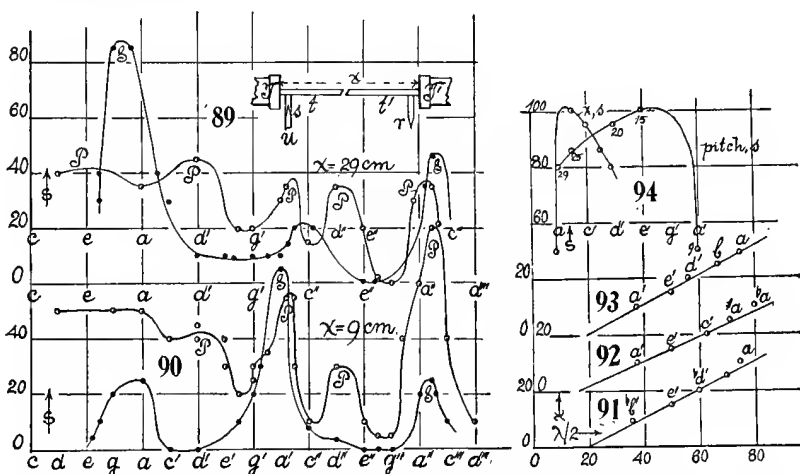
\* This has since succeeded both with resistance and inductance leading to interesting deductions to be given in the Proceedings of the National Academy of Sciences for May *et seq.*, 1925.



When the plates are in phase ( $P$ ), the pipe is rarely silent; not at all for  $x=9$  cm. It presents a remarkable case of multiple resonance. It is possible that the lower pitched maxima all evoke the strong upper harmonic near  $b''$ .

In figures 91, 92, and 93 the resonance pitch corresponding to different lengths of pipe  $x$  have been recorded. The experiments were completed at different times and in figures 91 and 92 the graph appears to be curved, as if an effect of pitch in relation to viscosity of air were here discernible; but in figure 93, which was made with great care in view of this question, there is no such effect appreciable. The discrepancy is thus referable to the difficulty of locating the very flat maximum of the 4-foot octave.

The curves have a common characteristic. Compared with figure 87 for 2 cm. pipes, their mean slope is very much less,  $2x=0.35$  being the mean



result. All the curves, however, demand an initial constant, as if referable to the space in the telephone mouthpieces. This is at present relatively large, so that (fig. 93) the equation  $x+10=0.51(\lambda/2)$  is a more suitable form. The results are now:

Observed $x$ .....	9	15	20	25	29 cm.
Observed $s$ .....	70	80	90	85	50 scale-parts.
Observed pitch .....	$a'$	$e'$	$d'$	$b'$	$a$
Observed $\lambda/2$ .....	37	50	56	67	75 cm.
Computed $\lambda/2$ .....	37	49	59	69	76 cm.
Computed pitch .....	$a'$	$e'$	$bd'$	$b$	$a$

These data are in places again disappointing as to pitch. In the case of somewhat flickering chromatic intervals, the ear occasionally overestimates its precision.

The data of figure 93 are given as to intensity and pitch in figure 94. The optimum appears as usual. The rapid drop of frequency ( $a'$  to  $e'$ ) for the first small elongation,  $x=9$  to  $x=15$ , is noteworthy.

If we take the equation  $x+a=b(\lambda/2)$  and compare the coefficients for tubes 2 cm. in diameter and the present quill tubes 0.4 mm. in diameter, the

respective coefficients are 0.92 and 0.51. Thus, while the ratio of diameters has gone down five times, the ratio of coefficients is but  $0.92/0.51=1.8$ . If we write the equation in  $u$  and  $v$ , § 51,

$$\frac{(x+a)-\lambda/2}{\lambda/2} = -\frac{1}{R} \sqrt{\frac{\eta}{2n\rho}}$$

Since no relation to  $n$  has been detected, this conforms to

$$\frac{(x+a)-\lambda/2}{\lambda/2} = -(1-b)$$

Thus for the two diameters  $2R=2$  cm. and 0.4 mm. the coefficients are  $1-b=0.08$  and 0.49, respectively. Hence, while  $R$  has decreased five times  $(1-b)$  has increased about six times and  $R(1-b)$  is no longer constant. Without violence to the observations this differential coefficient  $1-b=0.08$ , however, might be put 0.09 or even larger, in view of the difficulties in fixing pitch above pointed out. The discrepancy is therefore not decisive, except in the absence of the frequency effect  $\sqrt{\eta/2n\rho}$ .

**58. Vibration in transverse quill tubes.**—The adjustment is shown in figure 95 (inset),  $t''$  being the transverse quill tube activated when the telephone plates vibrate in the same phase. A difficulty is here encountered, inasmuch as the conical pin-hole tubes  $r$  and  $s$  are no longer negligibly small in comparison with the pipe  $t''$ . With 200 ohms in the telephone circuit, the response is good and figure 95, *a* shows that an optimum is probable, as usual. The rapid march of the note ( $e''$  to  $b'$ ) for the first small elongations ( $z=7$  cm. to  $z=12$  cm.) is noteworthy, here as in the above data (compare fig. 94,  $a'$  to  $e'$ ). While for telephone plates in opposite phases there was no response, a fringe displacement of 60 scale-parts was observed for like phases.

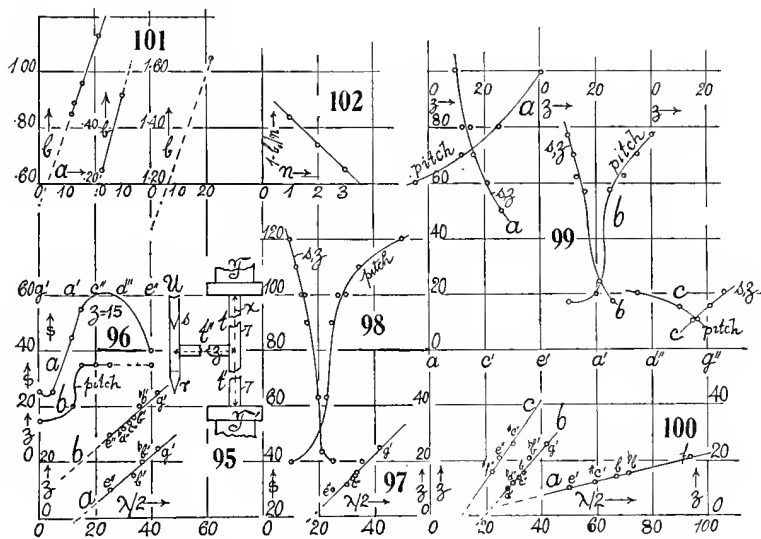
If the transverse length is called  $z$  (see fig. 95), the coefficient in  $z+a=b(\lambda/2)$  here comes out astonishingly large, and in figure 95, curve *a* conforms closely to  $z+12=0.85(\lambda/2)$ . This value for these thin quill tubes ( $2R=0.4$  cm.) recalls the value for tubes 2 cm. in bore. The work was repeated later (figs. 95 and 96, curve *b*) with modifications; but the results are of the same order,  $z+13=0.89(\lambda/2)$  so far as the coefficient is concerned.

In figure 97 the survey was repeated in such a way as to obtain large fringe displacements throughout (see fig. 98); but the mean coefficient is here even larger, the equation reading  $z+16=0.96(\lambda/2)$ . If the whole distance to the telephone plate  $t+t''$  or  $t'+t''$  is taken,  $z+23=0.96(\lambda/2)$  would adequately reproduce the data, which procedure does not, of course, modify *b*.

On comparing figure 97 for transverse pipes with figure 93 for straight pipes (longitudinal vibration), one notices that the frequency in the latter case is about an octave lower; but there is a full octave in figure 93 and more than an octave in figure 97. Yet no suggestion of a frequency effect appears. Moreover, the respective coefficients  $b$  are in the inverse order in which they should occur, for it is the higher octave (fig. 97) which has the largest

coefficient. The cause of this anomalous result will be considered in the next section.

Figure 98, indicating the large intensities  $s$  in relation to transverse-tube-length  $z$  and the observed pitch, imply an optimum within the smallest available tube-length  $z=10$  cm. Apart from this, the graphs of figures 98 and 94 are not dissimilar. Moreover, one would expect an optimum here when  $z=\pi/2$ , i. e., for three equivalent resonators. I refrain from putting stress on the absolute magnitude of the  $s$  data, as they are subject (as already intimated) to the play of the contact breaker and this is liable to vary in efficiency. Thus,



in figure 96, the curve  $b$  has probably encountered some such discrepancy, from which the curve  $a$  is free.

**59. The same. Overtones. Viscosity effect.**—After obtaining the anomalous results stated, I overhauled the apparatus as a whole, chiefly with regard to slight leakages at the telephone plates and elsewhere. The result was a considerably increased sensitivity ( $s$ ), as shown in table 16, 1,000 ohms being in circuit (see fig. 99). The slopes of the given series (fig. 100, curve  $b$ ) has even increased, so that now  $z+22=1.13(\lambda/2)$ . The observations as a whole were more regular. At the same time, however, I detected the graph ( $c$ ), a scant fifth above ( $b$ ) and reproduced by the equation  $z+22=1.65(\lambda/2)$ . Clearly this was the third harmonic of the transverse tube, so that the fundamental might be looked for an octave lower. The graph ( $a$ ) in figure 100 was accordingly sought and found. The initial tube-length  $a$  here is, as usual, smaller and the equation  $z+2.5=0.25(\lambda/2)$  adequately reproduces the data. The present coefficient  $b=0.25$  is thus astonishingly small, being but one-half of the preceding coefficient,  $b=0.51$ , for vibrating air filaments in straight tubes.

If one conceives the vibrations to take place along  $Tt''s$  and  $T't't''r$  (fig. 95, inset) and return, the structure in the tube  $t''$  (area of filament reduced one-half) and the expansion in the tube  $sr$  may have something to do with the increased resistance; but the initial lengths  $a$  seem to be adjusted by the tube itself in an arbitrary manner, being but  $a=2.5$  cm. for the graph  $a$ , and  $a=22$  cm. for the overtone graphs  $b$  and  $c$ . Unfortunately, in the case of curve  $a$ , the fringe displacements below  $f$  are nearly constant (compare graphs 89 and 90), so that resonances are continuous and can no longer be picked out. Figure 99 shows, however, that in curves  $a$  and  $b$  the optimum should lie below 10; and since the straight pipes  $t$  and  $t'$  (fig. 95, inset) are each 7 cm. long, this result would be consistent if the resonance of the  $x/2$  and  $z$  air filaments contributes to this end. Contrariwise, the optimum in the overtone graph  $c$  would lie considerably above 26 cm. (fig. 99), and for this there seems to be no suggestion at hand.

TABLE 16.

$z =$	10 cm.	12 cm.	14 cm.	16 cm.	21 cm.	26 cm.
B { Pitch .....	$d''$	$bd''$	$c''$	$b'$	$bb'$	$g'$ .
$\lambda/2$ .....	28	30	32	33	35	42 cm.
$s$ .....	77	70	62	57	24	17 scale-parts.
A { Pitch .....	$e'$	$\#c'$	$b$	$bb$	$f?$	(continuous).
$\lambda/2$ .....	50	59	67	71	94?	cm. (continuous).
$s$ .....	100	80	80	70	60	50 scale-parts (continuous).
C { Pitch .....	..	..	..	$\#f''$	$e''$	$\#c''$ .
$\lambda/2$ .....	..	..	..	22	25	30 cm.
$s$ .....	..	..	..	10	15	20 scale-parts.

The apparatus is active even if but one telephone is used, the other being silent. Thus at  $d''$ ,  $s=75$  fell to  $s=35$  with one telephone excluded. Care to guard against even small leakages is very necessary, or  $s$  will fall off.

With the graphs  $a$ ,  $b$ ,  $c$ , figure 100, another method of approaching the frequency correction becomes available. Since the first three harmonics are in question, the pipe-lengths  $z+a$  are respectively equivalent to  $\lambda'/2$ ,  $2\lambda'/2$ ,  $3\lambda'/2$ , where  $\lambda'$  is the wave-length within the quill tubes, and not to  $\lambda/2$ , as was postulated in the equations  $z+2.5=0.25(\lambda/2)$ ,  $z+22=1.13(\lambda/2)$ , and  $z+22=1.65(\lambda/2)$ . Thus, if the corrected coefficients  $b$  are called  $b$ ,  $b'$ ,  $b''$ , respectively, the following relations appear for the relative frequencies  $n$ ;

Curve (a) freq. ratio, $n=1$	$b=0.25$	$b=0.25$	$1-b=0.75$	$(1-b)\sqrt{n}=0.75.$
Curve (b)	2	1.13	$b'= .56$	$1-b'= .44$ $(1-b')\sqrt{n}= .62.$
Curve (c)	3	1.65	$b''= .55$	$1-b''= .45$ $(1-b'')\sqrt{n}= .78.$

In the preceding section for straight tubes,  $x+10=0.51(\lambda/2)$  was obtained, so that  $b=0.51$  is more probably the coefficient for the fundamental. True, figure 90 contains an  $a$  maximum below the  $a'$ ; but it is to be considered incidental and at all events too low for development. Thus it appears that a coefficient of this order could be identified with the data  $b'=0.56$  and  $b''=0.055$

for the second and third overtones in the table. But such a procedure leaves the datum  $b' = 0.25$ , here found, still more anomalous.

From the theoretical equations, as above put,

$$(\lambda/2 - (z+a))/(\lambda/2) = 1 - b = \sqrt{\eta/2n\rho}/R$$

$(1-b)\sqrt{n} = \text{const.}$  should follow for a given radius of tube  $R$ . These data have also been tabulated, and it is now the second harmonic which is inconsistent. There are, however, three earlier values (figs. 95 and 97) for this coefficient, respectively,  $b' = 0.45$ ,  $0.43$ , and  $0.48$ , and if their mean be taken  $(1-b')\sqrt{n} = 0.77$ , which would fit in better with the table.

The subject therefore is quite involved. Within the range of the separate graphs, figures 95, 97, and 100, no frequency effect can be detected. From the group of graphs for successive overtones, such a relation can not, however, with confidence be rejected. It seems more plausible that  $b = 0.51$  given by straight tubes is trustworthy and that, therefore  $(1-b)\sqrt{n}$  is not constant, whereas  $b$  probably is nearly so.

What is particularly puzzling is the interdependence of  $a$  and  $b$ . As obtained in different experiments,  $a$  and  $b$  vary proportionally for incidental causes not detected. Thus in figures 95, 97, and 100 for the octave

$$\begin{array}{ccc} a = 12 & 13 & 16 \\ b = 0.85 & 0.89 & 0.96 \end{array} \quad \begin{array}{c} 22 \\ 1.13 \end{array}$$

In figures 93 and 100 for the fundamental

$$\begin{array}{cc} a = 10 & 2.5 \\ b = 0.51 & 0.25 \end{array}$$

while the fifth in figure 100 stands alone. These data are constructed in figure 101 and the graphs are seen to be consistent and not very different for the fundamental and the octave.

TABLE 17.

	Freq. ratio, $n =$		
	1	2	3
$b_0$ .....	0.16	0.52	1.05
$b_0/n$ .....	.16	.26	.35
$1 - b_0/n$ .... {	.84	.74	.65 observed.
	.84	.74	.64 computed.

It is thus worth while to attempt to eliminate the  $a$  from the equation, if the incidental influences modifying  $b$  are to be removed. This may be done by estimating the  $b_0$  which holds for  $a = 0$  in an equation  $b = b_0 + \beta a$ , and since the slope for the octave is not very different from the fundamental, the slope for the fifth may be taken as the same as that of the octave. Thus the data are given in table 17.



fifths are deleted. The results, however, are very much smoother than heretofore and three successive octave groups are available for exploration.

The survey in pitch is summarized in figures 103 and 104, the telephone, small inductor, and circuit together constituting the electric siren. The lengths  $l$  are measured from  $s$  or  $r$  to  $n$ . Beginning with  $l=8$  cm. in the bend,  $l$  is increased in steps of 5 cm. on each side. Corresponding maxima are tabulated in table 18.

The chief maxima thus reappear at octave intervals. The optimum (see fig. 105) lies within 8 cm. There are small secondary maxima which it is difficult to construe.

The relations of  $l$  and  $\lambda$  are given in figure 106, with the pitch added at each observation. Their disposition is again as nearly linear as the ear can guarantee, the three lines  $n=1, 2, 4$  belonging to the successive octave groups. Each again demands an initial tube-length, but this ( $l=12, 12, 13$  cm.) is here nearly the same in the three cases, or is at least without systematic change.

TABLE 18.

$l$	Pitch.	$\lambda/2$	Pitch.	$\lambda/2$	Pitch.	$\lambda/2$	Remarks.
8 cm....	..	cm.	$g''-g''$	cm.	$g'$	cm.	Minima, $a', d'', a''$
Computed	..	..	..	21-22	..	42	Sec. max., $b'$ .
13 cm....	..	..	$e''-f''$	20	$e'$	41	Minima, $a' \#a''$
Computed	..	..	..	24-25	..	50	
18 cm....	$\#c''$	15	$\#c''$	25	$\#c'$	50	Minima, $g', f'', a''$
Computed	..	15	..	30	..	60	Sec. max., $g''$
23 cm....	$\#a''$	18	$\#a'$	30	$\#a$	60	Minima, $\#d' (c'', d'', e'')$
Computed	..	18	..	35	..	71	
28 cm....	$\#g''$	20	$\#g$	35	$\#g$	69	Minima ( $c', d', e'$ ) ( $d'', e'', g''$ )
Computed	..	20	..	40	..	80	
				40		79	

One might suppose that the tube ends  $Us$  and  $U'r$  are implicated, but their length is but 5 to 6 cm. The equations of the lines for the frequency ratios  $n$  may be written

$$\begin{array}{rcl} n=4 & l+12=2.0 & (\lambda/2) \\ 2 & l+12=1.0 & (\lambda/2) \\ 1 & l+13=.52 & (\lambda/2) \end{array}$$

The above shows the computed values which, on the whole, are about as near as the ear may expect to come. A few divergences could doubtless be resolved on repetition. Thus the viscosity here expresses itself in the coefficient together with an additional tube length.

A question presents itself, whether these octaves (of which the middle one is the most conspicuous) are not stimulated by overtones in the telephone-note. Thus when for  $l=8$  cm., the telephone sounds  $g'$ , it may be the  $g''$  evoked which produces the  $g'$  maximum; for  $l=18$  cm. the telephone note near  $c'$  may be active through  $c'', g'', c'''$  in the overtones, etc. In such a case, the above equations would be repetitions of each other. It is, however, improbable that the overtones should be of the observed intensity, and more important

still, the telephone overtone can only be operative if  $b$  is fractional. Thus  $b=0.25$  is the only case which could be evoked in this way. Consequently we may write with assurance as in the preceding section (if  $\lambda'$  is the wavelength under friction), taking the graph  $n=1$  as the fundamental:

$$\begin{array}{rcl} n=1 & (\lambda'/2)=l+13=0.52(\lambda/2) & \lambda'=0.52\lambda \\ 2 & 2(\lambda'/2)=l+12=1.0(\lambda/2) & \lambda'=.50\lambda \\ 4 & 4(\lambda'/2)=l+12=2.0(\lambda/2) & \lambda'=.50\lambda \end{array}$$

in the general form  $n(\lambda'/2)=l+a=b(\lambda/2)$ . Since the constant  $a$  is here the same (nearly) throughout, the coefficient  $b$  is probably less in need of reduction in relation to  $a$ . At all events, no observations could be devised to elucidate this dependence.

Thus it appears that the relations are simpler than in the preceding section,  $b=0.51$  being constant for the three octave groups  $n=1, 2, 4$  in frequency ratio. The values heretofore found were for straight tubes of about the same section  $b=0.51$ ,  $a=10$  cm.,  $n=1$ ; for transverse tubes,  $b=0.25$ ,  $a=2.5$  cm.,  $n=1$ ;  $b=0.56$ ,  $a=22$ ,  $n=2$ ;  $b=0.55$ ,  $a=22$ ,  $n=3$ . These are all of the same order of value, excepting the case  $n=1$  for transverse tubes, where  $b=0.25$  has but one-half its anticipative value. Thus in the four octave groups  $n=1, 2, 3, 4$ ,  $b$  does not vary, if the exceptional case specified, associated with the exceptional  $a=2.5$  cm., can be explained. The endeavor to reduce  $b$  to  $b_0$  for  $a=0$ , by the constants of figure 101, leads to no trustworthy results in the single telephone experiments;  $b_0/n$  (0.27, 0.31, 0.31) comes out more nearly constant than  $1-b_0/n$ . Tentatively, one may postulate that the transverse pipe on sounding its fundamental vibrates like a closed organ-pipe or that

$$\frac{n}{4}\lambda'=0.25(\lambda/2)$$

whence  $\lambda'=0.50\lambda$ , in keeping with the six other octave groups. The result remains none the less difficult to understand, and one more easily concedes here that it is the first overtone of the telephone-note which evokes this apparently low octave group. To make sure of its occurrence, I repeated the two telephone experiments (fig. 95, inset) and obtained for the transverse pipe somewhat differently mounted:

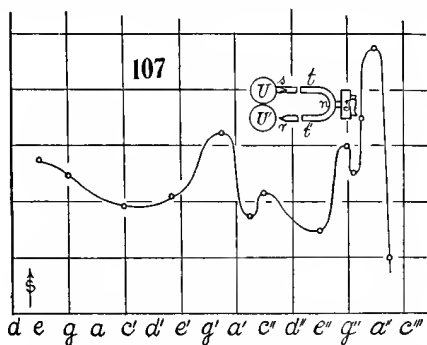
$$\begin{array}{rcl} z= & 8 & 13 & 18 \text{ cm.} \\ \text{Pitch} = & f'-g' & c' & a \\ s= & 35 & 30 & 50 \text{ scale-parts.} \\ \text{Observed } \lambda/2 = & 45 & 63 & 75 \text{ cm.} \\ \text{Computed } \lambda/2 = \left\{ \begin{array}{l} 45 \\ f'-g' \end{array} \right. & c' & 63 & 82 \text{ cm.} \\ & & \#g & \end{array}$$

results given by the equation  $z+4=0.27(\lambda/2)$ . The difficulty here, already foreshadowed in figures 89 and 90, lies in the plateau-like character of the low-pitched maxima; but the order of  $b=0.27$  is none the less definite.

A final question relative to the need of joining the pin-holes  $s$  and  $r$  to the respective shanks  $U$  and  $U'$  of the gage, deserves attention. In the inset, figure 107, the pin-hole  $r$  is disconnected and open to the atmosphere. Another telephone was used, but the endeavor was made to insert a tube-length  $l=8$

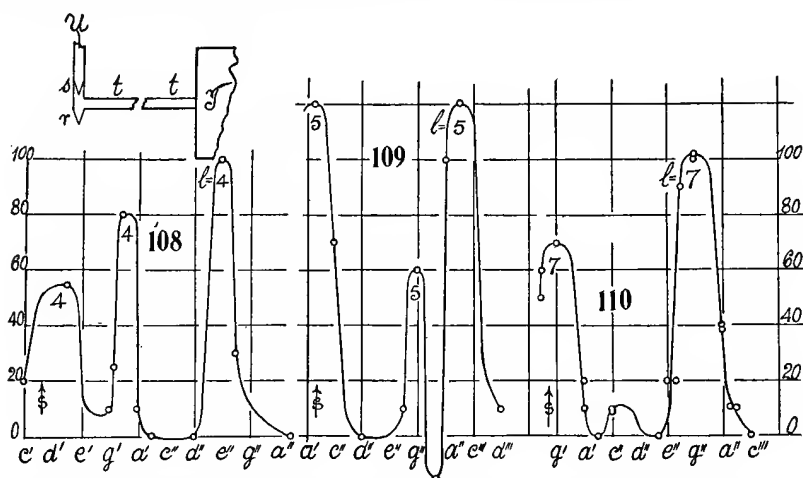


cm. so far as this can be done. The graph thus obtained (fig. 107) is closely similar to the graph for  $l=8$  cm. in figure 103, a little shift necessarily resulting from the  $l$ -difference. In figure 107, however, the secondary maxima were more carefully traced, showing one at  $g''$  which is ignored in figure 103. The



curve below  $g'$  in the 2- and 4-foot octaves was also followed at closer intervals. It is astonishing to find a strong 4-foot  $e$  in these short ( $l=8$  cm.) quill tubes, and the whole curve presents a case of multiresonance which only terminates at  $b''$ . Nowhere else is the response absent. It is conceivable that the  $g''$  and  $a''$  maxima may belong to the tubes  $t$  and  $t'$  separately.

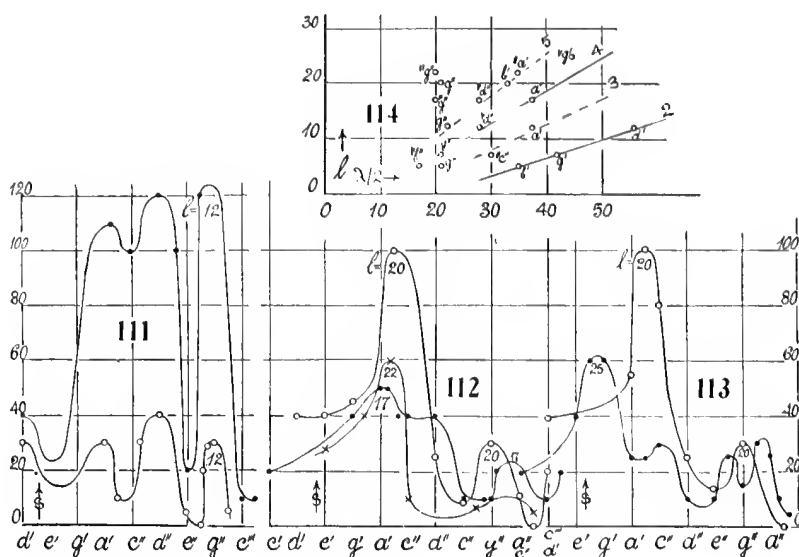
**61. The same. Single telephone and single tube.**—The final method tested (shown in the inset of fig. 108), though apparently the simplest, failed to give data as clear cut as was expected. Here the quill tube  $tt$  (0.35 cm. in



diameter) extends at one end to the plate of the telephone  $T$ , while the other carries a T-branch holding the salient and reëtrant pin-holes  $r, s$ . The latter is joined with a short end of tubing to one shank of the interferometer U-gage and  $r$  is open to the atmosphere. In this case the quill tube  $tt$  may be made

very short, and the graph (fig. 108) was obtained with  $tt$  less than  $l=5$  cm. With 2,000 ohms in circuit the strong maxima near  $e''$ ,  $ba'$ , and  $bc'$  appeared. There is marked response even at  $c'$  for this 4-cm. tube. It is possible, of course, that this low pitch may be evoked by the upper harmonics of the telephone-note, though one would not anticipate the observed intensity in such a case. The maxima obtained do not fit in with the results below, which, however, is not surprising, as the diameter for the short length was irregular.

A repetition of the work, with a quill tube slightly longer ( $l=5$  cm.) and of uniform bore, gave the data of figure 109, with two definite maxima at  $bb''$  and  $bb'$  and peculiar behavior near  $ba''$ , which I did not stop to investigate. Acoustic pressure here came out definitely negative, and this is the only case of negative pressure obtained in this group of experiments. Figure 110 shows



the results for a tube-length ( $tt$ ) of  $l=7$  cm., with two marked maxima about an octave apart and a minor one. In figure 111 the tube-length is increased to 12 cm. and two different intensities of current were used, producing similar but unequally developed curves.

Beyond this the graphs for  $l=17$ , 22 cm. gradually fall out of agreement. Resonance is continuous over large intervals and the appropriate maxima are harder to recognize. The crest near  $a'$  for  $l=17$  cm. is still acceptable, but the one for  $l=22$  cm., which should be at  $f'$ , is absent.

A repetition of the last case with  $l=20$  cm. and somewhat larger intensity is also given in figure 112. It closely resembles the graph for  $l=22$  in character, and the pitch of the chief but spurious maximum is about the same. Hence the orderly sequence of maxima stops at  $l=17$  cm. and between 17 and 22 cm. there is little progress. Between  $l=20$  and 25 cm. (fig. 113) the

sequence of maxima seems to recommence, though the details of the graphs for these long tubes naturally increase.

In figure 114, the  $l$  and  $\lambda/2$  values for the chief crests have been constructed. The values which may be taken as belonging together are (curve 4) :

Pitch.	$l$	$\lambda/2$
$bb''$	5 cm.	17.5 cm.
$g''$	7	21
$d''$	12	28
$a'$	17	37

conforming adequately with  $l + 5.5 = 0.60(\lambda/2)$ . The lower octaves are less definitely (curve 2) :

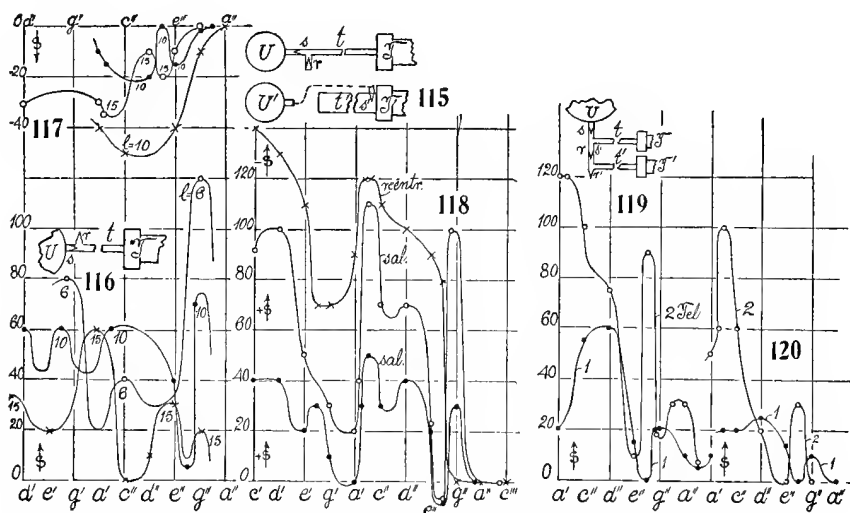
Pitch.	$l$	$\lambda/2$
$bb'$	5 cm.	35 cm.
$g'$	7	42
$d$	12	56

and their coefficient  $b=0.32$  agrees roughly with the preceding, if reduced. Both coefficients are larger for some reason than in the above experiments with double tubes, while the two maxima in figure 113 would correspond to a coefficient of less than  $b=0.5$ . Thus the conditions here are much more complicated than heretofore and a number of prominent crests (curves 3 and 5) can only tentatively be grouped together; the graphs are probably untrustworthy, even though their coefficients are roughly in the ratio of 2. 3. 4. 5. The crests near  $g''$ , which together lie nearly on a vertical for all values of  $l$ , are clearly to be referred to the resonance of independent vibrator like the telephone-plate.

**62. Reversal of pin-holes, etc.**—If the pin-holes are reversed at the same shank of the U-tube, so that, in figure 108, inset,  $s$  and  $r$  both point toward  $U$ , the graphs obtained are throughout negative. Pressures have been changed to dilatations within  $it$ . The arrangement, however (see also fig. 115 at  $UT$ ), is usually much less sensitive, and, what is more important, the resulting graphs are quite different in the disposition of their (negative) crests from the original case. Thus, for instance, the persistent  $g''$  crest (fig. 116 showing the direct and fig. 117 the reversed pin-hole adjustment, with two graphs for large and small intensity at  $l=10$  cm.) is quite absent ( $s=0$ ) in the reversed case, and similarly with other crests. In fact, these graphs are liable to be without harmonic character, showing response everywhere from  $a'$  to  $a''$ , with a maximum at about  $c''$ . The conditions under which reversal proceeds are

thus quite complicated and difficult to investigate; but they may be of considerable importance in their bearing on the phenomenon as a whole.

A number of other experiments of reversal were made, resulting in graphs of the same character as figures 116 and 117, which need not therefore be given. As in case of the curves for  $l=10$  cm., notes which fail in some adjustments come out in others, a result probably similar to difficulties of intonation in musical instruments. The amplitudes increase more rapidly than the electric currents actuating the telephone. The chief difficulty of comparison, however, lies in the unequal lengths of the tubes for reversed pin-holes, if the adjustment of figure 116 (inset) is used. I therefore returned to the adjustment of figure 108 (inset) where the pin-hole tubes are in the transverse branch. Results so obtained (length  $l=10$  cm.) are given in figure 118, the upper curve



showing the acoustic dilatations ( $-s$  charted upward) and the two lower the acoustic pressures ( $+s$  upward), for pitches from  $c'$  to  $c''$ . In the latter cases ( $+s$ ), fringes of different size were used in the two curves. Hence the difference of intensity. In figure 118 there is an obvious correspondence between all the graphs. Thus, the  $b'$  crest is a definite feature of all, as is also the march toward a lower maximum somewhere near  $b$ . In their details, however, the  $+s$  and  $-s$  graphs differ, particularly at the crest near  $g''$ , which comes out strongly with salient pin-holes, but is silent for reëtrant pin-holes, as already found in figure 116. Hence, while in the above I associated this persistent note with the telephone-plate, it now seems more probable that it is to be referred to the pin-hole tubes. That these in the salient position do respond quite appreciably I showed in an earlier report (Carnegie Inst. Wash. Pub. 310, § 25, figs. 34, 35, 1921). Similarly the negative  $f''$  in the salient cases does not appear in the reëtrant graph.

If the pin-hole between  $U$  and  $tt$  (fig. 116) is removed, so that a single pin-hole salient outward remains, the tube  $tt$  is virtually open at one end. The graphs are, of course, essentially different and the sensitiveness is liable to be very low unless the size of pin-hole is judiciously chosen.

Since in case of the use of two pin-holes  $r$  and  $s$  but a single shank of the  $U$ -tube is required, the other with reversed pin-holes may be used for any other acoustic purposes at the same time. Thus in figure 115, the quill tube  $t$  is set for acoustic dilatation, while the pin-hole  $s'$  salient as to  $U'$  measures the acoustic pressure in the wide tube  $t'$  open at one end, the telephones  $TT$  being in parallel. In this way, if  $t$  or  $t'$  is adjustable in length, the lengths of  $t$  and  $t'$ , which correspond to the same crest, may be directly compared. The fringe displacements are nearly summational; thus:

Tube  $t$  (alone)  $s$  equals 30;  $t'$  (alone) 45;  $t+t'$  (together) 70 scale-parts. The difficulties in tuning such pipes are, however, greater than I anticipated.

**63. Successive telephones in cascade.**—In the earlier reports the endeavor was repeatedly made to obtain increased acoustic pressure from a succession of pin-holes in series; but no relaying of this kind occurs. There should, however, be a definite result if (as in fig. 119), between each pair of pin-holes  $sr$ ,  $s'r'$ , etc., a telephone  $T$ ,  $T'$ , etc., is introduced. For the case of two identical telephones in parallel, the graphs (fig. 119) show this to be the case. But while the intensity for two telephones is as a whole much larger than for one, the positions of the crests and troughs is by no means the same. The two quill tubes  $t$  and  $t'$  do not behave identically. Thus near  $f''$ , while one telephone evokes a trough, the combined effect of two is a pronounced crest. Even in a repetition of the experiment with slightly altered tube-length  $tt'$  (fig. 120), this inversion at  $f''$  is sustained. The conditions are further complicated, inasmuch as the relative efficiency of the pin-holes enters fundamentally into the result. If the current in one telephone is reversed, the sum is also liable to be reduced.

It is not surprising, therefore, that with three telephones adjusted on the plan of figure 119, inset, an increase of the acoustic pressure produced by two (all left in parallel) is not as a rule attainable; at least I did not, after many trials, obtain a single marked result, and in many cases there was a reduction.

**64. Experiments with high resistance (binaural) telephones. Apparent hysteresis.**—In testing the radio telephones, the  $H$ -branch of figure 58 above was used for convenience, the cross-tube  $a$  being provided with a short branch and stopcock, so that the air within the  $H$ -branch could be partially exhausted. To make the telephones air-tight, a gasket of card-board, previously soaked in hot oil to expel air, was interposed between the cap and the telephone-plate.

Very small fringes, less than 0.5 scale-part of the ocular micrometer (1 cm. divided in 0.1 mm.), were used to admit of larger pressure ranges. Tested

with the slide micrometer  $\Delta x$ , at  $\theta = 45^\circ$  ( $2\Delta x \cos \theta = n\lambda = 2\Delta h$ ), the coefficient was at first  $\Delta x = 10^{-4} \times 1.07$  cm. per scale-part ( $\Delta s$ ); or  $\Delta h = 7.6 \times 10^{-5}$  mm. per ocular scale-part. The coefficient changed to  $\Delta x = 10^{-4} \times 1.03\Delta s$ , in the course of the work.

The small inductor of varying frequency (electric siren) actuating the telephone gave about 50 scale-parts ( $s$ ) of deflection at resonance, with 40,000 ohms in the telephone circuit. Between 20,000 and 40,000 ohms,  $sR$  was nearly constant; as, for instance,

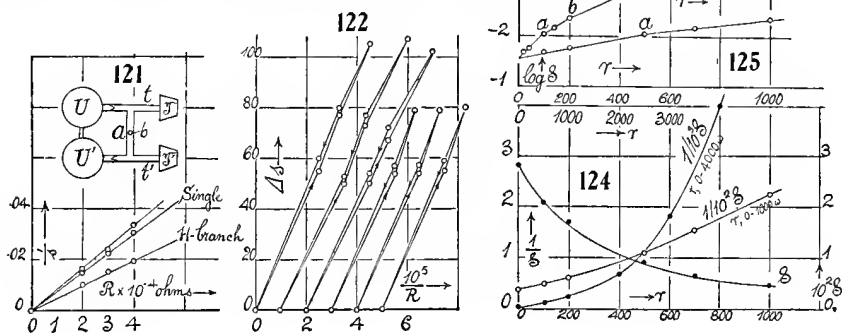
$$10^{-4} \frac{s}{R} = \frac{100}{2} \quad \frac{66}{3} \quad \frac{52}{4} \quad \begin{array}{l} \text{scale-parts.} \\ \text{ohms.} \end{array}$$

An example is given in figure 121, taking  $\frac{1}{s} = \frac{1}{e} R$ . The figure also gives data for single telephone, either the tube  $t$  or  $t'$  being stopped in this case. Usually, larger deflections were obtained with loose rubber connections than with very tight rubber connections at the branches, a result probably to be referred to the pressure introduced in making the latter connection, as will presently be shown. Closing the cross-piece  $a$  (fig. 58, or insert, fig. 121) with a screw pinch-cock, gradually cut off all deflection. If there is a slight leak in the **U**-gauge the deflections are scarcely reduced; but a continuous air current now passes against resistance from  $U'$  at lower pressure through  $a$  to  $U$  at higher pressure, in virtue of the acoustic mechanism. For the acoustic pressures at the pin-hole valves demand an excess of pressure of  $U$  over  $U'$ .

An interesting result is the detection of what appear to be hysteresis phenomena in the telephones. The **H**-branch method (fig. 121, inset) was again used. The deflections  $s$  were found to be smaller for gradually increasing telephonic currents than for decreasing currents to the extent of 5 or 10 per cent. Example of each result is given in figure 122, constructing the fringe deflections  $s = e \left( \frac{1}{R} \right)$ , both for the interval between  $R = \infty$  and 20,000 and between  $\infty$  and 30,000 ohms. As the **U**-gauge returns strictly to zero when the current is broken, the phenomenon can not easily be referred to the gage. It may therefore be in the telephone, which here appears more sensitive if it has recently been more highly stimulated. The effect quite disappears after the current is broken. It is, moreover, as might be expected, somewhat capricious, so that it varies in amount in different telephone adjustments and may even be absent. However, it is not improbable that the difficulties encountered in the density work (above, § 37, etc.) are producing similar discrepancies here.

**65. Telephonic effect at different air-pressures.**—The above result suggested the desirability of testing the telephone with a partial vacuum in the **H**-branch and the apparatus (fig. 121, inset), therefore, was made moderately air-tight, as above explained. Increased air-pressure on the front face of the plate wiped out all fringe deflection.

On removing the air from *a* (fig. 121, inset) through a side-branch with stop-cock by gentle suction, it was very curious to note that the mouth cavity frequently responded by resonance loudly to the telephone pitch, the latter being otherwise practically inaudible under the circumstances (distance, closed region). The run of experiment was usually something like this, remembering that a slight air leak remained in the telephone: Starting with a deflection of about 40 space-parts, this fell off to very small values immediately after suction and closing the stop-cock. In the lapse of time, however, the deflection increased, finally rapidly, until it reached even 85 or 90 scale-parts, *i. e.*, more than double the original value. The latter is a maximum; and on further waiting, it slowly decreased, more and more so, as it got smaller. To reach the original deflection again sometimes took an hour. Putting a mercury gage in connection with the closed region, it was found that the whole march of rapid increase and decrease of *s* occurs very nearly at atmospheric pressure. Thus one would naturally refer the occurrence to the telephone, the plate of which is successively spaced and momentarily conforms to maximum sensitiveness. The reason, however, for the long retention of increased sensitiveness, when once impressed, is by no means clear to me, though there is probably a connection between the present result and the preceding. In fact, both phenomena may vanish



at times; but they reappear on reclamping the plate of the telephone, and the like. They are interesting as showing the wide limits to which sensitivity is subject. Finally, the different rates at which air would (incidentally) transpire out of the U-gage, through the pin-holes if not of identical diameter, further complicates the observed occurrences.

**66. Telephonic response to varying current.**—Using the favorable conditions of a U-gage filled in vacuo (§ 2), tests were made of the relation of the resistance *r* inserted into the telephone circuit and the corresponding dis-

placement,  $S$ , of the slide-micrometer needed to bring the fringes back to the fiducial point in the telescope. This was done throughout as wide a range as the acoustic pressures in the branch adjustment (fig. 56, § 47) admitted. As it is often of practical interest to know to what extent the simple equation  $S(r+r_0)=\text{constant}$  applies when the external resistance  $r$  is diminished as far as zero ( $r_0$  being the total resistance in the telephone for a fixed frequency), graphs are given to show the change of  $1/S$  with  $r$ .

In the first survey a fixed resonance note was established in the telephone by aid of the electric siren at  $r=1,000$  ohms. The siren was then left untouched, while  $r$  was successively diminished or successively increased. The graphs, for  $1/S$  (example in fig. 123) were curved throughout, even with an apparent minimum at  $r=100$  ohms. It seemed probable that a part of this result must be attributable to the gradual loss of resonance between the telephone-note and the branch-pipe, owing to incidental occurrences.

The work was therefore repeated in such a way as to reestablish the resonance at each of the successive  $r$  values. The new results found are summarized in the graphs (fig. 124). It thus appears that only for an external resistance between  $r=500$  and  $1,000$  ohms is the relation of  $r$  and  $1/S$  practically linear. Below  $r=500$  ohms, the graph departs from the line, a result which one would naturally expect. The data obtained are as follows:

$r = 1000$	700	500	200	100	0	ohms.
$10^4 S = 44$	65	91	168	207	282	cm.
$1/10^2 S = 2.25$	1.53	1.09	.595	.482	.354	
$10^2 \Delta h = 32$	46	65	119	147	251	mm. Hg.

The corresponding acoustic pressure  $\Delta h$  in millimeters of mercury is also given, reaching a maximum of 0.25 mm. when all external resistance is excluded. For large resistances  $r$ , the data were (fig. 124):

$r = 1000$	2000	3000	4000 ohms.
$10^4 S = 44$	15	5.5	23 cm.
$s = 70$	25	10	5 scale-parts.
$1/10^2 S = 2.27$	6.67	18.2	40

Here the graph is characteristically curved.

In the preceding report (Carnegie Inst. Wash. Pub. 310, Part II, 1923, § 38), the relation  $S_0 = Se^{r/r_0}$  was proposed for these curves; but it was noticed that on plotting  $\log s$  and  $r$ , the straight lines obtained always showed a break of continuity. The broken lines again appear in the present experiments, as shown in figure 125. In the range between  $r=0$  and  $1,000$  there is a break at  $a$  ( $r=500$  ohms). In the range from  $r=0$  to  $4,000$  ohms there is a further break at  $b$  ( $r=1,000$  ohms). The line  $ab$  as a whole might suggest a continuous curve; but this is improbable in view of the similar results given for smaller ranges in the last report. The inference seems reasonable that at points  $a, b$  the vibration of the telephone-plate changes form and with it the acoustic pressure. There are thus a series of values  $\log s_0 = -1.55$  (observed),  $-1.75$ ,  $-1.88$ , to which  $r_0 = 448, 723, 923$  correspond.



## MISCELLANEOUS PIPES AND EXCITATION.

**67. Experiments with pin-hole resonators.**—The most sensitive form of this apparatus consisted of a cylindrical pipe closed at one end by a doubly perforated adjustable cork, through which the paired salient and reëtrant conical pin-hole tubes were to be thrust. The latter were then connected with the corresponding shanks of the interferometer **U**-tube. This requires two connecting-pipes. Now, in a variety of experiments since made (*cf.* § 60), it was a matter of indifference whether both pin-holes are thus connected with the **U**-tube, or whether one of the pin-holes is merely open to the air, so that but a single connecting-tube is needed. It was of interest to find out to what degree a similar principle would apply to the pin-hole resonator.

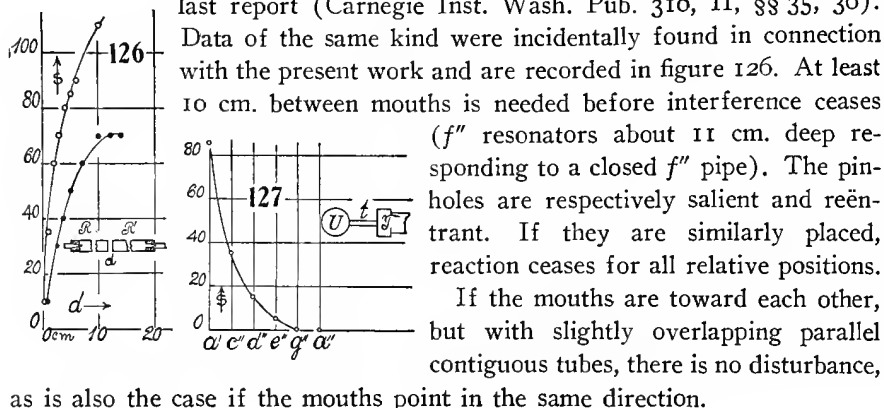
These experiments were made at some length, but the evidence obtained was not clear cut, chiefly, I think, because the organ-pipe with which the resonator is in step ( $f''$ ) changes its pitch, as usual, slightly with its intensity. If we denote by  $s$  and  $r$  the salient and reëtrant pin-holes, when joined to the **U**-tube, by  $s_0$  and  $r_0$ , the same when disconnected from the **U**-tube and open to the air, and by  $p$  a plug inserted in place of the pin-hole tube, the results obtained may be most clearly expressed as follows: The combination  $s+r$  always gives the maximum fringe displacement. The combination  $s+s$  or  $r+r$  gives no displacement; or if the pin-holes are not quite equally efficient, there may be a small residual displacement either positive or negative. On the other hand, as regards fringe displacement,  $s+r_0$  or  $s+p$  may come as near as 10 per cent of  $s+r$ . Rarely did it fall 30 or 40 per cent below it. The variable adjustment proved to be  $s_0+r$  or  $p+r$ . The latter often fell off 70 or 80 per cent, while the usual value of  $s_0+r$  was about 50 per cent of  $s+r$ , though it rose at times to 90 per cent. Supposing that in the last case there might be a small leak in the cork, I used different precautions without avail. The cause of the irregularity in the behavior of  $r$  was not detected. The  $r$  pin-hole differs from the  $s$ , inasmuch as the former lies at the bottom of a quill tube which necessarily becomes a part of the resonator.

As a result, perhaps, while  $s+s$  or  $r+r$  give a null effect (the pressures at the **U**-tube counterbalancing each other and the pin-holes therefore equally efficient), the  $r+s$  effect in fringe displacement is often not summational. A certain maximum of acoustic pressure seems to be producible which can not be exceeded by apparently favorable adjustment of the pin-holes. A typical series of data may be added

	$s+r$	$s+r_0$	$s_0+r$	$p+r$
Fringe displacement	100	70	50	30

If four identical pin-hole resonators be taken and the two salients joined to the **U**-shank, the two reëtrant to the **U'**-shank, the fringe deflection of a single pair is not increased. If the pin-holes for the same  $U$  are reversed the effect is zero.

68. Interference of resonators.—Results obtained for the interference of two identical single pin-hole resonators (inset, fig. 126), coaxially placed at a distance  $d$  apart with their mouths toward each other, were given in the last report (Carnegie Inst. Wash. Pub. 310, II, §§ 35, 36).



as is also the case if the mouths point in the same direction.

69. Immediate junction of U-gage and telephone.—In the earlier reports it was shown that in a rigorously closed tubular region no acoustic pressure could be registered. Thus in figure 127 (inset), where the telephone  $T$  is joined to one shank of the U-tube  $U$  by a short length of tubing  $t$ , no fringe displacement is observable, even when the telephone vibrates intensely with a loud burr, provided the plate, etc., are all sealed hermetically. But if there is a slight leak around the plate, even if tightly appressed by the cap, a very definite fringe displacement is observed, particularly at low pitch. It is again necessary that the telephone vibrate strongly.

The results obtained are given in fringe displacements  $s$ , for different pitches from  $a'$  to  $a''$ . Below  $a'$ ,  $s$  was found to decrease, so that there is probably a crest at  $a'$ , as is usual with these short tubes. Above  $a'$ ,  $s$  falls off rapidly and nothing was observable beyond  $a''$ . Conformably with the small leak in question, these fringe motions are very gradual, so that the experiment takes some time. If the sound ceases, the zero is regained with the same slowness.

The experiment is interesting, as it might be supposed to admit of an interpretation on the energy of the sound excitation. If the pressure in the atmosphere is  $p$ , the same pressure occurs within the region  $UtT$ , if the telephone is not sounding. When the telephone is actuated, therefore, the energy per cubic centimeter within the region is  $p + \rho v^2/2$ , where  $v^2$  is the average velocity squared of the vibrating air-particle. Thus the available energy would be in excess within; and  $p$  is therefore reduced to  $p'$ , such that  $p' + \rho v^2/2 = p$ . Thus  $\Delta p = \rho v^2/2$ .

Standardizing the fringes with the slide micrometer,  $\Delta h = 16 \times 10^{-6}$  cm. of mercury was found as the pressure equivalent to the displacement of 1 fringe; so that  $\Delta h = 0.213 \Delta s$  dynes/cm.<sup>2</sup> if  $\Delta s$  is the fringe displacement



with the cap all but tight gave evidence of marked dilatations. Loosening the cap a little further (fig. 133, upper curve) the pressures of the upper curve again result. In figure 134, with a cap just loose, the adjustment incidentally obtained is such that marked dilatations followed by marked pressures occur in succession. At  $g'$  the conditions are unstable and the fringes sweep suddenly from negative to positive values.

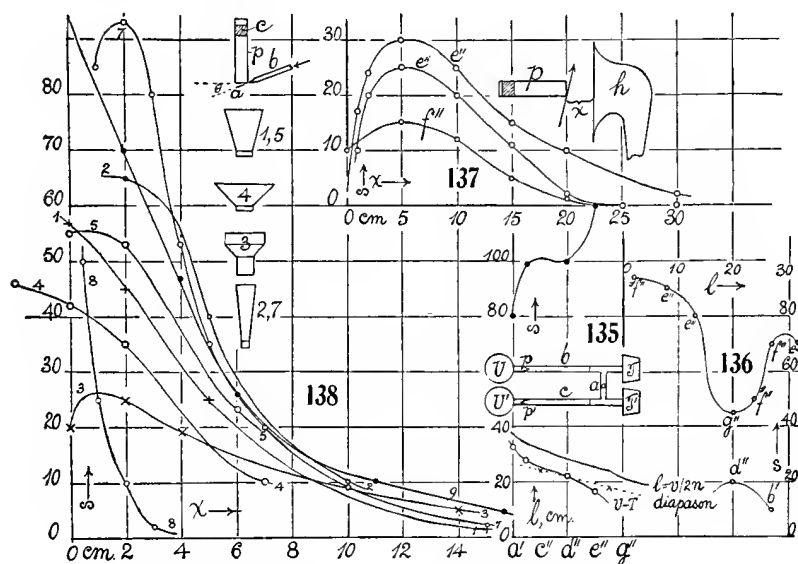
Thus in the long run the suggestions of the preceding section are not sustained. While the dilatations are more frequent, marked pressures may also occur, provided the nearly closed region (U-tube, quill tube, telephone) is not air-tight. This implies that the shape of the crevice at the telephone-plate, where there is slow escape of air, is solely instrumental in producing the acoustic pressures observed. The very thin air-gap acts like a pin-hole, though much less effectively; and it may to this degree replace either the reëtrant or salient pin-hole, depending on the chance condition of loosening the plate to produce an adequately fine crevice.

**71. Specially tuned H-pipe.**—The advantage of the H-branch (fig. 135, inset) is the ease with which it may be tuned to any note by elongating the pipes  $b$  and  $c$ , which may be made of quarter or eighth inch pure-rubber tubing. These are attached to the rigid elbow of very thin brass ( $\frac{1}{4}$ -inch) tube, the cross-pipe  $a$  corresponding to the distance between the telephones  $T, T'$ , which should be kept within 10 cm. A hole in  $a$  with a stopper allows of additional tuning; but as energy is lost here, the hole should be small. The behavior of open quill tubes attached to the hole  $O$  of the cross-branch  $a$  is peculiar and given in some detail in figure 136. Here  $l$  denotes the length of tube measured from  $O$  to the open end, and  $s$  is the corresponding fringe displacement. The relation is distinctly periodic, while the pitch changes from  $e''$  to  $g''$ , the latter curiously enough corresponding to minimum fringe displacement. Lower harmonics are also present, though in small intensity, as shown at  $d'', b'$ . When the hole  $O$  is closed, the note is  $e''$ ; when quite open  $\sharp f''$  to  $g''$ , with a displacement of  $s=95$  to 100 in each case. The pin-hole valves  $p, p'$  (fig. 135) should be at the end of very short tubes and placed as near the U-tubes as possible, as the sensitiveness depends very materially on this condition. Unfortunately, since an entrance tube to  $U$  and  $U'$  is necessary elsewhere, the length lost here in my apparatus was 3 to 5 cm.

The lower part of figure 135 gives a record of the length of  $b$  and  $c$  tube, between  $U$  and  $T$ , corresponding to different frequencies from  $a'$  to  $e''$ . The same figure shows the length of common wood diapason pipes. The mean rate at which pitch decreases with length is less in the latter case. At  $d''$  the lengths would coincide, though it is probable that about 4 cm. (to pin-holes) should be deducted from the  $UT$  length, in which case coincidence would occur at a lower pitch. Since the  $UT$  pipes are less than 0.25 inch in diameter and form a doubly closed acoustic pipe, this coincidence is rather curious, as one would anticipate a much greater viscous effect in the quill pipe. The ease with which low values of pitch (even to  $c'$ ) may be produced here is equally

surprising; for one would expect the slender air column to break up. Just above the two curves in question are the corresponding semi-wave-lengths in free air.

At the top of figure 135 I have given the fringe displacements  $s$  in scale-parts (scale-part about a double fringe) for the different pitches. The response is unquestionably stronger for high-pitch values ( $e''$ ) than for low values ( $a'$ ); but the curve is not simple. It is difficult to discuss this result, as much depends on the action of the contact breaker, which interrupts the current of the primary of the small inductor energizing the telephones. Moreover, even the latter, whenever there is marked change of temperature, are liable to show very different degrees of sensitiveness, so that it is necessary to reset the plates by unscrewing and refastening the mouthpiece.



**72. Experiments with horns.**—With the H-branch (fig. 135) tuned to  $e''$ , it is interesting to test the response of a wireless loud-speaking horn (fig. 137) to a closed  $e''$  pipe, blown in the vicinity of the flare. In this case the telephones  $TT'$  (fig. 135) receive the current from the moving coil attached to the diaphragm at the base of the horn. If  $x$  is the distance between the plane of the flare and the mouth of the closed  $e''$  pipe, the graphs (fig. 137) show the fringe displacements in their variation with  $x$ . It is necessary here to tune the  $e''$  pipe with great nicety if a strong response is desired (upper curve). Otherwise the fringe displacements,  $s$ , diminish very rapidly. An  $f''$  pipe gives scarcely half the corresponding resonant deflection. Again, the maximum response is obtained when the  $e''$  pipe is at a distance  $x$  of about 5 cm. from the plane of the flare. Within this distance the fringe displacements

fall off very rapidly, particularly so in the case of unison, less so ( $f''$  pipe) when there is slight difference in pitch. In other words, there are interferences between the pipe,  $e''$ , and the horn and its appurtenances which are quite audible; for when the mouth of the pipe is too near the flare, or within it, the fundamental note of the pipe is quenched. This occurs in marked degree when the current through the electro-magnet at the base of the horn is on, and the pipe-note often breaks out again when it is off. There is an evident case here of "back feeding," the diaphragm reacting through the horn on the pipe. A distance of 50 cm. (which is the  $e''$  wave-length) between mouth of pipe and diaphragm seems here to correspond with the maximum.

Beyond the maximum the graphs fall off regularly and there is little effect (for the present small size of fringes) beyond  $x=30$  cm. I had rather expected to find a second maximum in sequence, but it does not occur.

The endeavor to use the electro-magnetic diaphragm together with the closed  $e''$  pipe (in the same way in which I combined the latter with a corresponding resonator in the preceding report), to map out the nodal planes of waves reflected upward from the table, did not succeed. With the horn removed, all fringe displacement vanishes when the organ-pipe (mouth downward) is but a few centimeters above the diaphragm. The details are shown in figure 138, curve 8, where the distances  $x$  are measured upward from the connecting neck or ring, just above (3 cm.) the diaphragm. When the mouth is but a half centimeter from the neck (as close as it may be put without quenching the note) the response is strong, but at 4 cm. above there is practically no fringe displacement appreciable.

As the intervention of some form of horn is thus necessary, it seemed interesting to test a number of forms in succession. These are sketched in figure 138 (inset), the lower part always being the conical horn, No. 2, 7, with its mouth, 6 cm. in diameter, about 20 cm. above the diaphragm. The flares given under 1, 5, 4, and 3, fit the mouth snugly and vary its shape and height. The closed organ-pipe indicated at  $p$ , with a tuning-plug at  $c$ , is energized by the pipe-blower,  $b$ ,  $a$ , described in the preceding report. This must be rigidly attached to the pipe, as the pitch varies not only with the position of  $c$ , but with the angle  $\theta$  of the lamella  $a$  and the plane of the mouth.

To get large fringe displacements, it is necessary that the H-branch (fig. 135, inset) and the pipe  $p$  be sharply in tune; *i. e.*, the plug  $c$  must be placed within a millimeter. As would be expected, by far the largest displacements were obtained when the small horn 2, 7 was used alone, with the pipe just above it; for then the mouth subtends the largest conical or solid angle. Moreover, since the pipe and horn reciprocate acoustically, or make a single vibratory system, the tuning at  $c$  must be finally adjusted with relation to the horn. The graphs 2 and 7, figure 138, are examples of results in which this tuning was respectively good and moderate. Owing to the blowing mechanism of the pipe, the plane of the mouth of the horn can not be much nearer to the open end of the pipe than 1 cm. In fact, even here there is considerable interference, so that the pipe-note is only heard when the electro-magnet of the

loud speaker is energized. As soon as the current is broken, the shrill overtones of the pipe break forth. On closing it again, the pipe and diaphragm vibrate in unison and the normal pitch is reached by accommodation. The disturbances have not been actually eliminated, as is clearly apparent in the hooked part at the top of the graphs, indicating a breakdown of normal conditions of vibration. In general, it is not unusual to obtain small differences of pitch, according as the electro-magnetic current is on or off.

The graphs 1 and 5 were obtained by attaching the flare, 1, 5, which was about 15 cm. high and 15 cm. in diameter, above. The response as a whole is here less than in the preceding case; but it is much larger, of course, than the small horn would have given 15 cm. above its mouth. Here the pipe-mouth may be placed in the plane of the mouth of the wide flare. It is not unusual, nevertheless (curve 5), to meet interferences in this case also. Initially hooked graphs are common, showing that the normal increase of  $s$  has been reduced by secondary disturbances.

The wider attachment, No. 4, 20 cm. in diameter and 9 cm. deep, makes it possible to dip the pipe-mouth below the plane of the flare. Fringe displacement is, however, inferior, as shown by the graph 4.

The cylindrical flare (3), 15 cm. in diameter outward, 18 cm. deep, gave the worst response (graph 3) of the series; but in compensation, the small displacements  $s$  vanish much more slowly than in the other cases and at  $x=14$  cm. above the mouth of the flare, the present fringe displacements actually exceed them. The hooked form of graph indicates the usual disturbances at  $x=0$ .

The most effective coupling is always obtained with the pipe  $p$  coaxial with the horn. Moreover, the large fringe displacements are essentially a slow growth, showing that the amplitude of the diaphragm is gradually increasing to a maximum. No doubt the sensitiveness could in all cases be much increased by selecting a depth of horn in unison with the pipe and performing the final tuning at the H-branch of the interferometer U-tube. Using a well-tuned system of this kind, I attached the flare 1, 5 again, the mouth being about 35 cm. above the diaphragm. Care was also taken to sustain each note (30 to 60 seconds) until the fringe displacement crept to its maximum value. The results were (curve 9, fig. 138) surprising:

Pipe at $x=-2$	$+0$	$+2$	4	6	11	16	cm. above mouth.
$s=105$	93	70	47	26	10	5	scale-parts.

These data are as large as any obtained heretofore, showing the importance of the secondary disturbances. It has also been possible to dip into the mouth of the flare with some advantage.

With the same good adjustment at hand, it seemed worth while to prolong the horn to a length of about 1 meter by the insertion of a cylindrical tube about 60 cm. long, 5 cm. in diameter. Here the tube dominated the situation. Shrill overtones and beats were frequent. Nevertheless, fringe displacements of 50 scale-parts were at once obtained, and they could have been smoothed out to much larger values by tuning, as above.

## ELECTRIC EXCITATION OF CAPPED PIPES.

73. **Electric-spark excitation of quill tubes.**—The production of acoustic vibration in quill tubes by aid of a telephone vibrating at one end has the advantage of needing but small currents and potentials. It nevertheless seemed desirable to accomplish the same result by other methods. Thus a periodically heated wire has been used. In the thermophone (Bull. Nat. Res. Council, No. 23, VI, p. 16, 1922) a fine metal strip heated by an alternating current is in operation.

In the following experiments the millimeter electric spark of a little induction coil provided with the usual spring interrupter was employed. By tightening the spring, or weighting it more or less, something over an octave, naturally in the region of low frequency, was available. The acoustic part of the apparatus is shown in figure 139 (inset), *tt* being the quill tube, closed at one end by the plug carrying the platinum spark-gap *g* and the wires of the inductor *ww'*. The tube *tt* is closed at the other end of the salient (*s*) and reëntrant (*r*) pin-holes, the former leading to one shank of the interferometer U-gage.

As the spring platinum interrupter in the lapse of time changes its efficiency, the graphs obtained show considerable difference in detail. I will, therefore, give but two examples (fig. 139) of the many series tested, as all of them conform to the same type of variation. The quill tube *tt* in these cases was about 8 cm. long. The graph *a* was obtained with a heavy and, therefore, steadier vibrator of low pitch, the curve *b* with a lighter vibrator more liable to fail. Some of the curves were strongly concave upward.

The property apparently brought out by these graphs is the rapid increase of acoustic pressure (varying with *s*) with the increase of frequency *n*. Thus, for a two-fold increase of *n*, the increase of *b* is at least four-fold, *i. e.*, as  $n^2$ . The other feature is the absence (probably to be inferred for these low frequencies and very short tubes) of any certain evidence of resonance, such as was obtained strikingly in all the preceding experiments with telephone-blown tubes and higher pitch. Tubes *tt* from  $l=8$  cm. to  $l=25$  cm. in length behave about alike, in so far as discrimination is possible.

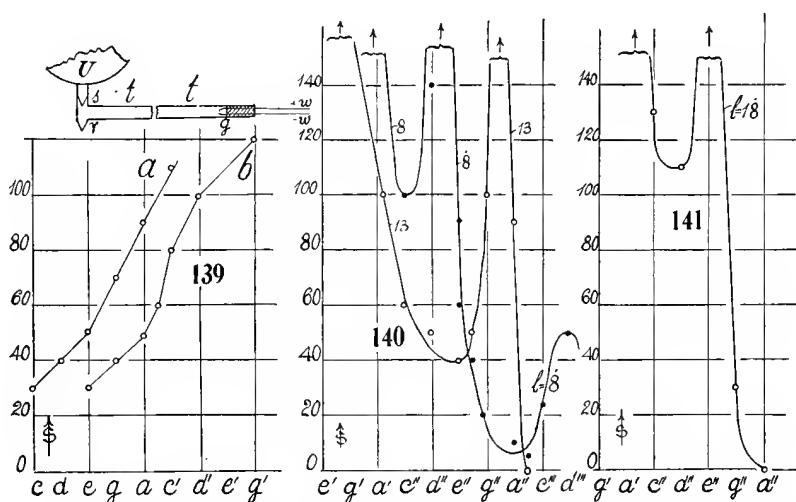
Since the intensity *i* of the vibration is proportional to squared ratio of amplitude and wave-length,  $a^2/\lambda^2 = a^2 n^2/v$ , where *v* is the velocity of the wave, the intensity  $i \propto n^2$  if  $a^2$  is constant. If the sparks at all frequencies be regarded as communicating the same energy to the sound-wave,  $a^2$  may indeed be regarded as constant. Hence, if at low frequency conformably with the graph, the acoustic pressure  $s \propto n^2$ , we should obtain  $i \propto s$ . From this point of view these experiments have some interest and should therefore be pursued with more carefully designed apparatus, always remembering that *s* varies with the shape and size of the pin-holes and may be either positively or negatively increasing with *i*.

The preceding experiments (fig. 139) are remarkable for the very low frequencies (4-foot octave *c*,  $n=131$ ) employed. The acoustic pressure is thus produced by pulses traveling in succession from the spark-gap to the



far end of the tube. They must therefore be supplemented by experiments at higher frequencies, in order that the approach to resonance conditions may be tested. Great difficulty was encountered in endeavoring to produce spark successions of this rapidity. The best results were obtained from a large induction coil (usual laboratory size), actuated by as weak a primary current as possible. In such a case the commutator interrupter (with small motor and resistance) could still be employed; but the break soon deteriorated and the fringe displacements (acoustic pressures,  $s$ ) are steady and comparable for only a short time, after which the break must again be cleaned and reset.

Notwithstanding these irregularities, the resonance conditions were very clearly made out. The intensities at the nodes were often enormously beyond the ocular micrometer, showing acoustic pressures exceeding 0.1 mm. of mercury, so that the slide micrometer had to be used.



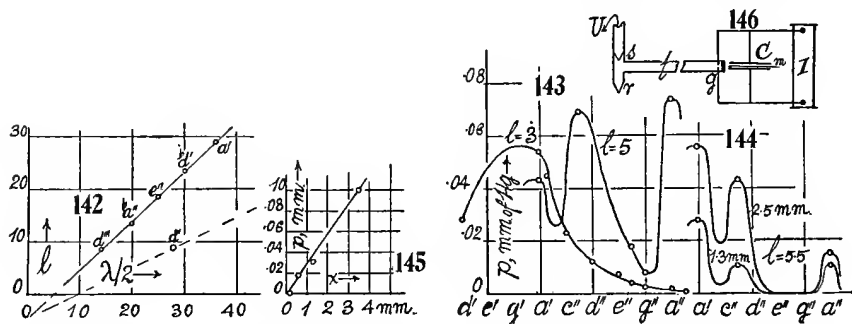
The survey for the tube-lengths 8.5 and 13.5 cm. is given in figure 140 and was made in some detail, so far as the method permitted. The resonance crests are far out of field. The low-pitch notes are continuously so, suggesting the relation to figure 139. For the longer tube-lengths (figure 141),  $l=18.5$ , 23.5, 29 cm., only the maxima were sought out, by using the displacement micrometer to bring the fringes in the field. These crests were often very sharp. In case of the tube,  $l=23.5$  cm., the  $bd''$  crest corresponded to the acoustic pressure ( $\Delta h = \Delta s \cos \theta$ ) of  $\Delta h = 0.092$  mm. of mercury. In case of  $l=29$  cm., the descent from the  $a'$  crest was measured as  $a'$ , 0.084;  $c''$ , 0.047;  $d''$ , 0.016;  $e''$ , 0.012, etc., mm. Hg, the latter ( $e''$ ) being of the order of the usual run of maximum acoustic pressures treated with telephones.

If we express the tube-length  $l$  in terms of the free semi-wave-length,  $\lambda/2$ , in air, the crests would lie as shown in figure 142. They are thus adequately reproduced by the equation  $l + 4.6 = 0.93\lambda/2$ . Interpreting this as the first overtone, the confined wave-length  $\lambda' + 4.6 = 0.46\lambda$ , agreeing in order of value

with the chief results obtained with telephones for the same tubes. Hence the strong  $d''$  in figure 140,  $l=8.5$  cm., belongs to the fundamental, as suggested in figure 142.

On further reducing the tube from 5.5 to 3.5 mm., the greater part of the length was made up of the T-branch and the spark-gap tube. This is equivalent to an appreciable increase of section, so that the crests no longer fit into figure 142. The acoustic pressures measured in millimeters of mercury are given in figure 143. At  $l=5.5$  cm. a succession of three crests,  $a'$ ,  $c''$ ,  $a''$ , is strongly apparent, but at  $l=3.5$  cm. only a diffuse crest at  $g'$  remains.

**74. Effect of spark-length, etc.**—The energy of the spark is caught within the closed quill tube and expressed, as it were, in terms of acoustic pressure. Moreover, all sparks are produced in the secondary from the same primary mechanism. Thus it seemed that the acoustic pressure should be independent of the length of spark-gap in the quill tube. But this is by no means the case, as shown, for instance, in the two graphs of figure 144, for tube-length  $l=5.5$



and spark-lengths 1.3 mm. and 2.5 mm., respectively. The crests have the same location as in figure 143, but the acoustic pressure for the longer gap is much in excess of that for the shorter. Similarly, for a tube-length of  $l=24$  cm., while the 1.3-mm. gap gave a pressure of 0.051 mm. of mercury, the 3.5-mm. gap gave a pressure of 0.100 mm. Small spark-lengths of 0.1 to 0.2 mm. produced a deflection of only a few fringes, i. e., less than 0.0005 mm. Hg, and were therefore inactive, while a spark-gap 0.6 mm. evoked a pressure of 0.0018 cm. Thus, in figure 145, the acoustic pressure (mm. Hg) at the nodes is roughly proportional to the spark-length, the values here obtained being something less than 0.03 mm. Hg per millimeter of gap. On the other hand, the long gap very much sooner misses fire as the pitch rises, owing to irregularities in the break circuit. The spark, moreover, is apt to be brighter at the resonance frequencies. This suggests that to start a vigorous acoustic wave, a sudden shock such as is conveyed by a single dense spark is necessary. A succession of small sparks of the same aggregate energy is relatively ineffective. (See § 76.) If  $N$  is the number of lines removed at each break of the primary, in a secondary circuit of resistance  $R$  and capacity  $C$ , we may

put  $N = QR$ , where  $Q$  is the constant charge available at each break. Hence if  $V$  is the potential corresponding to the spark-gap and if  $Q$  is discharged in  $n$  sparks, the total energy appears as  $n(Q/n)V = nCV^2$  or  $nC = N/RV$  is constant. If  $C$  is increased by the condenser,  $n$  is diminished.

The difficulties are increased when a capacity is inserted around the spark-gap, however; higher potentials being needed in the primary, the endeavor to eventually bring the electric oscillation of the spark into resonance with the quill-tube pitch is at the outset not very promising. A variety of subsidiary phenomena were observed. In figure 146,  $t$  is the quill tube, with its salient and reëntrant pin-holes at  $s$ ,  $r$ , the U-gage at  $U$ , and the spark-gap is at  $g$ ;  $I$  is the induction coil, and  $C$  the condenser. The latter is made variable by mounting the top plate on a micrometer screw (all properly insulated), so that it may be lifted up and down by a definite amount, as heretofore\* described. A thin plate of mica or hard rubber,  $m$ , is inserted between the plates of  $C$ . The current in  $I$  is controlled by the electric siren in the primary, which may be set at any pitch from  $a'$  to  $c'''$ . When the plates of  $C$  are gradually approached, the spark at  $C$  is quenched at a definite distance, as is to be expected. If on further approach the metal plates of the condenser are moderately pressed against the thin mica insulator between, a loud note is heard in the condenser, of the same pitch as the electric siren. This occurs strikingly when the mica plate is less than 1 mm. thick. The note is louder for thinner plates (0.2 mm.) and softer for thicker plates (0.6 mm.). With a hard-rubber plate 1.6 mm. thick, the note was still audible, but now only at the resonance notes of the quill tube  $t$ , when sparks passed at the gap  $g$ .

In spite of the fact that quite thick brass disks (6 inches diameter and 0.25 inch thick) are active, the phenomenon is probably nothing more than electrostatic attraction and sudden release, the elasticity of the air-film between plates playing an important part. The insulation  $m$  now virtually conducts electrically. No Chladni figures were obtainable.

There is another phenomenon here much more difficult to interpret; for the condenser note modified the resonance pitch of the pipe  $t$ , according as the condenser plates are pressed snugly against the insulator and sounding, or as they are loose and not sounding. Thus, for the pipe length  $l = 18$  cm., hard rubber (1.6 mm.) tight, sounding, crests at  $c''g''$ ; hard rubber (1.6 mm.) loose, silent, crests at  $e''b''$ ; mica (0.6 mm.) tight, sounding, crests at  $c''g''$ ; mica (0.6 mm.) loose, silent, crests at  $e''b''$ . Here mica and hard rubber behave alike and the pitch is raised to the normal value  $e''$  (see fig. 142) when the insulator plate is loose (millimeter or more clearance). But in other cases pitch was depressed, so that one can hardly call in temperature phenomena at  $g$  in explanation. One may note that  $c''$  and  $g''$ ,  $e''$  and  $b''$ , are not harmonics of the same series. These phenomena may be observed by the occurrence of sparking at the nodes, even without the measurement of fringe displacements at the U-gage.

---

\* Carnegie Inst. Wash. Pub. No. 310, p. 6, fig. 7, 1921.

When the spark-gap is sufficiently wide (1.5 to 2 mm.) the quill tube responds at all frequencies ( $a'$  and  $a''$  tested), the nodal effects appearing as an accentuation of the uniform response. They may even be observed. It follows, therefore, that each individual spark impulse produces marked acoustic pressure, irrespective of the pitch of their succession on the pitch of the quill tube. In the case of the higher frequencies ( $a'' \dots c'''$ ) it ought therefore to be possible to obtain evidences of electric oscillation. How to recognize them among other crests is thus next to be considered.

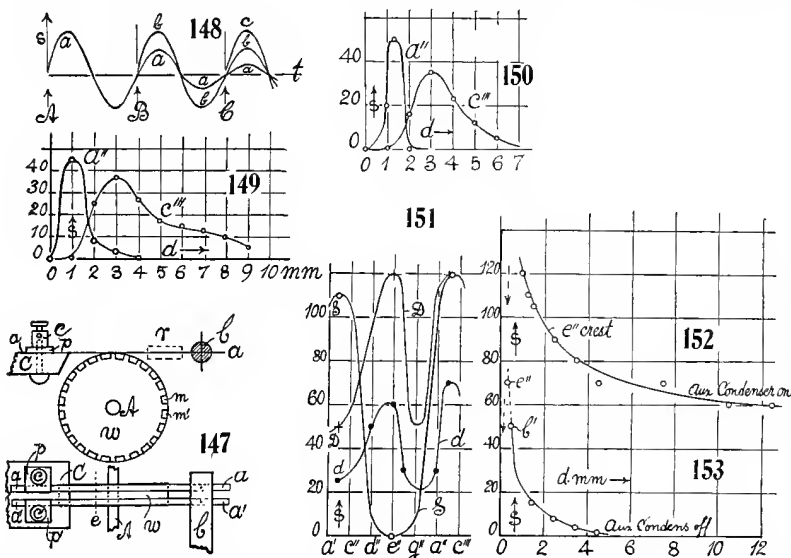
**75. Electric oscillation recognized. Inductance.**—It is obviously necessary to have a very large inductance in the secondary in order that a small voltage (1 storage-cell) in the primary may produce sparks. Even then the high-frequency break-circuit in the primary is apt to behave capriciously. The break-circuit which gave me the best results is shown in figure 147, where  $w$  is a wheel of insulating material carrying equidistant metallic segments at its circumference. It is mounted on the axle  $A$  of a small motor of controllable speed. The two thin metallic strips  $a, a'$ , through which the primary current circulates (clamp-screws  $cc'$ ) are made as short as possible, tightly stretched between the insulating holders  $C$  and  $b$ , the latter carrying a pin, the former a metallic plate  $p$  secured by a bolt. The holder  $b$ , being adjustable up and down, is so placed that the twin strips just touch the metallic commutator segments, to temporarily close the current. To deaden undesirable vibrations, pieces of soft rubber,  $r$ , may be wedged between the strips.

Though this break functions pretty well as far as  $c'''$  and above, it does not act equally well at all frequencies, owing to the incidental vibrations specified. Consequently, in the adjustment (fig. 146) the capacity only is to be changed to obtain different electro-magnetic frequencies, while the pitch at the break is kept constant. Furthermore, it is desirable to select a quill tube  $t$  of small length  $l$ , like the one for  $l=3.5$  cm. in figure 143, in which resonances at high pitch are usually absent. Low-pitch response ( $g', a'$ , etc.) is always present, as if these low notes broke up into higher harmonics. This is of little consequence, as they can not be reached electro-magnetically.

Under these circumstances the plan of attack is shown in figure 148, in which the acoustic pressure resulting from successive oscillations are given in the lapse of time. If  $a$ , the oscillation resulting from the first spark, is in phase with  $b$ , the oscillation of the second, and  $c$ , the oscillation of the third spark, etc., the acoustic pressure will reach a maximum.

Obviously, however, no distribution can be made between crests and troughs here, so that in relation to acoustic pressure all vibrations are rectified. Reinforcement occurs for acoustical half-period time differences between the impulses. A selection of an admissible period  $T$  is made by the experiment, among the available  $T/2, 2T/2, 3T/2$ , etc. The maximum interference occurs for phase differences of  $T/4$ . The compound rectified wave can not be annulled; but at it is far less oscillatory in character and with a period approaching  $T/4$ , it passes out of range as if it were annulled.

Examples of the results obtained in this way are given in figure 149, where the acoustic pressure is shown in terms of the distance apart  $d$  of the plates of the condenser. The break (fig. 148) was first set at  $c'''$ , which it held pretty well. The curve  $c'''$  was thus worked out for varying capacity, by separating the plates of the condenser from  $d=0$  to  $d=9$  mm. There is a distinct optimum at  $d=3$  mm. The break was then set at pitch  $a''$  and the corresponding curve worked out. It reaches higher intensities (probably owing to increased length of contact) and is much sharper. The spark-gap was but 1 mm. The sparks must cease at  $d=0$ . This might have influenced the left side of the  $a''$  curve, but not the  $c'''$  curve. A similar experiment with a condenser modified so as to secure greater precision in the separation of



plates gave the results shown in figure 150. They are essentially like the preceding. The  $a''$  crest, however, is sharper and has been somewhat displaced ( $d=1.25$  mm.) in the  $d$  direction.

The interpretation of these data is not at once evident. The main oscillation must occur in the circuit  $IC$  (fig. 146) modified by the spark-gap  $g$ . The oscillation in  $Cg$  is clearly of much higher frequency and out of comparison with the pitches  $a''$  and  $c'''$ . Leaving the spark-gap resistance out of consideration for lack of data, we may test the usual equation  $T=2\pi\sqrt{LC}$  (where  $L$  is the inductance of the coil and  $C$  the total capacity of coil and condenser), tentatively, and since the only change appeared in relation to the  $a''$  and  $c'''$  is the change of capacity, the coil capacity may be eliminated by writing

$$L=\Delta T^2/4\pi^2\Delta C$$

If, therefore,  $C=A/4\pi d$ , where  $d$  is the distance apart and  $A$  the area of the plates,  $C_0$  the capacity in the coil

$$\Delta C=C_0+A/4\pi d-(C_0+A/4\pi d')=A\Delta(1/d)/4\pi, \text{ els. units}$$

whence

$$L = 9 \times 10^{11} \Delta T^2 / \pi A \Delta (1/d) \text{ henries}$$

Since for  $c''$ ,  $T^2 = 10^{-6} \times 0.92$  and for  $a''$ ,  $T^2 = 10^{-6} \times 1.29$ ,  $\Delta T^2 = 10^{-6} \times 0.37$ .  $A = 78 \text{ cm.}^2$ , whence  $\pi A = 245$ . In figure 78,  $d = 0.1$  and  $0.3 \text{ cm.}$ , respectively, whence  $\Delta (1/d) = 6.7$ . This gives  $L = 200$  henries. In figure 79, however,  $d = 1.25$  and  $0.3 \text{ cm.}$ , respectively, whence  $\Delta (1/d) = 4.7$ , so that  $L = 290$  henries results. The order of these results would not seem to be unreasonable. If  $T$  for  $c''$  and  $a''$  are to be regarded as semiperiods, as explained, they would be too large; but, on the other hand, again, the conditions might be such that only when  $c''$  and  $a''$  represent a  $3/2$  period could response take place.

76. Further experiments.—In the summer I took up the work again, being in some doubt whether in the preceding experiments a state of resonance had actually been reached. The installation of apparatus was essentially the same, except that in addition to the variable condenser  $C$  (fig. 146), an auxiliary condenser was inserted in parallel. This consisted of two circular disks, each  $14.9 \text{ cm.}$  in diameter and spaced by one or two hard-rubber plates,  $0.154$  and  $0.207 \text{ cm.}$  thick. The difficulty with all these condensers is that with decreasing distance between plates and after some use, the insulator gradually conducts. Hence the descending branch on the left in figures 149 and 150 might be referred to this increasing conductivity, as it certainly is when  $d$  approaches zero and a loud condenser note is heard. In such a case the ascent of the curves in the right could be interpreted as a coalescence of a larger number of small sparks into a smaller number of larger ones and ultimately into a single spark, between successive breaks of the interrupter. If, then, the single spark is acoustically very active in exciting sound-waves, whereas the smaller sparks are relatively inactive, curves much like figures 149 and 150 would be obtained, implying a mere approach to electric resonance. With quill tubes no decisive results were reached, though one curious result may be mentioned: When the conical pin-holes were accidentally set pointing from each other (differentially) instead of in the same direction as in figure 146, pronounced negative deflections (*i. e.*, dilatations) were obtained from the spark excitation within the quill tube, the  $U$  pin-hole pointing away from the tube like the other.

In the following tests the interrupter (fig. 147) was also modified back again to the more conventional form. Stretched ribbons,  $aa''$  as such, were discarded by severing them at say  $e$ . This cut is to be parallel to the insulation crevices between the plates  $mm'$  on the wheel  $w$ . The upper strips are then pressed down on the wheel and held in contact elastically. The free ends  $aa'$  should be made as short as possible. The advantage lies largely in the ease with which the contact edges of  $aa'$  are trimmed and reset if worn, in the very high frequency of their own vibration, and on the fact that the pitch to be observed is always clearly audible, coming from  $w$ . The plates  $mm'$ , in spite of constant sparking, remain bright, or may be polished by light pressure from an old razor-blade. It is obvious that this break must function faultlessly.

Replacing the quill tube by a wide pipe 2.2 cm. in diameter and 13 cm. long, adjusted as at  $t$  (fig. 146), small single displacements only were obtained. The spark-gap was unable to produce a strong acoustic wave in this bulky tube and the harmonics were difficult to detect. An interesting and exceptional behavior was observed: On closing the spark succession, a violent throw of fringes toward larger pressures occurred, whereas in breaking the spark current, the throw was equally violent in the direction of dilatations. The appearance is thus very much like electric induction. A probable explanation is to be found in the fact that the air within the tube near the spark-gap is relatively warmer than sparkless air. Hence sudden thermal expansion of air or the reverse is put in evidence before the air escape at the pin-holes can reestablish equilibrium. The simultaneous occurrence of strong ionization is probably not appreciable in terms of pressure, though it would act similarly. The phenomenon is not observed with quill tubes, nor with the narrower tubes (diameter below 1 cm.) which follow. This, again, may be due to insufficient volume of air within the tube, so that the pin-holes are now large enough to maintain equilibrium at all times. Placing the spark-gap at the ends or at the middle made no difference in the unsatisfactory general performance of these wide tubes.\*

The tube  $t$  (fig. 146) was now replaced by one length 10 cm. and diameter 0.7 cm., and this showed clear-cut crests at  $e''$  and above  $b''$ , as indicated in curve  $d$ , figure 151; but the tube was never silent, provided the auxiliary condenser  $C$  was left in circuit. Without it, harmonics or crests could not be appreciably evoked in the tube. This is also indicated in figures 152 and 153, in which the abscissas denote the separation of plates (decreasing capacity)  $d$  of the variable condenser, in millimeters, while the auxiliary condenser is fixed in figure 152 and removed in figure 153. In the latter case the pipe shows no crests and the  $b'$  note was chosen at random. As the condenser space  $d$  decreases to the smallest value compatible with non-conduction, the fringe displacement rises very rapidly, and eventually with high capacity, even in figure 153, the  $e''$  harmonic is brought out. Thus one might infer that only dense sparks excite these air-waves, while small sparks in succession, though conveying the same energy, per second, have almost no effect, a view in keeping with the remarks at the beginning of the paragraph. On the other hand, if the capacity falls, the period of the resonance note also falls, so that it may rapidly fall above (high frequency) the available pitch interval. The question is best treated by computation, which can here be made to rest on more substantial data than in case of figures 149 and 150, where the  $a''$  and  $c''$  pitches are rather too high for the apparatus.

**77. Computation.**—Admitting the reservations of the preceding paragraph, there remain nevertheless certain observations, as already indicated (§ 75), when the condenser capacity alone changes, which seem explicable

---

\*A variety of other experiments with different lengths of wide tubes brought out only uncertain results. Sometimes a sharp tube crest appeared.

only in terms of electric resonance. The following results (fig. 151) are in some respects even more incisive. Using the glass pipe ( $l=10$  cm.,  $2r=0.7$  cm.), leaving the variable condenser constant, but changing the hard-rubber plates of the auxiliary condenser in parallel from a thickness  $d=0.154$  cm. to  $d=0.361$  cm., the two curves  $D$  and  $S$  of figure 151 were obtained. Here the graph  $D$ , more intense but identical in character with the former graph  $d$ , corresponds to the smaller capacity or  $d=0.361$  cm. Its salient feature is the crest at  $e''$ , very pronounced. Removing the extra hard-rubber plate ( $d=0.207$  cm.) the curve  $S$  was obtained for  $d=0.154$  cm. The feature here is the minimum at  $e''$ , whereas a crest appears at or below  $b$ . Both curves have crests near  $b''$ . The exchange may be repeated an indefinite number of times, always with the same results. The  $e''$  crest is invariably transformed into an  $e''$  trough, and (vice versa) similarly at  $b'$ . These crests are therefore of electric origin and do not belong to the tube, whereas the crest near  $b''$  to which both cases of capacity contribute may belong to the tube.

The two crests observed in figure 151, viz,  $e''$ , period  $T_1=1/658$  seconds and  $b'$ ,  $T_2=1/494$  seconds, would seem to be too low to be compatible with electric oscillations, unless they are stimulated by their octaves here beyond range of the siren. Accepting them and putting  $K$  for the fixed capacity and  $L$  for the inductance of the circuit, the periods  $T$  are

$$T_1=2\pi\sqrt{L(K+C_1)} \qquad T_2=2\pi\sqrt{L(K+C_2)}$$

where  $C_1$  and  $C_2$  are the smaller and larger auxiliary capacities. Hence

$$T_1^2/T_2^2=(K+C_1)/(K+C_2)$$

The capacities  $C_1$  and  $C_2$ , computed as  $\kappa A/4\pi d$  where  $\kappa=2.7$  is the specific inductive capacity of hard rubber, come out  $C_1=104$  els. U.,  $C_2=234$  els. U. Hence the value of  $K$  computed from the periods is 75 els. U. If, therefore, we use the first equation and reduce to henries

$$L=\frac{9 \times 10^{11} T_1^2}{4\pi^2 (K+C_1)}=293 \text{ henries}$$

This agrees so well (considering the difficulty of the experiment) with the results of § 75, where virtually the same equation but a totally different treatment is in question, that the datum should be trustworthy. Thus the  $e''$  and  $b'$  crests in figure 151 are to be regarded as placed by the electric oscillation and they have no bearing on the harmonics of the tube. It follows also that the construction of such relations as given in figure 142, if made with the spark exciters, must be interpreted with caution.



## CHAPTER V.

### MISCELLANEOUS EXPERIMENTS.

#### EXHIBIT OF TELEPHONIC EXCITATION OF ACOUSTIC PRESSURE.

78. **Apparatus.**—In Science (vol. 54, p. 155, 1921) I described a series of simple experiments bearing on the nature of the acoustic forces observed in connection with telephone-blown pipes. Having occasion to repeat this work in relation to the preceding chapter, I obtained a series of repulsions as well as the former attractions. This induced me to repeat the experiments with the bifilar suspension shown in figure 154. Here  $TT'$  are the telephones excited by a small inductor and break of variable frequency, each carrying the identical pipes  $PP'$ , about 13 cm. long and 5 cm. in diameter, with a note ranging from below  $b'$  to  $\sharp c''$ , depending on the degree to which the mouth is open.  $RR'$  are two identical cylindrical resonators of heavily varnished paper, about 9 cm. long and 2.2 cm. in diameter, responding to  $a''$  (in place), attached at right angles to a straw shaft  $ss'$  26 cm. long. The deflections were observed with mirror and scale at a distance of 142 cm. To guard against air currents, the box  $BB'$  surrounds the whole, in such a way that the telephone pipes  $PP'$  may be more or less withdrawn, or that  $R$  may dip more or less into  $P$ . The period of the needle was about 30 seconds, and the total weight 4.5 grams. The addition of adjustable closed cylinders  $DD'$  improves the damping, etc.

79. **Observations.**—When the resonators  $R$  extend to about 3 cm. within  $P$ , the full telephonic current throws the light spot off scale. The current was therefore diminished by inserting 500 ohms resistance, which reduced the sound to the loudness of an ordinary organ-pipe. The survey in pitch ( $a$  to  $c'''$ ) then gave the deflections  $s$  reproduced in the graph (fig. 155), repulsion laid off positively. There are two marked attractions at  $b'$ , the resonance pitch of  $P$  and at  $b$ , an octave lower, none at  $b''$ , an octave higher. Hence the overtones of the telephone note are probably responsible for  $b$ , though its intensity is surprisingly large. Similarly there are three repulsions, the strongest at  $a''$ , the resonance pitch of  $R$ , while  $a'$  and  $d'$  are probably again referable to the successive overtones of the telephone note.

When the pipes  $P$  are partially withdrawn, so that the mouths of  $R$  and  $P$  are coplanar, the deflections obtained are such as shown in figure 156. The repulsions ( $a''$ ,  $a'$ ,  $d'$ ) have nearly vanished, but the attractions (now at the resonance pitch  $\sharp c''$  of  $P$ ) is still strong.

At a distance of 4 cm. between the mouths (organ-pipe loudness) the attractions at  $\sharp c''$  also practically vanished; at a distance of 8 cm. quite so. One notes that  $P$  attractions are more persistent.

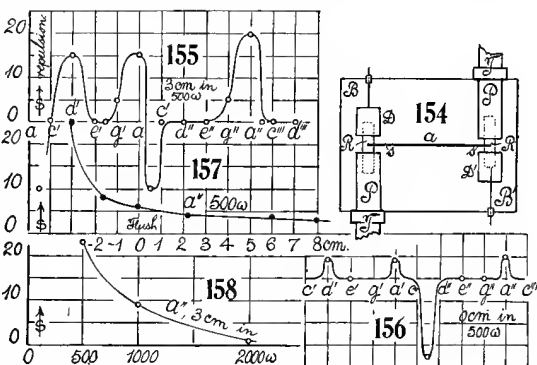
Thus the acoustic pressures fall off very rapidly with the distance apart of the systems  $R$  and  $P$ . In figure 157 with 500 ohms in circuit and the steady note  $a''$ , this relation is indicated, the mouth of the resonator  $R$  being within  $P$  for negative abscissas, in centimeters. The note is a little louder than in figure 156. The effect increases as the mouth of  $R$  approaches the telephone plate, though it is still 9 cm. off.

In figure 158, the deflections at  $a''$  pitch, with the mouth of  $R$  3 cm. within  $P$ , are shown for increasing resistances (abscissas) in the telephone circuit.

Similar experiments made

with a variety of resonators  $R$  of different lengths, widths, and shapes will presently be described, but the results were not essentially different from the above.

The tuning at the crests must be precise—more so than the inductor was able to hold steadily. Hence the needle is usually in motion, and this with the long period makes it difficult to obtain sharp data. It is clear, however, that forces fall off very rapidly beyond the organ-pipe.



**80. Estimates.**—The pipes  $R$  having an area of about  $4 \text{ cm.}^2$ , the deflections  $s$  with the above constants of the bifilar may be reduced to pressures by the equation  $10^4 p = 7s \text{ dyne/cm.}^2$ . Thus the maxima in the figures would not exceed an acoustic pressure of  $0.0007 \times 20 = 0.014 \text{ dyne/cm.}^2$ . If  $p = 10^6$  is the atmospheric pressure,  $\Delta p/p = 1.4 \times 10^{-8}$ . This is only about twice as large as Rayleigh's minimum audible ( $6 \times 10^{-9}$ ), although the pipe  $P$  could certainly be heard at several hundred feet away. The high value  $\Delta p = 0.25 \text{ dyne/cm.}^2$ , found for howling pipes, was similarly small, so that but a minute fraction of the acoustic energy per cubic centimeter is locked up in these acoustic pressures, the remainder being radiated.

**81. Equation.**—One may describe these phenomena \* as a whole, by putting the locally available energy in the form  $p + \rho v^2/2 = p_0 + \Delta p_0$ , where  $p_0$  is the atmospheric pressure and  $\Delta p_0$  an increment contributed by the acoustic vibration, increasing with its intensity, but constant within the region bounded by the hollow resonators. When the pipe  $P$  is in resonance, the waves are merely reflected, without nodes, within  $R$ . When  $P$  sounds loud enough, pressure  $p$  at the mouth of  $P$  may with increasing  $v$  have fallen below that of the atmosphere, while at the same time it has increased above atmospheric pressure

\* The rigorous treatment of pulsating sources is given by Bjerknes, *Hydrodynam. Fernkräfte*, Leipzig, 1902, J. A. Barth.

at the closed or nodal end of  $P$ .<sup>\*</sup> Thus the reduced pressure at the mouth of  $R$  is harbored within it, and it is thus thrust inward by the full atmospheric pressure on the outside. Conversely, when  $R$  is in resonance,  $P$  merely reflects (without nodes) the waves emerging from  $R$ . If the vibration is of sufficient intensity, the pressure at the mouth of  $R$  falls below that of the atmosphere, while the pressure within  $R$ , at its closed ( $v=0$ , nodal) end rises above atmospheric pressure, so that  $R$  is now thrust outward from  $P$ .

**82. Further experiments.**—In the introductory work, single resonators counterpoised on the other side of the bifilar were tried, largely to test the pressures obtainable with very loud sounds. The bifilar corresponded to  $p=1.37 \theta$  dynes/cm.<sup>2</sup> ( $\theta$  radians, deflection). When a resonator 13 cm. long and 2.1 cm. diameter was used, the resonance notes were  $e'$ ,  $e''$  for  $R$  and  $b'b'$  for  $P$ . The repulsions obtained reached 0.2 to 0.3 dynes/cm.<sup>2</sup>,  $R$  being well within  $P$ . With a shorter cylinder  $R$ , 8.1 cm. long, the results were about the same. Beyond the mouth pressures fell off rapidly, as above.

Supposing that long tubes (length 17.7 cm., diameter 2.25 cm., period of bifilar 40 seconds) would show increased sensitiveness, as these could be thrust more nearly to the telephone plate within  $P$ , they were tested at some length. The contrary was the case, as shown in figure 159, the  $R$  resonance observed being at  $d''$ . Slight attraction (at  $\#c''$ ) only was obtained when the mouths were flush and a few centimeters beyond this, there was no deflection appreciable. Going to the opposite extreme,  $R$  cylinders as short and wide as admissible (length 5.6 cm., diameter 3.8 cm., blowing  $b'e'''$ ) were examined in turn. Figure 160, where  $p=10^{-4} \times 2.5s$ , summarizes the  $s$ -effect of increasing resistance in the telephone circuit. The attractions of the  $P$  pipe (resonance notes now abnormally  $a'$  and  $a''$ ) only were obtainable. There were no repulsions. Moreover, these attractions, though never very large, were sustained throughout lower intensities (up to 4,000 ohms in the telephone circuit). Later, on careful searching a weak repulsion at  $\#c''$  was at times detected, which may be taken for an octave below the  $R$  pipe-note in place ( $\#c'''$ ). The occurrence of the  $a''$  resonance note for  $P$  is, however, quite puzzling; for  $P$  and  $R$  can not vibrate together as a double closed pipe without producing repulsion in  $R$ . Granting that the  $P$  frequency may be depressed from  $c''$  to  $a'$  because of the stopped mouth, the origin of the strong  $a''$  is left unexplained.

A careful survey in pitch with the mouths of  $P$  and  $R$  coplanar and with the full telephonic current ( $\omega=0$ ) is given in figure 161*a*. Here there is multiple resonance from  $a'$  to  $e''$  which naturally masks the possibility of repulsion at  $c''$ . Resonance at  $a''$  is very strong, the light spot passing out of scale. With a distance of 2 cm. between the mouths of  $R$  and  $P$ , an accentuated attraction (fig. 161*b*) of the usual note of the  $P$  pipe (now at  $d''$ ) shows itself with nothing else appreciable. The  $a'a''$  resonances of figure 161*a* are gone. To make sure that these attractions are due to  $P$  only,  $R$  was reversed

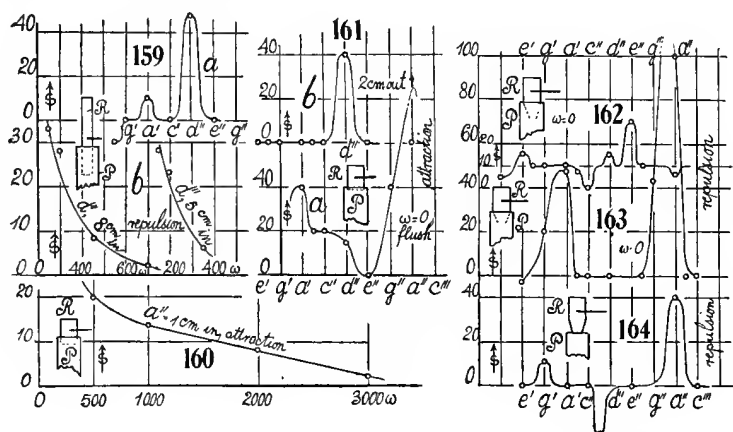
---

<sup>\*</sup> This may be tested by lowering a disk in  $P$ .

and its *closed* end just inserted into  $P$  (fig. 161, inset). The same graph, with its attractions at  $a'$ ,  $c''$ , and  $a''$ , appeared as before. Thus  $R$  as a resonator was throughout inactive.

The key to this dilemma is probably given in figure 114, where a pitch near  $a''$  appears as the resonance note of the telephone-plate. Thus the  $a''$  is to be regarded as a forced vibration impressed on  $P$  by the strongly resonant telephone, and the depression of  $a'$  is probably similarly influenced. Hence it makes no difference whether  $R$  presents its closed or open end to  $P$ , for the vibration of  $R$  does not appear. The frequent occurrence to  $a'$  and  $a''$  crests is probably of like origin.

The preceding short  $R$  pipe was now provided with a conical front 4 cm. long and 1.3 cm. in diameter at the mouth. Figure 162 (inset) gives the results with the cone only submerged in  $P$ . The system was very insensitive



throughout, the full telephonic intensity ( $\omega=0$ ) only just sufficing to bring out the graph characterized by cusplike repulsion at  $e''$  and a minor one at  $e'$ , the attraction near  $c''$  being slight. Nothing further was obtained by thrusting  $R$  into  $P$ .

The front was now cut down to a length of 2.5 cm., with a mouth 2.2 cm. in diameter, the cone being as before just submerged in  $P$  (fig. 163, inset). An enormous increase of sensitiveness is at once obvious (fig. 163), with the repulsion crests at  $a''$  and  $a'$ . No attraction (near  $c''$ ) was detected. With 500 ohms in circuit, the sensitiveness was reduced to the usual order, so that there is no gain ascribable to shape.

The experiment was next modified by placing the neck of  $R$  (fig. 164) flush with the mouth of the pipe  $P$ . With the telephone at full power (no external resistance), only moderate repulsions appear at  $a'$  and  $a''$ ; but the attraction of  $P$  at  $c''$  is now normal and distinct. Thus the insertion of the cone into the mouth of  $P$  has been sufficient to quench its resonant vibration, while a narrow mouth quenches  $R$  also.

To obtain further evidence of the influence of telephonic resonance, the pipe  $P$  was cut down from 13.5 cm. to 8.5 cm. from the telephone-plate until its resonance note was  $e''$ . Using the resonator  $R$  of figure 154, the data were obtained as given in figure 165. Here  $a'$  and  $a''$  are the  $R$  repulsions as before, while the  $e''$  is the new attraction of the shortened  $P$  pipe. Figure 166 summarizes the results found on making the same test with the short wide resonator of figure 160, and inserting the closed end of  $R$ . The  $e''$  appears correctly as the attraction of the resonant  $P$  pipe. Hence the two  $a'a''$  attractions can only be referable to telephone-plate resonance.

A long, wide resonator, No. VI, 10.5 cm. long and 4 cm. in diameter gave no new results. There were strong repulsions at  $a''$ , smaller at  $a'$ , and attraction at  $e''$  of the usual value. With a somewhat improved mounting of  $R$  No. III, the full telephone-note was effective to a displacement of about 20 cm. between the mouth of  $R$  and the telephone-plate.

**83. Disk explorer.**—By far the most sensitive arrangement is the plate or disk, probably because its diameter (here 5 cm.) may be large. At about 8 cm. from the phone-plate and 1.5 from the mouth of  $P$ , the light index passed off scale even with 1,500 ohms in the telephone circuit. At 3.5 cm. from the mouth of  $P$  it did so when the resistance was removed. Two resonances  $a'$  and  $a''$  were found; but the upper one extended from  $f''$  to  $hb''$ , thus probably including the free pipe-note. The lower crest was also broad. With a long  $P$  pipe (14 cm. from telephone-plate) the arrangement becomes insensitive. The objection to the disk is that attractions only are possible, and that these increase very rapidly as the disk approaches the mouth of  $P$ , while at the same time the resonance note changes. The forces here are much like those of a magnet pole.

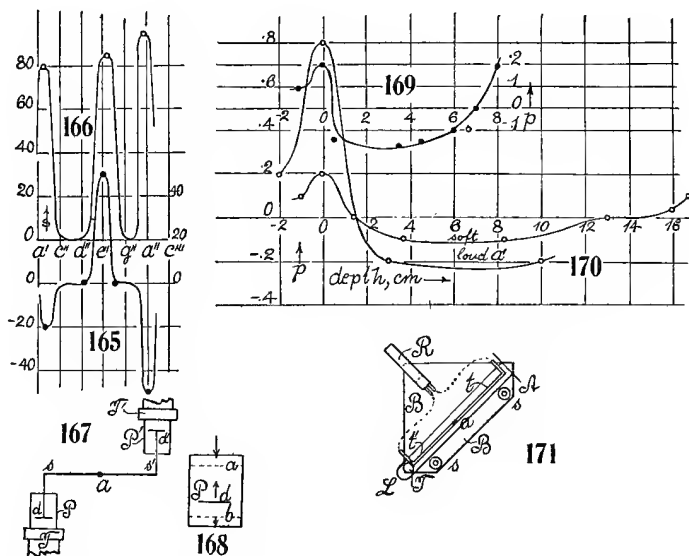
Pursuing the case further, the somewhat awkward arrangement, figure 167, was tried. Here two disks,  $d, d'$ , 4 cm. in diameter, could be inserted into the  $P$  pipe, almost as far as the telephone-plate ( $T$ ), the right-angled shaft  $s$  being supported by the bifilar at  $a$ . Although but small angles of rotation were possible, the nature of the forces was easily ascertained. From about 1 cm. inward within the mouth of  $P$ , these disks were strongly repelled when the  $a''$  resonance note sounded, almost but not quite as far as the plate. From about 1 cm., as stated, outward the attraction increased, being at a maximum near the mouth. Thus there is a normal plane slightly within  $P$ , say at  $a$ , figure 168, at which the conditions are neutral, but at a short distance from which, in or out, either attraction or else repulsion, respectively, are experienced. It follows, as in Lord Rayleigh's experiments, that a disk oblique to the axis of  $P$  would have its near half attracted and its far half repelled, or would tend to rotate, a form of apparatus highly developed by Professors F. R. Watson,\* G. W. Stewart, P. E. Sabine, and others.

Finally, on using the horizontal torsion-balance described in the last report (*l. c.*), these data were confirmed and extended. The accurate measurement

---

\* Bull. 127, Eng. Exp. Station, Univ. of Ill., Urbana, 1922.

of the forces would well repay research. The experiment is a delicate one, as the conditions are usually unstable, and the registration decreases rapidly above or below the resonance note. With the horizontal torsion system used (figure 168),  $d$  being the exploring disk, a second neutral plane at  $b$ , about 1 cm. from the plate of the telephone, was detected. Below this the disk actually flopped down upon the mouthpiece of the telephone. The forces are thus essentially as shown by the arrows of the figure. There is a jerk at resonance. In case of a disk 3.5 cm. in diameter, figure 169 gives a record of the actual distribution of pressures (dynes/cm.<sup>2</sup>) for the pipe 8.5 cm. long and 5 cm. in diameter. Figure 170 supplies two records for a loud and a softer note, in case of a glass cylinder 18 cm. long and 5 cm. in diameter and



the same disk. At the outer neutral plane (1 to 2 cm. within mouth of pipe) a slightly sharp note produces repulsion. The nearly constant repulsion within the shaft of the pipes, together with the relatively marked repulsion at the mouth, are throughout noteworthy.

#### PNEUMATIC GAGE FOR THE PIN-HOLE RESONATOR.

**84. Apparatus. Observations.**—Pressure measurement with the U-tube interferometer has the advantage of being absolute, sensitive, instantaneous, and with dead-beat fringe displacements. But the implicity of an inclined-plane arrangement consisting of a thread of liquid in a quill tube, so frequently used for measuring small pressures, commends itself, and I have often applied it. The apparatus is shown in figure 171, where  $BB$  is a triangular base-board on leveling screws  $ss'$ . The quill tube is seen at  $t$  with a thread of liquid at  $a$ . The ends of  $t$  are raised and communicate through short ends of rubber tubing

with the twin pin-hole resonator  $R$ , provided with salient and reëntrant pin-holes to the respective ends of  $t$ .

The quill tube  $t$  is fastened to a lath  $LA$ , hinged at  $A$  and carrying a tangent screw  $T$  at the other end, to give  $LA$  any desired small inclination.

The base-board is first leveled by the screws  $ss'$  until the liquid thread  $a$  is permanently stationary. An extra level on  $t$  may be used. In such a case it may be moved toward the pin-hole reëntrant in  $R$ , by blowing an organ-pipe in resonance with  $R$ , near it. Motion stops with the sound, but is always sluggish. At longer distances (1 or 2 meters) the thread creeps, but its speed increases as the pipe is moved closer.

With the pipe fixed, say at a foot,  $LA$  is raised at  $T$ , until the thread  $a$  is just stationary. It is then interesting to observe that when the pipe is moved slightly nearer, the thread rises, and falls with the pipe moved farther. In this way the pipe position for a given number of turns of  $T$  may be found.

As an example I give the following experiment chosen at random: The data were: length  $TA$ ,  $L=32.1$  cm.; inclination angle,  $\theta=0.0024$   $n$ ; pitch of screw,  $T=0.077$  cm.; length thread  $a$ ,  $l=1.9$  cm.; number of turns,  $n=7$ ; density (alcohol),  $\rho=0.8$ . Whence

$$p = l\rho g\theta = 3.6n; \text{ or } p = 3.6 \times 7 = 25 \text{ dynes/cm.}^2$$

The same resonator  $R$  tested by the U-tube interferometer gave about 60 fringe displacements for the same pipe and distance, so that

$$p = n(\lambda/2) 13.6g = 0.42n; \text{ or } p = 25 \text{ dynes/cm.}^2$$

which happens to agree exactly with the preceding datum, though the correspondence would not in general be so close. The resonator was not specially sensitive as to pin-hole adjustment.

#### EXPERIMENTS WITH INTERFEROMETERS.

**85. Modification of the Michelson interferometer.**—The purpose is two-fold—to eliminate the need of compensator and to permanently protect the half-silver plates against sulphur corrosion. This may be accomplished very simply by cementing the half-silver film  $H$ , figure 172, with Canada balsam between two glass plates of the same material and thickness. If  $M$  (on a micrometer) and  $M'$  are the two opaque mirrors, it will be seen that each of the component beams passes identically through 4 thicknesses of glass at  $H$ , effectively through 3. One hurtfully reflecting glass face has been eliminated.

Using mirrors 3 inches square and an arc lamp at  $A$ , about 0.5 meter from  $H$ , the fringes of white light are easily projected on a white screen  $S$ , 10 or 20 feet from  $H$ . To make the image brilliant and the lines sharp, a weak lens (2 diopters)  $L$  must be used near  $H$ . With common plate glass the fringes are then somewhat irregular ovals, and covering a surface 6 inches to a foot square, look much like grained wood. They may be seen and used in subdued daylight. Placing the finger lightly on the  $\frac{1}{2}$ -inch base-plate in front of or

behind  $M$ , the fringes all pass toward or away from the center, respectively, indicating the flexure of the plate. The micrometer at  $M$  can scarcely be used with common plate, for the ellipses vanish when 10 or 12 fringes have passed ( $3 \times 10^{-4}$  cm.). They are thus very easily lost and thereafter difficult to recover. It is easy to find them, however, by using a spectrotelescope in  $HS$  with a collimator in  $AH$ . The spectrum fringes are first found. These are made horizontal by aid of the micrometer at  $M$  and the white light fringes then almost always appear on removing the spectroscop. Compensators, if desired, may be introduced in pairs. Using the spectrum ellipses, however, a plate 0.5360 cm. thick required micrometer displacement of 0.2864 cm. to restore the yellow diameter of ellipses to its original position. Thus the index of refraction was 1.5344, correct to one or two units of the fourth place.

With the white-light fringes, only a soap film may be inserted. If such a film  $x$  cm. long and  $y$  cm. thick is stretched on a frame, we may write  $\Delta x/x = -\Delta y/y = -\lambda/2(\mu-1)y$ , so that  $y = x\lambda/2(\mu-1)\Delta x$  if  $\Delta x$  is the stretch per fringe. Thus a film 2 cm. long stretched to 4 cm. for one fringe, must have been  $7 \times 10^{-5}$  cm. thick originally. The experiment does not work out as smoothly as I expected, because the film is eventually a wedge-shaped bag covering several fringes from top to bottom.

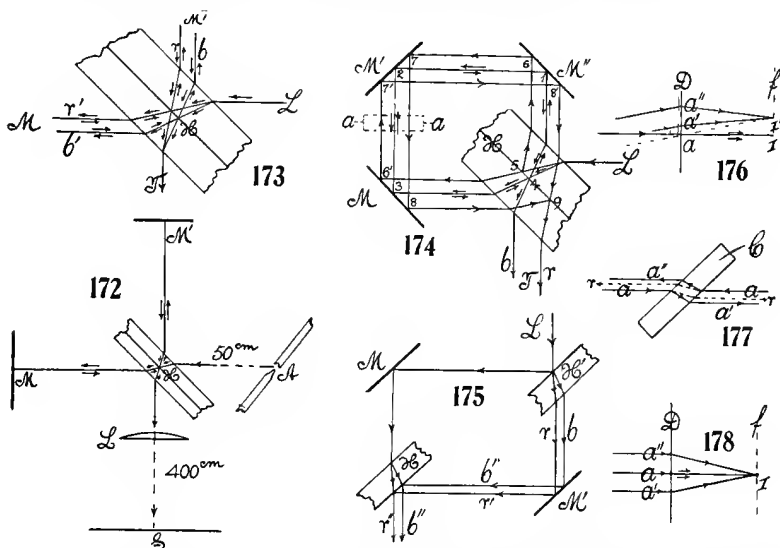
Although the micrometer is not available, the rings may be controlled by using a pair of identical compensator plates in the paths  $HM$  and  $HM'$ . On rotating one in a given direction, the central rings on the screen  $S$  move outward, leaving a blank field within, while the rings remain very sharp as they move to the limits of the field. The phenomenon is symmetrical for rotation in either direction. With the arc lamp the fringes are continually squirming. I at first supposed this to be due to air currents; but it results from the unsteadiness of the arc light, whereby the apex of the cone of light moves. With sunlight, condensed or not, the fringes are fixed. The fringes travel only if the condensing lens moves.

With the Michelson interferometer, the fundamental form is always oval, or was so in the many cases which I tested. If the two plates of the half-silver  $H$  in figure 172 are not equal, the spectrum fringes are small ovals and the white light fringes rapidly become too faint for projection. To obtain good achromatics, however, the fundamental form must be quasi-hyperbolic, as is always the case with the quadratic interferometer.

**86. Achromatic fringes.**—In the case of the Michelson interferometer, the fundamental fringe figure is elliptical, and the outer rings when the disk vanishes are progressively colored spectral rings. The achromatics are not producible. One may note (fig. 173) that even horizontally a ray of white light entering at  $L$  comes out at  $T$  as a ray of white light. There is no separation of colors if the half-silver is compensated, nor with additional compensators. There is dispersion in the absence of compensation, and in this case the displaceable and useful small spectrum ellipses occur.



In case of other interferometer adjustments, the displaceable achromatic fringes are producible with white light. The fundamental design may here be taken to consist of equilateral hyperbolas, with the horizontal black fringe as one of the asymptotes, though the figure is usually much more complicated, particularly with common plate glass, of course. This does not necessarily interfere with the occurrence of available small straight fringes (*cf.* Carnegie Inst. Wash. Pub. 249, Part IV, Chap. VII, §§ 54, 55). In these adjustments, one may note, an entering ray of white light issues with horizontal separation of colors. Thus, in the self-adjusting interferometer (fig. 174) with or without the compensator (the latter is here superfluous, except as a film protection), the incipient white ray  $L$  is replaced by the spectrum  $br$ . In the quadratic interferometer (fig. 175), in spite of the complete compensation in view of



the identical half-silvers  $H$  and  $H'$ , the entering white ray  $L$  is again changed to the horizontal spectrum  $r'$ ,  $b''$ . There must, therefore, in these cases also be vertical spectra with inclined rays.

The achromatic fringes, as I have called them,\* are in appearance like Young-Fresnel fringes, except that the central fringe is frequently not white but black. In other words, there is usually phase reversal corresponding to the black spot in thin plates. The black line flanked on either side by white lines is in fact the same thing. The slit-images in the telescope must be coincident throughout.

If, for convenience, we operate with the self-adjusting interferometer (fig. 174) and rotate the mirror  $M$  slightly about the horizontal axis, the fringes may be made to enlarge from horizontal hair-lines, through infinite size back again to hair-lines for the same sign of rotation. Here there is a change of

\*They are really superchromatic, as will appear presently.

obliquity of rays; in other words, the coincident slit-images rise or fall in the telescope; at the same time the black fringe is changed in position correspondingly; *i. e.*, it does not remain glued to the cross-hairs of the telescope, but moves with the slit-images. The whole phenomenon as to color, etc., passes through infinity, symmetrically with respect to the black line, in spite of the marked change in angle of the rays.

Since the distances 34 and 3214 are unequal, it is obvious that the spots of light at 4 move vertically over each other when  $M$  is rotated on a horizontal axis, although the rays remain parallel. Hence let  $D$ , figure 176 (elevation), be the principal plane of the objective of the telescope at  $T$ , and let the coincident parallel rays  $a$  have an image at  $I$  on the focal plane  $f$ ; then in case of rotation of  $M$ , the coincident rays  $a$  separate into the rays  $a'$ ,  $a''$  with their focus at  $I'$ , again coincident; but whereas the interference design from contiguous spots,  $a$ , is infinite in size, that of the separated spots is reduced proportionally to their distance apart. Thus we may regard  $a'a''$  similarly to the two slits in Young's experiment, except that the position of the black line of symmetry will depend on the initially opposed phases of  $a'$  and  $a''$ . The experimental evidence shows that this line of symmetry, initially at  $I$ , as one would expect, moves with  $I$  toward  $I'$ , though usually less than the slit-images.

If the mirror  $M'$  (fig. 175) is rotated on a horizontal axis, the slit-images move in the telescope as before, owing to the increasing obliquity of rays; but the fringes do not change in size because the distance  $a'a''$  is relatively constant.  $M''$  again operates like  $M$ .  $H$  rotated on a horizontal axis changes the size of fringes only, since but one component beam, 41234, is reflected. Being reflected in parallel,  $I$  remains in place, but  $a$  changes to  $a'a''$  with a focus at  $I'$ .

There is another method of changing the size of fringes with a particular bearing on the present experiment, since the direction of rays is not changed. This consists in placing a compensator of good plate glass ( $aa$ , fig. 174), capable of rotating on a horizontal axis in the path of the beams. In the oblique position (fig. 177), this converts the originally coincident opposed rays  $a$ ,  $a$  into the non-coincident but parallel rays  $a'a''$ . The result is, if  $D$  (fig. 178) is the principal plane of the objective of the telescope at  $T$  (fig. 174), that the coincident rays at  $a$  with an image at  $I$ , are converted into the symmetrically parallel rays  $a'a''$ , also with an image at  $I$ . The slit-images thus remain fixed, while the fringes decrease in size proportionally to the distance  $a'a''$ ; and since  $a'$  and  $a''$  are opposed in phase, the black line remains fixed at  $I$  throughout.

**87. Iceland-spar compensator. Extraordinary ray.**—With a plate-glass compensator, no matter how thick (glass columns up to 7 cm. were tried), the fringes remain appreciably the same on the two sides of the position for infinite size; *i. e.*, they pass from hair fringes, through infinity, to hair fringes again, symmetrically when the compensator is rotated in a given direction. This is no longer the case when a calcite prism ( $C$ , fig. 179) with short diagonal vertical, is introduced, as in the figure, even if the prism is less than

a centimeter thick. To bring out the phenomenon vividly, however, a calcite block 3 cm. thick is desirable. With a Nicol 7 cm. long the results are correspondingly striking.

In dealing with polarized light it is well to observe at the outset that the ray at  $T$  having undergone successive reflections, is itself very nearly polarized, with a plane of polarization horizontal. It is therefore necessary to make adjustments for vertical vibration only, as the horizontal effects are extremely faint. Furthermore, if the long diagonal of  $C$  is vertical, the ordinary ray is in question and the crystal there behaves like common glass (max. index,  $\mu=1.65850$ ), as it should.

Next let the short diagonal of  $C$  be vertical (extraordinary ray, min. index,  $\mu=1.48635$ ) and the rotation of  $C$  on a horizontal axis be made from hair fringes on one side to hair fringes on the other. It will be found that on one side of the position for infinitely large fringes they are pronouncedly achromatic and very numerous (15 to 20 counted), whereas on the other side of the infinite fringes they are few and usually highly colored. In view of the thickness of  $C$  (3 cm.), a very small angle of rotation is in question and the position of the crystal to the rays is about as shown at  $C'$ , figure 179, the edges sloping a little downward from the horizontal parallel to the ray. If an analyzer is used, it is possible to detect also the much fainter fringes corresponding to the horizontal vibration. Large-size fringes of one kind usually correspond to small-size fringes of the other kind of polarization, though of course the sizes pass in opposite directions through each other.

Using the Nicol 7 cm. long, with the short diagonal vertical, the number of achromatic fringes had further increased (contrasting therefore with the glass column 7 cm. long and its doubly symmetrical fringes). I counted 50, and they filled the field of the telescope from top to bottom. The colored fringes were much the same as with the calc-spar. In figure 180 I have given a record observed at successive stages of rotation, beginning on the colored side,  $b$  denoting black,  $w$  white,  $r$  red,  $g$  green,  $r'$  reddish, etc. The black fringe is stationary throughout the rotation. The  $\infty$ -fringes are of course too faint within the field of the telescope to be characterized. On the achromatic side (4, 5, 6) the fringes merely shut up, with loss of color, from large to small size. On the colored side (3, 2, 1) the few present are variegated, but also narrow down to hair-lines as the given rotation proceeds. The total rotation downward from the level edge, from small fringes to small fringes, will not exceed  $5^\circ$ ; but the fringes remain visible within an interval of about  $15^\circ$ , symmetrically enlarged. One of the light spots on the mirror may then be seen passing from above to below the other. The design 2 is most interesting, consisting of a strong black line flanked by two vividly white lines on either side, the remaining colors soon fading off. If this pattern can be maintained, the black line  $b$  as an index in displacement interferometry should be very useful. With an analyzer at the telescope, the color contrast is often sharpened. The group 2 (fig. 180) appearing with analyzer in parallel may

be changed to appear like middle white flanked by two blacks, if analyzer and polarizer are crossed.

**88. Theoretical remarks.**—In the treatment of achromatic fringes and thin plates, it is customary to use as the equation of condition  $\cos r/\lambda = \text{const.}$ , where  $r$  is the angle of refraction of the ray within the thin plate (here air,  $\mu = 1$ ) and  $\lambda$  the wave-length. There results (for instance for Talbot's fringes) an expression

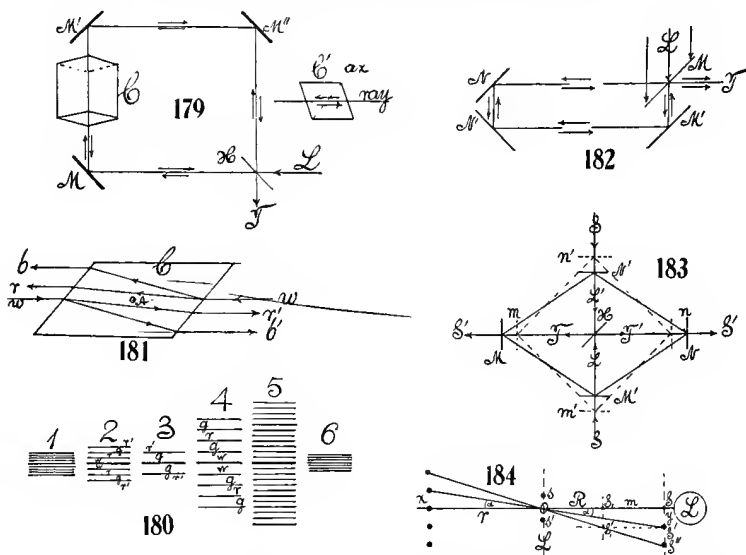
$$\cos^2 r / \sin r = \sin \phi \cdot \sec R \cdot \lambda d\mu / d\lambda$$

where  $\phi$  is the prism angle and  $R$  the angle of refraction at the initial incidence. In the Michelson interferometer the familiar method of rotating one of the rays on the trace of the half-silver reduces the treatment to the case of thin plates. The same may be done less directly with the self-adjusting interferometer; but as in all these instruments the angle  $\phi$  is essentially zero, the equation vanishes. True, in my experiments the square half-silver plate was probably a wedge of very small angle  $\phi$ ; but by trying this plate on all four sides and by using an indefinite assortment of other plates, there was no essential difference in the phenomenon. Nevertheless, it is probable that the color factor (which may be transformed to  $\lambda d\mu/\mu d\lambda$ ) will contribute to an explanation, quantitatively.

If we consider figure 180 as a whole, it is obvious that there must be two coefficients of vertical dispersion; one of these, resulting from the interference  $a'a''$ , changes its sign on the two sides of the black line of symmetry, while the other, resulting from the refractive dispersion of the compensators (compare fig. 177) also changes sign for the component rays  $a'$ ,  $a''$ . The dispersion instanced in figures 174, 175, being horizontal, is not available. Hence, in figure 180, groups 1, 3, 2, the coefficients cooperate; in groups 5, 6 particularly they annul each other and achromatism results. Thus it is also clear that the  $d(\log \mu)/d(\log \lambda)$  must have a particular value to establish the balance. Various glasses tested (plates of flint glass and of crown glass, quartz plates, quartz columns 4 cm. long, ordinary ray of calcite, etc.) had no appreciable effect, while the extraordinary ray of calcite fulfilled the conditions strikingly. If the refraction does not change in distribution of color the fringes are the same on both sides of  $\infty$ . This is the case with the regular achromatics, which are thus always on the dispersion cooperating side. For instance, in figure 177, for all positions of the plate-glass compensator  $C$ , the red rays  $rr$  will be innermost and the blue outermost. Hence in figure 178 the red rays  $a'a''$  will be closer together and will be additionally more dispersed than the blue rays in the interferences. The conditions will be symmetrical as  $C$  rotates through the vertical. There will be few fringes because of the large combined dispersion.

For the case of the calcite rhomb ( $C$ , fig. 181), the two spectra  $br$  above,  $r'b'$ , below, issuing from the corresponding white rays  $w$ ,  $w'$ , are opposite in direction. The red rays are nearer each other vertically than the blue rays.

Now, it is only an extraordinary ray that can pass through an oblique face collinearly. Hence when the rhomb is rotated on an axis  $A$  normal to the diagrams, so that  $r'b'$  is above and  $rb$  below, the blue rays are nearer together than the red rays. In the latter case they would therefore counteract the dispersion due to interference, so that achromatic spectra would result. In the former case they are in the same sense as the interferences and accentuate the color effects. Thus if  $c$  is the vertical distance  $a'a''$  in figure 178 (normal distance between  $r, r'$  or  $b, b'$  in figure 181), since  $a'$  and  $a''$  are in opposed phases, the equation of a dark line is  $n\lambda = cx/F$ , where  $n$  is the ordinal number of the fringe at a distance  $x$  from the center  $I$  and  $F$  the focal length of the objective. Hence if, within a certain range approximately,  $c = k\lambda$ , where  $k$



is a mean constant,  $n = kx/F$  (blues closer together) and is free from color. In the other case we should have to write consistently  $c = k/\lambda$  (reds closer together) and  $n\lambda^2 = kx/F$ , accentuating color.

#### INTERFEROMETRY AT LONG DISTANCES.

**89. Purpose.**—Preparatory to certain experiments on the detection of shearing displacements of points on the earth's surface, the use of the interferometer suggested itself. Under such circumstances the source of light appears as a mere point, even if examined by as strong a telescope as would be useful. The interferences of two light points are not available even if they can be seen, for it is the measurable displacement of fringes in a fixed white field which is needed.

At short ranges, when an ordinary collimator is used, the rays are parallel in a plane (horizontal) normal to the slit, only. The vertical extent of the slit-image in the telescope is therefore practically indefinite. Particularly at

long distances, the interference fringes produced by the interferometer are as a rule present in the focal plane only. The endeavor to get fringes out of focus, with the light filling the field of the eyepiece, does not usually succeed, except with very good plate glass.

The case is different, however, when the collimator is discarded and a beam of sunlight  $L$  is used directly, as in figure 182. For convenience, the self-adjusting interferometer pattern was used,  $M$  being a half-silver and  $NN'M'$  opaque mirrors with the distance  $NM$  very large. The telescope is at  $T$  and when focused for parallel rays shows a mere point of light, even when the mirrors (which must obviously be of optic plate) are a square decimeter in area. Nevertheless, the fringes must be present and are usually suggested by the irradiation. If, however, the telescope is put out of focus by thrusting the eyepiece either toward the front or rear, till the whole field is illuminated, the fringes will usually appear and may be enlarged by slight rotation of  $M'$  on a horizontal and vertical axis, supposing the other adjustments are nearly enough true. The beam  $MT$  is, as it were, lamellar throughout, even if the glass used is not exceptionally good. The conditions of good definition in the absence of the best optic glass may be further improved by narrowing the beam at  $L$  to small cross-section (5 mm. square), so that only a small part of the half-silver  $M$  is effective. In this case the fringes always come out strongly and there is, as a rule, still an abundance of light, if sunlight is the source. I have even used a condenser of 10 or 20 meters focal length in the beam  $L$ , without destroying the fringes and with a gain of illumination. Obviously the telescope itself is not needed and a good lens with a micrometer-plate in focus placed anywhere in the beam  $MT$  will suffice.

The available distances in the laboratory did not much exceed 11 meters; but this sufficed to make the tests, which succeeded at once in spite of rather poor glass plates. If the fringes are straight the spectrum fringes come out equally well, even with the grating, if the ruling is set at right angles to the fringes.

It will, of course, be very much more difficult to use the separated beams of Michelson's interferometer; but this either at  $90^\circ$  or  $60^\circ$  is essential for the purpose in view. If, as in figure 183, the rays were passed parallel to the directions of principal strain in a shear, the gradual increase of strain could hardly escape detection at an early date, particularly as the source of light  $L$  and receiving lens  $T$  could both be reversed  $180^\circ$  without any interference at the mirrors  $H$ ,  $NN'$  and  $MM'$ . In the figure  $mn'nn'$  suggest the original position of mirrors, and  $MM'NN'$  their position under advanced strain, relative to each other.

**90. Interferences resembling Michelson's diffractions for small angles.\***—In figure 184,  $L$  is the objective of a telescope. No light is admitted except that passing two fine parallel slits  $s$  and  $s'$  close together at a distance

---

\* Mr. Lloyd W. Taylor (Manual of Optics, p. 50 *et seq.*) describes somewhat similar experiments.

$c$  apart. Consequently, even with white light, interference fringes at a distance  $x$  apart are seen in the ocular. They are practically equidistant, and if  $r$  is the focal length of the telescope

$$a = x/r = \lambda/c$$

$\lambda$  being the mean wave-length of light and  $a$  the angle subtended by two fringes. With white light, three of these, flanked by two closed colored fringes, are usually obtained. A telescope of 20 cm. focal distance suffices. The plate  $ss'$  is best placed within the objective touching it, so that the distance  $r$  is definite. Two lines about 0.5 mm. apart, ruled with a needle in a black photographic gelatine-covered plate, if well chosen, do very well, though smoked plate glass is preferable.

**91. Same. Outer plate for angular measurement.**—This is shown at  $S, S'$  . . . and may be a similar but large black photographic plate with two parallel lines 1 or 2 mm. apart ruled across it with a needle. The incandescent lamp  $L$  is immediately behind  $SS'$ , attached to the same standard and a screen of oiled paper (paraffine tissue) is placed between to equalize the illumination. If the distance  $R$  (1 or 2 meters) is as given in the diagram, the fringes from  $S$  are in step with the fringes from  $S'$  and reenforce each other. Hence

$$a = \lambda/c = y/R; \text{ or } y = R\lambda/c$$

and the value of  $y$  is thus given in centimeters. In the Michelson device, the adjustment is made by separating the slits  $ss'$  to the required amount. In the present experiment, however, it is more convenient to place the plate  $SS'$  on a slide  $R$ , so that the normal distance  $R = Ss$  may be changed at pleasure. Thus for  $SS'$  the fringes are again in step and reenforced relative to the angle  $2a$ , while for a position of  $SS_1$  at  $m$ , the fringes interfere. I have not, with white light, been able to make the fringes vanish; but the interference is marked. The distance  $R$  must be relatively very large. If  $R$  is too small, each of the slits  $S$  and  $S'$  produces its own group of interference fringes, more and more separated.

**92. Data.**—To give an example: The distance  $ss'$  being 0.06 cm.,  $a = \frac{\lambda}{c} = \frac{6 \times 10^{-5}}{6 \times 10^{-2}} = 10^{-3}$ . The slits  $SS'$  were 0.15 cm. apart and produced clear fringes at about  $R = 70$  cm. and  $R = 130$  cm. Hence,  $y = 10^{-3} \times 130 = 0.13$  cm. instead of 0.15 cm. The criterion of clear fringes, is, of course, very coarse for white light. It would be interesting to repeat the experiment with homogeneous light and finer slits and fringes, when more alternations would appear. Instead of the telescope the eye itself might be used, the plate  $ss'$  being placed immediately in front of it; but though the fringes are obtained clearly, I had no success with the necessary alternations.

**93. Diffraction substituted for interferences.**—If in figure 184 the double slit  $ss'$  in front of the objective of the telescope is replaced by a single

micrometer slit of variable width  $ss' = c$ , the two slits at  $S$  being fixed in place, an experiment similar to the preceding may be made by successively widening  $ss'$ . When the slit at  $ss'$  is gradually opened, the broad white central patch gradually opens into two distinct and narrower patches corresponding to  $S$  and  $S'$ . On further widening, a sharp diffraction line appears between them for a slit, width  $c$ . We may then write, if  $x$  is the fixed distance apart of the images of  $SS'$  in the ocular:

$$\frac{x/2}{r} = \frac{y/2}{R} = 3 \frac{\lambda/2}{c}, \quad \text{whence} \quad y = 3R\lambda/c$$

In the experiment made,  $R = 110$  cm.,  $c = 0.125$  cm.,  $\lambda = 6 \times 10^{-5}$  cm., whence  $y = 0.16$  cm., the value measured.

On further widening the slit  $ss'$ , two ( $x/3$ ) and three ( $x/4$ ) fringes appear between the images of  $SS'$ . But they are fainter and the adjustment much less sharp. The equation may now be put

$$x/2r : x/3r : x/4r : \dots = y/2R : y/3R : y/4R : \dots = \\ 3\lambda/2c : 3\lambda/2c' : 3\lambda/2c'' : \dots$$

whence  $c, c', c''$  are the successive slit-widths when one, two, three, etc., fringes lie within the  $S$  images. The trial showed  $c = 0.125$ ;  $c' = 0.175$ ;  $c'' = 0.225$  cm.;  $y = 0.16$ ;  $y = 0.17$ ;  $y = 0.176$  cm., the march of  $y$  being due in part to back-lash in the slit micrometer and in part to the lack of sharpness specified.

If the opaque strip between  $S$  and  $S'$  is removed, so that  $S$  is now a single broad slit, the light is too strong for the fringes to appear within the white image.

#### THE CAPILLARY ELECTROMETER.

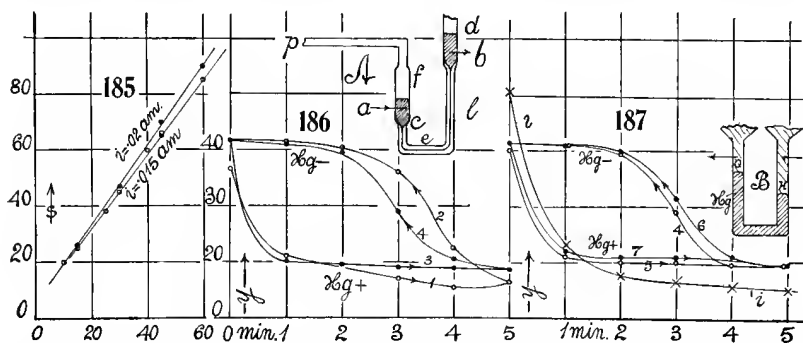
**94. Electrolysis.**—Experiments were made in the endeavor to register the excursions of the mercury meniscus of the capillary electrometer, by the aid of interference fringes. To do this, the capillary tube carrying the moving meniscus (fig. 186, inset *A*, at *l*) was directly coupled with a small end of pure-rubber tubing to one shank of the interferometer **U**-gage. It was not, at first, possible to detect any displacement of fringes in this way. Naturally the large volume of air above the mercury in the **U**-gage, compared with the small volume displacement in the capillary tube, militates against this plan. It would be necessary to reconstruct the **U**-gage for the elimination of as much of the former volume as possible.

Later, however, on devising an apparatus of the type of the diagram (fig. 187, inset *B*), in which both menisci (capillary bore less than 1 mm.) are utilized, the closed shanks suitably connecting with the corresponding shanks of the interferometer **U**-gage, 5 to 10 fringe displacements were regularly obtainable. This is too small a number to be of practical value.

With the former apparatus set up, however, it seemed interesting to test it in a different way by determining the electro-chemical equivalent of water ( $E = 0.174$  c. c. of gas under normal conditions per ampere per second). For this purpose it was only necessary to increase the potential difference (1 to 2 storage cells) at the wet meniscus (dilute  $H_2SO_4$ ) until evolution of gas



ensued, and to measure the current in the circuit with an ammeter. Naturally, the experiment, if so performed, is rough, both on account of the polarization incident to the use of filamentary non-blackened electrodes and to the heat produced during electric decomposition. The current, owing to the escape of bubbles of gas, was often fluctuating. The results, however, as seen in the examples (fig. 185; fringe displacement  $s$  in the lapse of seconds for currents 0.015 and 0.020 amperes, respectively), are better than was expected. The graphs are nearly linear, with a retardation at the beginning, owing to polariza-



tion. A curious feature of the results is the frequent increase of rates  $ds/dt$  with time, while the current  $i$  diminishes; for instance:

Time .....	0	15	30	45	60 seconds.
$s$ .....	0	26	45	66	85 scale-parts.
$i \times 10^8$ .....	19	17	16	16	15 amperes.

Between 15 seconds and 45 seconds  $ds/dt = 1.14$ ; between 30 seconds and 60 seconds,  $ds/dt = 1.33$ . This, however, is not always the case, as, for instance,

$t$ .....	0	15	30	45	60 seconds.
$s$ .....	0	25	47	70	90 scale-parts.
$i \times 10^8$ .....	21	..	21	19	.. amperes.

the corresponding rates being  $ds/dt = 1.5$  and  $1.43$ .

To compute the electrical equivalent,  $s$  must be reduced to heads of the mercury column, the equation of reduction being  $\Delta h = 10^{-8} \times 66 \Delta s$  in the first series and  $= 10^{-8} \times 69 \Delta s$  in the second. Hence we obtain the mean normal rates  $(dh/dt)/i = 10^{-8} \times 5.2$  and  $10^{-8} \times 5.1$  per second per ampere for the two series. Owing to the infinitesimal increments of pressure  $p$ , volume  $v$ , and mass of gas  $m$ , at the absolute temperature  $\tau$ , taken as constant, the intrinsic equation becomes

$$\frac{dp}{p} + \frac{dv}{v} = \frac{dm}{m} = \frac{dv'}{v}$$

where  $dv'$  is the fresh small increment of volume of electrolytic gas, practically at  $p$ ,  $v$ , and  $\tau$ . Thus, since  $v = Ah$ ,  $A$  being the area and  $h$  the mean depth of the relatively large volume of air in the U-tube,

$$Ah \frac{dh}{B} + \frac{1}{2} A dh = dv'$$

where  $B$  is the height of the barometer corresponding to  $p$ . Now,  $dv' = E$  per second per ampere, whence

$$E = A \frac{dh/dt}{2i} \left( 1 + \frac{zh}{B} \right)$$

For the diameter of **U**-tube, 9.4 cm.,  $A = 70 \text{ cm.}^2$ ;  $B = 77.5 \text{ cm.}$  at the temperature of  $dh$ ;  $h = 1 \text{ cm.}$  Thus  $A(1 + zh/B)/2 = 36.0$ . Hence, in case of the two series,

$$E = 36 \times 10^{-3} \times 5.2 = 0.187 \quad E = 36 \times 10^{-3} \times 5.1 = 0.184 \text{ cm.}^3/\text{sec.}$$

Reduced to  $0^\circ \text{ C.}$  and 76 cm., these become  $E = 0.178$  and  $0.175$ , data as near the normal equivalent ( $0.174 \text{ c. c./sec.}$ ) as the present form of method warrants. In a modification of the apparatus, larger platinized (non-filamentary) electrodes would be the chief desideration.

**95. Capillary electrometer.**—To return to the capillary electrometer: Since the direct coupling is of no marked interest, the question occurs whether on compensating the depression at the wet meniscus by a pressure applied at the dry meniscus and measuring the latter with the **U**-gage interferometer, any advantage can be secured. A variety of instruments were tested, including one given to me by Professor W. Nernst; but they did not suffice as well as the improvised form shown in the inset of figure 186. Here *dec* is the capillary tube, about 1.4 mm. in diameter. The end *cf* is wide and contains the charge of Hg, above which is *pf*, a quill tube for applying pressure. A screw plunger with stuffing-box (not shown) was used for the purpose, and the platinum terminal is seen at *a*. The end *d* is also widened and contained a charge of acidulated water, meeting the wet meniscus *l*, *b* being the terminal. Acid water insures more rapid action, but it is liable to clog the meniscus. The great difficulty of this otherwise very interesting apparatus for the present purposes is its indecision. For example, figures 186 and 187 give 7 consecutive series of readings of the head of the meniscus on the scale of an ocular plate micrometer ( $y = 24$  scale-parts per millimeter Hg in pressure) in the lapse of minutes. The first series are the more or less erratic; the last series are better, but one observes a wandering of the zero-point nevertheless. In view of the very weak electrolyte, it takes at least 2 minutes to obtain the full displacement  $y$  of the meniscus when it is positive, and at least 3 minutes when it is negative. One may therefore infer that the Hg meniscus itself contributes positive ions. The full displacement is here about  $y = 40$  scale-parts or about 1.7 mm. of mercury for the standard Daniell cell used. Initially, as shown by the curve *i*, the electrometer had been much more sensitive, suggesting an incidentally greater strength of electrolyte. Later, with a constant voltage of about 0.110 volt, I carried the measurements through and obtained  $y = 80$  scale-parts or 3.3 mm. of Hg depression, per Daniell. These microscope scale-parts were each found equivalent to  $s = 50$  scale-parts of the interferometer **U**-gage. Thus, the Daniell is equivalent to 4,000 *s*, or an *s* scale-part (**U**-gage) would be a little over 0.0002 volt. Theoretically, the

mercury head is  $\Delta h = 70 \times 10^{-6} \Delta s$  cm. and thus the Daniell at 3.3 mm. depression should be equivalent to  $0.33/70 \times 10^{-6} = 5,000$  s, or  $2 \times 10^{-4}$  volts to the scale-part, as nearly corroborative as measurements of this character may be. It is thus rather a pity that these results can not be realized, the failure being inherent in the usual behavior of capillary phenomena. The sensitiveness is of course ultimately dependent on the accuracy with which the capillary meniscus may be set. For these reasons I abandoned the interferometer designs which I had prepared.

In wider tubes (3 mm. diameter), in which the meniscus just moves per volt ( $y = 3$  scale-parts, about;  $h = 0.1$  mm.), it is interesting to note the annular horizontal vortices, turning in opposite directions as the mercury is charged positively or negatively. They are shown by small crystals, etc., on the surface and apparently attributable to the sudden advance or retreat of the axis of the Hg column. Such vortices, nevertheless, also occur when the meniscus is quite stationary.

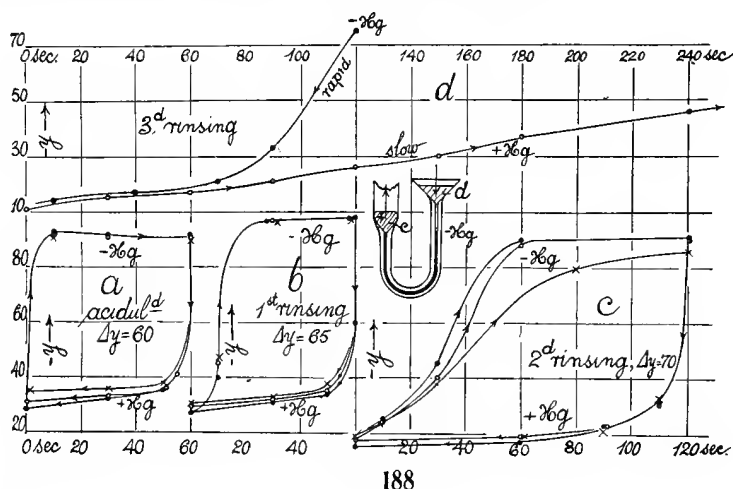
The addition of acid at the charged surface (always keeping the liquid very dilute, so that the meniscus remains clear) makes the displacements practically instantaneous, though there is residual adhesion and lag when the meniscus is positive. If the meniscus is previously raised and lowered by slight suction, the best results are obtained. I was unable, however, even after long trial, to render them sufficiently precise to be in keeping with the U-tube interferometer. As the phenomenon itself is of extreme interest, it has been discussed at great length, since the original discovery of Lippmann.\*

The occurrences are well exhibited in Professor Nernst's apparatus, if both ends of a capillary U-thread of mercury are used symmetrically, as in the diagrammatic inset *B*, figure 187. This design, in fact, behaves with greater precision than any of the others which I have tried. Helmholtz and Lippmann adduce a beautiful theory, based on the second law of thermo-dynamics, from which  $\partial T / \partial \phi = -\sigma$ ,  $T$  being the surface tension and  $\phi$  the potential difference in the double layer at the mercury meniscus and  $\sigma$  its electrical surface density. The mercury surface is thus naturally positive, and passes through zero at maximum  $T$  into negative charges under the influence of the cation layer. Other theories have been advanced. It occurred to me that if one postulates an ion evaporation or ionic vapor-pressure at the mercury surface, the phenomenon has a close analogy to Kelvin's theory of increased vapor-pressure at a convex surface. The lower or negative meniscus (fig. 187, inset *B*) is more convex than the upper or + meniscus, which may be coordinated with a more rapid evaporation, or a higher pressure of negative electrons from the negative mercury surface.

**96. Dilution of electrolyte.**—It may not be superfluous, therefore, to contribute the data which I obtained incidentally on the increasing slowness of

\* Cf. Chwolson, *Physik*, vol. iv, 1, p. 201 *et seq.* (Vierveg u. Sohn, 1908); Winkelmann, *Physik*, iv, 1, p. 850 *et seq.* (Barth, 1905.)

adjustment as the electrolyte approaches more nearly to the case of pure water. Necessarily using the one electrolyte apparatus (fig. 188, inset) a drop of very dilute acid was added to the pure water at  $d$  and the capillary column preliminarily agitated by suction at the other end. The results of displacement  $y$  ( $y=24$  scale-parts, equivalent to 1 mm. of mercury) produced by 1 Daniell are shown in the lapse of seconds by the graph  $a$ . Successive cycles are given by different kinds of points. The main displacements are reached within 10 seconds. They would have been more rapid with a stronger electrolyte. As above, the displacement of the negative surface (reversed by the microscope in the graphs) is more rapid than that of the positive surface; a meniscus rises more quickly than it falls, or the negative ions escape or evaporate more copiously than the positive ion, even at the beginning.



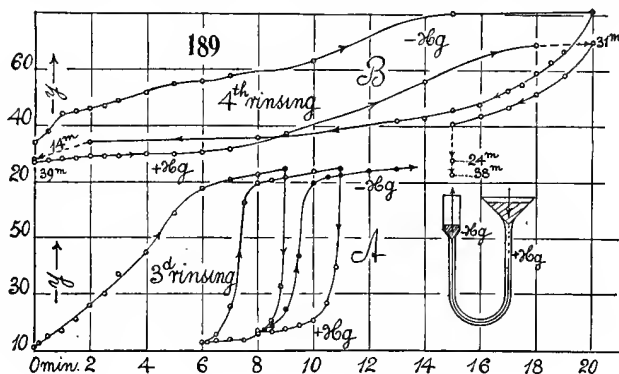
188

The liquid in the reservoir  $d$  (fig. 188, inset) was now removed by a capillary dropper and replaced by pure distilled water. After agitating by suction as usual, the graphs  $b$ , figure 188, were obtained. The response is, as a whole, slower than before, but not as much so as would be expected. Negative ions escape from the mercury meniscus much more rapidly than the positive ions, and the latter more slowly than before, in the first graph  $a$ . There is an enlargement of limits,  $\Delta y$ , of displacements, only partially reached, of course, in the single minute of observation.

The electrolyte was then cleansed in the same way with fresh distilled water at  $d$ , and the curves, figure 188,  $c$ , show that at least 2 minutes were needed to reach approximate constancy. The escape of positive ions is now relatively slow and not quite identical in the three cycles tested, as one would anticipate from the effect now producible by admixture of mere traces of impurity. The evaporation of negative ions, though still rapid by comparison, now shows a marked tendency to lag. The limits here are the largest obtained, being  $\Delta y = 70$  at least, as compared with 65 and 60 before.

The results of the fourth rinsing are given by the curves (fig. 188d) in the lapse of seconds. Only the beginning of each graph can be shown, as the time unit is too small. We now have an extremely slow dissipation of positive ions compared with the cases heretofore, and even the negative ions escape slowly from the mercury meniscus.

The results after the third and fourth cleansing are given by the graphs (fig. 189), in a scale of minutes. It is interesting to note that the initial slow discharge of positive ions (graph A) is not present in the same degree in the



second cycle of this graph, possibly because some solute has been accidentally picked up. In no case has the limiting asymptote been reached even in 10 minutes.

The graphs B in figure 189 are the results of the fourth rinsing. Both positive and negative ions are now dissipated from the mercury surface with extreme slowness, and there is not on the whole much to choose between them, except at the beginning of each graph, where the negative ions escape more rapidly; but they do not reach an asymptote in 24 or even 38 minutes of observation. In pure water, therefore, a mercury meniscus is as liable to be positive as negative, though favoring the former, so far as here observed. The merest trace of electrolyte in the water makes the mercury dominantly positive.

## CHAPTER VI.

### GRAVITATIONAL EXPERIMENTS.

#### THE CONSTANT OF GRAVITATION IN TERMS OF THE VISCOSITY OF AIR.

97. **Introductory.**—In the experiments heretofore, the occurrence of uniform motion in the case of a needle vibrating in air was not unusual, provided the quartz fiber used was not exceptionally thin, *i. e.*, provided the needle passed through the equilibrium position with sufficient velocity. Thus, in a preceding report (Carnegie Inst. Wash. No. 310, 1921, § 94, figs. 143, 150, and 151), the graphs of the excursions of the needle were often sharp zigzag lines. The straw shaft then used admitted of an estimate of the constant only. In the last report (Carnegie Inst. Wash. No. 310, Part II, 1923, § 62; also Proc. Nat. Ac. Sc. VIII, 1922, p. 66), the framework of the needle being filamentary, the equation for the motion of the balls at the end of the needle could be much more nearly given. In fact, when the needle passes through its equilibrium position, the torsion of the fiber is zero, and for a small angle, symmetrically on either side, the contribution of the fiber is respectively positive and negative. Hence the acceleration imparted is again removed. If, therefore, here the needle moves uniformly, the gravitational pull is exactly balanced by the frictional resistance, the latter rising asymptotically to a maximum, dependent on the speed imparted by the former. Only a very small excursion near the zero position is in question. In such a case Stokes' equation, as shown heretofore, leads to the value

$$\gamma = \frac{R^2}{Mm} \frac{3\pi\eta rl}{L} \frac{\Delta y}{\Delta t}$$

where  $M$  and  $m$  are the gravitating masses at a distance  $R$  apart,  $m$  of radius  $r$  being at the end of the needle of semilength  $l$ .  $L$  is the distance between the mirror on the needle and the scale along which, as seen telescopically, the small middle excursion  $\Delta y$ , is passed in  $\Delta t$  seconds. The viscosity of air is  $\eta$ , and is well known to be nearly independent of pressure, so that observation for the needle in moderate vacuo is permissible.

In this equation the resistance experienced by the filamentary design of the needle is neglected. It is supposed that the motion is slow enough that the viscosity of air (not any eddy resistance) is alone in question. This may be admitted in vacuo, I think.

To recognize the equilibrium position for the exhausted case of the needle, the attracting weights  $M$  are placed in the neutral position for a sufficient time. In work with a slow-moving needle, however, the observations are necessarily prolonged and the zero position of the needle changes in the lapse of time. Accordingly, different values of  $\Delta y$  will be found, according as the

needle moves toward or falls from the high numbers on the scale. If the difference is not large, the mean may be taken. Otherwise, if the swing of the needle has become steady in its repetitions, the mean of the extreme elongations of the swinging needle is probably a preferable value.

**98. Apparatus and method.**—As heretofore described, this consisted of a flat case (*cf.* fig. 191) capable of exhaustion. Each attracting weight  $M$ , near the corresponding end of the needle, could be moved expeditiously from one side to the other of the case, the reversible forces thus admitting of methods of multiplication. The quartz fiber was exceptionally delicate and the apparent period of the needle about 750 seconds, almost the whole of the effective weight being in the masses  $m$  at either end. The air-pump attached to the case was capable of exhaustion of about  $10^{-4}$  mm. of mercury and a McLeod gage was continually in connection with the case, even after the air-pump attachment had been shut off. The vacuum in the case was thus determinable at any time. All observations were here made at night.

The values of the constants in equation (1) were as follows:  $M=3,368$  g.,  $m=0.6295$  g.,  $R=5.67$  cm.,  $L=447.5$  cm.,  $l=11.0$  cm.,  $M'=2,947$  g.,  $m'=0.6295$  g.,  $R'=5.43$  cm.,  $r=0.23$  cm.,  $\eta=0.00019$ . This makes  $10^7\gamma=1.536\Delta y/\Delta t$  and  $1.609\Delta y/\Delta t$ , respectively, or conjointly  $^*\gamma=10^{-7}\times 1.572\Delta y/\Delta t$ .

To bring the needle into a steady state of vibration, the attracting weights are put on one side of it, and thereafter, when the needle has reached its maximum elongation, the weights  $M$  are quickly swung to the other side. The needle soon becomes steady. Two or three reversals usually suffice. When this is the case, observations are made for the time ( $\Delta t$ ) consumed in passing between points 1 cm. on each side of the equilibrium position ( $\Delta y=2$  cm.), a stop-watch or a chronometer being available for the time measurement.

In table 19, I have collected values of this kind. The question at issue is whether in case of a very delicate quartz fiber (the one in question gave a static double displacement of over  $\Delta y=13.4$  cm.), the needle will acquire sufficient velocity from the swinging of the weights  $M$ , to meet the conditions of the equation. In the first series the telescopic arc of vibration was but  $y-y'=20$  cm., the excursions being alternately positive and negative. The mean time taken was 20.5 seconds and 23 seconds, respectively, showing that the zero-point had wandered. The mean value of  $\gamma$  thus obtained is but  $1.5\times 10^{-8}$ , with the implication of a gravitating force considerably in excess of the frictional resistances. Consequently, in series 2 of table 19, the excursions were gradually pushed to the limit ( $y-y'=35$  cm.) by alternating the gravitational pull (reversal of  $M$ ) in step with the swing of the needle. Here again the original position of equilibrium changed in the lapse of time, so that the values of  $\Delta t$  for positive and negative arcs are not the same.  $\Delta y/\Delta t$  increases, though not quite regularly, with the size of the arc of vibration. Taking the last three data of the series, the value of  $\Delta y/\Delta t=0.157$  cm./sec.

\* In the original paper (*l. c.*), the sum instead of the mean constant was erroneously taken; *i. e.*,  $10^{-7}\times 3.145$  should be  $10^{-7}\times 1.572$ .

on the scale, from which  $\gamma = 10^{-8} \times 2.48$ . This is but 37 per cent of the standard value of  $\gamma$ . In figure 190 I have given the mean observed values of  $2\gamma$ , as depending on the arcs of vibration  $y - y'$ . If the curve is prolonged, an arc of  $y - y' = 2 \times 49$  cm. would be needed to bring out the full value of  $\gamma$ , whereas 35 cm. could not be exceeded.

The third series, made after an unsatisfactory day of variable temperature, was inferior to the preceding. Although the exhaustion was higher (mean 0.015 mm.), the maximum arcs were not so large as before.

The behavior of the needle at its reversals, sometimes rapid, at other times deliberate, has a bearing on its period and logarithmic decrement. For if the radiant forces are repulsive on both sides of  $m$ , the period will be shortened to a minimum; if they are attractive on both sides the period will be long for an equivalent of these forces added to or subtracted from the modulus

TABLE 19.—*Values of  $\Delta t$  for  $\Delta y = 2$  cm.  $10^8 \gamma = .314 \Delta y / \Delta t$ .*

Vacuum.	Arc.	$\Delta t$	$10^8 \times \Delta y / \Delta t$	$10^8 2\gamma$ (observed)	$T/2$	Vacuum.	Arc.	$\Delta t$	$10^8 \times \Delta y / \Delta t$	$10^8 2\gamma$ (observed)	$T/2$
<i>mm.</i>	<i>cm.</i>	<i>sec.</i>		<i>sec.</i>		<i>mm.</i>	<i>cm.</i>	<i>sec.</i>		<i>sec.</i>	
About 0.1	—20	24	83	2.61	...	Plenum.	—23.2	25	80	2.5	489
	+20	20	100	3.14	...		23.1	22	91	2.9	...
	—20	23	87	2.74	...		—23.4	26	77	2.4	449
	+20	21	95	2.99	...		22.8	23	87	2.7	...
	—20	23	87	2.74	...		—23.0	26	77	2.4	426
	+20	20	100	3.14	...	Mean ..	.....	.....	.....	2.6	...
	—20	23	87	2.74	...						
	+20	20.5	98	3.08	...	0.03 ...	>60	10	20	6.3	365
Mean ...	.....	.....	.....	2.92	...	.17 ...	>60	12	17	5.3	...
							>60	10	20	6.3	365
0.046 ...	—35	12.2	164	5.17	...		>60	10	20	6.3	...
	+35	13.3	150	4.73	...						
	—35	12.2	164	5.17	...						
Mean ...	.....	.....	.....	4.95	...						

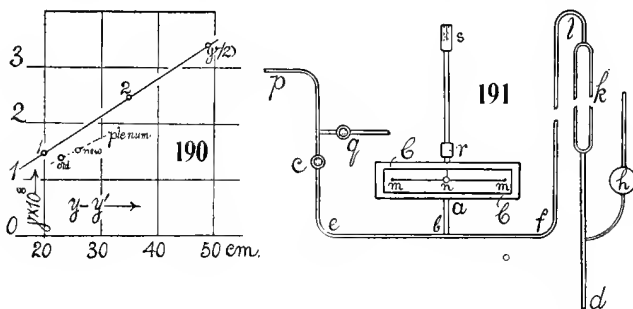
of the fiber. The periods will be intermediate if one side attracts and the other repels.

The data obtained in the third and subsequent series lay between 1 and 2 in figure 190 and were all in conformity, more or less closely, with the curve. They need not, therefore, be given. It is desirable, however, to determine the corresponding values for the case of the needle vibrating in a plenum of air. Data of this kind are also given in table 19; but they are far less trustworthy, chiefly, because the needle drifted at its high elongations gradually, from  $y = 32$  to  $y = 39$  cm., with a somewhat smaller drift, also towards high numbers, at the low elongations. The values of  $\Delta t$  for positive and for negative arcs of swing are thus unequal, though the mean position was aimed at in rating  $\Delta t$ . Although the needle moves very slowly, with an excessive period, it is questionable whether the frictional resistance is here purely viscous. The ("old") value of  $\gamma$  so found (necessarily small of course) even falls below the graph (fig. 190).



As a whole, the experiments show that the necessary arc of vibration under which the given equation would apply and for which there would be an equivalence of the gravitational and frictional forces, is not attainable with so fine a fiber by the mere passing of the weights  $M$  from one side of the needle to the other. As there was no other method for a safe use of the method of multiplication, the experiments were not carried further with this apparatus.

**99. Excessive arcs.**—During the course of the work in the succeeding paragraphs and in the presence of large radiant forces (July 30, 31), the needle fell through relatively very large arcs, probably exceeding 60 cm. A few measurements of the speed of the needle in passing through its equilibrium position (so far as determinable) were therefore also made. These are given at the end of table 19 and contain the closest approach ( $3.1 \times 10^{-8}$ )



to the standard value of  $\gamma$  which could be obtained. They do not fit into the locus of figure 190, because the arcs have not the same meaning. Other measurements made at this time were similar to the first and second series of the table.

**100. Recent summer tests.**—About a year later, in the ensuing summer, I took the work up again, the conditions being favorable for vibrations in a plenum. A brief example of the results ( $y_1 y_2$  telescopic elongations,  $\Delta t$  time of passing the middle collimeter) :

$y_1 = 7.9$			8.4		8.5	cm.
$\Delta t =$	10.4	10.4	10.2	10.4		seconds.
$y_2 =$		34.3		34.6		cm.
$\Delta y / \Delta t =$	0.0961	0.0961	0.0980	0.0961		cm./sec.
$\gamma \times 10^8 =$	1.51	1.51	1.54	1.51		

The apparatus remaining the same, the above constants may be considered as nearly enough applicable, so that  $10^7 \gamma = 1.573 \Delta y / \Delta t$ . So computed, the values of  $\gamma$  in table 19 adhere to the excessively low orders heretofore obtained. The normal speed  $\Delta y / \Delta t = 0.425$  second should have been found, equivalent to the time  $\Delta t = 2.35$  seconds in passing the middle centimeter. In fact, the observed data for  $\gamma$ , etc., are only about 23 per cent of the normal data. The

remainder of the gravitational attraction must therefore have been exerted in changing the momentum of the needle and in overcoming such additional friction as the framework of the needle may have introduced. So large a discrepancy was not expected, seeing that the difference of elongations,  $y_2 - y_1 = 26$  cm., is fairly constant; but the lower locus in figure 190 shows that it fits last year's datum for the plenum.

#### PERIODS, LOGARITHMIC DECUREMENT, AND STATIC DISPLACEMENTS.

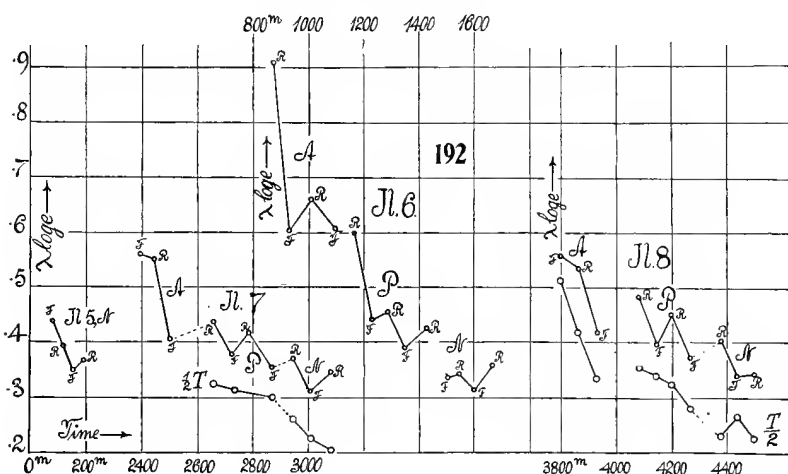
101. **Apparatus newly installed.**—The object of the present experiments is a completion of the work of the last report, by carrying the exhaustion of the case as far as practicable. Figure 191 is a sketch of the disposition of apparatus, where *mm* is the gravitation needle in its narrow case with plate-glass walls *CC*, *n* being the mirror. The attracting weights *M* are removed. The sides of the case are reëntrant, to receive the glass plates, and they and the quartz-fiber tube are sealed with resinous cement, poured into the crevices and the cups *rs* in the molten state. The exhaustion takes place through the pipe *ab*, communicating by a T-joint with the train of  $\frac{1}{8}$ -inch gas pipe *pefl*. All joints are sealed with cement. The pipe *p* comes from a large oil air-pump, with fore pump, capable of exhausting to about  $10^{-4}$  mm. of mercury. The MacLeod gage of the usual pattern is shown at *khd*. To shut off the case and gage there is a glass oil-sealed stop-cock at *c*, and a similar cock *q* allows of the admission of air. The pump is kept exhausted, no matter whether *c* is shut off or not. After the initial experiments, all parts of the apparatus worked very smoothly.

In spite of the care taken to seal all parts of the extended apparatus, it was not in the earlier work possible to hold the vacuum indefinitely. There remained a constant leak of 0.0038 mm. of mercury per hour, the seat of which I was unable to detect; but as experiments with gradually decreasing vacua were primarily contemplated, this leak was here no serious disadvantage, except that the highest exhaustions were not available. It is of course quite possible to keep the pump running and the stop-cock *c* open. When this is done, however, the needle (quite apart from tremor) is always in motion, so that gravitation measurements are out of the question. It is necessary to close the cock *c* and wait several hours until the case *CC* is in adequate thermal equilibrium. Thus the vacua below  $5 \times 10^{-3}$  mm. are lost.

102 **Data. Logarithmic decrement,  $\lambda$ .**—In the work of last year the logarithmic decrement, as obtained from observations largely made at night, seemed to remain fairly constant until the highest exhaustions were approached. This result needed the further qualification undertaken in the present paper. To compute  $\lambda \log e$ , the two arcs obtained from the first three elongations of the needle  $y - y'$ ,  $y' - y''$  were used. As there was a small leak in the apparatus of about 0.0038 mm./hour, the data for  $\lambda$  could be found with great accuracy in this way in the course of time, while the vacuum slowly

degenerated from about 0.0002 to 0.271. It was hoped that the viscosity of air in its relation to pressure could then be found; but this expectation was not realized, for reasons which will presently appear.

The data for  $\lambda$ , the time and the vacua to which they belong are given in table 20, observations being made in the morning (A), afternoon (P), and night (N). They are constructed relative to the lapse of time (minutes since exhaustion) in figure 192; and in relation to the vacua (mm. of mercury) in figure 193.  $F$  denotes that the attracting weight  $M$ , on the right, is in front, and  $R$  to the rear of the case and needle, the opposite conditions holding for the  $M$  near the left end of the needle. The first arc of swing was usually between  $y=20$  and  $y=30$  cm., depending on the time of day and the slow drift at either elongation, heretofore discussed.

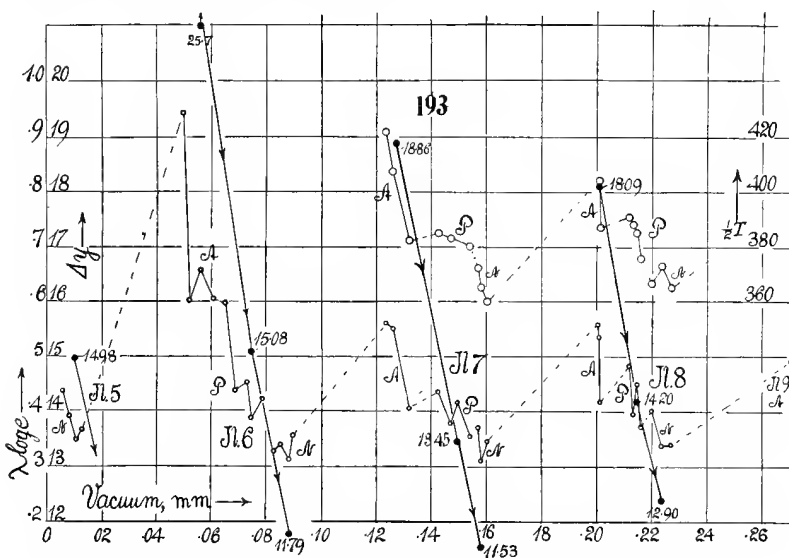


Inspection of figures 192 and 193 shows that changes of viscosity, due to changes of pressure, are not discernible in results of the present kind. In fact, the logarithmic decrement at the highest exhaustions (July 5) happens to be larger than at the lowest exhaustions (July 8, N). The logarithmic decrement is therefore also primarily and enormously under the influence of the radiant forces. It is largest in the morning and least at night. It therefore obviously oscillates once per day, though I did not make observations after 11 p. m. If  $d\theta/dt$  be the change of atmospheric temperature per second in the environment of the apparatus, then this coefficient is the controlling factor in the marked variations of  $\lambda \log e$ .

Moreover, the values of  $\lambda \log e$  are always larger for the rear positions  $R$  of  $M$  than for the front positions  $F$ , under otherwise like conditions. One or the other, or their mean, must therefore be taken in association with  $d\theta/dt$ . This may be due to a lack of symmetry of the position of the needle to the case; but it is more probably due to a lack of symmetry in the environment, as there is a wall immediately behind the case. The radiant forces from the

rear act as an attraction relatively to the radiant forces from the front, so that the first swing of the right end of the needle to the rear is excessive as compared with the swing from the rear. The conditions are reversed in the first swing toward the front.

**103. Periods.  $T$ .**—The accurate method of finding  $T/2$  from two successive passages of the needle through the position of equilibrium is very troublesome here; for  $T$  is long (over 12 minutes) and the position of equilibrium varies. Moreover, as the variations of  $T$  are large, precise values of it are here apparently of little use. Hence the measurement of  $T/2$ , from the first to the second elongation, was accepted as adequate for the purpose. These



values of the first semiperiod, so far as taken, are also given in table 20 and constructed in figure 193 (upper graph), in seconds. The variations may run from 6 to 7 minutes, and the  $T$  values are largest in the morning and least at night. They run about in parallel to the  $\lambda$  values, if either the  $R$  or the  $F$  position alone is taken.  $T$  thus also varies harmonically in the lapse of time with a period of 24 hours referable to  $d\theta/dt$ .

From these results it might be surmised that the true semiperiod  $T/2$  can be computed from the logarithm decrement observed at the same time, since, ordinarily,  $T = T_0 \sqrt{1 + \lambda^2/4\pi^2}$ ; but it is easily seen that the correction so obtained is of an order entirely too small to account for the existing divergencies. In fact, we are not at liberty to use the common theory of the damped pendulum at all, and the expression  $\lambda \log e$  is used merely as an analogy, for convenience. It must also be observed that the first semiperiod of the highly damped needle is alone in question.

104. Static displacements,  $\Delta y$ .—A continuous series of these data were given in the earlier report and obtained from night observations (7 to 11 p. m.), when they are liable to be most constant. Table 20 and figure 193 contrast these values for different parts of the same day.  $\Delta y$  is the static

TABLE 20.—*Logarithmic decrements ( $\lambda$ ), vacua, first semiperiods  $T/2$ , and static deflections  $\Delta y$ .*

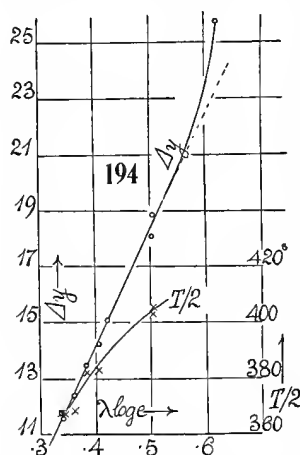
Date.	Time.	$10^4 \times$ vacuum.	$10^3 \times \lambda \log e$	$T/2$	$\Delta y$	Mean $10^3 \times \lambda \log e$	Mean $T/2$
	<i>min.</i>	<i>mm.</i>		<i>sec.</i>	<i>cm.</i>		
July 5, N.	0	2	...	...	...	...	...
	81	55	R438	...	...	...	...
	120	80	F393	...	...	...	...
	155	102	R350	...	14.98	370	...
	193	125	F367	...			
July 6, A. M.	876	490	R942	...	...	...	...
	930	518	F602	...			
	1010	560	R658	...			
	1098	606	F605	...	25.73	622	...
	P. M.	1169	R597	...			
	1229	685	F438	...			
	1290	730	R453	...	15.08	422	...
	1350	745	F388	...			
	1430	785	R424	...			
	N.	1505	F334	365	...	...	...
	1549	850	R341	...			
	1600	880	F313	...			
	1665	915	R357	369	11.79	337	367
July 7, A. M.	2392	1234	F560	421			
	2447	1260	R550	407	18.86	505	403
	2503	1320	F405	382			
	P. M.	2658	R435	385			
	2723	1470	F378	383	(13.74)	...	...
	2785	1495	R416	...			
	2869	1540	F354	380			
	N.	2945	R370	372	11.53	342	366
	3009	1580	F310	365			
	3082	1600	R345	360			
July 8, A. M.	3795	2006	F559	423	18.09	504	405
	3861	2010	R536	404			
	3930	2014	F418	387			
	P. M.	4080	R484	391	...	...	...
	4142	2133	F397	388			
	4197	2146	R451	385	14.20	407	383
	4265	2160	F373	376			
	N.	4375	R403	366			
	4435	2235	F340	373	12.40	362	368
	4499	2270	R342	365			
	5265	2710	F494	412			
July 9, A. M.					...	...	...

displacement finally obtained, when the attracting weights  $M$  are swung from one side of the needle to the other. As figure 193 shows,  $\Delta y$  is also markedly harmonic in the lapse of time or of the reduced exhaustion proportional to time, with a period of one day.

We thus come to the result that  $\lambda$ ,  $T$ , and  $\Delta y$  are similar time functions; that as a first approximation they are independent of the change of viscosity of rarefied air, and that their relative variation is such as to admit of their expression in terms of each other. It does not necessarily follow that a correct

value computed for one (for instance for  $\lambda$ ) would lead to correct values for  $T$  and  $\Delta y$ ; but it is a project well worth testing and will presently be considered.

**105. Comparison of  $\lambda$ ,  $T$ ,  $\Delta y$ .**—It is next necessary, therefore, to more specifically compare all the quantities obtained in the present investigation. This has been done in figure 194, where the abscissas are  $\lambda \log e$  and the ordinates  $T/2$  and  $\Delta y$  respectively.



Turning to the latter, it is at first astonishing to find that  $\lambda$  and  $\Delta y$ , in spite of the marked amplitude of radiant forces, make up a rather definite graph. In fact, if we omit the exception  $\Delta y=25.7$  (inadmissibly large radiant forces),  $\Delta y$  and  $\lambda$  are nearly proportional. The values of  $\lambda$  in hand lie on both sides of  $\lambda=1$  to the extent of about 15 to 19 per cent. If this curve were known,  $\Delta y$  could be computed from  $\lambda$ ; and vice versa.

The values of the first semiperiod of  $T/2$ , as already intimated, were not accurately taken, as I did not anticipate relations like the present. Nevertheless, figure 194 adequately shows that these also make out a definite graph, in which  $T/2$  increases more slowly than the logarithmic decrement; in other words, so far as the observations go,  $\lambda$  and  $T/2$  are not proportional.  $T/2$  also increases more slowly than  $\Delta y$ . If, for instance,  $\Delta y=13.4$  cm., about the mean value in the preceding report,  $T_1=758$  seconds should be its equivalent and  $\lambda \log e=0.385$  at the same time. If we take the vacuum period as  $T=T_1/\sqrt{1+\lambda^2/4\pi^2}$ , it would be  $T=750$  seconds.

**106. Observations in plenum.**—In contrast with the preceding oscillations under conditions of high exhaustion, the results of table 21, for the case of the needle vibrating in air under atmospheric pressure, are nearly aperiodic. The data for  $T/2$ ,  $\lambda$ ,  $\Delta y$ , are all enormously larger, and sometimes excessively so, as on July 10, 10<sup>h</sup>27<sup>m</sup> a. m., when the drift was correspondingly large. These values of  $\lambda$  are not analogous to logarithmic decrements, but result from the continued drift of the position of equilibrium of the needle toward the direction in which it is deflected by the attracting weights  $M$ . In this respect the present results are quite different from the preceding under exhaustion; for the latter are like real vibrations under the conditions imposed and  $\lambda$  has a definite meaning. One may ask, moreover, whether in a plenum, in spite of the slowness of motion, the resistance encountered by the needle is purely viscous, *i. e.*, whether a part of the resistance is not of the nature of dynamic pressure.

The motion of the needle in case of table 21 is peculiar. When the weights are exchanged, the needle falls from its high elongation to its low elongation

in the time given under  $T/2$ . It then turns toward a new high elongation for a time (usually about  $T/4$  seconds in length), after which it again moves toward low numbers by slow, indefinite creeping, without again turning. Exactly the same phenomenon occurs when the needle rises from a low elongation toward a higher. In other words, the needle, which is practically dead beat, may be said to oscillate about a position of equilibrium continually advancing in the direction of the deflection; or the radiant attractions in either direction continually increase. The following is an example:

Plenum: 7 <sup>h</sup> 35 <sup>m</sup> p. m.	$y = 15.90$	Exhaustion: 7 <sup>h</sup> 20 <sup>m</sup> p. m.	$y = 19.65$
	37.35		1.07
	36.90		9.00
8 <sup>h</sup> 36 <sup>m</sup>	40.15	8 <sup>h</sup> 24 <sup>m</sup>	7.87
	17.05		26.55
	17.40		17.40
9 <sup>h</sup> 34 <sup>m</sup>	16.62	9 <sup>h</sup> 37 <sup>m</sup>	19.15
	39.17		1.08
	38.95		9.25
10 <sup>h</sup> 10 <sup>m</sup>	41.40		....

In the exhausted case the next position of equilibrium lies between the preceding second and third elongations; in the presence of a plenum, it lies beyond the third of the preceding elongations.

Between these values of  $T/2$ ,  $\lambda$ , and  $\Delta y$  (unlike the above data for the exhausted chamber), no relation can be detected. Nevertheless, if mean values are taken, they conform with the theoretical viscous resistance much better than the vacuum values, as will presently be shown.

TABLE 21.—*Plenum values of  $\lambda$ ,  $T/2$ ,  $\Delta y$ .*

Date.	Time.	$T/2$	$\Delta y$	$\lambda \log e$	Mean $\Delta y$	Mean $\lambda \log e$	Mean $T/2$
July 9, P. M.	2 <sup>h</sup> 36 <sup>m</sup>	...	21.1	2.03	....	....	...
	3 00	520	20.7	1.54	....	....	...
	4 03	504	22.1	2.05	....	....	...
	5 00	543	21.5	1.53	....	....	...
	6 05	530	22.5	2.05	21.6	1.84	524
	N. 7 35	533	21.2	1.67	....	....	...
	8 36	520	22.9	1.82	....	....	...
	9 34	561	22.4	2.01	22.2	1.83	505
	July 10, A. M. 10 27	570	25.	(*)	....	....	...
	P. M. 1 30	585	23.	2.02	....	....	...
July 10, A. M.	6 03	533	18.10	1.49	....	....	...
	7 17	516	19.50	1.52	20.2	1.68	545
	N. 8 03	570	22.02	2.04	....	....	...
	9 05	585	23.43	1.45	....	....	...
	10 00	572	26.64	1.75	24.0	1.75	576

\* Creeping.

107. Comparison with computed values of frictional resistance.—It is now desirable to endeavor to construe the values obtained for  $\lambda$  and  $T$  by the aid of the familiar theory of the damped pendulum. If the needle be regarded

as consisting of the two balls at its end, the frictional forces should be  $6\pi\eta rv$ , and therefore the frictional coefficient  $b$  is

$$b = 6\pi\eta r$$

If  $T_1$  is the period of the damped needle and  $\lambda$  its logarithmic decrement

$$T_1 b = 2\lambda$$

and therefore

$$\lambda = 3\pi\eta r T_1$$

Hence  $\lambda$  should be proportional to  $T_1$  and if  $r = 0.23$  cm.,  $\eta = 0.00019$ , the datum in the tables becomes

$$\lambda \log e = 0.00112 T_1$$

or  $T_1 = 892\lambda \log e$  seconds. In figure 194, however, not only is proportionality of  $T$  and  $\lambda$  at long range excluded, but the factor would be for

$\lambda \log e = 0.35$	$T_1/\lambda \log e = 2,103$
.40	1,920
.50	1,720

i. e., about twice as large on the average. It would be necessary to suppose, therefore, that the viscosity  $\eta$  drops off in high vacua, which is untenable while in consequence of the resistance of the filamentary hanger of the needle  $\eta$  is effectively larger. The theoretical conditions of the equation do not, therefore, hold for the vibrations in vacua.

Curiously enough, however, if the mean be taken of the promiscuous experiments in a plenum (table 21), the results for two days are:

P. M.	$\lambda \log e = 1.84$	$T_1 = 1,048$	$T_1/\lambda \log e = 570$
	1.68	1,090	649
Night	1.83	1,010	553
	1.75	1,152	658

In consequence of the peculiar motion of the needle, these values are necessarily crude; nevertheless, they come much closer to the theoretical result (coeff. 892) than the vacuum values.

#### FURTHER INVESTIGATIONS.

**108. Change of apparatus.**—After concluding the experiments of the preceding section, the apparatus was taken apart for more rigorous sealing. Moreover, the pipe  $p$  (fig. 191) was bent down and the cocks  $c$ ,  $q$  placed in the down-going branch, so that all infiltrations from the oil-cups of the cock would pass into the pump. After putting the parts together again I found, to my astonishment, that the leak had increased to 0.042 mm./hour on the first day, which, however, on successive exhaustions fell off to 0.008 mm./hour at the end of the second. It was obvious, therefore, that the greater part of the leak was within the apparatus, and probably due to evaporation or sublimation from the resinous cements. The apparatus was then taken down again and put together with picein (rubber) cement, but with no great improvement.



Finally, I made use of tinned screws at the joints, so far as possible, and resolved to trust to continued exhaustion. The work began with a leak of 0.012 mm./hour on July 19, which had gradually decreased to 0.006 mm./hour on July 25, and fell continually thereafter. As a result of this labor (oil-cups and the connections separately were also tested), the apparatus showed a leak nearly twice as large as the original apparatus, in which the sealing happened to be nearly a year old. These annoyances seem to be inevitable in an apparatus necessarily to be sealed, and which can not be made wholly of glass.

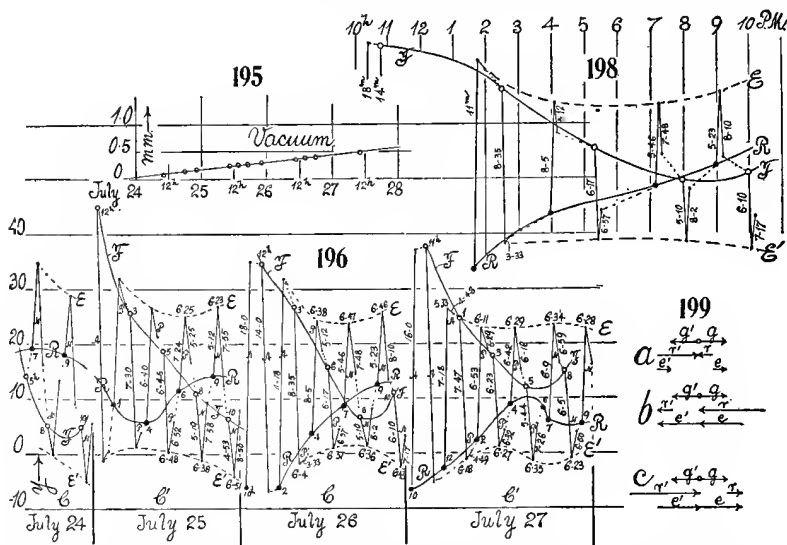
Fortunately, as shown in the preceding paragraph, the amount of high exhaustion is of little consequence in its bearing on the present experiments, for about half a day must elapse after exhaustion before the needle is in a sufficiently steady state for observation. In the present case, where the apparatus had been frequently slightly warmed to facilitate the preliminary exhaustions, the needle persisted in sticking to the glass plates, before or behind, for over 3 days before it was released by the radiant forces and available for excursions. The result is that the vacua in the following series, figure 195, are moderate, beginning with 0.0633 mm. on July 24 and ending with 0.466 mm. on July 27, indicating a mean leak of  $10^{-4}$  mm./minute.

Moreover, after the needle had swung free, a season of variable weather was at hand, with excessive and cold rains, etc., which seemed to make all normal observations useless. Nevertheless, as it proved, these very unsettled conditions afforded a means of exhibiting the interplay of gravitational and radiant forces more easily interpretable than any heretofore met with. The observations July 24 to 27 have therefore been very fully recorded in figure 196, where the ordinates denote the scale-reading  $y$  of the needle. The successive observations are inscribed at equal horizontal distances apart, with the nearest hour recorded, and not strictly chronologically, in which case the diagrams would be too diffuse. Little circles indicate the first of a set of three successive elongations (immediately after the reversal of the attracting weights,  $M$ ), from which two arcs are obtained. By the aid of two stop-watches, the semiperiods of these arcs were also measured and are recorded (by numerals in minutes and seconds) in place in the diagram. The mean semiperiod (in minutes and seconds) is given at the peaks. A, P, N refer to morning, afternoon, and night (after 6 p. m.) observations. Front and rear positions of the weight  $M$  near the right end of the needle are indicated by  $F$  (open circles) and  $R$  (black circles).

If we connect the little circles of the same kind by a curve, we get the successive positions of the needle in equilibrium, remembering that though the abscissas are not quite chronological, about an hour elapses on a given day between successive circles, as a rule, and about 6 or 7 ( $T/2$ ) minutes between the points of each triad. These equilibrium curves  $F$  and  $R$ , on July 24, 25, and 26, intersect at a time between 5 and 8 p. m., and they must intersect again late at night. When they do intersect, the equilibrium position

of the needle is the same, no matter whether the attracting weights  $M$  are on one side or the other of the needle. On July 27, the tendency of the  $F$ ,  $R$  graphs to intersect (which has been gradually decreasing) is just missed. Similarly interesting graphs  $E$ ,  $E'$  are obtained by drawing a line through the elongation of the first throw, after exchange of the weights  $M$ . These are, as a rule, convex towards each other, but they do not intersect. Their minimum distance apart in  $y$  is near the time of intersection of the equilibrium curves.

With regard to the successive semiperiods  $T_1/2$  and  $T_2/2$  obtained between elongations for the first two arcs of vibration, one may note that  $T_1 > T_2$ , as a rule, before the time of occurrence of the intersection of the equilibrium curves, and that  $T_2 > T_1$  after passing this intersection. Moreover, the total



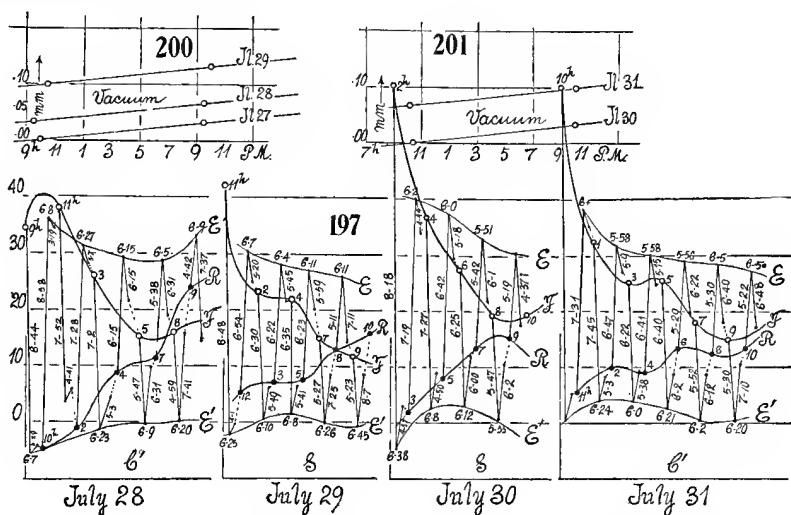
period  $T_1/2 + T_2/2$ , in spite of very large differences in the components, has more nearly the same value throughout. There is a determined attempt at compensation.

**109. Remarks on the graphs.**—What is extremely puzzling about these observations is the fact that the equilibrium curves  $F$  and  $R$  should intersect (*i. e.*, the needle occupy the same position of rest for either the front or rear positions of the attracting weights  $M$ ), and that nevertheless marked throws of the needle should occur immediately after the weights  $M$  are exchanged in position. I have therefore, in figure 198, constructed the results of July 26 on a time scale, instead of by observations (incidentally correcting a wrong entry at 8 p. m. in fig. 196). The curves  $F$ ,  $R$  and  $E$ ,  $E'$  now appear in less abrupt outline and remain close together after intersection. One may notice the  $T_1$  of the first arc becomes less than  $T_2$  of the second some hours before the intersection of  $F$  and  $R$ ; but the tendency remains. In figure 199 I have

represented the three force vectors,  $g$  for gravitation,  $r$  and  $r'$  for the radiant forces on the two sides and at one end of the needle (at  $m$  for instance), and  $e$  for the elastic force of the fiber. At the point of intersection we shall have ( $g$  taken positive) :

$$-g + r' = g + r = e \quad \text{or} \quad 2g = r' - r$$

In figure 199, case  $a$ , the  $r$  is negative and the sum  $r' + r$  is twice  $g$ , both radiant forces being repulsive. In cases  $b$  and  $c$ , both radiant vectors have the same sign and  $g$  is half their difference, taken positively. At the point of intersection of  $F$  and  $R$ ,  $r$  and  $r'$  may therefore, nevertheless, have any value, provided their difference is constant, i. e., the radiant forces on the two sides of the needle need not be equal.



Moreover, in case  $b$  we should expect  $T_2 > T_1$ , since in the latter case the needle moves against a repulsion. In case  $c$ ,  $T_1 < T_2$ , since the needle, in going toward the right in the diagram, moves away from an attraction. Thus  $T_1$  and  $T_2$  need not be equal at the intersection of  $F$  and  $R$ .

All this, however, affords no clue as to why there should be marked deflection in case of an exchange of weights  $M$ , when the positions of equilibrium  $F$  and  $R$  are the same. One possible suggestion is at hand. Whenever  $g'$  is changed to  $g$  there is a momentary removal of the gravitational force and hence a radiant impulse occurs. In case  $c$  this would act in the proper direction, but in case  $b$  it would act in the wrong direction; and since the deflection which follows an exchange of weights is, without exception, in the direction of gravitational attraction, the suggestion must be dismissed. Moreover, the impulse, lasting at best but a few seconds, would be altogether too small to account for the large throw of the needle observed. Again, the whole phenomenon is practically symmetrical; there is as marked a throw from curve  $R$

to curve  $E$ , as occurs from curve  $F$  to curve  $E'$ , on the average. The throw must therefore be essentially a gravitational phenomenon.

The next question is thus an inquiry into the seat of the radiant forces  $r$  and  $r'$ . If they arise in the glass-metal case they would be fixed; if in the weight  $M$  and fixed they would be indistinguishable from  $g$ . Hence the inference is suggested that the radiant forces are a relatively slow growth in the lapse of time and that their seat is effectively in the weights  $M$ . Immediately after the weights are exchanged, one may therefore assume that radiant forces are virtually absent. After the lapse of a fraction of an hour, however, they are again established in full equilibrium. The same mechanism acts in the next exchange. Hence, the view heretofore taken may be considered as corroborated, viz, that the weights  $M$  screen the case and needle from the radiation coming from without. The radiant forces grow in proportion as this radiation is absorbed by  $M$  and withheld from the case and needle. It may be conceded that the front and rear of the case make no difference here, since one of the two masses  $M$  is always in front and the other in the rear. The subject will be resumed in § III.

**110. New observations.**—Owing to the enormous difference between these fluctuating results and the exceptionally constant data obtained last summer, it seemed desirable to study the present conditions somewhat more at length. One may notice, for instance, that on July 24 (fig. 196), the  $F, R$  intersection actually occurs before 5 p. m. The apparent gravitational deflection  $\Delta y$  is thus zero and negative throughout the night. On July 25 and 26, the intersection occurs between 7 and 8 p. m. and on July 27 it just fails between 5 and 6 p. m. In contrast with this,  $\Delta y$  at night in the older results was almost constantly 13.5 after 6 p. m. for months, so that the observations were often much like repetitions of each other. Unfortunately,  $T/2$  was mostly observed for single arcs, as a rule; it should have been taken (as now appears) from two consecutive arcs of vibration.

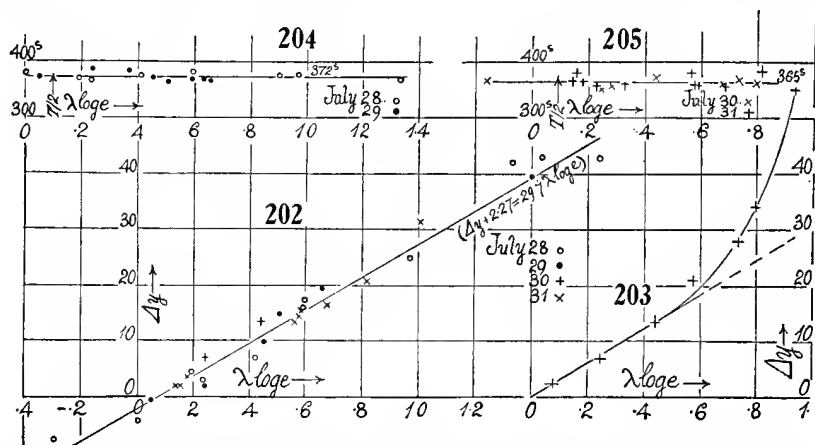
The new results obtained on July 28 and 29 after fresh exhaustion, in the same way as the preceding, are given in figure 197, with insets (figs. 200 and 201) showing the vacuum). Successive observations are horizontally equidistant, and the nearest hour is attached to the initial circles. The graph also gives the  $T/2$  for the ascending and descending branches and their mean  $T/2$  in minutes and seconds. The  $F, R$  curves are somewhat different in form from the preceding, but they nevertheless intersect at about 8 p. m., after which  $\Delta y$  is negative, or the radiant forces overpower gravitation.  $EE'$  curves, though much the same as before, are somewhat farther apart, as a rule. On July 28 (9 p. m.) there is a negative decrement  $\lambda$ .

The apparatus had been exhausted on the night before July 28. The vacua are therefore moderate, 0.06 to 0.26 mm. On July 30 the exhaustion was made at 10 a. m.; as it was necessary to wait until the needle was free from the sides of the case, observations were not available before 2 p. m. The  $F, R$  curves trend rapidly towards an intersection after 8 p. m., but they nevertheless

just fail, and thereafter diverge again. The day was clear, and hence the large  $d\theta/dt$  effect. On July 31 the  $F, R$  curves are more irregular; but they also fall short of intersection at 8 p. m., and recall the graphs of July 27. The vacuum has, meanwhile, been continually decreasing without producing any determinable impression on the graphs as a whole. On August 1 the equilibrium curves  $F, R$  have grown simpler, but they are as yet far removed from steady or normal  $\Delta y$  values, even at night.

After August 1, the extremely laborious procedure, involving much eye-strain, of determining  $T_1, T_2$ , and  $\lambda$  was dispensed with and measurements of  $\Delta y$  only, for time intervals about an hour apart, were taken. These, it was thought, would be adequate for comparison with similar data taken on the same day last summer. They will come up for consideration in § III.

111. Values of  $\lambda$  and  $\Delta y$ .—It seemed at first useless to look for any relations here, in view of the confusion of data and the frequent occurrence of



negative values of  $\lambda$  and  $\Delta y$  in the new results. Nevertheless, the indications of § 105 are sustained, though it has not been possible to adduce smooth graphs. The data so far as obtained are given in table 22. The quantity  $\lambda \log e$  was computed whenever two successive arcs were available and is merely the common logarithm of their ratio, no other connection with the theory of  $\lambda$  under normal conditions being implied. In the early forenoon the needle passes beyond the limits of the scale or touches one of its glass plates. Considerable difficulty is encountered in the proper selection of  $\Delta y$ , the static displacement. Table 22 gives the observed values; but these are about an hour apart, and during this time there has been considerable change of the position of equilibrium, as indicated by the  $F, R$  curves. The value of  $\lambda$ , however, is taken from two consecutive arcs and the time consumed is only about 13 minutes. Hence  $\lambda$  and  $\Delta y$  (observed) do not belong together. In this dilemma it is perhaps more trustworthy to associate  $\lambda$  with a value of  $\Delta y$  to be interpolated from the  $F, R$  curves for the same time interval. The

TABLE 22.—*Values of  $T_1/2$ ,  $T_2/2$ ,  $\lambda$ , and  $\Delta y$ .*

Date.	Vacuum.	mm.	Hour.	$T/2$ sec.	$10^8 \times$ $\lambda \log e$	$\Delta y$ cm.	Mean $T/2$ sec.
July 24	10 <sup>h</sup> 10 <sup>m</sup> a. m. 10 18 p. m.	0.0633 .1560	7 <sup>h</sup> 12 <sup>m</sup>	...	— 92	} —13.88	...
			8 3	...	—297		
			9 0	...	—263		
			10 0	...	— 29		
July 25	10 43 a. m. 10 0 p. m.	.2280 .2910	11 40	...	1,519	} 36	...
			1 35	...	700		
			2 53	...	972		
			3 50	...	611		
			4 46	408	514		
			5 55	385	246		
			7 40	398	62		
			8 50	393	— 54		
			9 42	410	— 63		
			2 56	364	1,453		
July 26	10 42 a. m. 10 11 p. m.	.357 .466	4 00	398	571	} 23	...
			5 35	397	496		
			7 6	407	214		
			8 4	396	87		
			9 3	406	31		
			9 55	403	377		
			11 20	...	...		
			12 20	333	1,497		
			1 23	378	1,180		
			2 22	371	717		
July 27	...	...	3 14	387	630	} 21.28	...
			4 18	389	268		
			5 13	395	289		
			...	...	...		
			7 15	394	388		
			8 19	383	514		
			9 19	388	418		
			...	...	...		
			9 12	367	1,642		
			10 27	368	1,335		
July 28	10 <sup>h</sup> 2 <sup>m</sup> p. m. 9 27 a. m. 9 27 p. m.	.0005 .0645 .1295	11 32	376	901	} 49	...
			2 10	377	970		
			3 22	383	597		
			4 25	375	413		
			5 22	369	194		
			7 5	365	237		
			8 10	380	50		
			9 10	369	—291		
			10 37	385	1,370		
			12 10	367	659		
July 29	10 <sup>h</sup> 25 <sup>m</sup> a. m. 10 8 p. m.	.197 .257	2 16	370	591	} 36.65	...
			3 36	364	509		
			4 30	368	633		
			5 34	371	453		
			7 10	386	241		
			8 00	371	522		
			9 8	...	159		
			10 6	...	...		
			2 5	...	932		
			2 57	362	796		
July 30	10 <sup>h</sup> 30 <sup>m</sup> a. m. 9 54 p. m.	.0006 .0651	4 00	368	735	} 60	...
			5 01	360	576		
			6 08	372	440		
			7 30	351	243		
			8 35	355	280		
			9 37	...	74		
			10 10	...	...		
			...	...	...		
			...	...	...		
			...	...	...		

TABLE 22.—*Values of  $T_1/2$ ,  $T_2/2$ ,  $\lambda$ , and  $\Delta y$ —Continued.*

Date.	Vacuum.		Hour.	$T/2$	$\frac{10^8 \times \lambda}{\log e}$	$\Delta y$	Mean $T/2$
		<i>mm.</i>		<i>sec.</i>		<i>cm.</i>	<i>sec.</i>
July 31	10 <sup>h</sup> 10 <sup>m</sup> a. m. 9 57 p. m.	0.1300 .1960	10 6	...	1,155	} 60	...
			11 20	...	1,090		...
			12 34	384	818		26.98
			2 20	358	680		22.60
			3 10	360	574		15.20
			4 00	358	588		15.90
			5 00	381	561		16.30
			5 56	356	227		12.00
			7 25	362	327		4.60
			8 9	365	176		4.08
			9 0	380	153		1.98
			9 45	365	140		1.70
			10 5	...	...		376
			12 0	374	1,042	} 25.68	...
Aug. 1	9 <sup>h</sup> 35 <sup>m</sup> a. m. 9 49 p. m.	.254 .318	1 45	368	645		...
			3 5	372	687		17.05
			4 15	...	381		15.15
			5 15	384	634		10.93
			6 5	342	389		10.15
			7 25	385	305		5.60
			8 25	365	243		4.65
			9 35	386	308		4.75
			10 5	...	...		6.80
			10 5	...	...		376

latter, however, are so irregular and vary so rapidly, particularly in the morning, that smooth curves can not be expected. I tested both cases of observed and interpolated  $\Delta y$ , finding that in afternoon and night values there was not much choice; but the forenoon data are unavailable in the former case. Hence in figure 206 (July 24–27) and figure 202 (July 28–31) the interpolated  $\Delta y$  is compared with  $\lambda$ . The high values are divergent for the reasons given; but both curves, as a whole, unquestionably point out a proportionality between these two quantities. The lines which I have drawn through both figures have the same slope, conformably with the equation

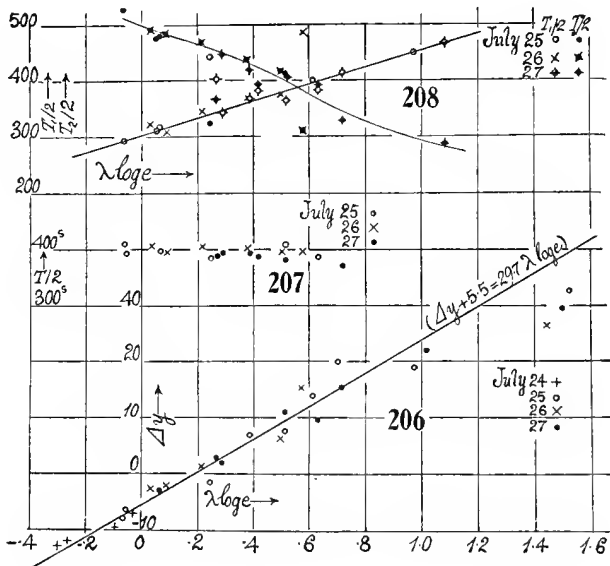
$$(\Delta y + \Delta y_0) = 29.7\lambda \log e = 12.9\lambda$$

The intercepts differ, being  $4.5 = \Delta y_0$  in figure 206 and 2.2 in figure 202.

The observations of July 30 seemed to depart from these results and are specially given in figure 203. It is, however, only the high values (above the abscissa  $0.5 = \lambda \log e$ ) which particularly diverge here, for some reason; the lower values conform to the same slope, but the intercept is zero. It is interesting to note that the negative values of  $\Delta y$  and  $\lambda$ , which I had supposed would rule out all possibility of comparison, conform pretty well with the locus as a whole, both in figures 202 and 206.

The values of  $T/2$  of table 22 are the means of the semiperiods for the first and second arc of vibration. It has already been pointed out that the two components differ widely and exchange relative magnitudes somewhere near  $\lambda \log e = 0.6$ . Since both components must here be found between the elongations of a very slow moving needle, they can not be measured. More-

over, there is some uncertainty during the exchange of weights at the first elongation. If the first half period is taken too long the second will be too short, so that their sum or mean is liable to be much more trustworthy than either and is therefore given under  $T/2$  in the table, as well as in figures 207, 204, and 205. The mean value on July 25 was  $T/2=399$  seconds; on July 26, 396 seconds; on July 27, 386 seconds. The values for this exhaustion are thus larger than for the next, viz, July 28,  $T/2=373$  seconds, July 29,  $T/2=373$  seconds, and for the last, viz, July 30,  $T/2=361$  seconds, July 31, 367 seconds. It is useless to speculate on the reason for the high values in the first exhaustion; but probably the later values, since the observer will gradually have gained skill in these difficult readings, are preferable. The final mean of this latter group will be  $T/2=368$  seconds, while the mean of all would be 379 seconds.



Although there is greater uncertainty attaching to the semiperiods (since if one is taken too long, the other will be too short, and vice versa), it is nevertheless worth while to give some examples of their relations, as in figure 208. Here the first half period  $T_1/2$  is plotted in open characters and the second,  $T_2/2$  in black characters of the same kind. There are a number of exceptions to the rule, no doubt; nevertheless, a glance at figure 208 indicates that first and second half periods lie on two lines which intersect somewhere before  $\lambda \log e = 0.6$ . Each of these quantities  $T_1$  and  $T_2$  is thus modified by the same agency as  $\Delta y$  and  $\lambda$ , which, however, is here nearly eliminated in their sum  $T_1 + T_2$ .

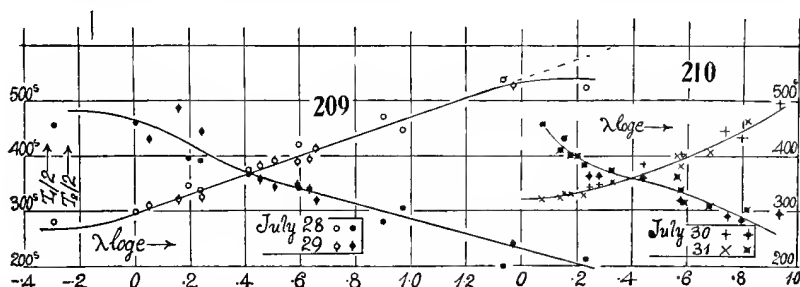
In figures 209 and 210, finally, the first and second semiperiods are taken from the data of July 28–29 and 30–31. There are no exceptions, though the



graphs naturally lack definiteness for the reasons given. The intersection of graphs takes place sooner ( $\lambda \log e = 0.4$ ) than in figure 208, so far as it can be located.

#### INFERENCES.

**112. Summary.**—It is now possible to bring these diverse data together in two groups: That of the morning, in which a gradual increase of the temperature of the environment ( $d\theta/dt$ , positive) supervenes, and that of the late afternoon and night, in which temperature gradually decreases ( $d\theta/dt$ , negative). Since the two sides of the case parallel to the needle are similarly circumstanced, it will suffice to consider the front face only. Hence when the weight  $M$  is on the right in front, that end of the needle is screened, while the left end receives radiation from without, if  $d\theta/dt$  is positive. The result is an excess of molecular bombardment on the left in front, manifesting itself as a repulsion of the left end of the needle towards the rear, *i. e.*, a virtual increase of the attraction of  $M$ . Again, if  $M$  is near the left end of the needle and in front of it, the conditions are exactly reversed. There is excess of



molecular bombardment or repulsion of the right end of the needle rearward, which is in turn equivalent to an increased attraction of  $M$ .

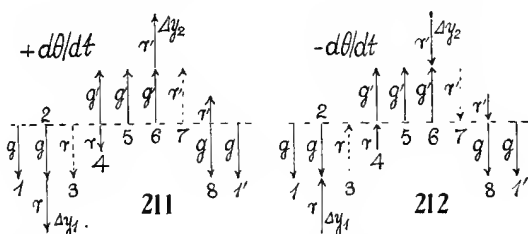
Finally, if  $d\theta/dt$  is negative, the radiant forces are again reversed, in each of the two cases. For it is now the end of the needle screened by  $M$  which is continually the warmer, *i. e.*, subject to excess of bombardment toward the rear. Hence the gravitational pull of  $M$  is reduced by the radiant forces.

These preliminaries granted, we may proceed with the analysis of the interaction of the gravitational vector  $g$ ,  $g'$  and the radiant vector  $r$ ,  $r'$ , assumed for convenience to be nearly equal (as they often are), in the way indicated in figures 211 and 212. It must be remembered that while  $g$  acts instantaneously with full strength,  $r$  requires time to reach its maximum value. Suppose, therefore,  $d\theta/dt$  is positive (fig. 211) and that at a given instant  $g$  is acting alone (case 1). Soon thereafter case 2 will be established and the resulting static deflection of the needle may be called  $\Delta y_1$ . Now let the attracting weight  $M$  be suddenly passed from front to rear. In the neutral position,  $r$  will then alone act prolonging the attraction (case 3), but with  $M$  newly located,  $g$  reversed ( $g'$ ) acts in full against a reduced value of  $r$  (case 4). In case 5,  $r$  has vanished and eventually in case 6,  $r$  has its maximum

negative value,  $r'$  and the static deflection of the needle is now  $\Delta y_2$ . The total deflection of the needle is thus  $\Delta y = \Delta y_1 + \Delta y_2$ . Finally, let the attracting mass  $M$  be again passed to the front, its first position. For an instant the radiant vector  $r'$  acts alone and prolongs the former attraction (case 7). In case 8 the gravitational pull  $g$  is reestablished with a reduced radiant vector  $r'$ . The latter vanishes, restoring the original case 1.

In figure 212,  $d\theta/dt$  is negative; but the consecutive cases are the same as before (*mut., mut.*), excepting that  $r$  is now negative. Here  $\Delta y_1$  and  $\Delta y_2$  and  $\Delta y$  may all be zero, an observation so common in the above results. The occurrence of large and small positive and negative values of  $\Delta y$  follows at once from the diagrams. In the latter case  $r$  must numerically exceed  $g$ .

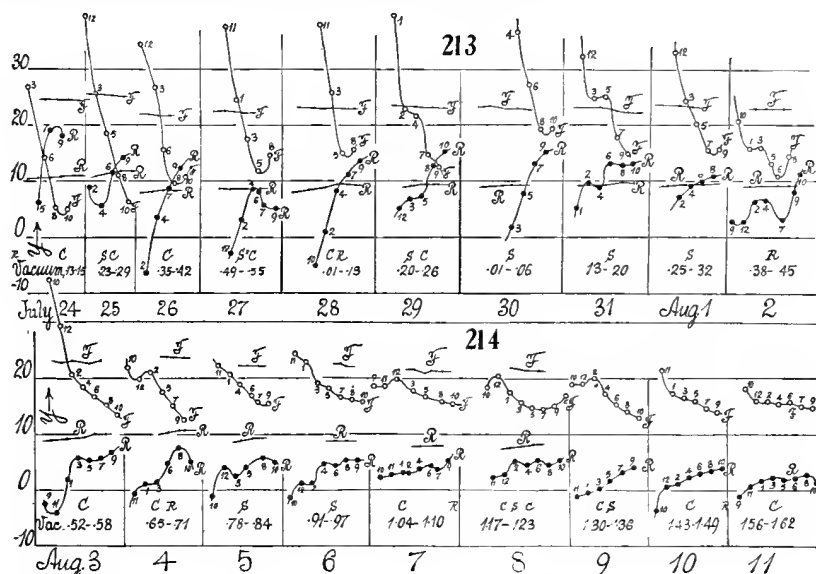
In figure 211,  $\lambda$  must also be large; for the first deflection occurs in the direction of an increasingly favorable vector  $r+g$ , whereas the second deflection is resisted by the same vector, probably still continually increasing. In the second case, figure 212 with  $d\theta/dt$  negative, the deflecting vector, algebraically  $g' + r'$ , passes through a maximum and may, if  $r'$  exceeds  $g$ , eventually become negative. Hence  $\lambda$  is smaller and may also be negative.  $\Delta y$  and  $\lambda$  are thus



fundamentally subject to the same radiant conditions. These must also determine, though perhaps less uniformly, the first and second semiperiods,  $T_1/2$  and  $T_2/2$ . For in case of figure 211,  $T$  is relatively long because the position of equilibrium is continually moving in the same direction as the pendulum, whereas in case of  $T_2$ , the pendulum moves in a direction opposite to the motion of the position of equilibrium. These relations may also be reversed in case of figure 212, so that  $T_2 > T_1$ . It is obvious also that  $T = T_1 + T_2$  will be more nearly constant than either component, though it does not follow that  $T$  will be quite constant.

113. Comparison of the equilibrium curves  $F$ ,  $R$ , of 1921 and 1922.—The apparatus used last year was identical with the present one, excepting only the minor appurtenances, added to secure greater convenience in exhaustion. These are without influence. Moreover, neither the location of the apparatus nor the mechanism of the weights  $M$  had been changed. The method of observation was substantially the same. It is thus very difficult to account for the erratic behavior of the gravitation needle during July and August of this year, as compared with the nearly constant deflections ( $\Delta y$ ,  $y$  being the scale reading) obtained under like conditions last year. I have, therefore, in

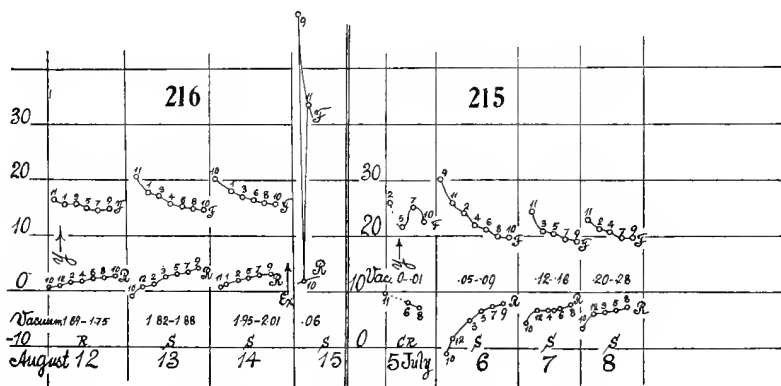
figures 213 and 214, put the scale readings of the elongations,  $y$ , obtained on the same day in 1921 and 1922, together, successive observations of the position of equilibrium (about an hour apart) being inserted equidistant horizontally. Data for 1922 are distinguished by little circles, with the nearest hour number of the observation attached. Data for 1921 are given in points, in corresponding positions, for easy comparison.  $F$  denotes that the attracting weight  $M$  on the right end of the needle is in front of it;  $R$ , that  $M$  is to the rear of the needle. Complete sets of observations (*i. e.*, equilibrium curves  $F$  and  $R$ ) are given between about 10 a. m. and 10 p. m. for each year from July 24 to August 11. The exhaustion (mm. of mercury) of the case in the morning and at night is shown on each day for 1922 only, as the data were not taken in 1921. In the same place  $C$  refers to cloudy,  $C'$  to partly cloudy



weather,  $S$  to sunshine or a clear day, and  $R$  to rain. It is seen at a glance that the variations of the position of equilibrium  $y$  in the lapse of time are of a different order in 1922 from their approximate constancy in the given scale in 1921. The contrast is startling, with nothing easily apparent to account for it. For the exhaustions, as a whole, were thought to be of about the same order of value in both years. In 1922 there was fresh exhaustion on July 24, 28, and 30. Thereafter I left the apparatus, with its slight leak, to itself. In 1921 there were no intermediate exhaustions, and unfortunately the McLeod gage was not attached to the case.

Figures 213 and 214 show, moreover, that all observations have a period of one day (24 hours). Consequently, the variations can not be contributed by anything within the laboratory, though enhancement is possible. They must, in other words, be originally meteorological, and due to solar radiation. Immediately after exhaustion (as on July 28 and 30) there are apt to be

large deflections, probably showing that the further exhaustion of the air within the case, though very rare, has nevertheless an appreciable cooling or other effect. The enhanced discrepancy persists half a day or longer. For this reason I ceased to make exhaustions after July 30, and the observations, possibly for this contributory reason among others, gradually grow smoother and more normal. Intersections of the curves  $F$  and  $R$  cease. Any slight cooling of the inside of the case would tend to exaggerate the daytime meteorological effect. If the cooling due to an exhaustion from 1 mm. to 0.001 mm. of pressure were instantaneous, one would estimate that about 0.01 calory would be abstracted from the air within the case. This is largely supplied, of course, by the massive case, and the exhaustion is very gradual. Nevertheless the effect on the needle is always very marked. One can not observe with the pump running. The needle in such a case clings to the glass plates.

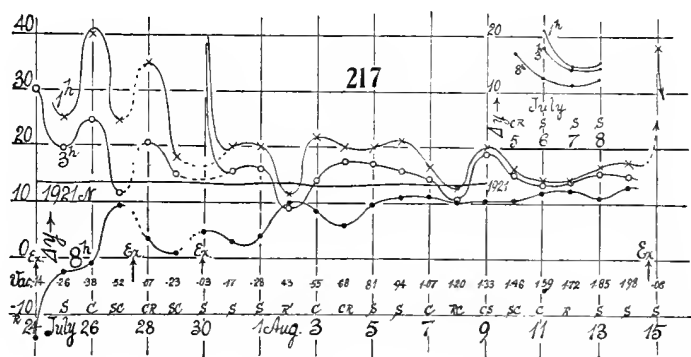


In figures 215 and 216 I have added a few supplementary observations obtained July 5-8 and August 12-15. The latter sustain the general run of figures 213 and 214 and the effect of the sun on August 13, after protracted cloudiness and rain, is marked but subdued when compared with the earlier graphs.

It was necessary to discontinue the observations on the morning of August 15. Consequently a final exhaustion was made to about 0.001 mm. 12 hours before that time, in order to test its effect on the now normal succession of results. Figure 217, like figure 216, shows (August 15) a relatively enormous enhancement of the radiation discrepancy, quite comparable with the earlier experiences. The conclusion is therefore trustworthy that the radiation forces are at a minimum in a partial vacuum of a few millimeters; that they are liable to be relatively very large in case of a plenum, or of a high vacuum, within a few tenths of a millimeter. The tendency of the needle to persistently cling to the walls of the case while the pump is running at high exhaustion is thus to be anticipated, in view of the excess of the radiant forces over gravitation, under conditions of high exhaustion. Moreover, since the slope of the  $F$ ,  $R$ ,

curves, always convergent, show a tendency to increase in proportion as the vacuum becomes more nearly perfect, the eventual intersection of these curves may be predicted and the enhancement be referred to causes within the apparatus accompanying the high exhaustions.

**114. Static deflections ( $\Delta y$ ) a year apart.**—To obtain a final comparison, it will be necessary to measure the distances apart  $\Delta y$  of the  $F$ ,  $R$ , graphs, at the same hour on successive days. As these graphs are often quite divergent, the interpolations will lose in accuracy; but the general relations of the results will nevertheless appear much more clearly. These static deflections,  $\Delta y$ , are given in table 23 and in figure 217. For 1922 the graphs are drawn for 1, 3, and 8 p. m. of the successive days, and are distinguished by circles or crosses. For 1921 the night observations (about 8 p. m. on the average) only are given, as the lines would lie too close to them at the other hours not to complicate



the diagram. In fact, the variations in 1921 are of a smaller order and must be given on a scale 10 times larger to be adequately shown.

The diagram brings out the striking difference of the results very well, and for 1921 the observations lie practically on a straight line,  $\Delta y = 13.42$ , for which the normal period of the needle in vacuo would be 752 seconds. In the results for 1922 the time of the successive exhaustions ( $ex$ ) is indicated approximately. It will be seen that the cooling or other effect of such an exhaustion (though carried from 1 mm. to 0.001 mm. only) is still effective in exaggerating the radiant forces for at least 6 hours or more (*cf.* July 24 and 30) after the exhaustion has been completed. Consequently, the graphs for 1 and 3 should probably be joined by the dotted lines, as indicated.

In all cases the extraneous radiant disturbance, which is strong in July 1922, gradually recedes more and more, as the observations enter the days in August. On July 24, at 8 p. m., the combined gravitation and radiant effect of the attracting mass  $M$  was strongly repulsive ( $\Delta y$  negative), the radiant repulsion being about twice the gravitational pull. Positive values are not reached until after July 26. From July 28 on, the 8 p. m. increase is determined, though it has not quite reached the values of  $\Delta y$  of 1921 even at the end of

the diagram (August 13). In the afternoon observations (1922) the rain effect (or the absence of sun effect) is brought out very clearly by the synclinal inflections on August 2, 8, 11, and 12. At night this effect may be reversed; *i. e.*, if radiation is scantily received by the apparatus during the day, there is an equivalent absence of radiation during the night.

In case of the observations of 1922, the small fluctuations of the  $\Delta y$  curves throughout a month showed instances of resemblance to the run of atmospheric temperature; but in the large variations recorded in 1922 (as a consequence perhaps) I was unable to detect such resemblances in the night observations, which are here alone of interest. The same is true of the change of temperature per day, etc. Nevertheless, it is possible the relatively short atmospheric temperature changes from without, such as would not be otherwise recorded, may make an impression on the 8 p. m. graph. This, however, would not bear upon the 1922 graph as a whole, from July 24 to August 13.

TABLE 23.—*Values of  $\Delta y$ , 1922, interpolated.*

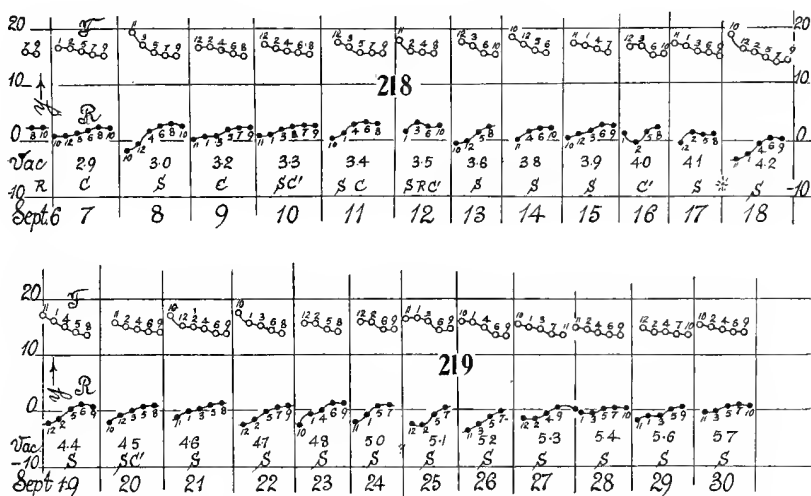
Date.	1 <sup>h</sup> p. m.	3 <sup>h</sup> p. m.	8 <sup>h</sup> p. m.	Date.	1 <sup>h</sup> p. m.	3 <sup>h</sup> p. m.	8 <sup>h</sup> p. m.
	<i>cm.</i>	<i>cm.</i>	<i>cm.</i>		<i>cm.</i>	<i>cm.</i>	<i>cm.</i>
July 24	....	>30.0	—14.0	Aug. 4	20	17.5	6.0
25	25	19.5	— 2.5	5	20	17.0	9.7
26	>40	24.5	— 1.0	6	21.2	15.7	11.0
27	24.5	11.5	+ 9.5	7	16.5	14.2	11.2
28	35	20.7	3.5	8	12.7	10.5	10.2
29	18	15.0	1.0	9	20.0	18.7	10.5
30	>40	43.0	4.7	10	16.0	15.0	10.5
31	20	15.5	3.0	11	14.0	13.2	11.8
Aug. 1	20	16.0	4.0	12	14.2	13.8	12.2
2	11.7	9.0	10.0	13	16.6	15.2	10.8
3	21.7	14.0	8.7	14	17.0	14.7	12.7

Supposing, moreover, that the medium within the apparatus is in some way modified by the high exhaustions (carried to within 0.001 mm.), it seems hardly probable that the apparatus would take so long to return to a normal condition, if radiation of some sort is alone in question.

What has gone down during this series of measurements is the vacuum. One would therefore conclude that states of high exhaustion (a few hundredths or tenths of a millimeter) are (like the plenum) more susceptible to the presence of radiant activity than the lower exhaustions of a few millimeters. The exhaustion made just prior to August 15 conspicuously bears this out. It not infrequently happens that night values are low when day values are high and, in general, there is a tendency of the graphs to converge toward rainy or densely cloudy weather. All this conforms with the view that the needle is screened from radiation by the large attracting mass  $M$  and that the radiant forces act with gravitation, if the temperature coefficient  $d\theta/dt$  is positive, and act against gravitation when  $d\theta/dt$  is negative, as elsewhere explained. I have been tempted to envisage a coefficient  $d\theta/dt$  which is not

all temperature; for there may be some other radiation or agency behind the recent rains (for instance), as well as behind the difference in the character of the results of 1922 and 1921 as exhibited by figure 217. Unfortunately, accumulation of evidence of this nature is very slow and laborious. It is safe to conclude, however, that the radiant discrepancy is at a minimum in a partial vacuum of a few millimeters. It increases enormously as a plenum is approached. It similarly increases in high exhaustions, within 0.1 mm. In fact, the needle is then liable to stick to the case.

However puzzling it may be to account for the discrepancy which persistently clings to the observations in July and early August, and which in its long duration would seem to be incompatible with the practically immediate daily cycle, the suggestions of the last paragraph are still quite valid. If, in



other words, the slope of the convergent  $F$ ,  $R$  graphs is increased by causes evoked by high exhaustion within the apparatus, these graphs will ultimately intersect, with the result that negative values of  $\Delta y$  and repulsive forces make their appearance at night.

#### CONCLUDING OBSERVATIONS AND COMPARISONS.

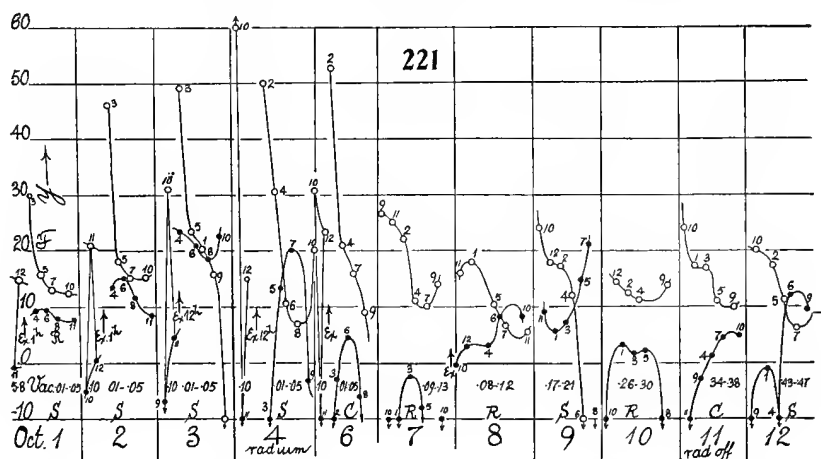
**115. Further observations.**—The observations interrupted after the exhaustion of August 15 were resumed (figs. 218 and 219) on September 6. In the meantime the vacuum had slowly decreased to about 3 mm. and it was under these conditions that the new observations were to be made. They are given ( $F$ ,  $R$ , equilibrium curves or elongations  $y$ ) in the same manner as in figure 216, with the successive observations horizontally equidistant and the nearest hour marked at the points. It is at once evident that the  $F$ ,  $R$  curves are very much more regular and more restricted in vertical extent than heretofore. This is the case until the arrival of the cold spell, September 15





The latter are given in full in table 22. If we throw out the observation on the cold day (September 17), which is evidently erroneous, the remaining 24 observations conform to the mean value (8 p. m.)  $\Delta y = 13.07 \pm 0.05$  cm. This is somewhat smaller than the mean of last year ( $\Delta y = 13.4$ ) owing to slight shifting of the weights  $M$ , from which the attraction proceeds, during the course of the year.

**116. The same. Higher exhaustions repeated.**—Having reproduced the conditions for the steady behavior of the needle as shown in figures 219 and 220, it seemed desirable to utilize the few remaining days of the season (steam heat was turned on October 13) to repeat the experiments with an intensified vacuum, in order to see whether anything could be made out of the chaotic behavior to be anticipated. The equilibrium curves are given in the same



manner as heretofore in figure 221, open circles referring to the front and dark circles to the rear position of the attracting weight  $M$  on the right end of the needle. The nearest hour at which the observation was made is attached in each case. The figure, furthermore, shows the successive vacua (vac. in mm. of mercury) and the meteorological conditions (S sun, C cloudy, R rain). The time at which the exhaustions (ex. to 0.0003 mm.) were made is also given. Observations were begun 2 or 3 hours later, or as soon as the needle ceased to cling to the glass walls of the case. It was customary to complete one observation for  $\Delta y$  in the morning and thereafter to exhaust the case for observations at the higher vacua. On October 1, the first pair of equilibrium values of  $y$  has about the same separation,  $\Delta y$  as in September, the vacuum being low, 5.8 mm. After the exhaustion, however, and for the mean vacuum of 0.03 mm., these relations are totally changed,  $\Delta y$  becomes very small, and the two equilibrium curves tend to intersect. On October 2 the  $\Delta y$  for the residual vacuum 0.1 mm. in the morning is now very large, so that the effect

of the low pressure of the preceding day has not vanished. After the renewed exhaustion, the tendency of the  $F$ ,  $R$  curves to intersect is accentuated and the drift of both into higher values of  $y$  is marked. The same effects are still further enhanced on October 3. The lower equilibrium curve has steadily risen in  $y$ ; the upper equilibrium curve on October 3 actually intersects the other at about 8 p. m. and thereafter marked repulsion replaces gravitational attraction, until the needle actually clings to the glass plates on the wrong side. This condition is indicated at the lower ends of all curves by the arrows. On October 4 the observations made in the residual vacuum, 0.1 mm., begin with the needle adhering successively to the walls of the case on both sides.

An important result thus stands out; obviously, the effect of exhaustion is cumulative. It does not vanish in 24 hours nor in a number of days, the inference already suggested by figure 217. Meantime the daily cycles are practically immediate. Thus it does not seem that what accumulates can be temperature, particularly in view of the small range of exhaustion (0.1 to 0.001 mm.), *i. e.*, of the very rare air contained.

Electric excitation on the outside, in the damp atmosphere, would be out of the question. Neither is electric excitation within (for instance when the needle strikes the glass walls) under favorable conditions, since the exhausted air is now a conductor. Nevertheless, it seemed worth while to increase the ionization within by aid of the gamma rays of radium. Accordingly a thin aluminum tube was suspended on the outside of the glass walls near the middle of the needle on October 4. The effect of this in no manner changes the chaotic nature of the curves between October 4 and October 10, so that electrostatic discrepancies are not in question. There is, however, a change in the character of the progression of curves during this interval, for whereas the mean positions of the  $F$ ,  $R$  curves were in general rising before, they are now gradually being depressed. The  $R$  curves, for instance, are deleted because the needle is usually at the walls. It does not follow, however, that this new condition is due to the presence of the  $\gamma$  rays (for on October 11, when the radium was removed, the same behavior continues), unless the effect of the rays on the air-content within the case is also cumulative. It is unfortunate that the observations after October 12 could not be continued in order to discern whether in the course of time the rise of  $y$  values of October 1-4 would have reappeared or whether the whole play of curves is merely an accentuated reproduction of meteorological conditions favored by high exhaustion.

It will be noticed that the exhaustions have the same range (average 0.03 mm.) between October 1 and 6. On October 3, the  $F$ ,  $R$  curves actually intersect and the aggregated forces are repulsive. On October 5 the needle remained at the walls of the case all day, so that no measurements could be made until October 6 in the residual vacuum. On October 7, the morning exhaustion was omitted; but the needle still shows a marked tendency to adherence in the  $R$  positions. Barring the slight incidental exhaustion at the end of the day, the case was thereafter left without fresh exhaustion. The

irregularity of behavior, however, continues even when the vacuum pressure is as high as 0.5 mm.

As a whole, even if the circumstances are very complicated, and if the discrepancies from meteorological temperature changes are enormously magnified by exhaustion for a certain range below 0.5 mm. of mercury, it seems to me that the observations of October 1 to 6 indicate that something cumulative in the lapse of time under high exhaustion is added to the inner content of the gravitation chamber. What that something may be I do not venture to state, but without it, the progressive character of the data from day to day, both at a pressure of 0.1 mm. and at the lower mean pressure of 0.03 mm., would be difficult to explain. For on these days observations were made under the same mean pressure, throughout.

The question as to what will happen when the chamber is rigorously exhausted to a limit is still outstanding, and under present circumstances particularly interesting. Everything should ultimately vanish short of light pressure. The present apparatus did not admit of that extension, as the needle with the pump running merely adheres persistently to the walls, not to become free for hours thereafter. Pressures blow  $10^{-4}$  mm. are thus essentially in question.

117. Conclusion. Observations of 1921.—The above experiments carry the work with the thin quartz fiber, under the given conditions, as far as the form of apparatus used warrants. Seeing that the latter was tightened with sealing-wax and that the air-pump can not be kept running during observations, a steady vacuum much within  $10^{-3}$  minutes could not be maintained; and it is just here that the radiant forces begin to be as formidable again, as they were for the plenum.

The work as a whole has yielded two series of systematic night observations (8 to 12 p. m.), one completed in the summer of 1921 and the other in the summer of 1922. Each is reasonably consistent, but different from the other, and it is therefore desirable to determine to what degree they have fallen short. Since the periods and logarithmic decrements are equally vitiated by the radiant forces, the only available procedure consisted in taking the apparatus apart and determining the torsion coefficient of this quartz fiber by a separate small mass of known moment of inertia. This was accomplished without accident to the fiber.

The damped period\* of the needle in 1921 was provisionally taken as 728 seconds, giving a free period of 724 seconds. The corrected moment of inertia of the needle was  $N = 159.4 \text{ gcm.}^2$  If in the equations  $M$  is the attracting,  $m$  the attracted mass,  $R$ , their distance apart,  $1 + s - t/\tau$  the correction for stem, etc., and  $\kappa$  the constant in  $\gamma = \kappa \Delta y$  (where  $\Delta y$  is the (double) static

---

\* Carnegie Inst. Wash. Pub. No. 310, § 55, 56, 57. By an error of entry, the datum  $T = 746.14$  seconds is given in § 55 and 57. This does not occur in  $\kappa'$ ,  $\kappa''$  and  $\kappa$ , where  $T = 724.3$  seconds is used.

displacement seen in the telescope), the values inserted or deduced were as given in table 24.

TABLE 24.

<i>M</i>	<i>R</i>	$1 + s - t/\tau$	$\kappa \times 10^8$
	<i>cm.</i>		
3,368 <i>g</i> .....	5.89	1.0206	0.9781
2,947 <i>g</i> .....	5.63	1.0212	1.0218
Together .....	....	.....	.4997

Thus the deflection 13.3 cm. was to be expected. The night observations actually gave  $\Delta y = 13.416 \pm 0.033$  for the mean result between July 17 and September 15.

As the equation (apart from corrections) reads

$$\gamma = \frac{\pi^2 N}{L T^2 l} \frac{R^2}{M m} \Delta y$$

or in a more useful form

$$\gamma = \frac{2\pi^2 l R^2 (1 + s - t/\tau)}{M L T^2}$$

it is merely necessary to put in place of the provisional period, the new value obtained by the aid of  $N'/T'^2$  of the auxiliary body. This gives the corrected value of  $\gamma$ , since  $T^2 = T'^2 (N/N') = T'^2 (159.5/N')$ .

Two smooth steel ball bearings of moments of inertia  $N' = 0.04166$  and  $0.04158$  and periods  $T' = 11.62$  seconds and  $11.56$  seconds on the given fiber, gave  $T = 719$  seconds and  $716$  seconds, respectively, the mean of the vibrations being taken. Although the arcs of vibration usually exceeded  $360^\circ$ , this disappointingly large difference suggested the possibility of an effect of the earth's magnetic field. The experiments were, therefore, checked by a pair of small brass cylinders which gave a mean value of  $T = 716.5$  seconds. The value  $T = 716$  seconds was accepted for the period of the needle, sufficing for the present critical purposes.

With  $T = 716$  seconds for the needle, the constants reduce to

$$10^8 \kappa' = 1.0011 \text{ and } 10^8 \kappa'' = 1.0458$$

or for the two balls conjointly

$$10^8 \kappa = 0.5117$$

whence

$$10^8 \gamma = \kappa \Delta y = 0.5117 \times 13.416 = 6.865$$

Thus, in spite of the care taken with the observations in 1921 and the encouraging uniformity of static deflections  $\Delta y$  from day to day, the radiant discrepancies were still present and equivalent to an excess of about 3 per cent in the value of  $\gamma$ . The reduced performance of the thin fiber has thus fallen below the first result, obtained with a much thicker fiber.

118. **Observations of 1922.**—The constants of the apparatus were nearly the same as in the previous year and the same needle was used, so that  $T=716$  seconds. The distances  $R$  measured are given in table 25.

TABLE 25.

$M$	$R$	$1 + s - t/\tau$	$\kappa \times 10^8$
	cm.		
3,368 $g$ .....	5.89	1.0206	1.0011
2,947 .....	5.67	1.0212	1.0606
Together .....	.....	.....	.5154

From this the values of  $\kappa$  in table 25 were computed. The mean value of  $\Delta y$  for the night observations from September 16 to 30, 1922, was found to be  $\Delta y = 13.07 \pm 0.05$  cm., hence

$$\gamma = \kappa \Delta y = 10^{-8} \times 0.5154 \times 13.07 = 10^{-8} \times 6.736$$

Thus the 1922 datum for  $\gamma$  obtained later in the season than was the case in 1921 are nearer the normal value of  $\gamma$ . Nevertheless the discrepancy produced by the presence of radiant forces is equivalent to an excess about 1 per cent of the value of  $\gamma$ . By using the largest values of  $T'$  found with the auxiliary body, both  $\gamma$  values could be reduced about 1 per cent; but this is of no interest as the divergence remains.







